

Introduction to Modern Nuclear Physics

Qun Wang

May 16, 2019

Department of Modern Physics, University of Science and Technology of China, Anhui 230026
China, qunwang@ustc.edu.cn, <http://staff.ustc.edu.cn/~qunwang>

Contents

1	Introduction	5
1.1	Why nuclear physics	5
1.2	From cgs-Gaussian to natural unit system	5
1.3	Conventions	8
2	Properties of Nuclei	11
2.1	Discover atomic nucleus	11
2.2	The size and density distribution of nucleus	12
2.3	Spin and magnetic moment	13
2.4	Parity	20
2.5	Electric multipole moment	21
2.6	The mass formula and binding energy	23
3	Radioactivity and nuclear decay	28
3.1	General property of radioactivity	28
3.2	Radioactive dating	37
3.3	α decay: strong interaction at work	38
3.4	β decay: weak interaction at work	46
	3.4.1 Fermi theory of β decay	53
	3.4.2 Parity violation in β decay	65
3.5	γ decay: electromagnetic interaction at work	66
	3.5.1 Classical electrodynamics for radiation field	66
	3.5.2 Quantization of radiation field	69
	3.5.3 Interaction of radiation with matter	71
	3.5.4 Multipole expansion	76
3.6	Mössbauer effect	91
4	Nuclear models	93
4.1	The shell model	93
	4.1.1 Phenomena related to shell structure	93
	4.1.2 Main points of the shell model	94
4.2	Collective models	101
4.3	Hartree-Fock self-consistent method	103
5	Nuclear reaction	109
5.1	Conservation laws and kinematics	110
5.2	Partial wave analysis and optical potential	113
5.3	Resonance and compound nuclear reaction	115
5.4	Direct reaction	118
5.5	Nuclear fission	119
	5.5.1 Spontaneous fission	119

5.5.2	Induced fission	123
5.5.3	Self-sustaining nuclear fissions and fission reactor	127
5.5.4	Time constant of a fission reactor	128
5.6	Accelerator-Driven System	129
5.6.1	Spallation neutron source	129
5.6.2	Thorium as fission fuel	129
5.6.3	Nuclear waste incinerator	130
5.7	Nuclear fusion	130
6	Nuclear force and nucleon-nucleon interaction	140
6.1	Properties of nucleons	140
6.2	General properties of nuclear force	140
6.3	Deuteron nucleus	145
6.3.1	S-state	145
6.3.2	S and D states	147
6.4	Low energy nucleon-nucleon scatterings	151
6.5	Nucleon-Nucleon scatterings in moderate energy	152
6.6	Meson exchange model for NN potentials	152
6.6.1	One pion exchange potential (OPEP)	153
6.6.2	One boson exchange potential	155
7	The structure of hadrons	161
7.1	Symmetries and Groups	161
7.1.1	The group $SU(2)$	164
7.1.2	$SU(2)$ isospin, fundamental representation	166
7.1.3	Conjugate representation of $SU(2)$	167
7.1.4	$SU(3)$ symmetry	168
7.1.5	Tensor representation of $SU(3)$	173
7.1.6	Reduction of direct product of irreducible representations in $SU(3)$	174
7.1.7	Quarks as building blocks for hadrons	175
7.1.8	Mesons as quark-anti-quark states	177
7.1.9	Baryons as three-quark states	181
7.1.10	Gell-Mann-Okubo relations	185
7.2	Quarks and gluons	188
7.2.1	Color degrees of freedom	188
7.2.2	Gluons as color carriers	191
7.2.3	Asymptotic Freedom	194
7.2.4	Phenomenological illustration of the confinement [7]	196
8	Acknowledgement	200
A	Nucleon-nucleon scattering theory	201
A.1	Nucleon-nucleon scatterings	201
A.2	The stationary scattering wave function	201
A.3	Cross section	202
A.4	The optical theorem	203
A.5	Partial wave method	204
A.5.1	Scattering amplitude and cross section	205
A.5.2	Inelastic scattering and total cross section	207
A.5.3	Phase shifts in square well scattering	209
A.5.4	Breit-Wigner formula	210
A.6	Scatterings of identical particles	211

A.7 Lippman-Schwinger equation and Green function method	212
B A: Bessel functions	216
C B: Spherical harmonic functions	220
D Solutions to problems	223

Chapter 1

Introduction

1.1 Why nuclear physics

Nuclear physics is one of the most important branches and milestones in modern physics in the last century. It has intrinsic connections to quantum mechanics and can be regarded as a laboratory for quantum physics. The aim of nuclear physics is to understand the properties of nuclei and their applications. Among many applications are (a) The origin of nuclei in the universe, i.e. nuclear nucleosynthesis, nuclear cross section is the key to understanding of nuclear reaction in astrophysics; (b) Nuclear energy, nuclear fission and fusion; (c) Nuclear transmutation of radioactive waste with neutrons; (d) Radiotherapy for cancer with proton and heavy ion beams; (e) Medical Imaging, such as nuclear Magnetic Resonance Imaging (MRI), X-ray imaging with better detectors and lower doses, Positron-Electron Tomography (PET); (f) Radioactive Dating, such as C-14/C-12 dating for dead lives, Kr-81 dating for ground water; (g) Element analysis, such as forensic (as in hair), biology (elements in blood cells) and archaeology (provenance via isotope ratios).

1.2 From cgs-Gaussian to natural unit system

We use natural units [\hbar, c, eV] (the Planck constant, speed of light, and electro-Volt) for angular momentum, velocity and energy to replace [g,cm,s] (gram, centimeter and second) for mass, length and time [1]. So any quantities in the cgs unit can be expressed as $\text{g}^a \text{cm}^b \text{s}^c$, and in the natural unit it can be expressed by $\hbar^\alpha c^\beta \text{eV}^\gamma$.

For electromagnetic phenomena, there are several unit system, here we will use cgs-Gaussian units, in particular, the unrationalized Gaussian units (not Lorentz-Heaviside ones). We will explain it in more details. In dealing with thermal phenomena, we have an additional unit k_B (Boltzmann constant) in the natural unit or equivalently K (Kelvin) in the cgs unit. The relations between two systems of units are given by

$$\begin{aligned} 1 \hbar &= 1.05 \times 10^{-27} \text{g} \cdot \text{cm}^2 \cdot \text{s}^{-1} \\ 1 c &= 2.99792458 \times 10^{10} \text{cm} \cdot \text{s}^{-1} \end{aligned} \tag{1.1}$$

$$\begin{aligned} 1 \text{eV} &= 1.60217653 \times 10^{-12} \text{g} \cdot \text{cm}^2 \cdot \text{s}^{-2} \\ 1 k_B &= 1.3806488 \times 10^{-16} \text{g} \cdot \text{cm}^2 \cdot \text{s}^{-2} \cdot \text{K}^{-1} \end{aligned} \tag{1.2}$$

From the above we can get the inverse relation

$$\begin{aligned}
 1 \text{ cm} &= 5.06 \times 10^4 \hbar \cdot \text{eV}^{-1} \cdot c \\
 1 \text{ g} &= 5.6 \times 10^{32} \text{ eV} \cdot c^{-2} \\
 1 \text{ s} &= 1.52 \times 10^{15} \hbar \cdot \text{eV}^{-1} \\
 1 \text{ K} &= 8.617 \times 10^{-5} \text{ eV} \cdot k_{\text{B}}^{-1}
 \end{aligned} \tag{1.3}$$

Now we explain the feature of unrationalized Gaussian units in electromagnetics. In this unit system, the Maxwell equations are written as

$$\begin{aligned}
 \nabla \cdot \mathbf{E} &= 4\pi\rho, \\
 \nabla \times \mathbf{B} &= \frac{4\pi}{c} \mathbf{j} + \frac{1}{c} \frac{\partial \mathbf{E}}{\partial t}, \\
 \nabla \cdot \mathbf{B} &= 0, \\
 \nabla \times \mathbf{E} &= -\frac{1}{c} \frac{\partial \mathbf{B}}{\partial t},
 \end{aligned} \tag{1.4}$$

where the electric and magnetic fields have the same unit. The inverse-square force laws are written as

$$\begin{aligned}
 \mathbf{F} &= \frac{q_1 q_2}{r^3} \mathbf{r}, \\
 \mathbf{F} &= \frac{1}{c^2} \iint \frac{I_1 d\mathbf{l}_1 \times (I_2 d\mathbf{l}_2 \times \mathbf{r})}{r^3}.
 \end{aligned} \tag{1.5}$$

We see that two of Maxwell equations (1.4) have the factor 4π while there is no such a factor in the force laws. However in Lorentz-Heaviside units or rationalized Gaussian units, one can absorb 4π in Maxwell equations by redefining fields and charges. As a price there are 4π factors in the force laws. The fields and charges in two unit systems are related by

$$\begin{aligned}
 \mathbf{E}_{\text{LH}} &= \frac{1}{\sqrt{4\pi}} \mathbf{E}_{\text{unrat-Gauss}}, \\
 q_{\text{LH}} &= \sqrt{4\pi} q_{\text{unrat-Gauss}}.
 \end{aligned} \tag{1.6}$$

In nuclear physics, the unit for thermal system is not used very often. So we stick to the unit $[\hbar, c, \text{eV}]$ or $[\text{g}, \text{cm}, \text{s}]$ for convenience. From the relations in Eq. (1.2) we can derive following useful conversion factors

$$\begin{aligned}
 \hbar c &= 197 \text{ MeV} \cdot \text{fm} \\
 e^2 &\approx \frac{1}{137} \hbar c
 \end{aligned} \tag{1.7}$$

We have $e^2 \approx 1/137$ in unrationalized Gaussian units. In contrast this relation becomes $e^2/(4\pi) \approx 1/137$ in rationalized Gaussian or Lorentz-Heaviside units.

In the cgs-Gaussian units, the charge is in the electrostatic unit (esu) which can be determined from the Coulomb law

$$\begin{aligned}
 \mathbf{F} &= \frac{q^2}{r^3} \mathbf{r} \rightarrow \text{esu}^2 = \text{g} \cdot \text{cm} \cdot \text{s}^{-2} \times \text{cm}^2 = \text{g} \cdot \text{cm}^3 \cdot \text{s}^{-2} \\
 &\rightarrow \text{esu} = \text{g}^{1/2} \cdot \text{cm}^{3/2} \cdot \text{s}^{-1}
 \end{aligned} \tag{1.8}$$

We know that the Coulomb force law in the SI system has the following form

$$\mathbf{F} = \frac{1}{4\pi\epsilon_0} \frac{q^2}{r^3} \mathbf{r} \tag{1.9}$$

where $\epsilon_0 = 8.8542 \times 10^{-12} \text{ C}^2\text{N}^{-1}\text{m}^{-2}$ and the charge unit is Coulomb (C). We can determine the conversion rule for C to esu. In the SI system, we have $q = 1 \text{ C}$ and $r = 1 \text{ m}$, then the force is $F = 8.99 \times 10^9 \text{ N}$. In the unrationalized Gaussian units, we have $q = 1 \text{ esu}$ and $r = 1 \text{ cm}$, then the force is $F = 1 \text{ dyn} = 10^{-5} \text{ N}$. Comparing two units, we obtain $1 \text{ C} = 3 \times 10^9 \text{ esu}$. An electron carries the charge

$$1 \text{ e} = 1.602 \times 10^{-19} \text{ C} = 4.8 \times 10^{-10} \text{ esu} \quad (1.10)$$

In the SI system, the unit of the electric field is Volt/m = N/C, while in the unrationalized Gaussian units, the electric and magnetic fields have the same unit: Gauss (G). So we have

$$\begin{aligned} 1 \text{ Gauss} &= \frac{\text{dyn}}{\text{esu}} = \text{g}^{1/2} \cdot \text{cm}^{-1/2} \cdot \text{s}^{-1} \\ 1 \text{ Volt} &= 1 \text{ N} \cdot \text{m}/\text{C} = \frac{10^7 \text{ dyn} \cdot \text{cm}}{3 \times 10^9 \text{ esu}} \\ &= \frac{1}{3} \times 10^{-2} \text{ esuVolt} \\ \text{esuVolt} &= \text{g}^{1/2} \cdot \text{cm}^{1/2} \cdot \text{s}^{-1} \end{aligned} \quad (1.11)$$

where we have the static Volt unit: esuVolt. Then we obtain $1 \text{ eV} = 1.6 \times 10^{-12} \text{ g} \cdot \text{cm}^2 \cdot \text{s}^{-2}$, the third line of Eq. (1.2). Also we obtain

$$\begin{aligned} e^2 &= 2.304 \times 10^{-19} \text{ esu}^2 = 2.304 \times 10^{-19} \text{ g} \cdot \text{cm}^3 \cdot \text{s}^{-2} \\ \hbar c &= 3.15 \times 10^{-17} \text{ g} \cdot \text{cm}^3 \cdot \text{s}^{-2} \end{aligned} \quad (1.12)$$

which give the second line of Eq. (1.7). We can express $\hbar c$ by

$$\begin{aligned} \hbar c &= 3.15 \times 10^{-17} (\text{g} \cdot \text{cm}^2 \cdot \text{s}^{-2}) \cdot \text{cm} \\ &= 3.15 \times 10^{-4} (\text{g} \cdot \text{cm}^2 \cdot \text{s}^{-2}) \cdot \text{fm} \\ &= 197 \text{ MeV} \cdot \text{fm} \end{aligned} \quad (1.13)$$

which is the first line of Eq. (1.7).

Now we can convert some quantities in natural units. For electric and magnetic fields in cgs units, we have

$$\begin{aligned} 1 \text{ Gauss} &= \text{g}^{1/2} \cdot \text{cm}^{-1/2} \cdot \text{s}^{-1} \\ &= 6.92 \times 10^{-2} (\hbar c)^{-3/2} \cdot \text{eV}^2 \end{aligned} \quad (1.14)$$

We can convert the proton and neutron masses in cgs unit to natural unit.

$$\begin{aligned} m_{\text{p}} &= 1.672622 \times 10^{-24} \text{ g} = 938.27208 \text{ MeV} \cdot c^{-2} \\ m_{\text{n}} &= 1.674927 \times 10^{-24} \text{ g} = 939.56541 \text{ MeV} \cdot c^{-2} \end{aligned} \quad (1.15)$$

Atomic mass unit is defined as 1/12 of the mass of ^{12}C , i.e. N_{A}^{-1} ·gram where $N_{\text{A}} = 6.022142 \times 10^{23}$ is the Avogadro constant. Atomic unit is

$$1 \text{ u} = 1.66 \times 10^{-27} \text{ kg} = 931.494 \text{ MeV}/c^2, \quad (1.16)$$

The proton and neutron mass in the atomic mass unit are

$$\begin{aligned} m_{\text{p}} &= 1.007276 \text{ u} \\ m_{\text{n}} &= 1.008665 \text{ u} \end{aligned} \quad (1.17)$$

Here is an example involving another natural unit k_{B} . The shear viscosity is defined by $F = \eta S \frac{dv}{dx}$ and entropy density is defined as thermal energy $sT\Omega$ (Ω is the volume). Their dimensions are determined from knowns,

$$\begin{aligned} [\eta] &= \text{g} \cdot \text{cm}^{-1} \cdot \text{s}^{-1} \\ [s] &= \text{cm}^{-3} \cdot k_{\text{B}} \end{aligned} \quad (1.18)$$

So the ration η/s has the dimension

$$[\eta/s] = \text{g} \cdot \text{cm}^2 \cdot \text{s}^{-1} \cdot k_{\text{B}}^{-1} = \hbar \cdot k_{\text{B}}^{-1} \quad (1.19)$$

In this book we take the natural unit $\hbar = c = k_{\text{B}} = 1$. In summary, a quantity has the dimension $[D] = \text{g}^a \text{cm}^b \text{s}^d \text{K}^f = \hbar^\alpha c^\beta \text{eV}^\gamma k_{\text{B}}^\delta$, by using Eq. (1.2) and (1.3), we can obtain following relations

$$\begin{aligned} \alpha &= a + d \\ \beta &= a - 2b \\ \gamma &= -a + b - d + f \\ \delta &= -f \end{aligned} \quad (1.20)$$

1.3 Conventions

We list conventions for notations as follows. All superscripts or subscripts standing for texts in mathematical expressions are shown in roman letters, those standing for variables are shown in normal mathematical mode.

Table 1.1: Conventions for notations.

Symbols	Physical Quantities
J, J_A	(1) Total angular momentum quantum number; (2) Nuclear spin quantum number
\mathbf{J}, \mathbf{J}_A	(1) Total angular momentum; (2) Nuclear spin
L	Orbital angular momentum quantum number
\mathbf{L}	Orbital angular momentum
M	(1) Atomic mass of an element; (2) Quantum transition amplitude; (3) Orbital angular momentum quantum number along one particular direction
S	(1) Spin quantum number; (2) S-matrix; (3) S-factor in WKB approximation; (4) Area in coordinate space
m	(1) Nuclear mass; (2) Nucleon mass
\mathbf{x}, \mathbf{r}	3-dimensional coordinates space points
x, r	Modula of 3-dimensional coordinate space points, $x = \mathbf{x} $, $r = \mathbf{r} $
x_i, r_i	Three components of coordinates space points, $i = 1, 2, 3$
R	Nuclear radius
q	Particle charge
e	Electric charge of a proton
Q	(1) Electric quadrupole; (2) Q-value
μ	Magnetic moment
g	(1) g-factor in magnetic moment; (2) Coupling constant
\mathbf{k}, \mathbf{p}	3- dimensional momentum
k, p	Modula of 3-dimensional momentum, $k = \mathbf{k} $, $p = \mathbf{p} $
A	Nucleon number in a nucleus
Z	Proton number in a nucleus
N	(1) Neutron number in a nucleus; (2) Particle number; (3) Quantum number in harmonic oscillator
n	(1) Radial quantum number; (2) Occupation quantum number; (3) Particle number
\mathbf{E}	Electric field
\mathbf{B}	Magnetic field
\mathbf{A}	Electromagnetic vector potential
E	Energy
B	Binding energy

Exercise 1. *Unit transformation.* Shear viscosity is a measure of the resistance of a fluid when it is deformed by shear stress, often denoted as η . Entropy density is the entropy per unit volume, denoted as s . Please try to express the unit of η/s in terms of \hbar and k_B , with $\hbar=h/2\pi$ the reduced Planck constant, and k_B the Boltzmann constant. [Note: In International System of Units, the unit of η is Pascal·Second.]

Exercise 2. *Nuclear magneton.* Convert the nuclear magneton in the natural unit $\mu_N = \frac{e}{2m_p}$ to the unit of Hertz/Tesla, where e is the electric charge of the proton in unit of Coulomb, and m_p is the proton mass.

Exercise 3. *Given* $1 \text{ Volt} = \text{esuVolt} \times \frac{1}{3} \times 10^{-2}$, *calculate* $e^2/(\hbar c)$.

Chapter 2

Properties of Nuclei

The static properties such as the charge, radius, spin, magnetic moment, electric quadrupole etc. are basic properties of nuclei. The dynamic properties include the structure and decay of nuclei.

2.1 Discover atomic nucleus

The beginning of particle and nuclear physics started from Rutherford's alpha scattering experiments, which was the first experiment where a microscopic particle was shot as projectiles into another microscopic particle as target to detect the content of the target particle. This is the prototype of modern particle and nuclear physics experiments.

To quote Rutherford in his original paper, "By means of a diaphragm placed at D, a pencil of alpha particles was directed normally on to the scattering foil F. By rotating the microscope [M] the alpha particles scattered in different directions could be observed on the screen S."

To quote Rutherford, "I had observed the scattering of alpha-particles, and Dr. Geiger in my laboratory had examined it in detail. He found, in thin pieces of heavy metal, that the scattering was usually small, of the order of one degree. One day Geiger came to me and said, "Don't you think that young Marsden, whom I am training in radioactive methods, ought to begin a small research?" Now I had thought that, too, so I said, "Why not let him see if any alpha-particles can be scattered through a large angle?" I may tell you in confidence that I did not believe that they would be, since we knew the alpha-particle was a very fast, massive particle with a great deal of energy, and you could show that if the scattering was due to the accumulated effect of a number of small scatterings, the chance of an alpha-particle's being scattered backward was very small. Then I remember two or three days later Geiger coming to me in great excitement and saying "We have been able to get some of the alpha-particles coming backward . . ." It was quite the most incredible event that ever happened to me in my life. It was almost as incredible as if you fired a 15-inch shell at a piece of tissue paper and it came back and hit you."

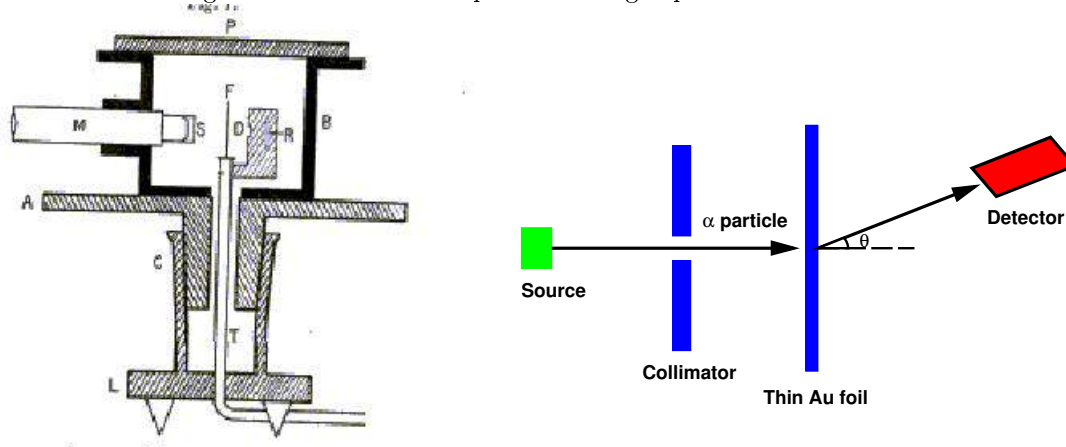
The Rutherford alpha scattering experiment proved that in the center of an atom locates its hard core called nucleus with positive charge due to the large angle scatterings.

In 1932, Chadwick found neutron by bombarding Beryllium with α particles to produce Carbon-12, ${}^4_2\text{He} + {}^9_4\text{Be} \rightarrow {}^{12}_6\text{C} + \text{n}$. He was awarded the Nobel prize later in 1935 for this discovery. Heisenberg proposed that a nucleus is made of protons and neutrons. This marked the birth of nuclear physics.

A Nucleus is labeled by ${}^A_Z X_N$ (in simple version, people also use ${}^A_Z X$ or ${}^A X$), where X is the name of the nucleus, A is the number of proton and neutrons $A = Z + N$, with Z/N the number of protons/neutrons. A nuclide is the nucleus with specific proton and neutron number. Isotope is the nuclide with the same Z but different N , isotone is that with the same N but different Z . Isobar: the same A but different Z .

The nucleus mass can be measured by mass spectrometer. Often the material is heated to produce an atomic vapor. Then the electron beam in transverse direction are used to strip the electrons out

Figure 2.1: Rutherford alpha scattering experiments.



of the atoms to make them ions. These ions are accelerated by an electric field and then pass through an area with a magnetic field exerted in upward direction perpendicular to the ion velocity. These ions are then bent in a circular motion and some finally enter the detector, see Fig. 2.4. Those ions that pass through the magnetic zone to enter the detector satisfy $qv|\mathbf{B}| = mv^2/R$, where q, v, m, R are the charge, circulating velocity, mass and radius of the circle the particle moves, respectively. Then we can get the mass from $m = qR|\mathbf{B}|/v$.

The Segre chart is the chart for nuclides in Z versus N . For light nuclei, we have $Z \sim N$, but for heavier nuclei, we have $Z < N$.

2.2 The size and density distribution of nucleus

A nucleus is a collection of protons and neutrons which can be regarded as a bulk of nuclear matter. If the nucleus is treated as a sphere, while the volume of a nucleus is proportional to the number of nucleons A , then the radius of the nucleus is in the form,

$$R = r_0 A^{1/3}, \quad (r_0 \approx 1.2 \text{ fm}) \quad (2.1)$$

We can estimate the density of a nucleus. The number and mass densities are

$$\begin{aligned} n_0 &= \frac{A}{V} \approx \frac{A}{(4/3)\pi r_0^3 A} \approx 0.138 \text{ fm}^{-3} \approx 1.38 \times 10^{38} \text{ cm}^{-3} \\ \rho_0 &= nm_N \approx 2.3 \times 10^{14} \text{ g} \cdot \text{cm}^{-3} \end{aligned} \quad (2.2)$$

Actually it is not very precise to regard the nucleus as a sphere with a uniform density. The electron scatterings tell us that a nucleus does not have a rigorous boundary but a surface with the width of 2-3 fm where the charge density gradually drops to zero. One can use the Woods-Saxon distribution (or the Fermi distribution) to describe the nuclear charge density,

$$\rho(r) = \frac{\rho_0}{1 + \exp[(r - R)/a]} \quad (2.3)$$

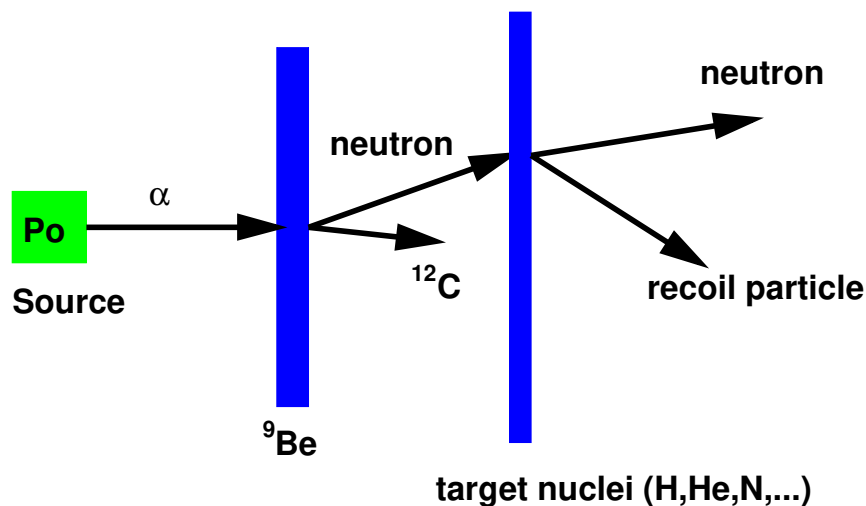
where $a \approx 0.54$ fm. The width of the surface t can be defined by the criterion that the density drops from 90% to 10% of ρ_0 ,

$$t \approx 4.4a \approx 2.4 \text{ fm} \quad (2.4)$$

One can introduce the angular dependence of the radius $R(\theta)$ to describe the non-spherical shapes of the nuclei,

$$R(\theta) = R_0[1 + \beta_2 Y_{20}(\theta) + \beta_4 Y_{40}(\theta) + \dots] \quad (2.5)$$

Figure 2.2: Chadwick found neutrons. The unknown particles carry no charges and has almost the same mass as proton.



where only even numbers l appear in spherical harmonic functions Y_{l0} .

2.3 Spin and magnetic moment

Any microscopic particles have angular momenta. If they contain charged constituents they also have magnetic moments. Here is the classical picture for magnetic moment. When a charged particle has orbital angular momentum it must have a magnetic moment. Suppose it carries a charge q and move in a circle with radius r and velocity v . Then its angular momentum is $L = mvr$. The magnetic moment is the area times the current, $\mu = \pi r^2 \frac{qv}{2\pi r} = \frac{q}{2m} L$.

Now let us consider the Maxwell equations (1.4) for magnetostatics,

$$\begin{aligned}\nabla \times \mathbf{B} &= 4\pi\mathbf{j}, \\ \nabla \cdot \mathbf{B} &= 0.\end{aligned}\tag{2.6}$$

Using $\mathbf{B} = \nabla \times \mathbf{A}$, we obtain

$$\nabla(\nabla \cdot \mathbf{A}) - \nabla^2 \mathbf{A} = 4\pi\mathbf{j}.\tag{2.7}$$

We impose Coulomb gauge condition $\nabla \cdot \mathbf{A} = 0$ and the above becomes

$$\nabla^2 \mathbf{A} = -4\pi\mathbf{j},\tag{2.8}$$

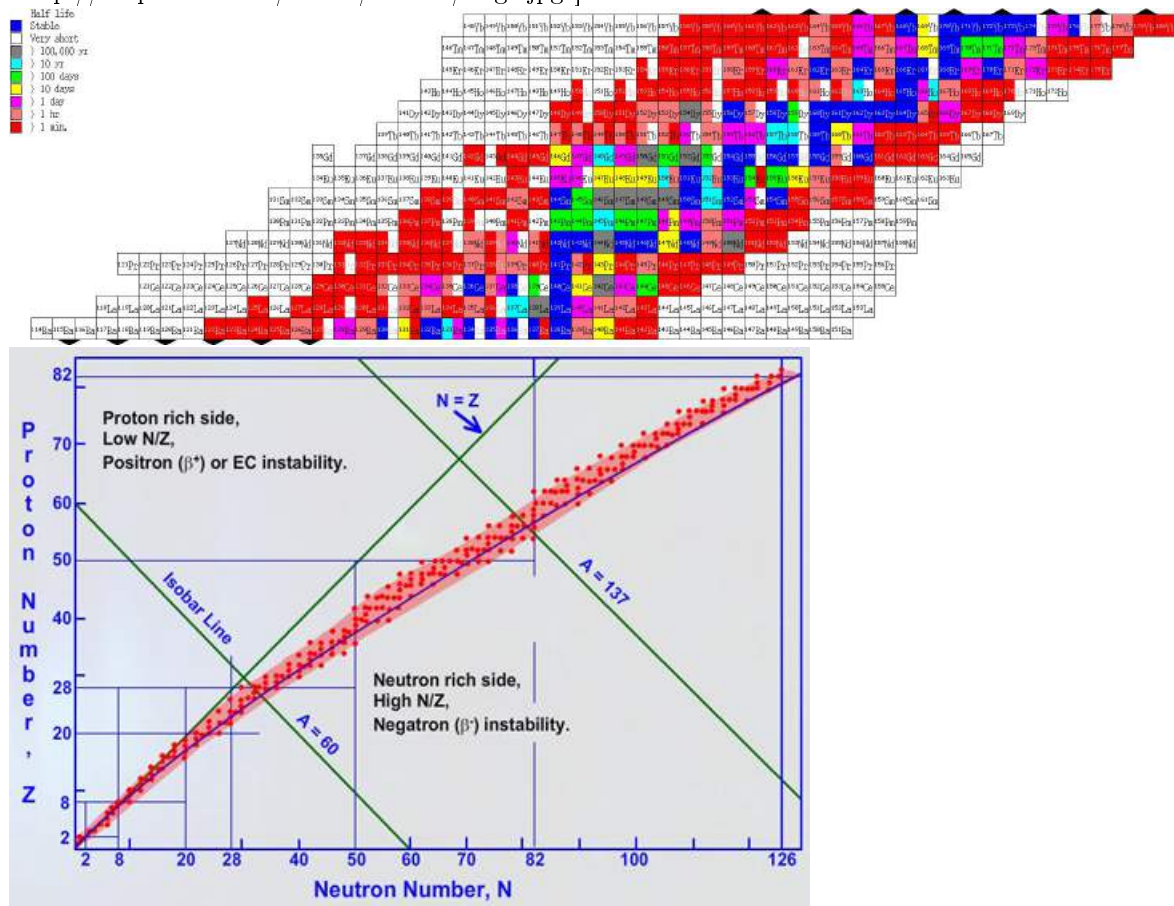
whose solution is

$$\mathbf{A}(\mathbf{r}) = \int d^3r' \frac{\mathbf{j}(\mathbf{r}')}{|\mathbf{r} - \mathbf{r}'|}\tag{2.9}$$

We can make expansion of the integrand for $r = |\mathbf{r}| \gg r' = |\mathbf{r}'|$,

$$\frac{1}{|\mathbf{r} - \mathbf{r}'|} = \frac{1}{r} - r'_i \partial_i \frac{1}{|\mathbf{r} - \mathbf{r}'|} \Big|_{r'=0} + \dots = \frac{1}{r} + r'_i \frac{r_i}{r^3} + \dots\tag{2.10}$$

Figure 2.3: Chart of Nuclide [see, e.g. “<http://atom.kaeri.re.kr/ton/nuc8.html>” and “<http://nsspi.tamu.edu/media/878612/img1.jpg>”]



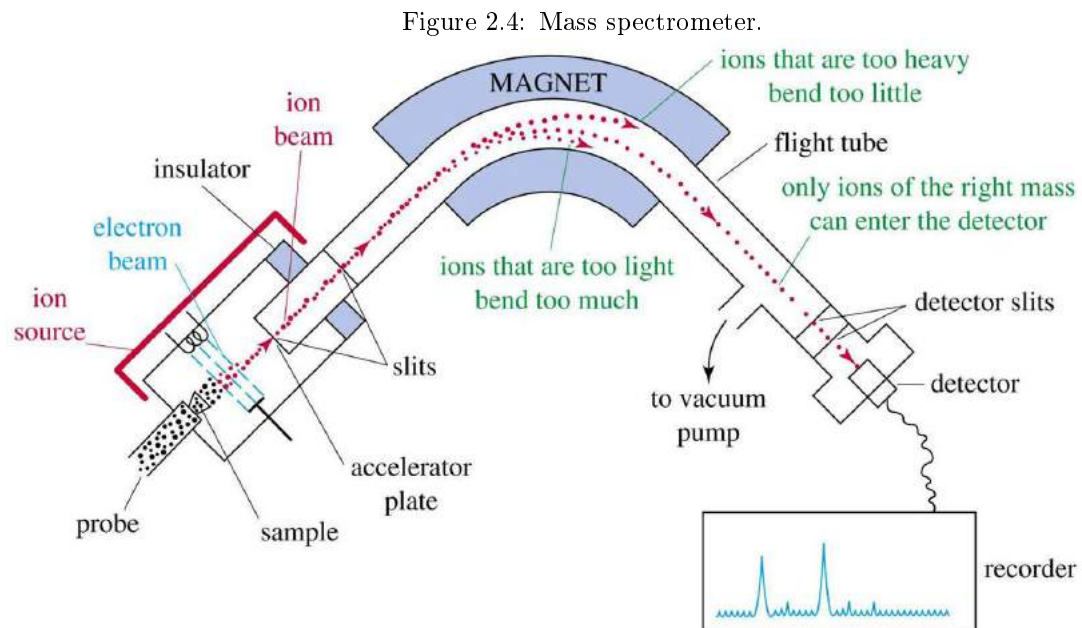


Figure 2.5: The nuclear density distribution.

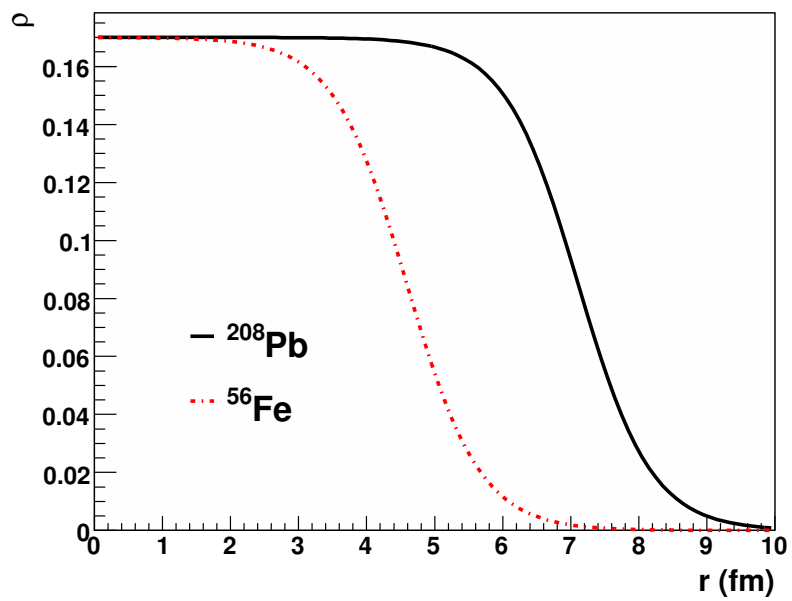
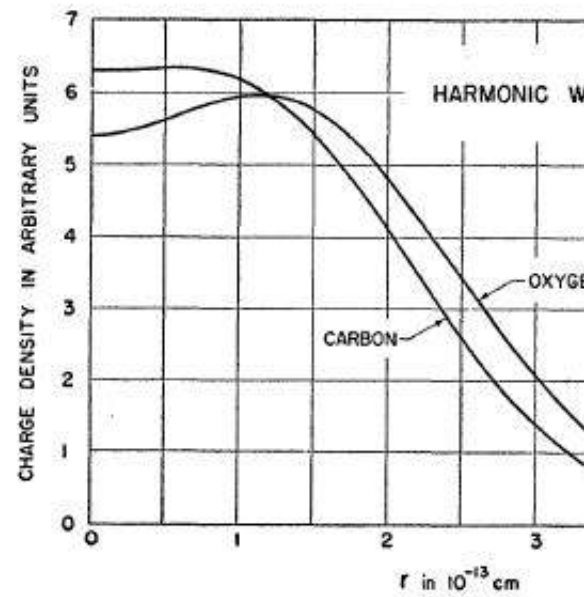
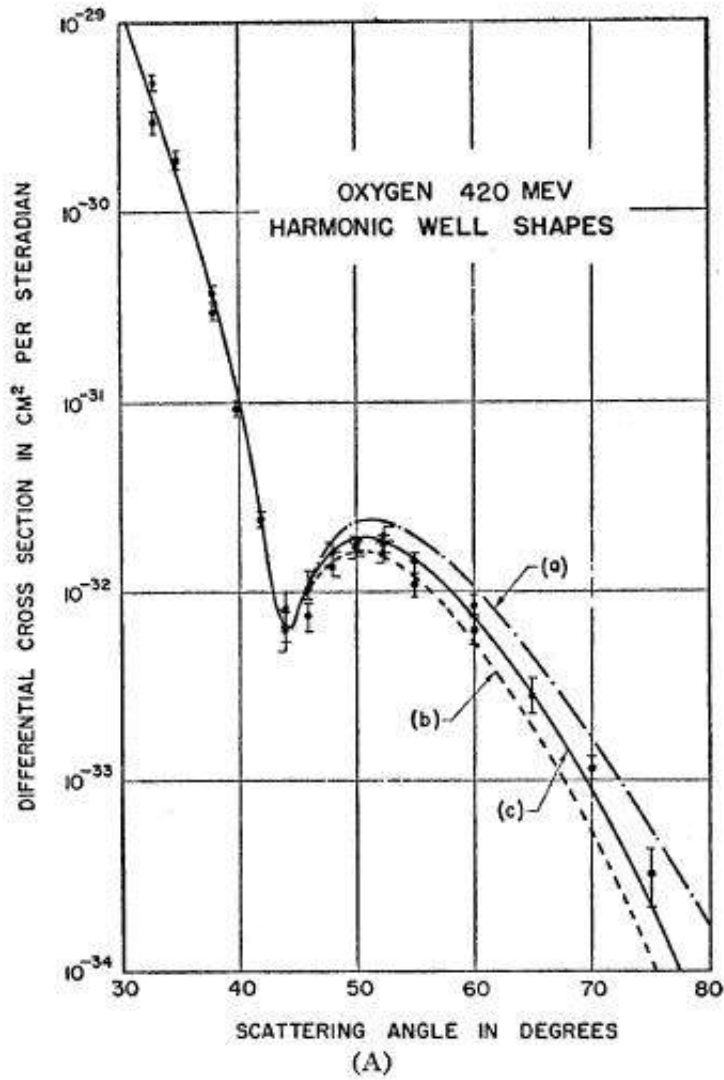


Figure 2.6: Elastic electron scattering of the charge distribution of ^{16}O , see Fig. 1(A) and Fig. 5 of Ref. [23].



Then Eq. (2.9) becomes

$$\begin{aligned}\mathbf{A}(\mathbf{r}) &= \frac{1}{r} \int d^3r' \mathbf{j}(\mathbf{r}') + \frac{r_i}{r^3} \int d^3r' r'_i \mathbf{j}(\mathbf{r}') + \dots \\ &= \frac{r_i}{r^3} \int d^3r' r'_i \mathbf{j}(\mathbf{r}') + \dots\end{aligned}\quad (2.11)$$

where the first term is vanishing $\int d^3r' \mathbf{j}(\mathbf{r}') = 0$. This can be shown by using $\nabla \cdot \mathbf{j} = 0$ and

$$\begin{aligned}0 &= \int d^3r' \nabla' \cdot (r'_i \mathbf{j}) = \int d^3r' (j_i + r'_i \nabla' \cdot \mathbf{j}) \\ &= \int d^3r' j_i\end{aligned}\quad (2.12)$$

We can also have the following identity for \mathbf{j} ,

$$\begin{aligned}0 &= \int d^3r' \nabla' \cdot (r'_i r'_k \mathbf{j}) = \int d^3r' (r'_k j_i + r'_i j_k + r'_i r'_k \nabla' \cdot \mathbf{j}) \\ &= \int d^3r' (r'_k j_i + r'_i j_k)\end{aligned}\quad (2.13)$$

Then we can re-write Eq. (2.11) as

$$\begin{aligned}\mathbf{A}(\mathbf{r}) &= -\mathbf{e}_k \frac{r_i}{2r^3} \int d^3r' [r'_k j_i(\mathbf{r}') - r'_i j_k(\mathbf{r}')] \\ &= -\mathbf{e}_k \frac{1}{2r^3} \epsilon_{kil} r_i \int d^3r' [\mathbf{r}' \times \mathbf{j}(\mathbf{r}')]_l \\ &= -\frac{1}{r^3} \mathbf{r} \times \boldsymbol{\mu}\end{aligned}\quad (2.14)$$

where the magnetic moment is defined by

$$\boldsymbol{\mu} = \frac{1}{2} \int d^3r' \mathbf{r}' \times \mathbf{j}(\mathbf{r}')\quad (2.15)$$

If we consider a system of charged particles, the current density is given by

$$\mathbf{j}(\mathbf{r}) = \sum_i q_i \mathbf{v}_i \delta(\mathbf{r} - \mathbf{r}_i)\quad (2.16)$$

where \mathbf{r}_i and \mathbf{v}_i are position and velocity of the particle i . Then the magnetic moment in Eq. (2.15) can be re-written as

$$\begin{aligned}\boldsymbol{\mu} &= \frac{1}{2m} \sum_i q_i \int d^3r' (\mathbf{r}' \times \mathbf{p}_i) \delta(\mathbf{r}' - \mathbf{r}_i) \\ &= \frac{1}{2m} \sum_i q_i \mathbf{L}_i\end{aligned}\quad (2.17)$$

where $\mathbf{L}_i = \mathbf{r}_i \times \mathbf{p}_i$ is the orbital angular momentum for the particle i .

The quantum origin of the magnetic moment can be seen as follows. When a charged particle is placed in an external magnetic field, its kinetic energy term is modified to

$$\begin{aligned}\frac{\mathbf{p}^2}{2m} &\rightarrow \frac{(\mathbf{p} - q\mathbf{A})^2}{2m} \rightarrow \frac{(-i\nabla - q\mathbf{A})^2}{2m} \\ &\rightarrow \frac{iq(\nabla \cdot \mathbf{A} + \mathbf{A} \cdot \nabla)}{2m} = \frac{iq}{m} \mathbf{A} \cdot \nabla \\ &= -\frac{iq}{2m} (\mathbf{r} \times \mathbf{B}) \cdot \nabla = \frac{iq}{2m} \mathbf{B} \cdot (\mathbf{r} \times \nabla) \\ &= -\frac{q}{2m} \mathbf{B} \cdot \mathbf{L},\end{aligned}\quad (2.18)$$

where the vector potential \mathbf{A} is related to the constant magnetic field \mathbf{B} by

$$\mathbf{A} = -\frac{1}{2}\mathbf{r} \times \mathbf{B} \quad (2.19)$$

One can verify

$$\begin{aligned} (\nabla \times \mathbf{A})_k &= -\frac{1}{2}\epsilon_{ijk}\partial_i(\mathbf{r} \times \mathbf{B})_j = -\frac{1}{2}\epsilon_{ijk}\epsilon_{l sj}\partial_i(r_l B_s) \\ &= \frac{1}{2}(\delta_{il}\delta_{ks} - \delta_{is}\delta_{kl})B_s\partial_i r_l \\ &= \frac{1}{2}B_k\partial_i r_i - \frac{1}{2}B_i\partial_i r_k = B_k \\ \nabla \cdot \mathbf{A} &= \partial_i A_i = -\frac{1}{2}\epsilon_{ijk}B_k\partial_i r_j = 0 \end{aligned} \quad (2.20)$$

One can define the orbital magnetic moment from Eq. (2.18),

$$\boldsymbol{\mu}_L = \frac{q}{2m}\mathbf{L} \quad (2.21)$$

so that the magnetic energy due to orbital angular momentum is

$$H_L = -\boldsymbol{\mu}_L \cdot \mathbf{B} \quad (2.22)$$

The spin magnetic interaction can only be derived from the Dirac equation,

$$H_S = -\boldsymbol{\mu}_S \cdot \mathbf{B} \quad (2.23)$$

where

$$\boldsymbol{\mu}_S = g\frac{q}{2m}\mathbf{S} \quad (2.24)$$

with the factor of g and the spin \mathbf{S} of the particle. We see that a non-zero spin always gives a non-zero magnetic moment. For electrons with $q = -e$, where e is the charge modula of the electron, we have $g_e = 2$ following the Dirac equation.

We know that nucleons have magnetic moments,

$$\begin{aligned} \boldsymbol{\mu}_p &= g_p\mu_N\mathbf{S}_p, \quad g_p = 5.586 \\ \boldsymbol{\mu}_n &= g_n\mu_N\mathbf{S}_n, \quad g_n = -3.82 \end{aligned} \quad (2.25)$$

where $\mu_N \equiv e/(2m_p)$ is the nuclear magneton for nucleons with the proton mass m_p , $S_p = S_n = 1/2$. The value of the nuclear magneton is,

$$\begin{aligned} \mu_N &= \frac{1/\sqrt{137}}{2 \times 938.3}\text{MeV}^{-1} = 4.55 \times 10^{-11} \frac{\text{eV}}{\text{eV}^2} \\ &\approx 4.55 \times 10^{-11} \times 1.05184 \times 10^{14} (\text{s}^{-1} \cdot \text{gauss}^{-1}) \\ &\approx 4.79 \times 10^3 \text{s}^{-1} \cdot \text{Gauss}^{-1} = 4.79 \times 10^7 \text{Hz} \cdot \text{T}^{-1}. \end{aligned} \quad (2.26)$$

Here we express eV in s^{-1} by Eq. (1.3) and eV^2 by Eq. (1.14) and then set to the natural unit. The nuclear magneton can also be expressed in $0.105 e \cdot \text{fm}$. Normally people use the maximum value of the magnetic moment for a particle in unit μ_N , for example, the magnetic moments of proton and neutron are $5.586/2 = 2.793$ and $-3.82/2 = -1.91$. Note that the magnetic moment of the neutrons has the same sign as the electrons. The non-zero magnetic moment of the neutrons indicates an inhomogeneous charge distribution. We know that a nucleon is composed of three constituent quarks, so its magnetic moment can be given by those of three quarks.

The nucleus behaves as a single entity with an angular momentum \mathbf{J}_A , which is referred to as the nuclear spin and is a vector sum of those of all constituent nucleons,

$$\mathbf{J}_A = \sum_{i=1, \dots, A} (\mathbf{L}_i + \mathbf{S}_i) \quad (2.27)$$

A nucleus has a magnetic moment which is proportional to its spin,

$$\boldsymbol{\mu}_A = g_A \mu_N \mathbf{J}_A \quad (2.28)$$

with g_A the g -factor for the nucleus. There are pairing forces in the nucleus to make two nucleons coupled so that their spins and orbital angular momenta add up to zero. So the pairing nucleons do not contribute to magnetic moments. We only need to count a few valence nucleons. This makes the magnetic moments of heavy nuclei much smaller than expected. Actually there are no nuclei whose magnetic moments exceed $6\mu_N$.

Generally for even- A (even-even and odd-odd) nuclei, nuclear spin is an integer since the angular momentum of each nucleon is a half integer and there are even number of nucleons, while for odd- A nuclei, the nuclear spin is a half-integer. If we consider the shell structure and pairings, for even-even nuclei, we have $J_A = 0$ due to spin-0 pairings of every two protons or neutrons. For even-odd nuclei, J_A is determined by the unpaired nucleon. For odd-odd nuclei, J_A is an integer and is determined by unpaired nucleons. For example, the J_A of ^{13}C and ^{13}N are $1/2$, the spin is determined by the nucleon outside the fully occupied shell. For nuclei with $A > 10$, nuclear spins come from $J \cdot J$ couplings of constituent nucleons, i.e. $\mathbf{J} = \sum_{i=1} \mathbf{J}_i$ where $\mathbf{J}_i = \mathbf{L}_i + \mathbf{S}_i$. For nuclei with $A < 10$, there are LS couplings, $\mathbf{J} = \mathbf{L} + \mathbf{S}$ where $\mathbf{L} = \sum_i \mathbf{L}_i$ and $\mathbf{S} = \sum_i \mathbf{S}_i$.

The nucleus magnetic moment can be measured by exerting an external magnetic field, the associated energy is

$$E = -\boldsymbol{\mu}_A \cdot \mathbf{B} = -g_A \mu_N M_A B \quad (2.29)$$

where $M_A = -J_A, -J_A + 1, \dots, J_A - 1, J_A$. The energy difference of the neighboring levels is

$$\Delta E = g_A \mu_N B \quad (2.30)$$

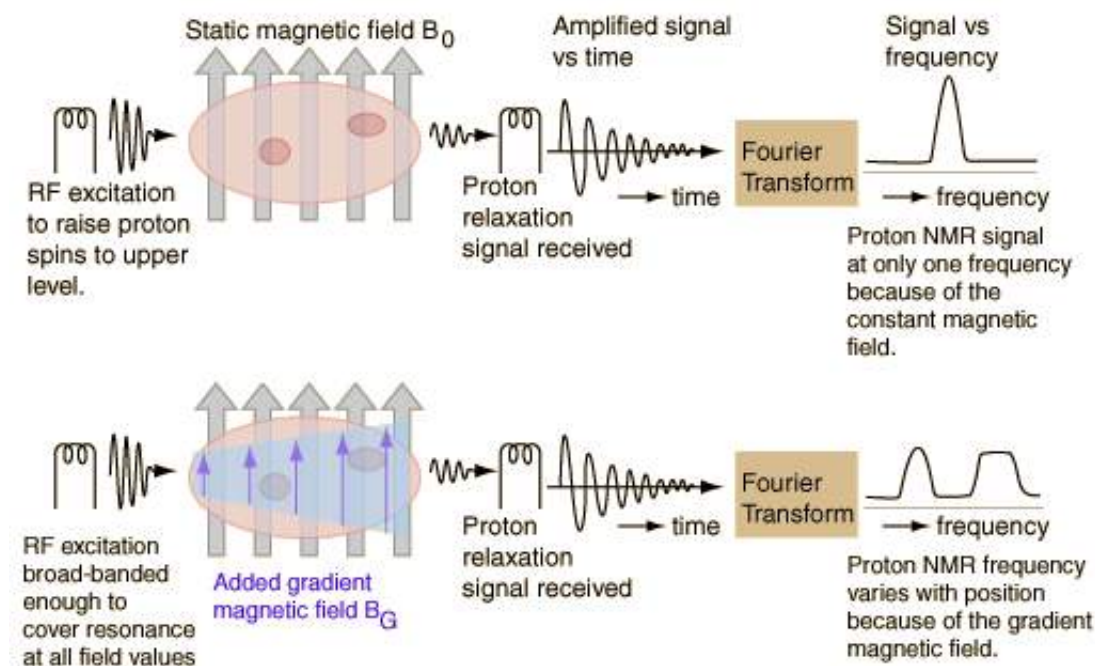
If the magnetic field oscillates with a high frequency which satisfies

$$2\pi\nu = \Delta E \quad (2.31)$$

there is a strong resonance absorption or emission. This phenomenon is called nuclear magnetic resonance (NMR), and the frequency ν is called resonance frequency. This energy is at about 60-1000 MHz in the range of VHF and UHF in television broadcasts. NMR allows the measurement of magnetic properties of atomic nuclei in molecules, crystals, and non-crystalline materials and becomes a useful tool for condensed matter physics and material sciences. There are two gradients in NMR, one is the constant magnetic field exerting on the sample to align the nuclear spin, another one is the electromagnetic pulse at radio frequency to produce perturbation of this alignment. At the NMR frequency, there are nuclei which can be excited to the higher energy level by resonance absorption and flip their spins. After the electromagnetic pulse, those nuclei on the higher energy level can jump back into the thermal state and emit photons at the same frequency. By analyzing the radiation spectrum captured, we can build up a picture of the nuclear distribution.

Use this property for protons to make image of living tissues is called magnetic resonance imaging (MRI). The MRI technology was developed in 1973. Most substance of human body is water whose molecule has two hydrogen nuclei or protons. When a constant magnetic field of the scanner is exerted onto the body, the alignment of magnetic moments of these protons in the direction of the field will take place. An oscillating electromagnetic field is then turned on at resonant frequency, and the protons will absorb or emit the electromagnetic quanta to flip their alignment relative to the field.

Figure 2.7: Nuclear magnetic resonance imaging.



When the field is switched off they go back to their original ground state or magnetization alignment in the constant magnetic field. By measuring the signal from the alignment changes people can build up an image of the body. The position of the body can be located by using gradient magnetic field so the resonant frequency depends on the position. By analyzing signals of different frequency one can know where the signals are from the body. Diseased tissue, such as tumors, can be identified from the different rates at which the tissue protons return to their equilibrium state. One can make images of different organs by the contrast between different types of body tissue.

The resonance phenomenon for protons was demonstrated in 1946 by F. Bloch and E. M. Purcell who were awarded the Nobel Prize in Physics in 1952. Further significant discovery in magnetic resonance led to two Nobel Prizes in Chemistry and one in Physiology or Medicine: R. Ernst (1991, Chemistry), K. Wüthrich (2002, Chemistry), and P. C. Lauterbur and P. Mansfield (2003, Physiology or Medicine).

Exercise 4. We know that the nuclear magneton is defined by $\mu_N = \frac{e}{2m_p}$ in natural unit, try to find its form in the cgs unit. [Hint: in accordance with the interaction energy from the magnetic moment we can determine the real unit of the nuclear magneton.]

2.4 Parity

Parity is one of the property of the wave function for a particle under spatial reversion $\mathbf{r} \rightarrow -\mathbf{r}$,

$$P\psi(\mathbf{r}) = \psi(-\mathbf{r}),$$

where P is the parity operator satisfying $P^2 = 1$. So the eigenvalue of P is either $+1$ or -1 , i.e. $P\psi(\mathbf{r}) = \pm\psi(\mathbf{r})$, corresponding to the even or odd parity. For a particle moving in a central potential,

the wave function is written in the form,

$$\psi(r, \theta, \phi) = R(r)Y_{LM}(\theta, \phi),$$

where $Y_{LM}(\theta, \phi)$ are spherical harmonics. Under spatial reversion $\theta \rightarrow \pi - \theta$ and $\phi \rightarrow \phi + \pi$, $Y_{LM}(\theta, \phi)$ transform as

$$Y_{LM}(\theta, \phi) \rightarrow Y_{LM}(\pi - \theta, \phi + \pi) = (-1)^L Y_{LM}(\theta, \phi)$$

So the parity corresponding to the orbital angular momentum is $(-1)^L$.

Now we turn to the nuclear parity. The orbital parity of a single nucleon in the central potential is $(-1)^L$. The intrinsic parity of nucleons is $+1$. Suppose a nucleon moves in the potential formed by other nucleons, we can obtain its wave function and then its parity. If we know the wave function of each nucleon we could determine the parity of the nucleus by the product of the parities of all nucleons. But in practice this is impossible. Like the nuclear spin, we regard the parity as an overall property of the nucleus. The nuclear parity can be measured by the decay products of the nucleus. We can denote the parity of a nucleus by J^P where J denotes the nuclear spin and P the parity.

2.5 Electric multipole moment

The charge distribution of any charged systems can be described by electric multipole moments. The lowest multipole moment is monopole moment, followed by the dipole and quadrupole ones. The multipole expansion is a useful tool to describe the electromagnetic field of a remote source. Now we consider electric multipole moments. Consider the electric potential from an electric source $\rho(\mathbf{r}')$,

$$\phi(\mathbf{r}) = \int d^3r' \frac{\rho(\mathbf{r}')}{|\mathbf{r} - \mathbf{r}'|} \quad (2.32)$$

which satisfies Poisson equation

$$\nabla^2 \phi(\mathbf{r}) = -4\pi\rho(\mathbf{r}) \quad (2.33)$$

because

$$\nabla^2 \frac{1}{|\mathbf{r} - \mathbf{r}'|} = -4\pi\delta(\mathbf{r} - \mathbf{r}') \quad (2.34)$$

We define $r = |\mathbf{r}|$. If $r \gg r'$, we can expand

$$\begin{aligned} \frac{1}{|\mathbf{r} - \mathbf{r}'|} &= \frac{1}{r} - r'_i \partial_i \frac{1}{|\mathbf{r} - \mathbf{r}'|} \Big|_{r'=0} + \frac{1}{2} r'_i r'_j \partial_i \partial_j \frac{1}{|\mathbf{r} - \mathbf{r}'|} \Big|_{r'=0} + \dots \\ &\approx \frac{1}{r} + r'_i \frac{r_i}{r^3} + \frac{1}{2} r'_i r'_j \frac{3r_i r_j - r^2 \delta_{ij}}{r^5} \end{aligned} \quad (2.35)$$

where we have used

$$\partial_i \frac{1}{r} = -\frac{r_i}{r^3}, \quad \partial_i \partial_j \frac{1}{r} = -\partial_j \frac{r_i}{r^3} = -r_i \partial_j \frac{1}{r^3} - \frac{1}{r^3} \partial_j r_i = \frac{3r_i r_j - r^2 \delta_{ij}}{r^5} \quad (2.36)$$

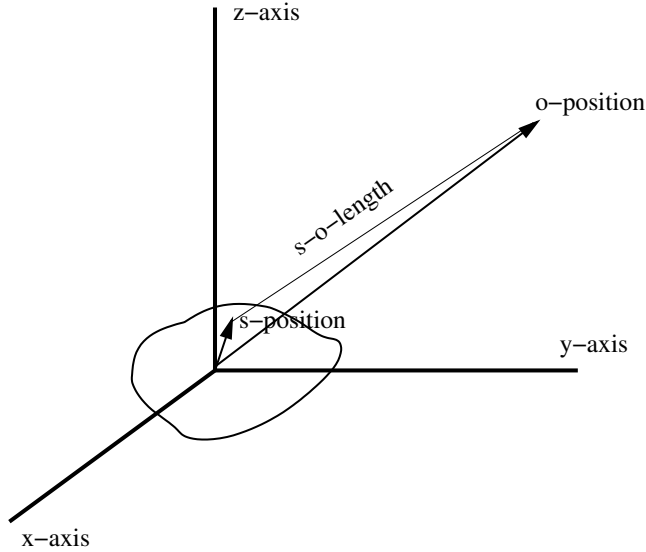
Then the potential in Eq. (2.32) becomes

$$\phi(\mathbf{r}) = \int d^3r' \frac{\rho(\mathbf{r}')}{|\mathbf{r} - \mathbf{r}'|} = \frac{Q}{r} + \frac{r_i D_i}{r^3} + \frac{1}{2} \frac{r_i r_j Q_{ij}}{r^5} \quad (2.37)$$

where

$$\begin{aligned} Q &= \int d^3r' \rho(\mathbf{r}') \\ D_i &= \int d^3r' r'_i \rho(\mathbf{r}') \\ Q_{ij} &= \int d^3r' [3r'_i r'_j - r'^2 \delta_{ij}] \rho(\mathbf{r}') \end{aligned} \quad (2.38)$$

Figure 2.8: Multipole expansion.



There is restriction on multipole moments from the symmetry of the nucleus, namely the parity of the nuclear state in quantum mechanical sense. Each electromagnetic moment has a parity depending on its property under parity transformation. The parity of the electric multipole moment is given by $(-1)^L$, the magnetic multipole moment is given by $(-1)^{L+1}$, where L is the order of the moment. In quantum mechanics, the moment can be obtained by the expectation value of moment operator \hat{O} on the nuclear wave function, $\langle \hat{O} \rangle = \int \psi^* \hat{O} \psi \sim \int \hat{O} |\psi|^2$. For electric dipole, the operator is $\hat{O} = \mathbf{r}$; for the magnetic moment, the operator is $\hat{O} = -i\mathbf{r} \times \nabla$. The parity of the wave function does not influence the result, but the parity of the moment operator does. For \hat{O} with odd parity, the integral is vanishing. So we conclude that all electric/magnetic moments of the odd/even order are vanishing. So a nucleus does not have electric dipole moment and magnetic quadrupole moment. This fact has been verified by experiments.

The next non-vanishing moment is the electric quadrupole moment. From Eq. (2.38), if the nucleus is a sphere, we can clearly see that the dipole and quadrupole moments D_i and Q_{ij} are zero. For non-vanishing electric quadrupole moments, we consider the nucleus in ellipsoid, it has rotational symmetry along z-axis, the length of the z-axis is $2c$ and the radius in xy -plane is a . The equation for the ellipsoid is:

$$\left(\frac{x}{a}\right)^2 + \left(\frac{y}{b}\right)^2 + \left(\frac{z}{c}\right)^2 \leq 1,$$

where we have $a = b$. We can parametrize the ellipsoid coordinates as $x = a\xi \sin\theta \cos\phi$, $y = a\xi \sin\theta \sin\phi$, $z = c\xi \cos\theta$, where $\xi \leq 1$. In terms of (ξ, θ, ϕ) , the volume element becomes $d^3r = dx dy dz = a^2 c d\xi d\theta d\phi \xi^2 \sin\theta$. Then the quadrupole moment is diagonal $Q_{ij} = Q_i \delta_{ij}$. Normally the quadrupole moment is defined by $Q \equiv Q_3$ and given by

$$\begin{aligned} Q &= \int d^3r (3z^2 - r^2) \rho(\mathbf{r}) = \int d^3r (2z^2 - x^2 - y^2) \rho(\mathbf{r}) \\ &= 2 \frac{Z}{V} \left(\frac{1}{5} c^2 V - \frac{1}{5} a^2 V \right) = \frac{2}{5} Z (c^2 - a^2) \end{aligned} \quad (2.39)$$

Table 2.1: Some values of nuclear electric quadrupole moments. Data from V. S. Shirley, Table of Isotopes, Wiley, New York, 1978, Appendix VII.

Nuclide	^2H	^{17}O	^{63}Co	^{63}Cu	^{133}Cs	^{161}Dy	^{176}Lu	^{209}Bi
Q(eb)	$+2.88 \times 10^{-3}$	-2.578×10^{-2}	+0.40	-0.209	-3×10^{-3}	+2.4	+8.0	-0.37

where we have used

$$\begin{aligned}
 \int d^3r z^2 &= a^2 c^3 \int_0^1 d\xi \xi^4 \int d\theta \cos^2 \theta \sin \theta \int d\phi \\
 &= \frac{4\pi}{15} a^2 c^3 = \frac{1}{5} V c^2 \\
 \int d^3r x^2 &= a^4 c \int_0^1 d\xi \xi^4 \int d\theta \sin^3 \theta \int d\phi \cos^2 \phi \\
 &= \frac{4\pi}{15} a^4 c = \frac{1}{5} V a^2
 \end{aligned} \tag{2.40}$$

Note that $Q_1 = Q_2 = -Q/2$. For spherical shape, the quadrupole moment is vanishing, $Q = 0$; for prolate or cigar-like shape, it is positive, $Q > 0$; for an oblate (discus-like) shape, it is negative, $Q < 0$. So the quadrupole part of the potential is

$$\phi_4(\mathbf{r}) \equiv \frac{1}{2} \frac{r_i r_j Q_{ij}}{r^5} = -\frac{1}{4} \frac{(x^2 + y^2 - 2z^2)Q}{r^5} \tag{2.41}$$

The deviation of the nuclear shape from a sphere is characterized by $\varepsilon \equiv \Delta R/R$ with R the radius of the sphere with the same volume as the ellipsoid, then we have $c = R(1 + \varepsilon)$ and $a = R/\sqrt{1 + \varepsilon}$ given by equating two volumes $\frac{4\pi}{3} R^3 = \frac{4\pi}{3} a^2 c$. Inserting a and c back into Q in Eq. (2.39), we get

$$Q \approx \frac{6}{5} Z R^2 \varepsilon \approx \frac{6}{5} Z r_0^2 A^{2/3} \varepsilon \tag{2.42}$$

The value of ε can be obtained by using the above formula and by measuring Q in experiments. The electric quadrupole moment can be measured by the violation of the separation rule in atomic hyperfine spectra. It can also be measured by the resonant absorption from the interaction between the nuclear electric quadrupole and electrons outside the nucleus.

Table 2.1 shows the electric quadrupole moments of some nuclides. The unit is barn which is 10^{-24} cm^2 . Usually the quadrupole moment is about one tenth of electron-barn (eb) for nuclides with $A < 150$ until it reaches about 2 for $A > 150$.

Exercise 5. *Electric quadrupole moment. Calculate the electric quadrupole moment of an ellipsoid whose long axis is $2a$ and short axis is $2b$. This ellipsoid is uniformly charged, and the total electric charge is Q . [Hint: The volume of this ellipsoid is $\frac{4}{3}\pi ab^2$.]*

Exercise 6. *From Table 2.1 and Eq. (2.42), determine ε for each nuclide.*

2.6 The mass formula and binding energy

A nucleus is a bound state of protons and neutrons. The binding energy of a nucleus is defined as

$$B(Z, A) = Zm_p + (A - Z)m_n - m(Z, A) \tag{2.43}$$

Table 2.2: The binding energies per nucleon for some nuclei. The data are taken from Ref. [28].

	${}^3_1\text{H}$	${}^4_2\text{He}$	${}^5_2\text{He}$	${}^6_3\text{Li}$	${}^7_3\text{Li}$	${}^8_4\text{Be}$	${}^9_4\text{Be}$	${}^{10}_5\text{B}$	${}^{11}_5\text{B}$	
B/A (MeV)	2.8273	7.0739	5.4811	5.3323	5.6063	7.0624	6.4628	6.4751	6.9277	
	${}^{12}_6\text{C}$	${}^{13}_6\text{C}$	${}^{14}_7\text{N}$	${}^{15}_7\text{N}$	${}^{16}_8\text{O}$	${}^{17}_8\text{O}$	${}^{18}_9\text{F}$	${}^{19}_9\text{F}$	${}^{20}_{10}\text{Ne}$	${}^{21}_{10}\text{Ne}$
B/A (MeV)	7.6801	7.4698	7.4756	7.6995	7.9762	7.7507	7.6316	7.7790	8.0322	7.9717

A nucleus can be regarded as an incompressible liquid drop which reflects the saturation property of the nuclear force. According to the liquid drop model, the binding energy can be expressed by the Weizsäcker's formula,

$$B(Z, A) = a_V A - a_S A^{2/3} - a_C Z^2 A^{-1/3} - a_{\text{sym}} I^2 A + s a_P A^{-1/2} \quad (2.44)$$

where $I = (N - Z)/A$. Here $a_V \approx 15.75$ MeV is the volume energy, $a_S \approx 17.8$ MeV the surface energy, $a_C \approx 0.71$ MeV the Coulomb energy, $a_{\text{sym}} \approx 23.3$ MeV the symmetric energy, $a_P \approx 12$ MeV the pairing energy. The sign of the surface energy is negative because the binding force of the nucleons in the surface is weakened compared to those inside the volume. The Coulomb energy comes from the static electric energy which is repulsive, so it is to decrease the binding energy. The symmetric energy is a quantum effect. For the pairing energy, the coefficient s is given by

$$s = \begin{cases} 1, & \text{even - even nuclei} \\ 0 & \text{odd A} \\ -1 & \text{odd - odd nuclei} \end{cases} \quad (2.45)$$

For the even-even nuclei are more stable because of the pairing of nucleons. See Table 2.2.

The volume energy is due to the short distance and saturation properties of nuclear force. If nuclear force is between any pair of nucleons, the volume term would be proportional to $A(A - 1)/2 \sim A^2$. The surface term is like the surface tension in liquid since a nucleus is like a liquid droplet. We know the larger the droplet's surface, the less stable the droplet is. So the surface term is to reduce the binding energy. The Coulomb term is from Coulomb energy of a charged sphere. With the constant charge density $\rho_C = \frac{Q}{V}$ where $V = \frac{4\pi}{3} R^3$ and $Q = Ze$, the electric potential inside a nucleus is

$$\phi(r) = \frac{Q}{R} + \frac{Q}{2R^3}(R^2 - r^2) \quad (2.46)$$

So the Coulomb energy is

$$E_C = \frac{1}{2} \int d^3r \rho_C \phi(r) = \frac{3}{5} \frac{Z^2 e^2}{R} \approx \frac{3e^2}{5r_0} \frac{Z^2}{A^{1/3}} \quad (2.47)$$

Therefore $a_C = \frac{3\alpha}{5r_0} \approx 0.71$ MeV with $\alpha = e^2 = 1/137 = 1.44 \text{ fm} \cdot \text{MeV}$ the fine structure constant and $r_0 \approx 1.25$ fm.

The binding energy for nuclei, Eq. (2.44), can be described by the model of the Fermi gas. We now sketch the idea of this model. We consider a potential of a cubic box,

$$V(\mathbf{x}) = \begin{cases} 0, & 0 < x_1, x_2, x_3 < L, \\ \infty, & \text{otherwise} \end{cases} \quad (2.48)$$

One particle wave function under the periodic condition at the box boundaries is

$$\psi \sim \sin(k_1 x_1) \sin(k_2 x_2) \sin(k_3 x_3)$$

where $k_i = \frac{2\pi n_i}{L}$ for $i = 1, 2, 3$ with n_i being integers. The eigen-energy is given by

$$E = \frac{1}{2m}(k_1^2 + k_2^2 + k_3^2) = \frac{1}{2m} \frac{(2\pi)^2}{L^2} (n_1^2 + n_2^2 + n_3^2)$$

An eigenstate can be denoted by a 3-integers set (n_1, n_2, n_3) . The number of states for a given energy, $E \equiv k_F^2/(2m)$ where k_F is called the Fermi momentum k_F , can be obtained by

$$\begin{aligned} n_1^2 + n_2^2 + n_3^2 &= 2mE \frac{L^2}{(2\pi)^2} = k_F^2 \frac{L^2}{(2\pi)^2} \\ \frac{N_{\text{state}}}{L^3} &= d_g \frac{4}{3} \pi k_F^3 \frac{1}{(2\pi)^3} \end{aligned} \quad (2.49)$$

where d_g is the degeneracy of each state, for a particle with spin $1/2$, we have $d_g = 2$. We see that the density of states is proportional to k_F^3 .

Now we consider a nucleus as a system of nucleons in a volume. The nucleon number density is related to the Fermi momentum k_F ,

$$\rho = \frac{A}{V} = d_g \frac{1}{(2\pi)^3} \frac{4\pi}{3} k_F^3 = \frac{d_g}{6\pi^2} k_F^3 = \frac{2}{3\pi^2} k_F^3 \quad (2.50)$$

where $d_g = 4$ is the degeneracy factor from the number of the spin states (2) and the isospin states (2). Here we treat protons and neutrons as identical particles with different isospins. From $\rho = 0.16 \text{ fm}^{-3}$, we can determine $k_F = 1.36 \text{ fm}^{-1} = 268 \text{ MeV}$. The corresponding kinetic energy is $E_F = k_F^2/(2m_N) \approx 38 \text{ MeV}$. The average kinetic energy per nucleon is then

$$\bar{E} = d_g \frac{1}{2\pi^2 \rho} \int_0^{k_F} dk k^2 \frac{k^2}{2m_N} = \frac{3}{5} E_F \approx 23 \text{ MeV} \quad (2.51)$$

When the numbers of protons and neutrons are not equal, the proton and neutron number densities are

$$\frac{Z}{V} = \frac{1}{3\pi^2} k_{F,p}^3 = \frac{1}{2} \left(\frac{k_{F,p}}{k_F} \right)^3 \frac{A}{V}, \quad \frac{N}{V} = \frac{1}{3\pi^2} k_{F,n}^3 = \frac{1}{2} \left(\frac{k_{F,n}}{k_F} \right)^3 \frac{A}{V} \quad (2.52)$$

where the degeneracy factors for protons and neutrons are the same $d_g = 2$ accounting for two spin states. Then the Fermi momenta for the protons and neutrons are given by

$$k_{F,p} = k_F \left(\frac{2Z}{A} \right)^{1/3}, \quad k_{F,n} = k_F \left(\frac{2N}{A} \right)^{1/3} \quad (2.53)$$

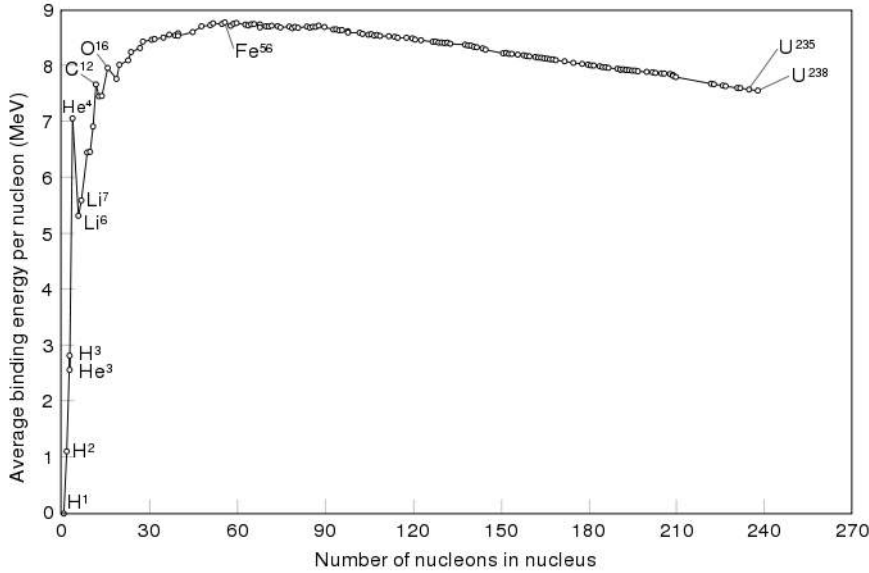
The average kinetic energies are

$$\begin{aligned} \bar{E}(I) &= \frac{1}{\pi^2 \rho} \left(\int_0^{k_{F,p}} dk k^2 \frac{k^2}{2m_N} + \int_0^{k_{F,n}} dk k^2 \frac{k^2}{2m_N} \right) \\ &= \frac{3}{10} E_F \left[\left(\frac{2Z}{A} \right)^{5/3} + \left(\frac{2N}{A} \right)^{5/3} \right] = \frac{3}{10} E_F \left[(1-I)^{5/3} + (1+I)^{5/3} \right] \\ &\approx \frac{3}{5} E_F + \frac{1}{3} E_F I^2 \end{aligned} \quad (2.54)$$

where $I = (N - Z)/A$. We can also obtain the surface energy after taking the boundary condition into account, the nucleon number element is

$$\begin{aligned} dA &= d_g \frac{L^3}{(2\pi)^3} 4\pi k^2 dk - 3d_g \frac{L^2}{(2\pi)^2} 2\pi k dk \\ &= d_g \frac{V k^2}{2\pi^2} \left(1 - \frac{\pi S}{2kV} \right) dk \end{aligned} \quad (2.55)$$

where the second term comes from three circle area corresponding to $k_1 = 0$ ($k_2^2 + k_3^2 \leq k_F^2$) or $k_2 = 0$ ($k_1^2 + k_3^2 \leq k_F^2$) or $k_3 = 0$ ($k_1^2 + k_2^2 \leq k_F^2$). Here $S = 6L^2$ and $V = L^3$ are the surface area and

Figure 2.9: The nuclear binding energy. From http://en.wikipedia.org/wiki/Nuclear_energy.

volume of the cube box with length L . Due to the wave function proportional to $\sin k_1 x \sin k_2 y \sin k_3 z$ all boundary states with $k_i = 0$ have to be excluded. The average kinetic energy is

$$\bar{E} = \frac{\int_0^{k_F} dA \frac{k^2}{2m_N}}{\int_0^{k_F} dA} = \frac{1}{2m_N} \left(\frac{V}{10\pi^2} k_F^5 - \frac{S}{16\pi} k_F^4 \right) \approx \frac{3}{5} E_F \left(1 + \frac{\pi S}{8V k_F} \right) \quad (2.56)$$

where we have treated the surface energy as a perturbation. The surface energy is then

$$E_S \approx \frac{3}{5} E_F \frac{\pi S A}{8V k_F} = E_F \frac{9\pi}{40r_0 k_F} A^{2/3} \approx 16.5 A^{2/3} \text{ MeV} \quad (2.57)$$

The nuclear binding energies of all nuclei per nucleon are shown in Fig. 2.9, which is a benchmark for how tight the nucleons are bound in nuclei. From the first three terms of the binding energy in Eq. (2.44), we can estimate the most tightly bound nuclide by looking at the extrema point of binding energy per nucleon,

$$\frac{\partial}{\partial A} \left[\frac{B(Z, A)}{A} \right] \approx \frac{\partial}{\partial A} \left(-a_S A^{-1/3} - \frac{a_C}{4} A^{2/3} \right) = 0, \quad (2.58)$$

which gives $A \approx 2a_S/a_C \approx 51$ roughly in agreement with the atomic numbers of iron or nickel. The binding energies per nucleon are largest for nuclei with mediate atomic number and reach maximum for iron nucleus ^{56}Fe . So the splitting of heavy nuclei into lighter ones or the merging of lighter nuclei into heavy ones can release substantial energy called nuclear energy by converting nuclear mass difference of initial and final state nuclei to kinetic energy, following Einstein's mass-energy formula $E = mc^2$. The splitting and merging processes are called nuclear fission and fusion respectively.

Exercise 7. The nuclear binding energy can be expressed by

$$B(Z, A) = a_V A - a_S A^{2/3} - a_C Z^2 A^{-1/3} - a_{\text{sym}} I^2 A + s_{\text{ap}} A^{-1/2}$$

where $I = (N - Z)/A$. Using the model of the fermion gas, determine the coefficients a_C , a_S and a_{sym} for Coulomb, surface and asymmetric energy respectively.

Exercise 8. Draw the binding energy per nucleon as a function of mass number as in Fig. 2.9 using data from the database NuDat2.6 of IAEA nuclear data services (<https://www-nds.iaea.org/>).

Chapter 3

Radioactivity and nuclear decay

3.1 General property of radioactivity

Unstable nuclides will undergo spontaneously decays by emitting particles. The phenomenon is called radioactivity. There two groups of elements or isotopes on the earth, one group were created by the s-process or the r-process in stars, the other group were created in the big bang earlier than 4.5 billion years ago. Most of lighter elements than lithium and beryllium belong to the first group, they are called primordial, meaning that they were created by the universe's stellar processes. All unstable nuclides are subject to a series of radioactive decays (decay chains) until they become stable. All nuclides with their half-lives less than 100 million years on the earth almost disappear by radioactive decays.

In addition to naturally occurring radioactivity, we can also produce radioactive nuclei in laboratory. The first experiment was first done by Irene Curie and Pierre Joliot in 1934. They used the α particles to bombard aluminum to produce the isotope of Phosphorus ${}_{15}^{30}\text{P}$ (Phosphorus-31 is stable) which decay through positron emission with half-life of 2.5 min. For the discovery of artificially produced radioactivity, the Joliot-Curie team won the Nobel prize in Chemistry in 1935. It is interesting to note that Pierre and Marie Curie and Becquerel was also awarded Nobel prize in physics in 1903 for their discovery of the natural radioactivity.

There are three main forms of radioactivities: (1) α decay. The nuclei emit α particles, i.e. the Helium nuclei; (2) β decay, including β^- and β^+ decay for electron and positron emissions, and electron capture (EC) where an orbital electron is captured by a nucleus; (3) γ decay and internal conversion (IC). In the γ decay, excited nuclei transits to the lower energy levels by emitting the short wave length photons. In the internal conversion, nuclei transfer energy to the orbital electrons directly.

The units for radioactivity are 1 Ci (Curie)= 3.7×10^{10} decays/s and 1 Bq(Becquerel)=1 decay/s. The SI unit for radioactivity is Bq, but Ci is widely used. The activity is not a good quantity to measure the radioactive strength for different decays. For example, how can one compares the strength of 1 μ Ci of γ decays with that of α decays? To this end, one can define the exposure X as the total electric charge Q on the ions produced by radiation in a given mass m of air, i.e. we can define $X = Q/m$. It measures the strength of the radiation in terms of its ability to ionize the atoms in the medium into which it propagates. The traditional unit of the radiation exposure is Roentgen (R), which is defined as ionization of 1 esu charge in 1 cm^3 of air at 0°C and 760 mm pressure ($m = 1.293 \times 10^{-3}\text{g}$), so we have

$$1 \text{ R} = \frac{1 \text{ esu}}{1.293 \times 10^{-3} \text{ g}} = 2.58 \times 10^{-4} \text{ C/kg} = 1.61 \times 10^{12} \text{ e} \cdot \text{g}^{-1} \quad (3.1)$$

where e is the charge (no sign) of the electron or proton, and we have used $1 \text{ C} = 3 \times 10^9 \text{ esu}$ and Eq. (1.10). From above one can see that 1 R is to produce 1.61×10^{12} electrons (ions) per gram or

Table 3.1: (a) Quality factors or weighting factors for radiations. (b) Quantities and Units for radiation.

		Radiation type	QF or WF
		β, γ	1
(a)		p,n (\sim keV)	2-5
		p,n (\sim MeV)	5-10
		α	20

Quantity	Definition	Traditional unit	SI unit
Activity	Decay rate	$3.7 \times 10^{10} \text{ s}^{-1}$, Curie (Ci)	s^{-1} , Becquerel (Bq)
(b) Exposure	Ionization in air	esu/(0.001293g), $\text{erg} \cdot \text{g}^{-1}$ Roentgen (R)	Coulomb/kg
Absorption dose	Energy absorption	$100 \text{ erg} \cdot \text{g}^{-1}$, rad	$\text{J} \cdot \text{kg}^{-1}$, Gray (Gy)
Dose equivalent	Biological effectiveness	$100 \text{ erg} \cdot \text{g}^{-1}$, rem	$\text{J} \cdot \text{kg}^{-1}$, Sievert (Sv)

2.08×10^9 electrons (ions) per cubic cm. On average, it costs about 34 eV energy to produce an ion carrying one unit electron charge in the air. So the radiation exposure of 1 R in the air is equivalent to energy absorption of $5.474 \times 10^{13} \text{ eV} \cdot \text{g}^{-1} = 88 \text{ erg} \cdot \text{g}^{-1}$.

The ionization by the γ ray depends on its energy. With about 34 eV to produce an ion in the air, 1 MeV γ ray may produce 3×10^4 ions. To describe the energy absorption, one uses the absorbed dose D defined as the energy deposited in the material by ionization. The unit for radiation absorbed dose is rad, 1 rad = 100 erg/g. For radiation in the air, we have 1 R=0.88 rad. The SI unit of the absorbed dose is Gray (Gy), defined as 1 Joule of energy absorbed in 1 kilogram of material. We have 1 Gy=1 J/kg=100 rad.

In the above quantities, we have not yet considered the radiation effects on biological systems like human body. For biological systems, the effects of the β and γ radiation are very different from that of α radiation. The energy absorption of the α particles per unit length is much more significant than that of β and γ radiation. To account for the effectiveness of radiation on biological systems, one uses quality factor (QF) or weighting factors (WF) to measure the energy absorption of a given type of the radiation per unit length. The QF of the β and γ radiation is set to 1. The QF of other types of radiation can then be determined by comparing to the β and γ radiation. The effects of radiation on biological systems depend on the quality factor and the absorption dose, so one define the dose equivalent (DE) as

$$\text{DE} = D \cdot \text{QF} \quad (3.2)$$

The unit of DE is rem (Roentgen Equivalent Man) when D is in rad. In the SI unit when the unit of D is Gray (Gy), the unit of DE is Sievert (Sv). We have 1 Sv=1 J/kg, and 1 Sv=100 rem.

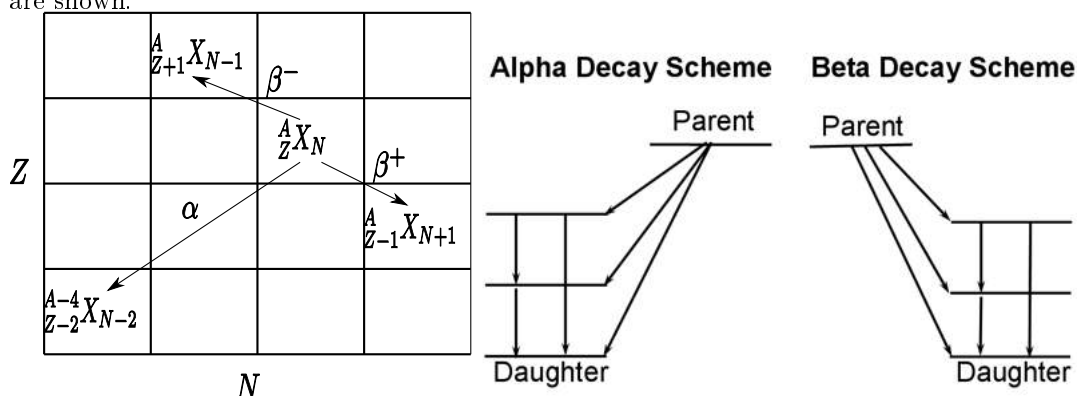
The recommended safe dose for general public should be lower than 0.5 rem = 0.005 Sv per year.

The radioactive decay follows the power law,

$$\begin{aligned} \frac{dN}{dt} &= -\lambda N \\ N(t) &= N_0 e^{-\lambda t} \\ \bar{t} &= \int dt t e^{-\lambda t} / \int dt e^{-\lambda t} = 1/\lambda \\ T_{1/2} &= \ln 2/\lambda \end{aligned} \quad (3.3)$$

where λ is the decay constant whose inverse gives the mean life \bar{t} of the nuclei, $T_{1/2}$ is the half-life which is the time when the number of nuclei reaches half of its original value. For nuclei with only one decay channel, they are identical. But for those with multiple channels they are different.

Figure 3.1: Type of nuclear decays in the nuclide chart. The scheme plots for alpha and beta decays are shown.



Normally it is very hard to measure the number of nuclei to determine λ . It is easier to measure $A(t) = \lambda N(t) = A(0)e^{-\lambda t}$ defined as the activity. One can read out λ from the plot of $\ln A(t)$ vs t . This method is workable for nuclei of half-life which is not too long or not too short. For those nuclei with very long half-lives we would not be able to observe substantial reduction of the activity. For those nuclei with very short half-lives such as $10^{-6} - 10^{-12}$ s, one has to use other precise techniques.

Usually many nuclei have more than one decay channels. Suppose there are two decay ways for a nuclide with λ_a and λ_b as decay constants respectively, the total decay rate is given by

$$\begin{aligned} \frac{dN}{dt} &= -N(\lambda_a + \lambda_b) \\ N &= N_0 e^{-(\lambda_a + \lambda_b)t} \end{aligned} \quad (3.4)$$

We note that the only observable decay constant is $\lambda_a + \lambda_b$ instead of each λ_a or λ_b alone. There is no way to turn off one and measure the other. We can generalize the above example to multi-channels cases

$$\begin{aligned} dN/dt &= -\lambda N \\ N(t) &= N_0 e^{-\lambda t} \end{aligned} \quad (3.5)$$

where $\lambda = \sum_i \lambda_i$. The branching ratio for the channel i is given by $R_i = \lambda_i/\lambda$.

Sometimes we have to deal with nuclear production, e.g. in materials bombarded by proton or neutron in reactors. The nuclei will capture a neutron or other charged particles to produce radioactive nuclear species. The rate R depends on the number of target atoms N_0 , the flux of incident particles I and the reaction cross sections σ . We assume R is very small and N_0 is a constant, which is valid for most cases in accelerators or reactors, we have

$$R = N_0 \sigma I \quad (3.6)$$

Typically I is of order $10^{14} \text{ s}^{-1} \text{ cm}^{-2}$ in reactors and the cross section is of few barns (10^{-24} cm^2), so we have $R \sim 10^{-10} N_0 \text{ s}^{-1}$, i.e only 10^{-10} of original nuclei are transmitted to radioactive nuclei. In

presence of nuclear production, the nuclear activity follows the law

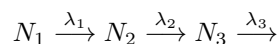
$$\begin{aligned}
 \frac{dN}{dt} &= R - \lambda N \\
 \frac{d(R - \lambda N)}{R - \lambda N} &= -\lambda dt \\
 R - \lambda N(t) &= [R - \lambda N(t_0)]e^{-\lambda t} \\
 N(t) &= \frac{1}{\lambda}R(1 - e^{-\lambda t}) + N(t_0)e^{-\lambda t} \\
 &\rightarrow \frac{1}{\lambda}R, \quad t \rightarrow \infty
 \end{aligned} \tag{3.7}$$

We can consider the case $N(t_0) = 0$, then we have

$$\begin{aligned}
 A(t) &= R(1 - e^{-\lambda t}) \\
 &\approx \begin{cases} R\lambda t, & t \ll t_{1/2} \\ R, & t \gg t_{1/2} \end{cases}
 \end{aligned} \tag{3.8}$$

We see the activity is linear in time for short time of bombardment and reach equilibrium for long time.

For subsequent decay



the decay rates are

$$\begin{aligned}
 \frac{dN_1}{dt} &= -\lambda_1 N_1 \\
 \frac{dN_2}{dt} &= \lambda_1 N_1 - \lambda_2 N_2 \\
 \frac{dN_3}{dt} &= \lambda_2 N_2 - \lambda_3 N_3
 \end{aligned} \tag{3.9}$$

A general solution to Eq. (3.9) has the form,

$$\begin{aligned}
 N_1 &= a_{11}e^{-\lambda_1 t} \\
 N_2 &= a_{21}e^{-\lambda_1 t} + a_{22}e^{-\lambda_2 t} \\
 N_3 &= a_{31}e^{-\lambda_1 t} + a_{32}e^{-\lambda_2 t} + a_{33}e^{-\lambda_3 t}
 \end{aligned} \tag{3.10}$$

The initial conditions are assumed to be

$$\begin{aligned}
 a_{11} &= N_0 \\
 a_{21} + a_{22} &= 0 \\
 a_{31} + a_{32} + a_{33} &= 0
 \end{aligned} \tag{3.11}$$

i.e. we assume that we only have A species at the initial time. Inserting the above solution into Eq. (3.9) to determin a_{ij} , the second and third lines becomes

$$\begin{aligned}
 -a_{21}\lambda_1 e^{-\lambda_1 t} &= \lambda_1 a_{11}e^{-\lambda_1 t} - a_{21}\lambda_2 e^{-\lambda_1 t} \\
 -a_{31}\lambda_1 e^{-\lambda_1 t} - a_{32}\lambda_2 e^{-\lambda_2 t} &= a_{21}\lambda_2 e^{-\lambda_1 t} + a_{22}\lambda_2 e^{-\lambda_2 t} \\
 &\quad - a_{31}\lambda_3 e^{-\lambda_1 t} - a_{32}\lambda_3 e^{-\lambda_2 t}
 \end{aligned} \tag{3.12}$$

Then we get

$$\begin{aligned}
a_{21} &= \frac{\lambda_1}{\lambda_2 - \lambda_1} a_{11} \\
a_{22} &= -a_{21} \\
a_{31} &= \frac{\lambda_2}{\lambda_3 - \lambda_1} a_{21} = \frac{\lambda_1 \lambda_2}{(\lambda_3 - \lambda_1)(\lambda_2 - \lambda_1)} a_{11} \\
a_{32} &= \frac{\lambda_2}{\lambda_3 - \lambda_2} a_{22} = \frac{\lambda_1 \lambda_2}{(\lambda_3 - \lambda_2)(\lambda_1 - \lambda_2)} a_{11} \\
a_{33} &= -a_{31} - a_{32} = \frac{\lambda_1 \lambda_2}{(\lambda_2 - \lambda_3)(\lambda_1 - \lambda_3)} a_{11}
\end{aligned} \tag{3.13}$$

Then Eq. (3.9) becomes

$$\begin{aligned}
N_1 &= N_0 e^{-\lambda_1 t} \\
N_2 &= N_0 \frac{\lambda_1}{\lambda_2 - \lambda_1} (e^{-\lambda_1 t} - e^{-\lambda_2 t}) \\
N_3 &= N_0 \frac{\lambda_1 \lambda_2}{(\lambda_3 - \lambda_1)(\lambda_2 - \lambda_1)} e^{-\lambda_1 t} + N_0 \frac{\lambda_1 \lambda_2}{(\lambda_3 - \lambda_2)(\lambda_1 - \lambda_2)} e^{-\lambda_2 t} \\
&\quad + N_0 \frac{\lambda_1 \lambda_2}{(\lambda_2 - \lambda_3)(\lambda_1 - \lambda_3)} e^{-\lambda_3 t}
\end{aligned} \tag{3.14}$$

We can generalize the above case to any number of generations,

$$N_1 \xrightarrow{\lambda_1} N_2 \xrightarrow{\lambda_2} \dots \xrightarrow{\lambda_{n-1}} N_n \xrightarrow{\lambda_n} N_{n+1} \xrightarrow{\lambda_{n+1}}$$

Assume that we already know all N_k ($k = 1, \dots, n$) which have the form

$$N_k = N_0 \lambda_1 \lambda_2 \cdots \lambda_{k-1} \sum_{i=1}^k \prod_{j \neq i}^k \frac{1}{(\lambda_j - \lambda_i)} e^{-\lambda_i t} \tag{3.15}$$

we can determine N_{n+1} by

$$\frac{dN_{n+1}}{dt} = \lambda_n N_n - \lambda_{n+1} N_{n+1} \tag{3.16}$$

We assume N_{n+1} has the following form,

$$N_{n+1}(t) = \sum_{i=1}^{n+1} a_{n+1,i} e^{-\lambda_i t} \tag{3.17}$$

Inserting the above into Eq. (3.16) we obtain

$$\begin{aligned}
-\sum_{i=1}^n a_{n+1,i} \lambda_i e^{-\lambda_i t} &= \sum_{i=1}^n (\lambda_n a_{n,i} - \lambda_{n+1} a_{n+1,i}) e^{-\lambda_i t} \\
&\rightarrow \\
-a_{n+1,i} \lambda_i &= \lambda_n a_{n,i} - \lambda_{n+1} a_{n+1,i} \\
&\rightarrow \\
a_{n+1,i} &= \frac{\lambda_n}{\lambda_{n+1} - \lambda_i} a_{n,i}, \quad i = 1, \dots, n
\end{aligned} \tag{3.18}$$

From the initial condition, $N_{n+1}(0) = 0$, we can obtain $a_{n+1,n+1}$,

$$a_{n+1,n+1} = -\sum_{i=1}^n a_{n+1,i} = N_0 \lambda_1 \lambda_2 \cdots \lambda_n \prod_{i=1}^n \frac{1}{\lambda_i - \lambda_{n+1}} \tag{3.19}$$

So we finally get

$$N_{n+1} = N_0 \lambda_1 \lambda_2 \cdots \lambda_n \sum_{i=1}^{n+1} \prod_{j \neq i}^{n+1} \frac{1}{\lambda_j - \lambda_i} e^{-\lambda_i t} \quad (3.20)$$

Assuming $\sum_{i=1}^n a_{n,i} = 0$, one can prove Eq. (3.19), this method is called mathematical induction method. The trick for the proof is to replace $a_{n,1}$ in the last line of Eq. (3.18) with $-\sum_{i=2}^n a_{n,i}$.

If we have

$$\frac{dN_1}{dt} \simeq \frac{dN_2}{dt} = \frac{dN_3}{dt} = \cdots = 0 \quad (3.21)$$

i.e. N_i ($i = 1, \dots, n$) are all constants in time, this means

$$\lambda_1 N_1 = \lambda_2 N_2 = \lambda_3 N_3 = \cdots \quad (3.22)$$

In order for N_1 to be nearly a constant in time, it is required that λ_1 is very small. Then we have a decay chain with a very long half-life isotope followed by shorter half-life isotopes as decay products. This is called secular equilibrium.

There are about 200 or so stable nuclei in the universe, all decay chains end up there. Stable nuclei have p/n ratios from 1 for light nuclei to about 0.7 for heavy nuclei like Pb. Any nuclei heavier than Pb-208 are not stable, they will lose their weight mainly through alpha decays. Neutron-rich nuclei normally adjust their high n/p ratio through beta decays. Sometime we call nuclei heavier than Pb transuranics. For transuranic nuclei, there are only four types of decay chains, represented by $A=4n$, $4n+1$, $4n+2$, $4n+3$. This is because they undergo the alpha decays in which their mass numbers change by 4 and beta decays in which their mass numbers do not change but their proton/neutron numbers increase/decrease by 1. Three of them start from long half-lives nuclei, U-238 ($4n+2$ series, 4.5 billion years), U-235 ($4n+3$ series, 700 million years) and Th-232 ($4n$ series, 14 billion years), known as natural decay chains. There are no natural decay chains of the $4n+1$ series because there are no natural nuclei with mass number of the $4n+1$ type which have longer half-lives than the earth. But artificially produced Np-237 have the decay chain of the $4n+1$ series.

Figure 3.2: The decay chain of thorium-232 (4n series). The energy released from Thorium to Pb-208 is 42.6 MeV. From wiki page about decay chain "http://en.wikipedia.org/wiki/Decay_chain".

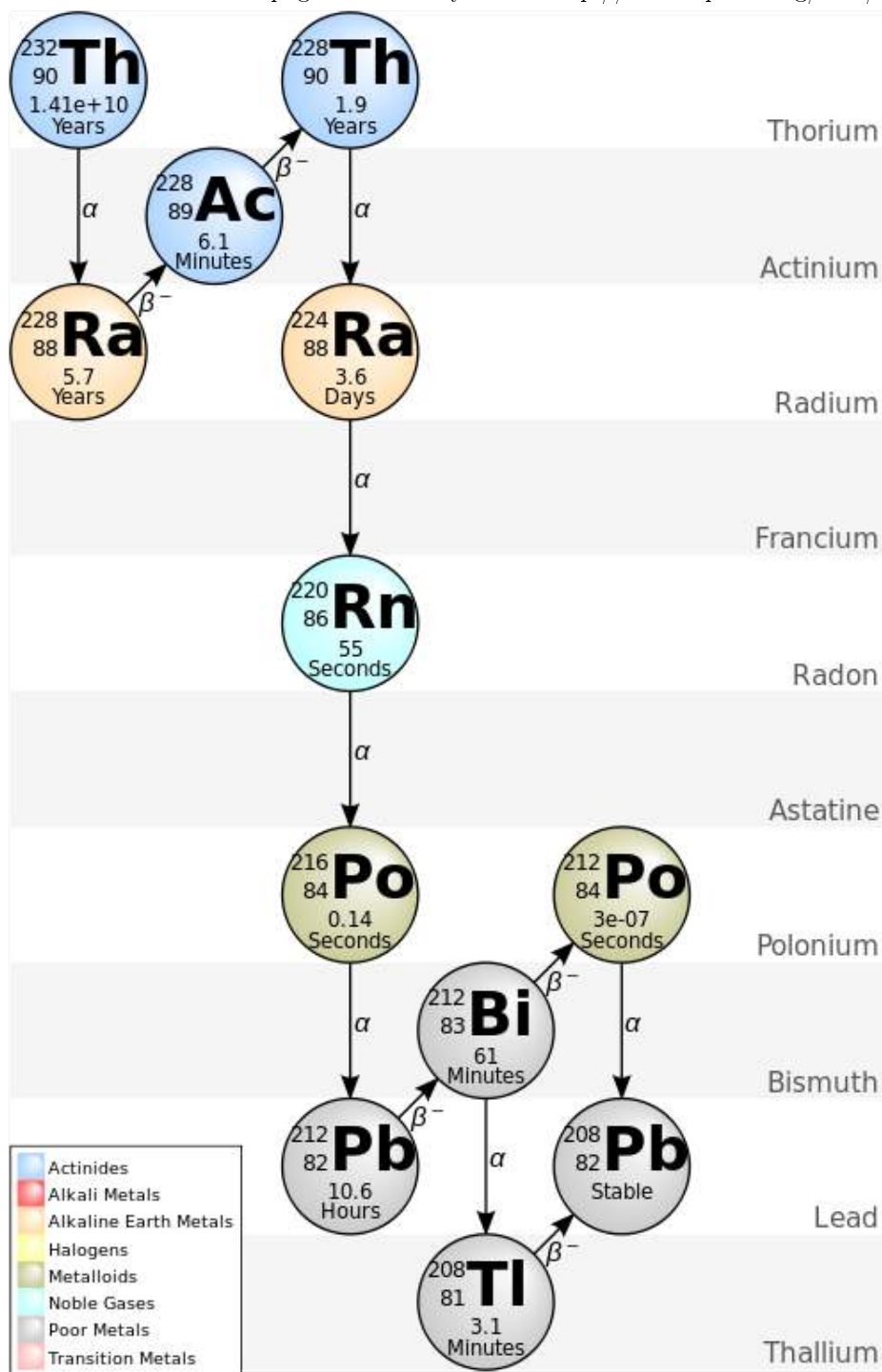


Figure 3.3: The decay chain of Uranium-238 ($4n+2$ series). The energy released from Uranium-238 to Pb-206 is 51.7 MeV. From wiki page about decay chain "http://en.wikipedia.org/wiki/Decay_chain".

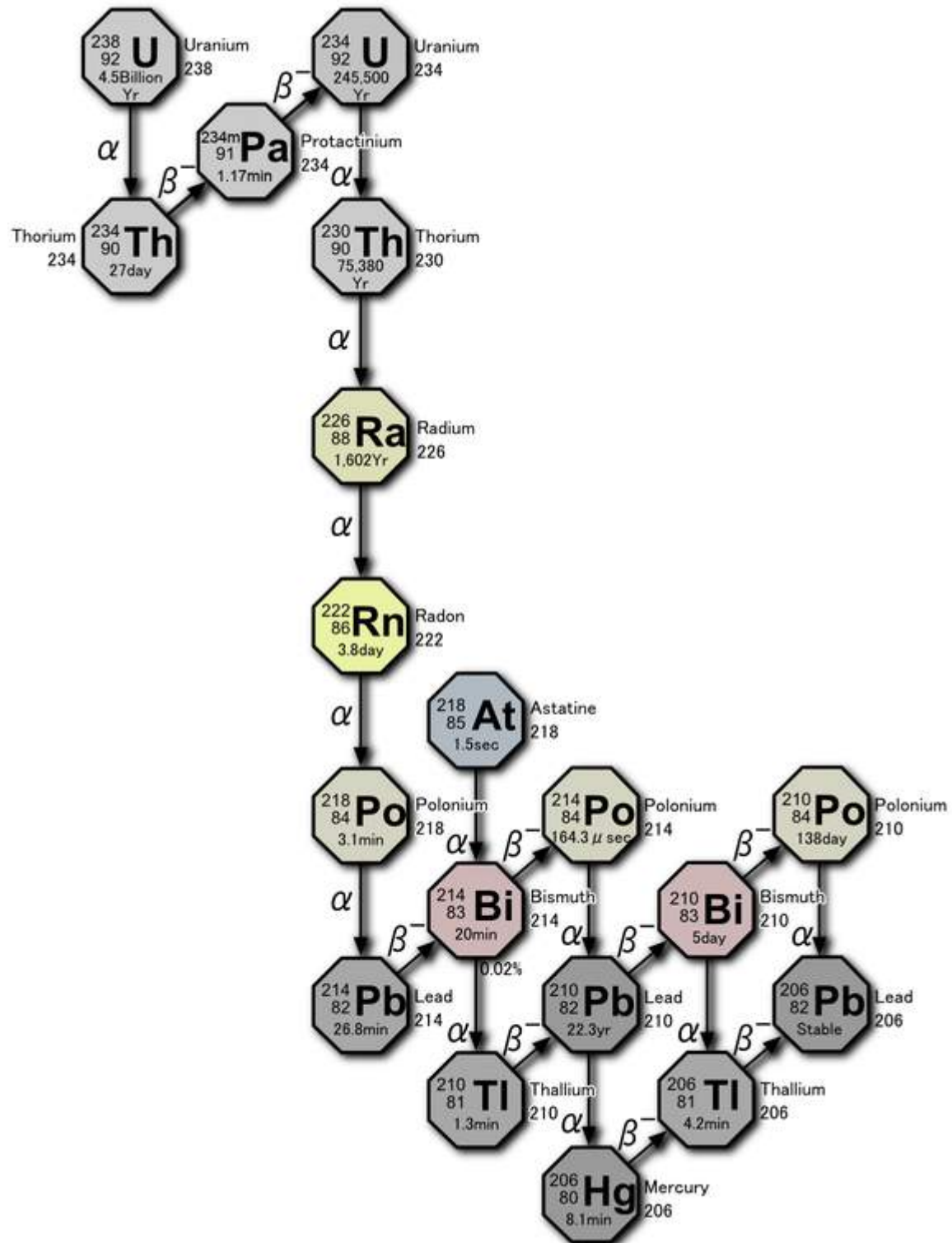
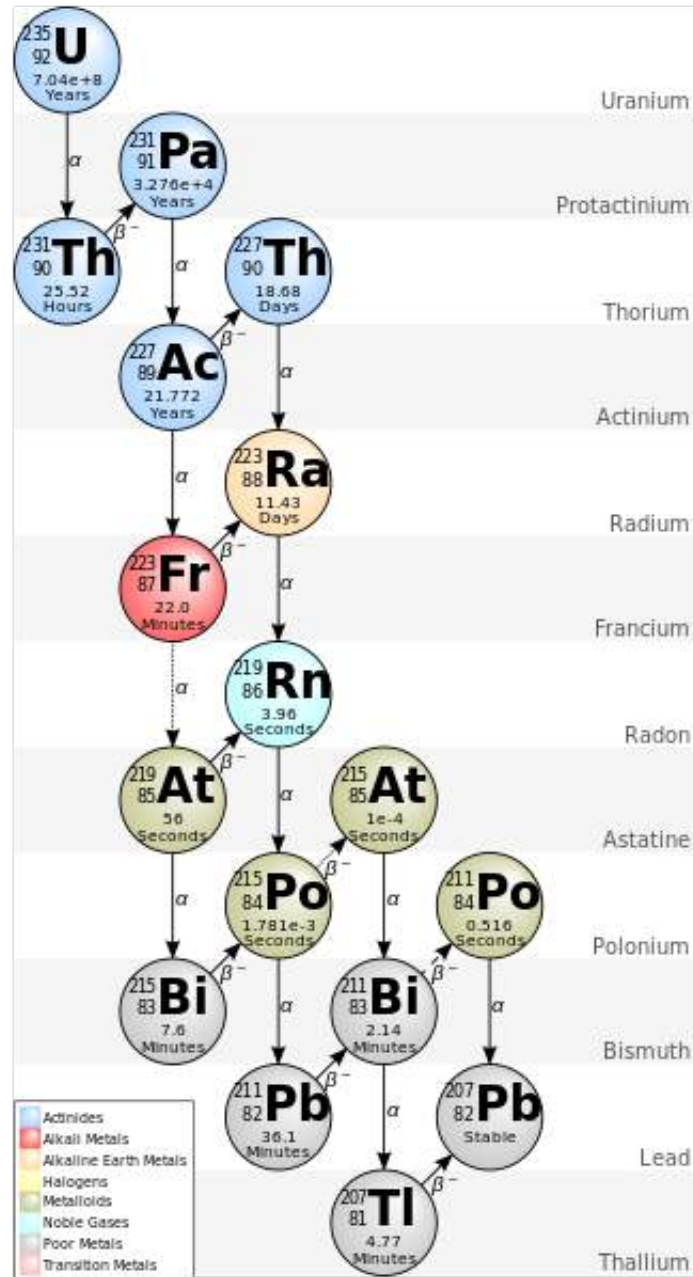


Figure 3.4: The decay chain of Uranium-235 ($4n+3$ series). The energy released from Uranium-235 to Pb-207 is 46.4 MeV. From wiki page about decay chain "http://en.wikipedia.org/wiki/Decay_chain".



Exercise 9. *The Chernobyl disaster was a well-known nuclear accident of catastrophic proportions that occurred at 1:23 a.m. on 26 April 1986, at the Chernobyl Nuclear Power Plant in Ukraine (then in the Ukrainian Soviet Socialist Republic, part of the Soviet Union). It is considered the worst nuclear power plant accident in history. The radioactive materials were released immediately into the environment as radioactive dust. The most important radioactive releases were: (i) Noble gases like radioactive isotopes of Kr and Xe in fission products. Fortunately they do little harm to human body since once inhaled they are promptly exhaled and so they do not remain in the body. (ii) ${}_{53}^{131}\text{I}$ that has 8.04 days half-life. Since it is highly volatile it is readily released. When taken into the human body by inhalation or by ingestion with food and drink, they can be transferred to the thyroid gland and cause thyroid nodules or thyroid cancers. These diseases represent a large fraction of all health effects predicted from nuclear accidents, but only a tiny fraction would be fatal. (iii) ${}_{56}^{137}\text{Cs}$ that has 30.1 years half life. It decays mostly (94.6%) by emission beta particle with maximum energy 0.512 MeV to a metastable nuclear isomer ${}_{56}^{137\text{m}}\text{Ba}$, the rest 5.4% decays to the ground state ${}_{56}^{137}\text{Ba}$. ${}_{56}^{137\text{m}}\text{Ba}$ has a half-life of about 2.55 minutes by emissions of gamma rays with energy 0.662 MeV. It does harm by being deposited on the ground where its gamma radiation continues to expose those nearby for many years. It can be picked up by plant roots and therefore get into the food chains. On May 2 of 1986, the main isotopes detected are (with activity in Bq/m³ and half life)*

Te-132	(18; 78.2 h)	Ru-103	(4.5; 39.4 d)
I-132	(10.6; 2.3 h)	Mo-99	(1.4; 6.02 h)
I-131	(8.5; 8.04 d)	Te-129	(3.5; 33.6 d)
Cs-137	(4.3; 30.1 y)	Ba-140	(2.3; 12.8 d)
Cs-134	(2.1; 2.04 y)	La-140	(2.3; 40.2 h)
Cs-136	(0.6; 13.0 d)		

(1) What is the total activity per cube meter at the time of the measurement and after 10 days? (2) Write the decay scheme plot for ${}_{56}^{137}\text{Cs}$. (3) About 0.4 tons of ${}_{53}^{131}\text{I}$ were released into the environment at the time of the accident, what's the radioactivity of ${}_{53}^{131}\text{I}$ at 11:00 a.m. on May 2 of 1986? [Hints: 1 Bq=1 decay/s]

3.2 Radioactive dating

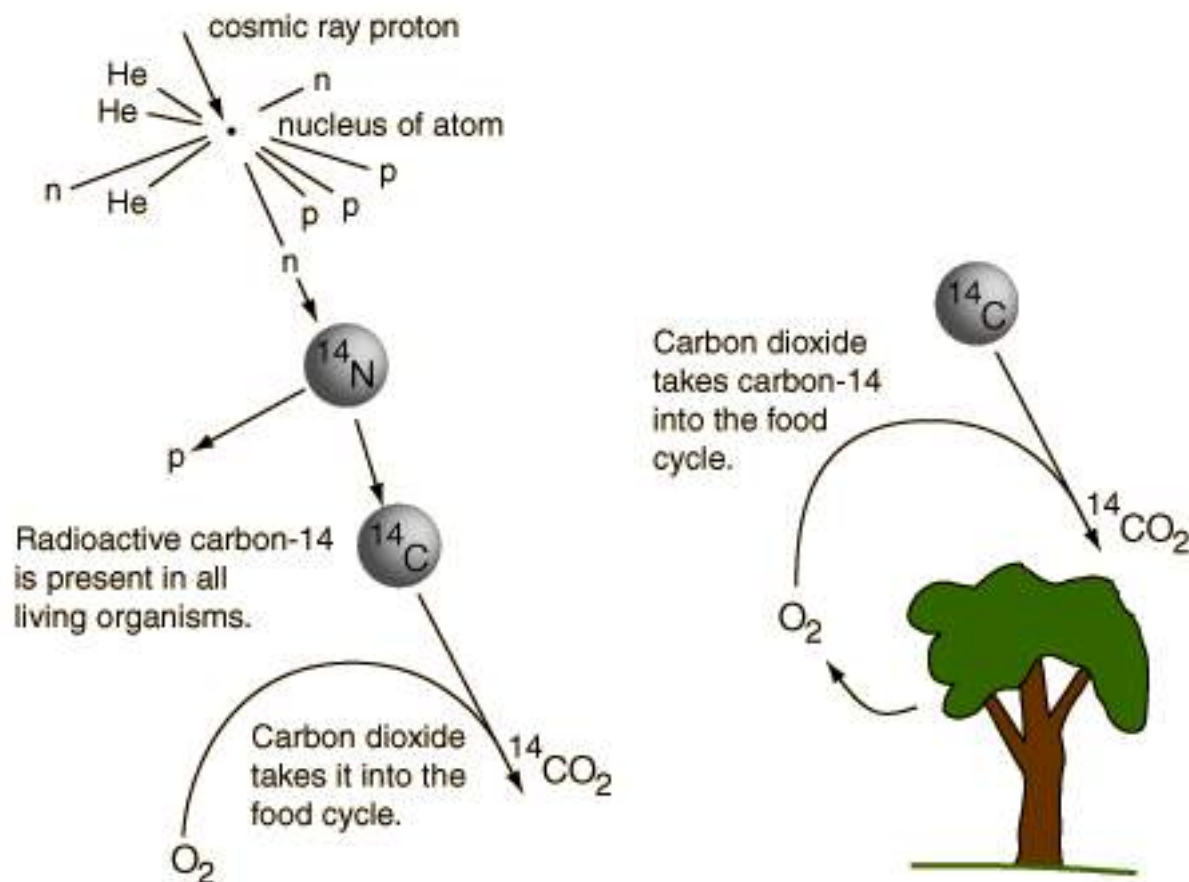
Radiocarbon dating or carbon dating is a method to determine the age of carbonaceous materials up to about 60,000 years using the radioactive isotope ${}^{14}\text{C}$. One use of carbon dating is to determine the age of organic remains from archaeological sites. The idea is as follows. Carbon has two stable isotopes ${}^{12}\text{C}$ (98.9%) and ${}^{13}\text{C}$ (1.1%) in atmosphere. There is a small portion of radioactive isotope ${}^{14}\text{C}$ in atmosphere produced by collisions of neutrons from cosmic ray and ${}^{14}\text{N}$,



All ${}^{14}\text{C}$ in atmosphere exists in the form of carbon dioxide CO_2 . The production rate of ${}^{14}\text{C}$ can be approximated as almost constant for thousands of years assuming that the flux of the cosmic ray does not vary much with time. The plants absorb ${}^{14}\text{C}$ by photosynthesis. The abundance of ${}^{14}\text{C}$ in living plants maintains the same level as in atmosphere. When plants die or eaten by animals or humans the density of ${}^{14}\text{C}$ will not be in equilibrium with atmosphere but will decrease by decay. By measuring the current amount of ${}^{14}\text{C}$ and comparing with that in atmosphere one can determine the age of plants, animals or humans after they die.

The decay channel of ${}^{14}\text{C}$ is β -decay, ${}^{14}\text{C} \rightarrow {}_7^{14}\text{N} + \text{e}^- + \bar{\nu}_e$, with half-life $T_{1/2} = 5730 \pm 40$ years. There is one atom of ${}^{14}\text{C}$ for 10^{12} atoms of ${}^{12}\text{C}$. We know that 1 g of carbon has about $N_A/12 \approx 5 \times 10^{22}$ atoms of ${}^{12}\text{C}$ and 5×10^{10} atoms of ${}^{14}\text{C}$, the radioactivity of ${}^{14}\text{C}$ is estimated as $5 \times 10^{10} \times \ln 2/T_{1/2} \approx 11.5$ decays per minute. The atomic composition (mass composition) of

Figure 3.5: Production of Carbon-14 in atmosphere.



carbon in a human body is about 12% (18%). Suppose a human has a weight of 60 kg, then he/she has about 9×10^{-10} mol of ^{14}C in the body. So there are about $5.4 \times 10^{14} \times \ln 2/T_{1/2} \approx 2.06 \times 10^3$ decays of ^{14}C in a second.

The carbon dating technique was developed by W. Libby and his colleagues at the University of Chicago in 1949. The concept was first suggested by E. Fermi in a seminar at University of Chicago, according to E. Segre. Libby was awarded Nobel prize in chemistry in 1960.

Exercise 10. Read the article and write a report: [C. B. Ramsey, "Radiocarbon Dating: Revolutions in Understanding", *Archaeometry* 50(2), 249-275(2008).]

3.3 α decay: strong interaction at work

Rutherford showed in his experiments in 1903 and 1909 that the α particles are actually Helium nuclei. The α decay is one of the most important decays for heavy nuclei. Especially the decay chains of naturally occurring nuclei involve only the α decay from strong interaction. The binding energy per nucleon for a Helium-4 nucleus or an α particle is much larger than its neighbors (much more stable), so it should be present in the heavy nuclear as clusters. In the binding energy formula of nuclei, the

Coulomb term behaves as $A^{5/3}$ while the volume term does as A . So for heavy nuclei, the Coulomb repulsion effects increase rapidly and match or even exceed the volume effects. This makes the nuclei unstable against cluster emission. The α decay is the most frequently occurring cluster decay.

The α -particles carry positive charges, so they can be measured by the spectrometer. The results show that there is fine structure in the energy spectra of the α -particles. They consist of some discrete peaks indicating that the energies are almost discrete.

The α decay can be written as



Here X is the mother nucleus with the mass m_X and Y the daughter particle with the mass m_Y . The mass of the α -particle is m_α . Their velocities are denoted v_X , v_Y and v_α . For the decay to take place, the following decay energy must be satisfied:

$$\begin{aligned} E_0 &= B(Z-2, A-4) + B(2, 4) - B(Z, A) \\ &= m_X - m_Y - m_\alpha \\ &= (M_X - Zm_e) - [M_Y - (Z-2)m_e] - (M_{\text{He}} - 2m_e) \\ &= M_X - M_Y - M_{\text{He}} > 0 \end{aligned} \quad (3.25)$$

The decay energy can also be expressed in terms of binding energies

$$\begin{aligned} E_0 &\approx -2\frac{\partial B}{\partial Z} - 4\frac{\partial B}{\partial A} + B(2, 4) \\ &\approx 4a_C Z A^{-1/3} - 4(a_V - \frac{2}{3}a_S A^{-1/3} + \frac{1}{3}a_C Z^2 A^{-4/3}) + 7.074 \times 4 \\ &\approx 4a_C Z A^{-1/3} - \frac{4}{3}a_C Z^2 A^{-4/3} + \frac{8}{3}a_S A^{-1/3} - 4a_V + 28.3 \\ &\approx \frac{5}{3}a_C A^{2/3} + \frac{8}{3}a_S A^{-1/3} - 4a_V + 28.3 \end{aligned} \quad (3.26)$$

Inserting Eq. (2.44) into the above (we keep only the first three terms), we can get the decay energy as a function of Z and A . We see that only when $A > 100$ is the positive decay energy possible. In reality we have the positive decay energy when $A > 140$.

The momentum conservation leads to

$$v_Y = v_\alpha \frac{m_\alpha}{m_Y} \quad (3.27)$$

The energy conservation is

$$\begin{aligned} E_0 &= \frac{1}{2}m_\alpha v_\alpha^2 + \frac{1}{2}m_Y v_Y^2 = E_\alpha \left(1 + \frac{m_\alpha}{m_Y}\right) \\ &\approx E_\alpha \frac{A}{A-4} \end{aligned} \quad (3.28)$$

where E_α is the kinetic energy of the α -particle. The kinetic energy is related to the decay energy

$$E_\alpha = \frac{A-4}{A} E_0 \quad (3.29)$$

If A is very large, the kinetic energy is almost the decay one.

For example, the followings decay of polonium isotopes

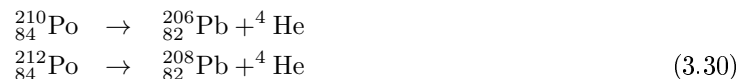
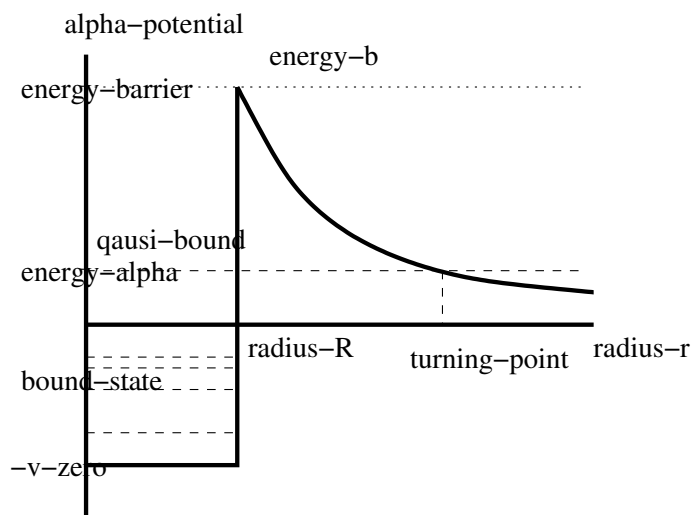


Table 3.2: Comparison the Q-value of $^{210}_{84}\text{Po}$ (209.9829 u) in different reaction channels. The unit is MeV.

$^{209}_{84}\text{Po} + n$ (208.9824, 1.00867) u	-7.6	$^{205}_{82}\text{Pb} + ^5\text{He}$ (204.9745, 5.01222) u	-3.5
$^{209}_{83}\text{Bi} + ^1\text{H}$ (208.9804, 1.00783) u	-4.96	$^{204}_{82}\text{Pb} + ^6\text{He}$ (203.9730, 6.01889) u	-8.3
$^{208}_{83}\text{Bi} + ^2\text{H}$ (207.9797, 2.01410) u	-10.15	$^{204}_{81}\text{Tl} + ^6\text{Li}$ (203.9739, 6.01512) u	-5.7
$^{207}_{83}\text{Bi} + ^3\text{H}$ (206.9785, 3.01605) u	-10.85	$^{203}_{81}\text{Tl} + ^7\text{Li}$ (202.9723, 7.016) u	-5.03
$^{206}_{82}\text{Pb} + ^4\text{He}$ (205.9745, 4.0026) u	5.4		

Figure 3.6: The potential for the α particles.

can happen. We can check

$$\begin{aligned}
 M(^{210}\text{Po}) &= 209.9829 \text{ u} \\
 M(^{212}\text{Po}) &= 211.9889 \text{ u} \\
 M(^{206}\text{Pb}) &= 205.9745 \text{ u} \\
 M(^{208}\text{Pb}) &= 207.9766 \text{ u} \\
 M(^4\text{He}) &= 4.0026 \text{ u}
 \end{aligned} \tag{3.31}$$

where $1 \text{ u} = 931.494027 \text{ MeV}$ is the atomic mass unit, for example, the deuteron has 2.014 u. Then the decay energies are

$$\begin{aligned}
 E_0 &= 209.9829 - 205.9745 - 4.0026 = 0.0058 \text{ u} \\
 &\approx 5.4 \text{ MeV for } ^{210}\text{Po} \\
 E_0 &= 211.9889 - 207.9766 - 4.0026 = 0.0097 \text{ u} \\
 &\approx 9.03 \text{ MeV for } ^{212}\text{Po}
 \end{aligned} \tag{3.32}$$

All these masses can be found in NuDat at IAEA nuclear data services.

Before we deal with the α decay problem. We review the tunneling effect in quantum mechanics. Suppose we have a potential $V(r)$ which has only radial dependence. In spherical coordinates, the

Hamiltonian reads,

$$\begin{aligned}
 \hat{H} &= -(1/2m)\nabla^2 + V \\
 &= -\frac{1}{2m} \left[\frac{1}{r^2} \frac{\partial}{\partial r} \left(r^2 \frac{\partial}{\partial r} \right) + \frac{1}{r^2 \sin \theta} \frac{\partial}{\partial \theta} \left(\sin \theta \frac{\partial}{\partial \theta} \right) + \frac{1}{r^2 \sin^2 \theta} \frac{\partial^2}{\partial \phi^2} \right] + V(r) \\
 &= -\frac{1}{2m} \left[\frac{1}{r^2} \frac{\partial}{\partial r} \left(r^2 \frac{\partial}{\partial r} \right) - \frac{L^2}{r^2} \right] + V(r)
 \end{aligned} \tag{3.33}$$

with \hat{L}^2 given by

$$\hat{L}^2 = - \left[\frac{1}{\sin \theta} \frac{\partial}{\partial \theta} \left(\sin \theta \frac{\partial}{\partial \theta} \right) + \frac{1}{\sin^2 \theta} \frac{\partial^2}{\partial \phi^2} \right] \tag{3.34}$$

whose eigenfunctions are spherical harmonics $Y_{lm}(\theta, \phi)$ which satisfies

$$\hat{L}^2 Y_{LM}(\theta, \phi) = L(L+1) Y_{LM}(\theta, \phi)$$

One can verify

$$[\hat{H}, \hat{L}^2] = [\hat{H}, \hat{L}_z] = 0 \tag{3.35}$$

Because the operators $\{\hat{H}, \hat{L}^2, \hat{L}_z\}$ all commute to each other, the state can be labeled by quantum numbers $\{n, L, M\}$, where n labels the energy level, L the angular momentum, M the projection to the third axis. The wave function can be expanded by

$$\psi(k, \mathbf{r}) = \sum_{L=0}^{\infty} \sum_{M=-L}^{+L} c_{LM}(k) R_{LM}(k, r) Y_{LM}(\theta, \phi) \tag{3.36}$$

The Schrödinger equation is

$$\hat{H}\psi = E\psi \tag{3.37}$$

whose radial part reads

$$-\frac{1}{2m} \left[\frac{1}{r^2} \frac{\partial}{\partial r} \left(r^2 \frac{\partial}{\partial r} \right) - \frac{L(L+1)}{r^2} \right] R_L(k, r) + V(r) R_L(k, r) = E R_L(k, r) \tag{3.38}$$

There is no dependence on the magnetic quantum number M , so $R_{LM}(k, r)$ is written as $R_L(k, r)$. The above equation can be written as

$$\left[\frac{d^2}{dr^2} + \frac{2}{r} \frac{d}{dr} + k^2 - \frac{L(L+1)}{r^2} - U(r) \right] R_L(k, r) = 0 \tag{3.39}$$

where $U(r) = 2mV(r)$. It is convenient to use

$$R_L(k, r) = \frac{u_L(k, r)}{r} \tag{3.40}$$

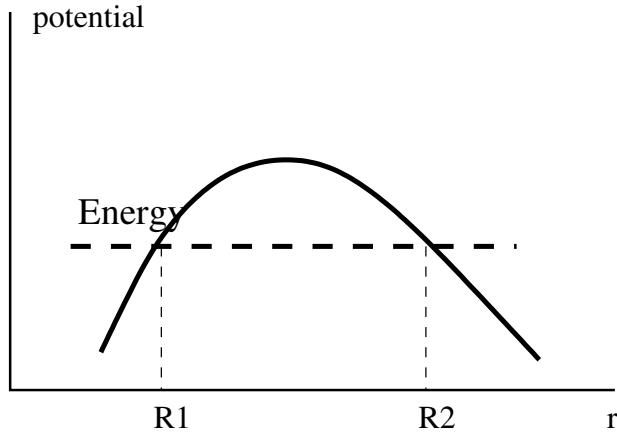
to rewrite Eq. (3.39),

$$\left[\frac{d^2}{dr^2} + k^2 - \frac{L(L+1)}{r^2} - U(r) \right] u_L(k, r) = 0 \tag{3.41}$$

If we consider the most simple case, $l = 0$, the above equation becomes similar to one dimensional Schrödinger equation,

$$\left[\frac{d^2}{dr^2} + k^2 - U(r) \right] u_0(k, r) = 0 \tag{3.42}$$

Figure 3.7: Potential barrier.



For simplicity of notation, we will suppress the subscript $u_0(k, r) \rightarrow u(k, r)$.

We consider a particle with energy $E = k^2/2m$ moving toward a potential barrier $U(r)$, see Fig. 3.7. We denote the regions bounded by the classical turning points, $r < R_1$, $R_1 < r < R_2$, and $R > R_2$, as I, II and III respectively. The regions I and III are classical allowed regions and the region II is the classical forbidden region. The corresponding wave functions are denoted as $u_1(k, r)$, $u_2(k, r)$ and $u_3(k, r)$, they satisfy the continuity conditions,

$$\begin{aligned} u_1(k, R_1) &= u_2(k, R_1) \\ u_1'(k, R_1) &= u_2'(k, R_1) \\ u_2(k, R_2) &= u_3(k, R_2) \\ u_2'(k, R_2) &= u_3'(k, R_2) \end{aligned} \quad (3.43)$$

Remember that we have suppressed the factor \hbar^2 in front of the second order differential operator ∇^2 in the Schrödinger equation since we use the natural unit. We can use the Wenzel-Kramers-Brillouin (WKB) method to solve the one dimensional Schrödinger equation (3.41, 3.42). In the WKB method, one assumes that the wave function has the following form,

$$u(k, r) = \exp \left[\frac{i}{\hbar} S(r) \right] \quad (3.44)$$

Substitute the above into Eq. (3.42) and make expansion of the equation in powers of the Planck constant \hbar or in the number of spatial derivatives, we can solve $S(x)$ or the wave function order by order. We assume $S(r)$ can be expanded as

$$S(r) = S_0(r) + (-i\hbar)S_1(r) + (-i\hbar)^2 S_2(r) + \dots \quad (3.45)$$

Inserting Eq. (3.44) into Eq. (3.42), we derive

$$\begin{aligned} 0 &= \left[\hbar^2 \frac{d^2}{dr^2} + k^2 - U(r) \right] u(k, r) \\ &= i\hbar S''(r) \exp \left[\frac{i}{\hbar} S(r) \right] - [S'(r)]^2 \exp \left[\frac{i}{\hbar} S(r) \right] \\ &\quad + [k^2 - U(r)] \exp \left[\frac{i}{\hbar} S(r) \right] \end{aligned} \quad (3.46)$$

Using Eq. (3.45), up to $O(\hbar)$ we obtain

$$\begin{aligned} [S_0'(r)]^2 &= k^2 - U(r) \\ S_0'' + 2S_0' S_1' &= 0 \end{aligned} \quad (3.47)$$

Then we can solve

$$\begin{aligned}
 S_0 &= \pm \int dr \sqrt{k^2 - U(r)} \\
 S'_1 &= -\frac{1}{2} [\ln S'_0(r)]' \\
 &\rightarrow \\
 S_1 &= \ln[k^2 - U(r)]^{-1/4}
 \end{aligned} \tag{3.48}$$

Let's define a new variable $\tilde{k} \equiv \sqrt{k^2 - U(r)}$. So the wave function has the form (we resume the use of natural unit),

$$u(k, r) = \exp[iS(r)] = \frac{1}{\sqrt{\tilde{k}}} \exp\left(\pm i \int_{r_0}^r dr \tilde{k}\right) \tag{3.49}$$

For the classically allowed region, i.e. $k^2 > U(r)$ or \tilde{k} is real, the general form of the wave function is

$$\begin{aligned}
 u(k, r) &= \frac{C_1}{\sqrt{\tilde{k}}} \exp\left(i \int_{r_0}^r dr \tilde{k}\right) + \frac{C_2}{\sqrt{\tilde{k}}} \exp\left(-i \int_{r_0}^r dr \tilde{k}\right) \\
 &= \frac{C'_1}{\sqrt{\tilde{k}}} \sin\left(\int_{r_0}^r dr \tilde{k} + C'_2\right)
 \end{aligned} \tag{3.50}$$

where $C_{1,2}$ and $C'_{1,2}$ are constants to be determined by the boundary and normalization condition. For the classically forbidden region, i.e. $k^2 < U(r)$, \tilde{k} in Eq. (3.49) is purely imaginary, so the wave function has the following form,

$$u(k, r) = \frac{C_1}{\sqrt{|\tilde{k}|}} \exp\left(-\int_{r_0}^r dr |\tilde{k}|\right) + \frac{C_2}{\sqrt{|\tilde{k}|}} \exp\left(\int_{r_0}^r dr |\tilde{k}|\right) \tag{3.51}$$

where $C_{1,2}$ are constants to be determined by the boundary and normalization condition. One can observe that the solution in the classically allowed region is oscillating while that in the forbidden region is exponential. Note that at classical turning points, the points at which $k^2 = U(r)$, the WKB solutions in Eqs. (3.50,3.51) are not valid since they are divergent.

Now we consider the boundary at $r = R_1$ with the classically allowed region in the left-side and the classically forbidden region in the right-side. The wave functions in the both sides have following correspondence,

$$\begin{aligned}
 \frac{2}{\sqrt{\tilde{k}}} \sin\left(\int_r^{R_1} dr \tilde{k} + \frac{\pi}{4}\right) &\iff \frac{1}{\sqrt{|\tilde{k}|}} \exp\left(-\int_{R_1}^r dr |\tilde{k}|\right) \\
 r < R_1 & \quad r > R_1
 \end{aligned} \tag{3.52}$$

Note that the wave function in the left-side is the superposition of an incident and reflection wave with equal amplitude (we assume the loss from transmission is small),

$$\begin{aligned}
 \sin\left(\int_r^{R_1} dr \tilde{k} + \frac{\pi}{4}\right) &= -i \exp\left[i\left(\int_r^{R_1} dr \tilde{k} + \frac{\pi}{4}\right)\right] \\
 &\quad + i \exp\left[-i\left(\int_r^{R_1} dr \tilde{k} + \frac{\pi}{4}\right)\right]
 \end{aligned} \tag{3.53}$$

We can rewrite the right-side wave function in Eq. (3.52) as

$$\frac{1}{\sqrt{|\tilde{k}|}} \exp\left(-\int_{R_1}^{R_2} dr |\tilde{k}|\right) \exp\left(\int_r^{R_2} dr |\tilde{k}|\right) \tag{3.54}$$

The second factor has following correspondence to the wave function in the right side of the turning point at $r = R_2$,

$$\exp\left(\int_r^{R_2} dr|\tilde{k}|\right) \iff -\exp\left[i\left(\int_{R_2}^r dr\tilde{k} + \frac{\pi}{4}\right)\right] \quad \begin{array}{l} r < R_2 \\ r > R_2 \end{array} \quad (3.55)$$

With the factor in Eq. (3.54), we obtain the wave function in the region $r > R_2$,

$$u(k, r > R_2) = -\frac{1}{\sqrt{|\tilde{k}|}} \exp\left[-\int_{R_1}^{R_2} dr|\tilde{k}|\right] \exp\left[i\left(\int_{R_2}^r dr\tilde{k} + \frac{\pi}{4}\right)\right] \quad (3.56)$$

So the transmission current is

$$j \sim \tilde{k}|u(k, r > R_2)|^2 = \exp\left(-2\int_{R_1}^{R_2} dr|\tilde{k}|\right) \quad (3.57)$$

The transmission probability is then

$$P = \exp\left(-2\int_{R_1}^{R_2} dr|\tilde{k}|\right) \quad (3.58)$$

For the α decay, there are two forces in the nuclei, nuclear and Coulomb. We can assume the nuclear and Coulomb forces reach balance for the α particles which can be treated as free inside the nuclei. The potential for the α particles is

$$V(r) = \begin{cases} -V_0, & r < R \\ \frac{Z_1 Z_2 e^2}{r}, & r > R \end{cases} \quad (3.59)$$

where $Z_1 = 2$ and $Z_2 = Z$. See Fig. 3.6. Let us estimate the height of potential barrier,

$$\begin{aligned} E_B &= \frac{Z_1 Z_2 e^2}{R} \approx \frac{2Z \times 1.44}{1.2(A^{1/3} + A_\alpha^{1/3})} = 2.4 \frac{Z}{A^{1/3} + A_\alpha^{1/3}} \\ &\approx 27 \text{ MeV for } {}_{84}^{212}\text{Po}, \end{aligned} \quad (3.60)$$

where $R \approx 1.2(A^{1/3} + A_\alpha^{1/3}) = 9 \text{ fm}$.

One sees $E_B \gg E_0$. According to classical theory the α decay cannot escape. But in quantum theory the penetration probability is given

$$P = e^{-G} = \exp\left(-2\sqrt{2m_\alpha} \int_R^b \sqrt{V - E_0} dr\right) \quad (3.61)$$

where $b = \frac{Z_1 Z_2 e^2}{E_0}$. When $b/R \gg 1$,

$$\begin{aligned} G &= 2\sqrt{2m_\alpha} \int_R^b \sqrt{\frac{Z_1 Z_2 e^2}{r} - E_0} dr = 4\sqrt{2} \sqrt{\frac{m_\alpha}{E_0}} Z_1 Z_2 e^2 \int_{y_{min}}^1 \sqrt{1 - y^2} dy \\ &\approx 4\sqrt{2} \sqrt{\frac{m_\alpha}{E_0}} Z_1 Z_2 e^2 \left[\int_0^1 \sqrt{1 - y^2} dy - \int_0^{y_{min}} \sqrt{1 - y^2} dy \right] \\ &\approx 4\sqrt{2} \sqrt{\frac{m_\alpha}{E_0}} Z_1 Z_2 e^2 \left(\frac{\pi}{4} - \sqrt{\frac{R}{b}} \right) = 2\sqrt{2}\pi Z e^2 \sqrt{\frac{m_\alpha}{E_0}} - 8\sqrt{e^2 m_\alpha} \sqrt{ZR} \\ &= 2\sqrt{2}\pi \frac{1}{137} \sqrt{3750} \frac{Z}{\sqrt{E_0}} - 8\sqrt{3750/197/137} \sqrt{ZR} \\ &= 3.97 \frac{Z}{\sqrt{E_0}} - 2.98 \sqrt{ZR} \end{aligned} \quad (3.62)$$

where $y \equiv \sqrt{\frac{r}{b}}$ and $y_{min} = \sqrt{\frac{RE_0}{Z_1 Z_2 e^2}} = \sqrt{\frac{R}{b}}$. We have used the fine structure constant $e^2 = 1/137$. Obtaining the last line, we have used $Z_1 = 2$, $Z_2 = Z$, $m_\alpha = 3750$ MeV. In the last equality, R is in unit fm and E_0 is in MeV. The collision times per second for an α particle inside the nucleus is

$$n = \frac{v}{2R} \approx \sqrt{\frac{2E_k}{m_\alpha}} \frac{1}{2R} \approx 3 \times 10^{21} A^{-1/3} E_k^{1/2} \text{ sec}^{-1} \quad (3.63)$$

where $E_k = E_0 + V_0$ is the kinetic energy of the α particle inside the nucleus in unit MeV. In transforming the speed v from the natural unit to cgs one, we note that it has to times the speed of light c . Then the average life for α decay is

$$\tau = \frac{1}{\lambda} = \frac{1}{nP} \approx 3.5 \times 10^{-22} A^{1/3} E_k^{-1/2} e^G \quad (3.64)$$

We can take logarithm of above and obtain,

$$\ln \tau = a_1 + a_2 \frac{1}{\sqrt{E_0}}, \quad (3.65)$$

where $a_1 = \ln(3.5 \times 10^{-22} A^{1/3} E_k^{-1/2}) - 2.98\sqrt{ZR}$ and $a_2 = 3.97Z$. Eq. (3.65) was first obtained as an empirical law by Geiger and Nutall in 1911 and later confirmed by quantum mechanics.

Let us estimate the half life of ^{210}Po from α decay,

$$\begin{aligned} T_{1/2}(^{210}\text{Po}) &= \frac{\ln 2}{\lambda} = \ln 2 \times 3.5 \times 10^{-22} A^{1/3} E_k^{-1/2} e^G \\ &\approx \ln 2 \times 3.5 \times 10^{-22} \times 210^{1/3} \times (5.4)^{-1/2} \times \exp(3.97 \times 84/\sqrt{5.4} - 2.98 \times \sqrt{84 \times 9}) \\ &\approx 6.2 \times 10^{-22} \times \exp(61.6) \\ &\approx 4.06 \text{ days} \end{aligned} \quad (3.66)$$

$$\begin{aligned} T_{1/2}(^{212}\text{Po}) &\approx \ln 2 \times 3.5 \times 10^{-22} \times 212^{1/3} \times (9.03)^{-1/2} \\ &\quad \times \exp(3.97 \times 84/\sqrt{9.03} - 2.98 \times \sqrt{84 \times 9}) \\ &\approx 4.81 \times 10^{-22} \times \exp(29) \\ &\approx 1.98 \times 10^{-9} \text{ s} \end{aligned} \quad (3.67)$$

We can compare with the data, $T_{1/2}(^{210}\text{Po}) = 138.4$ days and $T_{1/2}(^{212}\text{Po}) = 3 \times 10^{-7}$ s.

In the above simple model, we have made several approximations. (1) We have neglected the influence of initial and final state wave functions. (2) we did not consider the angular momentum of alpha particles. When the angular momentum is taken into account, there will be centrifugal potential $V_{\text{cent}} = \frac{L(L+1)}{2mr^2}$ which will modify the half life of alpha decay. (3) We used the nuclear radius formula $R = 1.2A^{1/3}$ fm, which is not correct for many heavy nuclei with strong deformation. Since the half-lives are very sensitive to the nuclear radius, it becomes a method to measure the shape of the nuclei through α decay half-lives.

The alpha decay is strong interaction which conserves parity. The parity of an alpha particle is $(-1)^L$ where L is the quantum number of the orbital angular momentum. So parity conservation requires the selection rule $P_i = (-1)^L P_f$, where P_i and P_f are the parity of the initial and final state respectively.

A full description of alpha decay using time dependent quantum mechanics can be found in Ref. [34, 35].

Exercise 11. Use the data at the IAEA nuclear data services [28] to draw the binding energy per nucleon as a function of the number of nucleons in Fig. 2.9. Also draw the α particle decay energy E_0 in Eq. (3.25) as a function of the number of nucleons.

Exercise 12. Calculate the half life of ${}_{92}^{238}\text{U}$ from emission of 4.2 MeV α -particles. One assumes $E_k \approx E_0$.

Exercise 13. In the above we do not consider the angular momentum of alpha particles. When the angular momentum is taken into account, the centrifugal potential $V_{\text{cent}} = \frac{L(L+1)}{2mr^2}$ will modify the half life of alpha decay. Estimate its correction to $T_{1/2}({}^{210}\text{Po})$.

Exercise 14. A full description of alpha decay using time dependent quantum mechanics can be found in Ref. [34, 35]. Read one of the articles and write a report of 2000 chinese words.

Exercise 15. Calculate the α decay half-lives of thorium isotopes ($A=220,222,224,226,228,230,232$) and compare to the experimental data.

Exercise 16. Consider the alpha decay ${}_{Z+2}^{A+4}X \rightarrow {}_Z^AY + \alpha$. The potential for the α particles is

$$V(r) = \begin{cases} -V_0, & r < R \\ \frac{Z_1 Z_2 e^2}{r}, & r > R \end{cases}$$

where $Z_1 = 2$, $Z_2 = Z$ and $R \approx 1.2(A^{1/3} + A_\alpha^{1/3})$. The kinetic energy of the alpha particle is E_0 , from which we can determine classical turning point $b = \frac{Z_1 Z_2 e^2}{E_0}$. The transmission probability for the alpha particle to go through the Coulomb barrier is

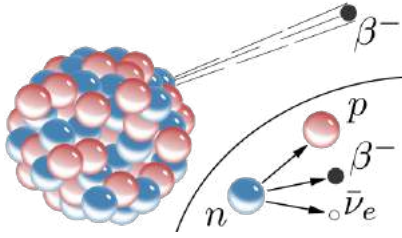
$$P = e^{-G} = \exp\left(-2\sqrt{2m_\alpha} \int_R^b \sqrt{V - E_0} dr\right)$$

We assume $b/R \gg 1$. (1) Work out the integral to express P as a function of E_0 , Z and R . (2) Write down the formula for the half-life of the alpha decay in terms of $E_k = E_0 + V_0$ and R .

3.4 β decay: weak interaction at work

In the α decay, when the recoil energy of the daughter nucleus is negligible, the energy of the α particle reflects its energy inside the mother nucleus. The energy spectrum is not continuous since the α particle and the daughter nucleus form a quasi-bound state inside the mother nucleus and the bound state energies form energy levels. Unlike the α decay, the energy spectrum of the β particle or electron in the β decay is continuous ranging from the zero to the decay energy which is the energy difference between the initial and final state. This poses a puzzle or a challenge for theorists. In order to explain the continuous energy spectra in the β decay or the 'missing' energy Pauli proposed the neutrino hypothesis, accompanying the emission of electrons is emitted a tiny particles called neutrinos which escape the catch of the detector. Neutrinos are spin-one-half neutral particles with very small mass. The β decay is then written as



Figure 3.8: Beta minus decay. From http://en.wikipedia.org/wiki/Beta_decay.

as a three body decay. The electron anti-neutrino is denoted as $\bar{\nu}_e$. The simplest example is the decay of neutron into proton accompanying emission of electron and neutrino [see Fig. 3.8],



From Table 6.1, we know that the neutron and proton masses are 939.56536 MeV and 938.27203 MeV respectively. The electron has rest mass 0.51 MeV. The mass difference between neutron and proton plus electron is $\Delta m = m_n - m_p - m_e = 0.78$ MeV. Then the Q-value of the neutron β -decay is $Q = \Delta m - m_\nu$. The measured value of the maximal endpoint energy of the electron is about 0.78 MeV, so we conclude that the neutrino mass is very small.

Let us discuss all forms of the β decays in general sense. The first form is the β decay of electrons in Eq. (3.68), whose decay energy is given by

$$\begin{aligned} E_0 &= m_X(Z, A) - m_Y(Z + 1, A) - m_e \\ &= M_X(Z, A) - M_Y(Z + 1, A) \end{aligned} \quad (3.70)$$

where m_X and M_X are the nuclear and the atomic mass respectively. In order for the β decay to occur, it is required that $M_X > M_Y$.

The energy-momentum conservation for β decay in (3.68) reads

$$\begin{aligned} \mathbf{p}_e + \mathbf{p}_\nu + \mathbf{p}_Y &= 0 \\ E_e + E_\nu + E_Y &= E_0 \end{aligned} \quad (3.71)$$

where E_0 is the decay energy, E_i ($i = e, \nu, Y$) are kinetic energies. Let us consider two extreme cases. If $\mathbf{p}_\nu = 0$, we have

$$\begin{aligned} E_Y &= \frac{p_Y^2}{2m_Y} = \frac{p_e^2}{2m_Y} \approx \frac{E_e(E_e + 2m_e)}{2m_Y} \\ E_0 &= E_e + E_Y \approx \frac{E_e(E_e + 2m_e)}{2m_Y} + E_e \approx E_e \end{aligned} \quad (3.72)$$

for $E_e \ll m_Y$. Here we have used for the kinetic energy E ,

$$E = \sqrt{p^2 + m^2} - m = \frac{p^2}{2m} - \frac{1}{2m} \left(\frac{p^2}{2m} \right)^2 \approx \frac{p^2}{2m} - \frac{E^2}{2m} \quad (3.73)$$

If $\mathbf{p}_e = 0$, then $E_e = 0$. We see that the energy of the electron is in the range between 0 and E_0 .

Neutrinos are neutral fermions with spin one-half and are almost massless. We can define the helicity for massless fermions, $H = \boldsymbol{\sigma} \cdot \hat{\mathbf{p}}$, see Fig. 3.10. Anti-neutrinos have positive helicity and are right-handed meaning that their spins are along the momentum direction. Neutrinos have negative helicity and are left-handed. Neutrinos rarely interact with other particles. The cross section of neutrino-nucleus interaction is about $\sigma \sim 10^{-44}$ cm². If the matter density is about $n \sim 10^{23}$ cm⁻³,

Figure 3.9: Decay scheme for beta decay for Cobalt-60 and Gold-198. From http://en.wikipedia.org/wiki/Decay_scheme.

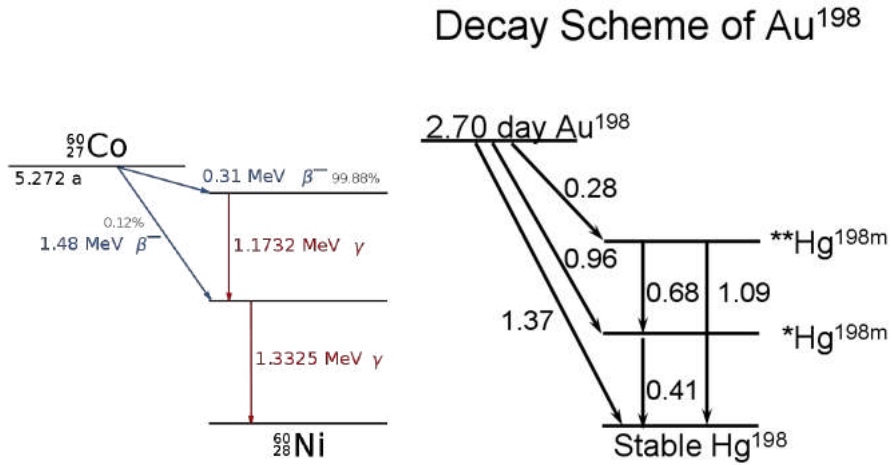


Figure 3.10: Neutrino helicity.

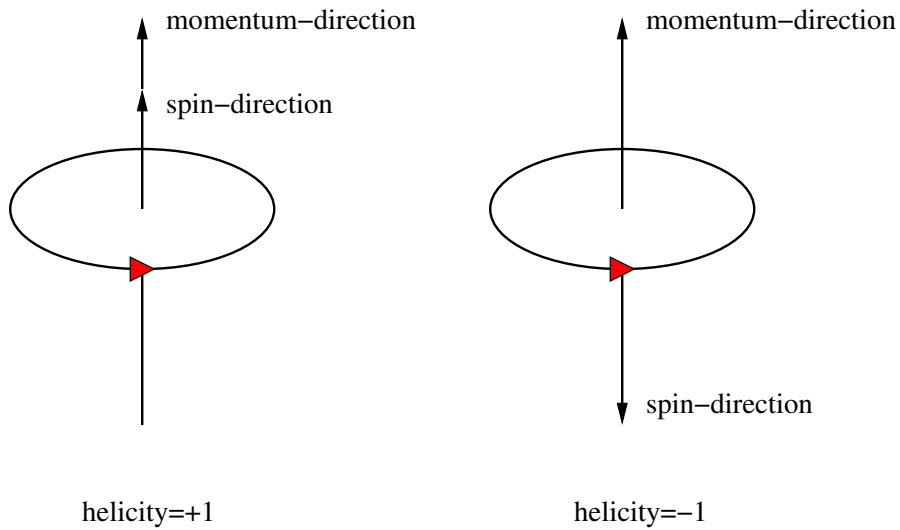
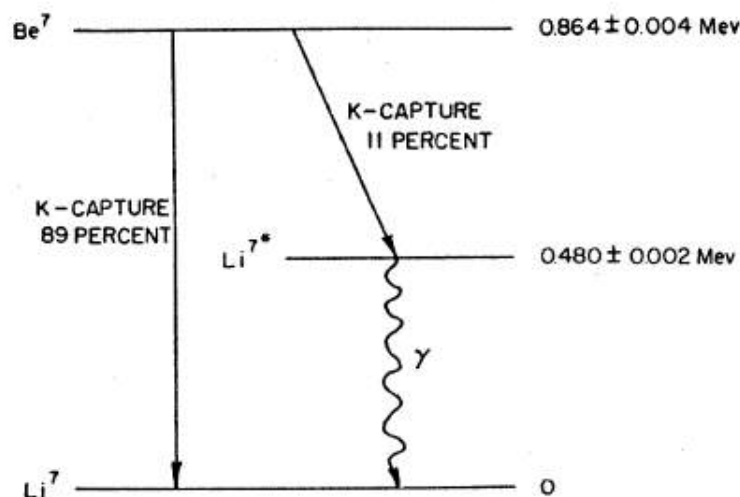


Figure 3.11: The K-electron capture isotope ${}^7_4\text{Be}$, taken from Ref. [24].

the mean free path is about $l_{\text{mfp}} = 1/(n\sigma) \sim 10^{16}$ km. Direct experimental tests of neutrinos are hard to carry out. But there are some indirect evidences for their existence, for example, the beta particle can be emitted at any angles with respect to recoiling nucleus. The measurement of the recoil energy spectrum of an electron capture isotope is a good test of the single neutrino hypothesis. The kinetic energy of the recoiling nucleus is

$$E_Y = \frac{p_Y^2}{2m_Y} = \frac{p_\nu^2}{2m_Y} \approx \frac{E_0^2}{2m_Y} \sim \frac{\text{MeV}^2}{10,000 \text{ MeV}} \sim 100 \text{ eV} \quad (3.74)$$

We see that the recoil energy is very small. In order to enlarge the recoiling energy the light nuclei are favorable. Davis Jr. measured the recoil energy of the process [24]



which gave the expected result $E_R \sim 56$ eV.

The direct detection of neutrinos was made by F. Reines and C. L. Cowan in 1959 [25]. They measured the cross section of the following process



The anti-neutrinos were emitted from a powerful fission reactor. They used 1400 liter liquid scintillation detector as the proton source, where a cadmium compound was added to the scintillator solution mainly of triethylbenzene for the detection of the reaction by the delayed coincidence technique. The positrons will annihilate with electrons emitting photons, while the neutrons are captured by cadmium also producing photons.

The β decay of ${}^3_1\text{H}$ put a more stringent limit on the neutrino mass,



The atomic masses of ${}^3_1\text{H}$ and ${}^3_2\text{He}$ are 2809.431984 MeV and 2809.413284 MeV respectively. The atomic mass difference between ${}^3_1\text{H}$ and ${}^3_2\text{He}$ is $\Delta m = M_{\text{H}} - M_{\text{He}} \approx 0.0186$. The nuclear mass difference between ${}^3_1\text{H}$ and ${}^3_2\text{He} + e^-$ becomes $\Delta m = (M_{\text{H}} - m_e) - (M_{\text{He}} - 2m_e) - m_e = M_{\text{H}} - M_{\text{He}} \approx 0.0186$

Figure 3.12: The anti-neutrino detector used by Reines and Cowan, taken from Ref. [25].

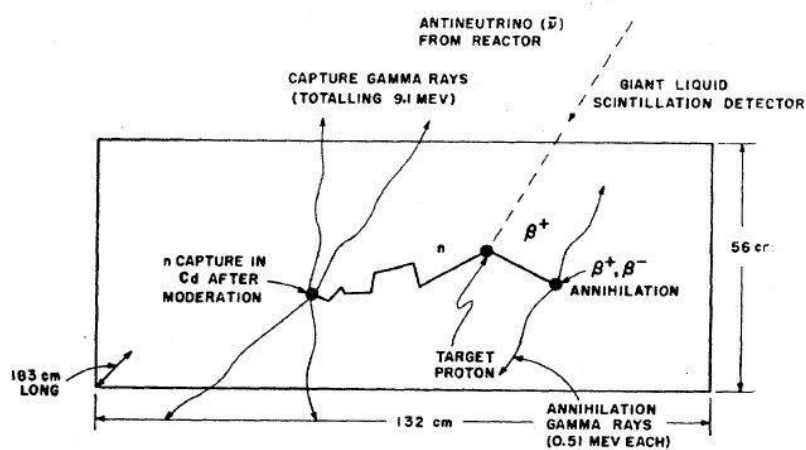


FIG. 1. Schematic of antineutrino detector. This 1.4×10^3 -liter detector is filled with a mixture which consists primarily of triethylbenzene (TEB) with small amounts of *p*-terphenyl (3 g/liter), POPOP wavelength shifter (0.2 g/liter) and cadmium (1.8 g/liter) as cadmium octoate. An antineutrino is shown transmuting a proton to produce a neutron and positron. The positron slows down and annihilates, producing annihilation radiation. The neutron is moderated by the hydrogen of the scintillator and is captured by the cadmium, producing capture gamma rays.

MeV. The upper limit for neutrino mass is only about 18.6 KeV. The further study of momentum spectrum of electrons gives an upper limit of only about 60 eV.

We provide two another examples for beta decays, Co-60 and Au-198, in Fig. 3.9. Co-60 is widely used as radioactive source for radiotherapy. Co-60 mainly decay to two excited states of Ni-60 through beta emission with a half life of 5.27 years. The excited states of Ni-60 emit two gamma rays with energies at 1.1732 MeV and 1.33 MeV. The decay energies are 0.31 MeV and 1.48 MeV respectively. For Au-198, it has three beta decay channels, to excited states of Hg-198 at 1.09 MeV and 0.41 MeV, and to the ground state. The excited states decay to the ground state by emitting three gamma rays of 0.68 MeV, 0.41 MeV and 1.09 MeV. The decay energies are 0.28 MeV, 0.96 MeV and 1.37 MeV respectively.

The second form of beta decay is the β^+ decay for positron emission,



The decay energy is given

$$\begin{aligned} E_0 &= m_X(Z, A) - m_Y(Z-1, A) - m_e \\ &= M_X(Z, A) - M_Y(Z-1, A) - 2m_e \end{aligned} \quad (3.79)$$

In order for the β^+ decay to take place, one requires $M_X(Z, A) > M_Y(Z-1, A) + 2m_e$.

The third form of beta decay is the orbital electron capture (EC),



where e_i^- is the electron in the i-shell. The decay energy is

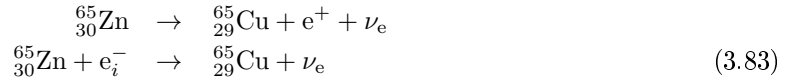
$$\begin{aligned} E_{0i} &= m_X + m_e - m_Y - W_i \\ &= M_X(Z, A) - M_Y(Z-1, A) - W_i \end{aligned} \quad (3.81)$$

where W_i is the binding energy of the electron in the atom. The K-level electron capture takes place with the largest probability, next to it is the L-level one. When

$$W_K > M_X(Z, A) - M_Y(Z-1, A) > W_L \quad (3.82)$$

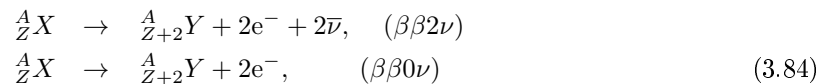
the K-level electron capture cannot happen but the L-level one can. Since $2m_e \gg W_i$, the nuclei which can β^+ decay can also capture orbital electrons.

As an example, we look at the β^+ decay and EC of Zn-65:



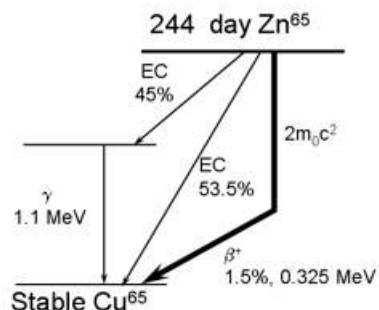
The scheme plot is shown in Fig. 3.13. There are two EC channels, whose decay energies are 0.236 MeV (45%) and 1.34 MeV (53.5%). The decay energy of the β^+ decay is 0.325 MeV. ${}^{64}_{29} \text{Cu}$ is the nucleus where all β^- , β^+ and EC can happen.

There are two kinds of double β decays, one with two neutrinos produced ($\beta\beta 2\nu$) and another without neutrinos $\beta\beta 0\nu$.



The neutrinos in $2\nu\beta\beta$ are Dirac neutrinos for which anti-neutrinos and neutrinos are different fermions, those in $0\nu\beta\beta$ are Majorana ones for which anti-neutrinos and neutrinos are identical. The neutrinoless double β decay ($\beta\beta 0\nu$) is the combination of two processes,

$$\begin{aligned} n &\rightarrow p + e^- + \bar{\nu} \\ \nu + n &\rightarrow p + e^- \end{aligned} \quad (3.85)$$

Figure 3.13: β^+ decay and electron capture of Zn-65.Decay Scheme for β^+ Emitting Zn⁶⁵

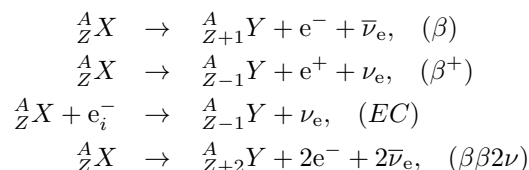
Vertical line represents the rest mass of the 2 electrons. Energy equivalence: 1.02 MeV

No experiments so far have succeeded in proving that neutrinos are of Dirac or Majorana types. In β decay, the final nucleus must have a larger binding energy than the initial nucleus. For some nuclei the β decay cannot happen since the nucleus with one more proton and one less neutron has smaller binding energy, the nucleus with two more protons and two less neutrons has larger binding energy so that the double β decay can happen. Germanium-76 is an example, which can in principle decay to selenium-76 via the double β decay. Here are isotopes which have been observed to have double β decay: $^{48}_{20}\text{Ca}$, $^{76}_{32}\text{Ge}$, $^{82}_{34}\text{Se}$, $^{96}_{40}\text{Zr}$, $^{100}_{42}\text{Mo}$, $^{116}_{48}\text{Cd}$, $^{128}_{52}\text{Te}$, $^{130}_{52}\text{Te}$, $^{150}_{60}\text{Nd}$, $^{238}_{92}\text{U}$.

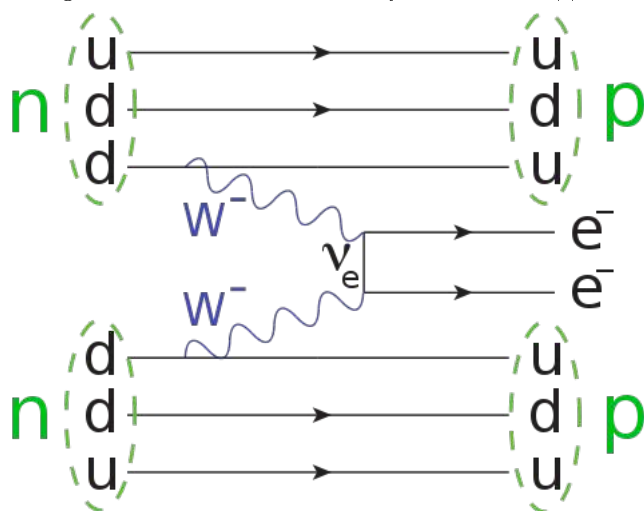
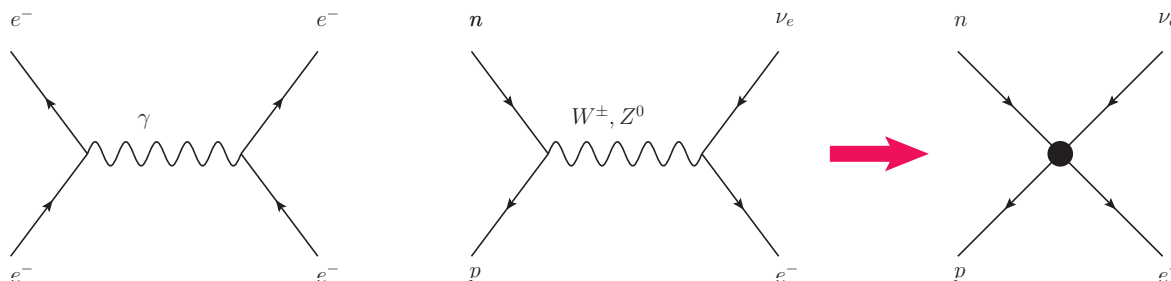
Exercise 17. Write down the reaction formula for the β and β^+ decay for the nucleus $^A_Z X$, where the daughter nucleus is $^{A'}_{Z'} Y$ with A' and Z' the nucleon and proton numbers. What are conditions for these decays to take place? Express the conditions using the atomic masses of X and Y .

Exercise 18. Write down the reaction formula for the $\beta\beta 2\nu$ and $\beta\beta 0\nu$ decay for the nucleus $^A_Z X$, where the daughter nucleus is $^{A'}_{Z'} Y$ with A' and Z' the nucleon and proton numbers. What is the difference in the electron energy spectra between the $\beta\beta 2\nu$ and $\beta\beta 0\nu$ decays?

Exercise 19. For following beta-type decays,



Using atomic masses of X and Y to express the energy, what are the energy conditions for the reactions to take place?

Figure 3.14: Double beta decay. From: http://en.wikipedia.org/wiki/Double_beta_decay.

 Figure 3.15: Similarity between an electron scattering and a beta decay-type reaction. The propagator of the W^\pm and Z^0 can be approximated as a point contact interaction due to their heavy masses.


Exercise 20. List all mass data for mother and daughter nuclei for nuclides which can undergo double beta decays. These are ${}_{20}^{48}\text{Ca}$, ${}_{32}^{76}\text{Ge}$, ${}_{34}^{82}\text{Se}$, ${}_{40}^{96}\text{Zr}$, ${}_{42}^{100}\text{Mo}$, ${}_{48}^{116}\text{Cd}$, ${}_{52}^{128}\text{Te}$, ${}_{52}^{130}\text{Te}$, ${}_{60}^{150}\text{Nd}$, ${}_{92}^{238}\text{U}$. Calculate the Q -values of each decay.

3.4.1 Fermi theory of β decay

In 1934 Fermi proposed a theory to describe the β decay. Fermi made an analogy of the β decay to the quantum transition of two atomic states radiating light or electron-electron scatterings, see Fig. 3.15. Similarly in β decay a quantum transition takes place where a neutron changes to a proton with emission of an anti-neutrino and an electron. In quantum electrodynamics, the amplitude of electron-electron scatterings can be written as $\bar{\psi}\gamma_\mu\psi\bar{\psi}\gamma^\mu\psi$ where ψ is a spinor field for electrons and can be understood as the electron wave function. Fermi then proposed the four-fermion model for the β decay. In this subsection, we will illustrate how the model works.

Before we discuss about the Fermi theory of the β decay. Let's first derive the Fermi golden rule for the rate of a quantum transition process from the Schrödinger equation. Suppose the transition is the consequence of the perturbative part of the Hamilton, H_{int} . The free part of the Hamilton is denoted as H_0 . The Schrödinger equation reads,

$$i\hbar\frac{\partial\psi}{\partial t} = (H_0 + H_{\text{int}})\psi \quad (3.86)$$

where $H_{\text{int}} \ll H_0$. The eigenstates of H_0 form a complete and orthogonal set $\{|n\rangle, n = 0, 1, 2, \dots\}$ with $H_0|n\rangle = E_n|n\rangle$. Suppose at the initial time $t = 0$, the system is in one eigenstate of H_0 , $\psi(0) = |i\rangle$. At a later time t , the wave function is in the form,

$$\psi(t) = \sum_n C_{ni}(t) \exp\left(-\frac{i}{\hbar} E_n t\right) |n\rangle \quad (3.87)$$

So we have $C_{ni}(0) = \delta_{ni}$. We can calculate the amplitude $C_{nk}(t)$ by substituting the above wave function into the Schrödinger equation,

$$i\hbar \sum_{n_1} \frac{d}{dt} C_{n_1 i}(t) \exp\left(-\frac{i}{\hbar} E_{n_1} t\right) |n_1\rangle = \sum_{n_1} C_{n_1 i}(t) \exp\left(-\frac{i}{\hbar} E_{n_1} t\right) H_{\text{int}} |n_1\rangle \quad (3.88)$$

We can determine $\dot{C}_{ni}(t)$ by projecting the above state on $|n\rangle$,

$$\begin{aligned} \dot{C}_{ni}(t) &= \frac{1}{i\hbar} \sum_{n_1} C_{n_1 i}(t) \exp\left[\frac{i}{\hbar}(E_n - E_{n_1})t\right] \langle n | H_{\text{int}} |n_1\rangle \\ &\approx \frac{1}{i\hbar} \exp\left[\frac{i}{\hbar}(E_n - E_i)t\right] \langle n | H_{\text{int}} |i\rangle \end{aligned} \quad (3.89)$$

where we have used $C_{ni}(t) \approx C_{ni}(0) = \delta_{ni}$. Then we can solve $C_{ni}(t)$ as

$$C_{ni}(t) = \delta_{ni} + \frac{1}{i\hbar} \int_0^t dt \exp\left[\frac{i}{\hbar}(E_n - E_i)t\right] \langle n | H_{\text{int}} |i\rangle \quad (3.90)$$

If $n \neq i$, we get the transition probability for $|i\rangle \rightarrow |n\rangle$,

$$P_{ni} = \frac{1}{\hbar^2} \left| \int_0^t dt \exp\left[\frac{i}{\hbar}(E_n - E_i)t\right] \langle n | H_{\text{int}} |i\rangle \right|^2 \quad (3.91)$$

If H_{int} is independent of time, the probability for $t \rightarrow \infty$ becomes,

$$\begin{aligned} P_{ni} &= \frac{1}{\hbar^2} |\langle n | H_{\text{int}} |i\rangle|^2 \left| \int_0^t dt \exp\left[\frac{i}{\hbar}(E_n - E_i)t\right] \right|^2 \\ &= \frac{1}{\hbar^2} |\langle n | H_{\text{int}} |i\rangle|^2 \frac{\sin^2[(E_n - E_i)t/(2\hbar)]}{(E_n - E_i)^2/(4\hbar^2)} \\ &\rightarrow |\langle n | H_{\text{int}} |i\rangle|^2 2\pi t \delta(E_n - E_i), \quad (t \rightarrow \infty, \text{ in natural unit}) \end{aligned} \quad (3.92)$$

where we have used

$$\lim_{x \rightarrow \infty} \frac{\sin^2(x)}{x^2} = \pi \delta(x) \quad (3.93)$$

Taking the density of final states into account, we obtain the transition rate

$$\begin{aligned} \lambda &= \int dn(E_n) |\langle n | H_{\text{int}} |i\rangle|^2 2\pi \delta(E_n - E_i) \\ &= 2\pi \rho(E_i) |\langle n | H_{\text{int}} |i\rangle|^2 \end{aligned} \quad (3.94)$$

where $\frac{dn}{dE} = \rho(E)$ is the energy density of states. Eq. (3.94) is called the Fermi golden rule.

Now we deal with the β decay with the Fermi golden rule. The initial state is the state of the mother nucleus and the final state is made up of daughter nucleus, an electron and an anti-neutrino,

$$\begin{aligned} |i\rangle &= \left| \frac{A}{Z} X \right\rangle = u_i(\mathbf{x}) \\ |f\rangle &= \left| \frac{A}{Z+1} Y, e^-, \bar{\nu}_e \right\rangle = u_f(\mathbf{x}) \phi_e(\mathbf{x}_e) \phi_{\nu}(\mathbf{x}_{\nu}) \end{aligned} \quad (3.95)$$

Here $u_{i,f}$ are eigenstates of mother and daughter nuclei respectively, and ϕ_e and ϕ_ν are the wave function of the electron and neutrino. According to the Fermi golden rule the differential decay rate reads

$$d\lambda = 2\pi |\langle f | H_{\text{int}} | i \rangle|^2 \delta(E_f + E_e + E_\nu - E_i) d\rho(e^-, \bar{\nu}_e) \quad (3.96)$$

where $d\rho(e^-, \bar{\nu}_e)$ is the number of final states for electrons and (anti-)neutrinos. The matrix element of the Hamiltonian between the initial and final state is

$$\begin{aligned} \mathcal{M}_{fi} &= \langle f | H_{\text{int}} | i \rangle \\ &= \int d^3\mathbf{x} d^3\mathbf{x}_e d^3\mathbf{x}_\nu u_f^*(\mathbf{x}) \phi_e^*(\mathbf{x}_e) \phi_\nu^*(\mathbf{x}_\nu) H_{\text{int}} u_i(\mathbf{x}) \\ &= G \int d^3\mathbf{x} d^3\mathbf{x}_e d^3\mathbf{x}_\nu u_f^*(\mathbf{x}) \phi_e^*(\mathbf{x}_e) \phi_\nu^*(\mathbf{x}_\nu) u_i(\mathbf{x}) \delta(\mathbf{x}_e - \mathbf{x}) \delta(\mathbf{x}_\nu - \mathbf{x}) \\ &= G \int d^3\mathbf{x} u_f^*(\mathbf{x}) \phi_e^*(\mathbf{x}) \phi_\nu^*(\mathbf{x}) u_i(\mathbf{x}) \end{aligned} \quad (3.97)$$

where we assumed the interaction part of the Hamiltonian is in a point contact form,

$$H_{\text{int}} = G \delta(\mathbf{x}_e - \mathbf{x}) \delta(\mathbf{x}_\nu - \mathbf{x}) \quad (3.98)$$

with G the effective coupling constant for β decay.

The differential decay rate for emitting an electron within the momentum range $[k_e, k_e + dk_e]$ is,

$$d\lambda \approx G^2 \left| \int d^3\mathbf{x} u_f^*(\mathbf{x}) \phi_e^*(\mathbf{x}) \phi_\nu^*(\mathbf{x}) u_i(\mathbf{x}) \right|^2 2\pi \delta(E_f + E_e + E_\nu - E_i) d\rho. \quad (3.99)$$

Assuming that the electron and the neutrino are free particles, their wave functions can be approximated by the plane waves

$$\begin{aligned} \phi_e &= \frac{1}{\sqrt{V}} e^{i\mathbf{k}_e \cdot \mathbf{x}} \\ \phi_\nu &= \frac{1}{\sqrt{V}} e^{i\mathbf{k}_\nu \cdot \mathbf{x}} \end{aligned} \quad (3.100)$$

Substituting the above into Eq. (3.99), we obtain

$$\begin{aligned} d\lambda &= G^2 \frac{1}{V^2} \left| \int d^3\mathbf{x} u_f^*(\mathbf{x}) u_i(\mathbf{x}) e^{-i(\mathbf{k}_e + \mathbf{k}_\nu) \cdot \mathbf{x}} \right|^2 2\pi \delta(E_f + E_e + E_\nu - E_i) d\rho \\ &= G^2 \frac{1}{V^2} \frac{V d^3\mathbf{k}_e}{(2\pi)^3} \frac{V d^3\mathbf{k}_\nu}{(2\pi)^3} 2\pi \delta(E_f + E_e + E_\nu - E_i) |M_{fi}|^2, \end{aligned} \quad (3.101)$$

where we have used

$$\begin{aligned} d\rho &= \frac{V d^3\mathbf{k}_e}{(2\pi)^3} \frac{V d^3\mathbf{k}_\nu}{(2\pi)^3} = k_e^2 k_\nu^2 dk_e dk_\nu \frac{V d\Omega_e}{(2\pi)^3} \frac{V d\Omega_\nu}{(2\pi)^3}, \\ |M_{fi}|^2 &\equiv \left| \int d^3\mathbf{x} u_f^*(\mathbf{x}) u_i(\mathbf{x}) e^{-i(\mathbf{k}_e + \mathbf{k}_\nu) \cdot \mathbf{x}} \right|^2, \end{aligned} \quad (3.102)$$

where we used $k_{e,\nu} \equiv |\mathbf{k}_{e,\nu}|$. Note that $|M_{fi}|^2$ is dimensionless. If we neglect the neutrino mass $m_\nu \approx 0$ and integrate over final state phase space where electron momenta are in the range $[k_e, k_e + dk_e]$, Eq. (3.101) becomes

$$\begin{aligned} d\lambda &= 2\pi G^2 k_e^2 dk_e \int \frac{d\Omega_e}{(2\pi)^3} \int \frac{d^3\mathbf{k}_\nu}{(2\pi)^3} \delta(E_f + E_e + E_\nu - E_i) |M_{fi}|^2 \\ &= \frac{G^2}{2\pi^3} dk_e k_e^2 (E_i - E_f - E_e)^2 |M_{fi}|^2 \end{aligned} \quad (3.103)$$

So the probability distribution is

$$\frac{d\lambda}{dk_e} = \frac{G^2}{2\pi^3} k_e^2 (\Delta E - E_e)^2 |M_{\text{fi}}|^2 \quad (3.104)$$

where $\Delta E = E_i - E_f$ is the energy between the mother and daughter nucleus in the beta decay or the decay energy.

Here we have neglected the influence of the Coulomb field on electrons from the nucleus. Normally the plane wave function of an electron can be distorted in the Coulomb field from protons inside the nucleus. The distortion to the electron wave function can be described by a Coulomb modification factor $F(Z, E_e)$,

$$F(Z, E_e) = \frac{x}{1 - e^{-x}} \quad (3.105)$$

where $x = \pm 2\pi Z e^2 / v_e$ for the β^\mp decay with $v_e = m_e^{-1} \sqrt{E_e^2 - m_e^2}$ being the electron velocity. The final form of the probability distribution is now

$$\frac{d\lambda}{dk_e} = \frac{G^2}{2\pi^3} k_e^2 (E_0 - E_e)^2 F(Z, E_e) |M_{\text{fi}}|^2 \quad (3.106)$$

We can re-write the above spectrum as

$$\begin{aligned} \sqrt{\frac{d\lambda/dk_e}{k_e^2 F(Z, E_e)}} &\sim C(\Delta E - E_e) \\ &= C(E_0 - T_e) \end{aligned} \quad (3.107)$$

where $E_e = T_e + m_e$, E_0 is the Q-value, and C is a constant. We can see that $\sqrt{(d\lambda/dk_e)/[k_e^2 F(Z, E_e)]}$ is in linear relation to E_e , which is known as the Kurie plot. From the Kurie plot we can determine the maximum energy ΔE or the Q-value from the intercept with the energy-axis. In Eq. (3.106), we see that the electron spectrum is in the range $k_e = [0, \sqrt{(\Delta E)^2 - m_e^2}] \approx [0, \Delta E - m_e^2/(2\Delta E)]$, see Fig.3.16 for the electron momentum and kinetic energy spectra of electrons and positrons in β^\pm decays of ${}^{64}_{29}\text{Cu}$.

If we recover the neutrino mass in Eq. (3.106) we obtain

$$\frac{d\lambda}{dk_e} = \frac{G^2}{2\pi^3} k_e^2 (\Delta E - E_e)^2 F(Z, E_e) \sqrt{1 - \frac{m_\nu^2}{(\Delta E - E_e)^2}} |M_{\text{fi}}|^2, \quad (3.108)$$

where we have used $k_\nu^2 dk_\nu = k_\nu E_\nu dE_\nu$. The zero points read $E_e^{(0)} = \Delta E$ and $E_e^{(0)} = \Delta E \pm m_\nu$, where the lowest zero point $E_e^{(0)} = \Delta E - m_\nu$ is physical. So we can determine the neutrino mass from the intercept with energy axis once we know ΔE .

We can obtain the integrated rate from Eq. (3.106) by using dimensionless variable $w \equiv E_e/m_e$ and $w_0 = \Delta E/m_e$,

$$\begin{aligned} \lambda &= \frac{G^2}{2\pi^3} \int_{m_e}^{E_0} dE_e F(Z, E_e) E_e k_e (\Delta E - E_e)^2 |M_{\text{fi}}|^2 \\ &\approx \frac{G^2 m_e^5}{2\pi^3} f(Z, w_0) |M_{\text{fi}}|^2, \end{aligned} \quad (3.109)$$

where $f(Z, w_0)$ is defined as

$$f(Z, w_0) = \int_1^{w_0} dw F(Z, w) \sqrt{w^2 - 1} (w_0 - w)^2 w \quad (3.110)$$

Figure 3.16: Momentum and kinetic energy spectra of electrons and positrons in β^\pm decays of $^{64}_{29}\text{Cu}$. Taken from Fig. 5.9 on p129 of Ref. [37].

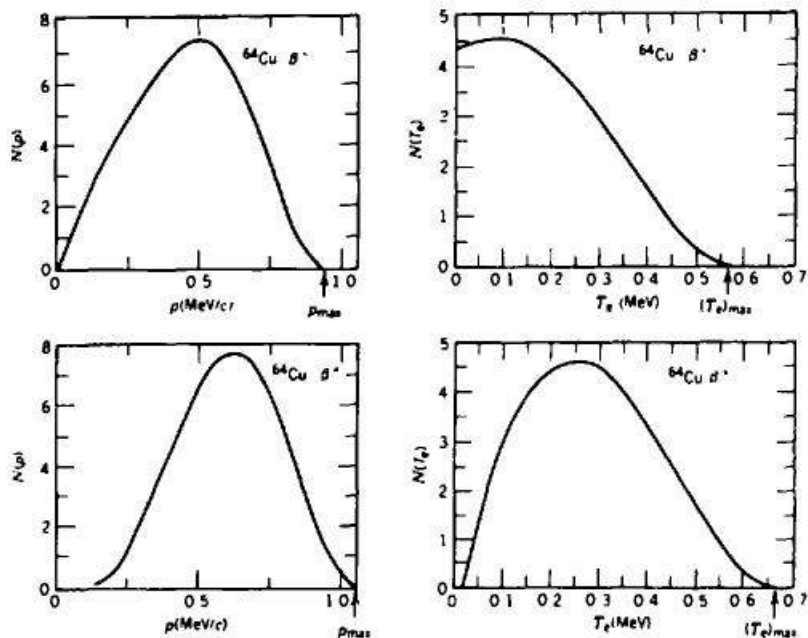


Figure 3.17: Illustration of the Fermi-Kurie plot for $^3\text{H} \rightarrow ^3\text{He} + e^- + \bar{\nu}_e$. Suppose $m_\nu = 30$ eV, there is difference between massive and massless neutrinos. Taken from Fig. 5.11 on p130 of Ref. [37].

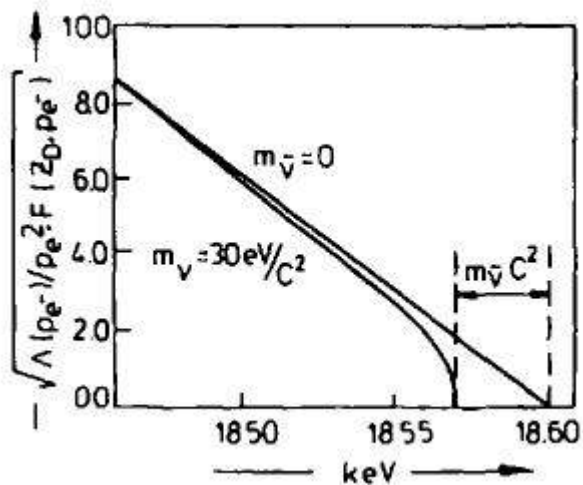


Figure 3.18: $T_{1/2}f(Z, w_0)$ for superallowed transition. Taken from Table. 5.3 on p133 of Ref. [37].

Decay	fT (s)
$^{10}\text{C} \rightarrow ^{10}\text{B}$	3100 ± 31
$^{14}\text{O} \rightarrow ^{14}\text{N}$	3092 ± 4
$^{18}\text{Ne} \rightarrow ^{18}\text{F}$	3084 ± 76
$^{22}\text{Mg} \rightarrow ^{22}\text{Na}$	3014 ± 78
$^{26}\text{Al} \rightarrow ^{26}\text{Mg}$	3081 ± 4
$^{26}\text{Si} \rightarrow ^{26}\text{Al}$	3052 ± 51
$^{30}\text{S} \rightarrow ^{30}\text{P}$	3120 ± 82
$^{34}\text{Cl} \rightarrow ^{34}\text{S}$	3087 ± 9
$^{34}\text{Ar} \rightarrow ^{34}\text{Cl}$	3101 ± 20
$^{38}\text{K} \rightarrow ^{38}\text{Ar}$	3102 ± 8
$^{38}\text{Ca} \rightarrow ^{38}\text{K}$	3145 ± 138
$^{42}\text{Sc} \rightarrow ^{42}\text{Ca}$	3091 ± 7
$^{42}\text{Ti} \rightarrow ^{42}\text{Si}$	3275 ± 1039
$^{46}\text{V} \rightarrow ^{46}\text{Ti}$	3082 ± 13
$^{46}\text{Cr} \rightarrow ^{46}\text{V}$	2834 ± 657
$^{50}\text{Mn} \rightarrow ^{50}\text{Cr}$	3086 ± 8
$^{54}\text{Co} \rightarrow ^{54}\text{Fe}$	3091 ± 5
$^{62}\text{Ga} \rightarrow ^{62}\text{Zn}$	2549 ± 1280

If w_0 is very large, we have $f(Z, w_0) \sim w_0^5/5$. The the half life is given by

$$T_{1/2} = \frac{\ln 2}{\lambda} = \frac{2\pi^3 \ln 2}{G^2 m_e^5 f(Z, w_0) |M_{\text{fi}}|^2} \quad (3.111)$$

If we know $T_{1/2}$ and $|M_{\text{fi}}|^2$, we can determine the coupling G . It turns out that the quantity $T_{1/2}f(Z, w_0)$ is almost a constant for certain type of beta decays. It is called the comparative half-life. For $0^+ \rightarrow 0^+$ transition, we have $|M_{\text{fi}}|^2 = 2$, $T_{1/2}f(Z, w_0)$ should be a constant, see Fig. 3.18 for the experimental data. From the data G can be determined to be $0.89 \times 10^{-4} \text{ MeV} \cdot \text{fm}^3 = 1.16 \times 10^{-5} \text{ GeV}^{-2}$. Eq. (3.111) can be put into a simple form,

$$T_{1/2}f(Z, w_0) \approx \frac{6185}{|M_{\text{fi}}|^2} \text{ second}$$

So the dimensionless coupling constant is $Gm_p^2 \approx 1.026 \times 10^{-5}$ with nucleon mass m_p . This can be compared to the couplings in strong and electromagnetic interactions whose coupling constants are of the order 1 (strong) and 10^{-2} (electromagnetic). We see that the strength of the β decay is much weaker, this is why the so-called weak interaction is at work in the β decay.

We can estimate the free neutron half life from the beta decay by Eqs. (3.110,3.111). We can neglect $F(Z, w)$. We can further neglect the recoil effect and approximate $|M_{\text{fi}}|^2 \sim 1 + 3g_A^2/g_V^2 \sim 5.8$, with $\Delta E \approx 1.29 \text{ MeV}$, $G = 0.89 \times 10^{-4} \text{ MeV} \cdot \text{fm}^3 = 1.16 \times 10^{-5} \text{ GeV}^{-2}$, and

$$f(Z, w_0) = \int_1^{w_0} dw \sqrt{w^2 - 1} (w_0 - w)^2 w \approx 1.63, \quad (3.112)$$

we obtain the neutron's half life

$$\begin{aligned} T_{1/2}(\text{n}) &\sim \frac{197 \times 10^{12} 2\pi^3 \ln 2}{1.15^2 \times 10^{-10} \times 0.51^5 \times 1.63 \times 5.8} (\text{fm}/c) \\ &\approx 654 \text{ s.} \end{aligned}$$

The data give $T_{1/2}(\text{n}) \approx 661 \text{ s}$. We see the perfect agreement between the data and the theoretical value.

Let us discuss about the transition amplitude $|M_{\text{fi}}|^2$, Eq. (3.102). Note that the phase is very small $(\mathbf{k}_e + \mathbf{k}_\nu) \cdot \mathbf{x} \sim 0.1 - 0.01 \ll 1$, so we can make an expansion of the phase factor $e^{i(\mathbf{k}_e + \mathbf{k}_\nu) \cdot \mathbf{x}}$ in terms of powers of $(\mathbf{k}_e + \mathbf{k}_\nu) \cdot \mathbf{x}$. We can also make an expansion of it in terms of spherical harmonic functions,

$$\begin{aligned} e^{i(\mathbf{k}_e + \mathbf{k}_\nu) \cdot \mathbf{x}} &= \sum_{L=0} (2L+1)(-i)^L j_L(|\mathbf{k}_e + \mathbf{k}_\nu|x) P_L(\cos \theta) \\ &\approx \sum_{L=0} \frac{(2L+1)(-i)^L}{(2L+1)!!} |\mathbf{k}_e + \mathbf{k}_\nu|^L x^L P_L(\cos \theta) \end{aligned} \quad (3.113)$$

Therefore the amplitude can be written as

$$\begin{aligned} M_{\text{fi}} &= \sum_{L=0} \frac{(2L+1)(-i)^L}{(2L+1)!!} \int d^3\mathbf{x} u_{\text{f}}^*(\mathbf{x}) u_{\text{i}}(\mathbf{x}) |\mathbf{k}_e + \mathbf{k}_\nu|^L x^L P_L(\cos \theta) \\ &= \sum_{L=0} M_{\text{fi}}^L \end{aligned} \quad (3.114)$$

The matrix elements corresponding to two lowest partial waves are

$$\begin{aligned} M_{\text{fi}}^{L=0} &= \int d^3\mathbf{x} u_{\text{f}}^*(\mathbf{x}) u_{\text{i}}(\mathbf{x}) \\ M_{\text{fi}}^{L=1} &= -i \int d^3\mathbf{x} u_{\text{f}}^*(\mathbf{x}) u_{\text{i}}(\mathbf{x}) |\mathbf{k}_e + \mathbf{k}_\nu| x P_L(\cos \theta) \end{aligned} \quad (3.115)$$

If $M_{\text{fi}}^{L=0} \neq 0$, it is called the allowed transition. If $M_{\text{fi}}^{L=1} \neq 0$, it is called the first order prohibited transition and etc.. The partial wave contribution M_{fi}^L drops very fast as L increases. The suppression of higher order contributions can be seen by

$$\frac{M_{\text{fi}}^{L+1}}{M_{\text{fi}}^L} \sim \frac{kr}{2L+1} \sim 10^{-2} \quad (3.116)$$

for $r \sim 5$ fm and $k \sim 1$ MeV. So we see that the lowest order, $L = 0, 1$, contributions play the role.

In the original version of the Fermi model of the beta decay, the spin part is absent. Nucleons and leptons are spin-1/2 fermions, we can recover the spin part in Eq. (3.114),

$$|M_{\text{fi}}|^2 = \sum_{L, S_{e\nu}} |M_{\text{fi}}^{L, S_{e\nu}}|^2 \quad (3.117)$$

where $\mathbf{S}_{e\nu} = \mathbf{S}_e + \mathbf{S}_\nu$ is the lepton spin. The angular momentum conservation reads

$$\mathbf{J}_i = \mathbf{J}_f + \mathbf{S}_{e\nu} + \mathbf{L} \quad (3.118)$$

where \mathbf{L} denotes the angular momentum of the leptons, and $\mathbf{J}_i(\mathbf{J}_f)$ is the nuclear spin of the mother (daughter) nucleus or the initial (final) nuclear state. The spin of the leptonic system $S_{e\nu}$ can be 0 (singlet) or 1 (triplet), which correspond to Fermi and Gamow-Teller transition respectively. The strength for Fermi and Gamow-Teller transition are different. The coupling strength is characterized by $G_{\text{GT}}/G_{\text{F}} \sim -1.26$. For allowed transitions of the pure Fermi type ($L = 0, S_l = 0$), we have $|M_{\text{fi}}^{L=0, S_l=0}|^2 = 1$. For allowed transitions of the pure Gamow-Teller type, we have $|M_{\text{fi}}^{L=0, S_l=1}|^2 = 3$, because there are three spin states. For super-allowed transition, we have $|M_{\text{fi}}^{L=0, S_l=0}(0^+ \rightarrow 0^+)|^2 = 2$ due to two pairing nucleons outside the shell in the initial 0^+ state. For the mixed type decays, there are both Fermi type and Gamow-Teller type contributions. We denote the matrix element squared as $G_{\text{F}}^2 |M_{\text{F}}|^2 + G_{\text{GT}}^2 |M_{\text{GT}}|^2$. From Eq. (3.114) we have parity selection rule:

$$P_i P_f = (-1)^L, \quad (3.119)$$

Table 3.3: Classification for the beta decay. Parity selection rule: $P_i P_f = (-1)^L$.

	$S_l = 0$: Fermi	$S_l = 1$: Gamow-Teller
$L = 0$: allowed	$J_i - J_f = 0$, $P_i P_f = 1$ $0^+ \rightarrow 0^+$: super-allowed	$J_i - J_f = 0, \pm 1$, $P_i P_f = 1$ $0^+ \rightarrow 1^+$: unique Gamow-Teller
$L = 1$: 1st forbidden	$J_i - J_f = 0, \pm 1$ $P_i P_f = -1$	$J_i - J_f = 0, \pm 1, \pm 2$ $P_i P_f = -1$

where $P_i(P_f)$ is the parity of the initial (final) nuclear state.

For $S_{e\nu} = 0$ and the allowed transition ($L = 0$), we get $J_i - J_f = 0$ and $P_i = P_f$, this is called Fermi selection rule. For $S_{e\nu} = 1$ and the allowed transition ($L = 0$), we get $J_i - J_f = 0, \pm 1$ and $P_i = P_f$, this is called Gamow-Teller selection rule.

The classification for the beta decay is in Table 3.3. For various types of transitions, the decay strengths vary to many orders of magnitude: $\log_{10}[T_{1/2} f(Z, w_0)] = 2.9-3.7$ (super-allowed), 4.4-6.0 (allowed), 6-10 (1st forbidden), above 15 (2nd forbidden), where $T_{1/2}$ is in the unit of second.

Here are some examples for the allowed β -decays. (1) ${}^{14}_8\text{O} \rightarrow {}^{14}_7\text{N}^*$, ${}^{10}_6\text{C} \rightarrow {}^{10}_5\text{B}^*$, ${}^{18}_{10}\text{Ne} \rightarrow {}^{18}_9\text{F}^*$ and ${}^{34}_{17}\text{Cl} \rightarrow {}^{34}_{16}\text{S}$ are $0^+ \rightarrow 0^+$ super-allowed Fermi-type transitions. The scheme plots for these decays are shown in Fig. 3.19. (2) ${}^{10}_6\text{C} \rightarrow {}^{10}_5\text{B}$ ($0^+ \rightarrow 1^+$), ${}^6_2\text{He} \rightarrow {}^6_3\text{Li}$ ($0^+ \rightarrow 1^+$), ${}^{13}_5\text{B} \rightarrow {}^{13}_6\text{C}$ ($3/2^- \rightarrow 1/2^-$), ${}^{28}_{12}\text{Mg} \rightarrow {}^{28}_{13}\text{Al}^*$ ($0^+ \rightarrow 1^+$) and ${}^{60}_{24}\text{Cr} \rightarrow {}^{60}_{25}\text{Mn}$ ($0^+ \rightarrow 1^+$) are Gamow-Teller transitions. The scheme plots for these decays are shown in Fig. 3.20. There are mixed type of decays, here are some examples. (3) Mirror decays: $n \rightarrow p$ ($1/2^+ \rightarrow 1/2^+$), ${}^3_1\text{H} \rightarrow {}^3_2\text{He}$ ($1/2^+ \rightarrow 1/2^+$), ${}^{13}_7\text{N} \rightarrow {}^{13}_6\text{C}$ ($1/2^- \rightarrow 1/2^-$), ${}^{21}_{11}\text{Na} \rightarrow {}^{21}_{10}\text{Ne}$ ($3/2^+ \rightarrow 3/2^+$), ${}^{41}_{21}\text{Sc} \rightarrow {}^{41}_{20}\text{Ca}$ ($4^+ \rightarrow 4^+$); Non-mirror decays: ${}^{24}_{11}\text{Na} \rightarrow {}^{24}_{12}\text{Mg}$ ($3/2^+ \rightarrow 3/2^+$), ${}^{41}_{11}\text{Ar} \rightarrow {}^{41}_{12}\text{K}$ ($7/2^- \rightarrow 7/2^-$), ${}^{46}_{21}\text{Sc} \rightarrow {}^{46}_{22}\text{Ti}$ ($4^+ \rightarrow 4^+$), ${}^{52}_{25}\text{Mn} \rightarrow {}^{52}_{24}\text{Cr}$ ($2^+ \rightarrow 2^+$), ${}^{65}_{28}\text{Ni} \rightarrow {}^{65}_{29}\text{Cu}$ ($5/2^- \rightarrow 5/2^-$).

We now discuss about the Fermi model of the orbital electron capture process. If the mass difference between the mother nucleus and the daughter nucleus is larger than the electron's binding energy, the orbital electron capture can take place. The electron capture process leads to an electron vacancy in the orbit. The filling of this vacancy by a free electron can release the binding energy by emission of X-rays or Auger electrons. The decay constant can be obtained through the Fermi golden rule,

$$d\lambda_{\text{EC}} = 2\pi |\mathcal{M}_{\text{fi}}|^2 \delta(E_\nu - E_0) \frac{dn}{dE_\nu} dE_\nu, \quad (3.120)$$

where E_0 is the Q-value of the process and

$$\begin{aligned} \mathcal{M}_{\text{fi}} &= G \int d^3\mathbf{x} u_{\text{f}}^*(\mathbf{x}) \phi_\nu^*(\mathbf{x}) \phi_{\text{e}}(\mathbf{x}) u_{\text{i}}(\mathbf{x}), \\ \frac{dn}{dE_\nu} &= V \frac{1}{2\pi^2} E_\nu^2. \end{aligned} \quad (3.121)$$

Here $\phi_{\text{e}}(\mathbf{x})$ is the electron wave function in the atomic shell. Capture is most likely for 1s electrons in the K-shell, since the s-wave function is maximal at the origin,

$$\phi_{\text{e}}(\mathbf{x}) = \frac{1}{\sqrt{\pi}} (Ze^2 m_{\text{e}})^{3/2} \exp(-Ze^2 m_{\text{e}} |\mathbf{x}|). \quad (3.122)$$

The neutrino wave function is still a plane wave, $\phi_\nu = \frac{1}{\sqrt{V}} e^{i\mathbf{k}_\nu \cdot \mathbf{x}}$. Then we have

$$\begin{aligned} |\mathcal{M}_{\text{fi}}|^2 &= G^2 \frac{1}{V} \frac{1}{\pi} (Ze^2 m_{\text{e}})^3 |M_{\text{fi}}|^2, \\ M_{\text{fi}} &= \int d^3\mathbf{x} u_{\text{f}}^*(\mathbf{x}) u_{\text{i}}(\mathbf{x}) \exp(-i\mathbf{k}_\nu \cdot \mathbf{x} - Ze^2 m_{\text{e}} |\mathbf{x}|), \end{aligned} \quad (3.123)$$

Figure 3.19: The scheme plots for the allowed β -decays of the Fermi type. The half-lives are shown as $\log_{10}(fT_{1/2})$. From IAEA database NuDat 2.6 at "<http://www.nndc.bnl.gov/nudat2/>".

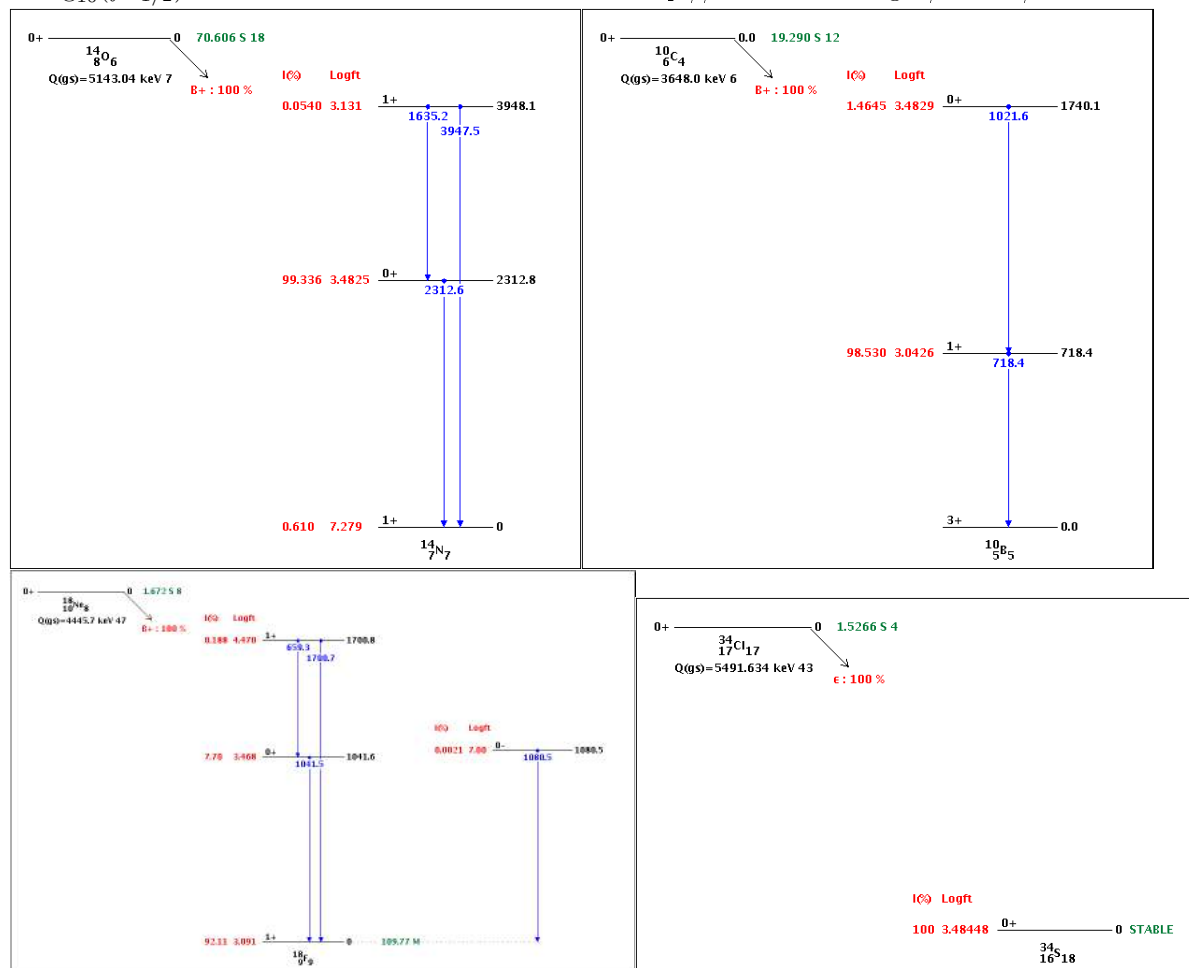
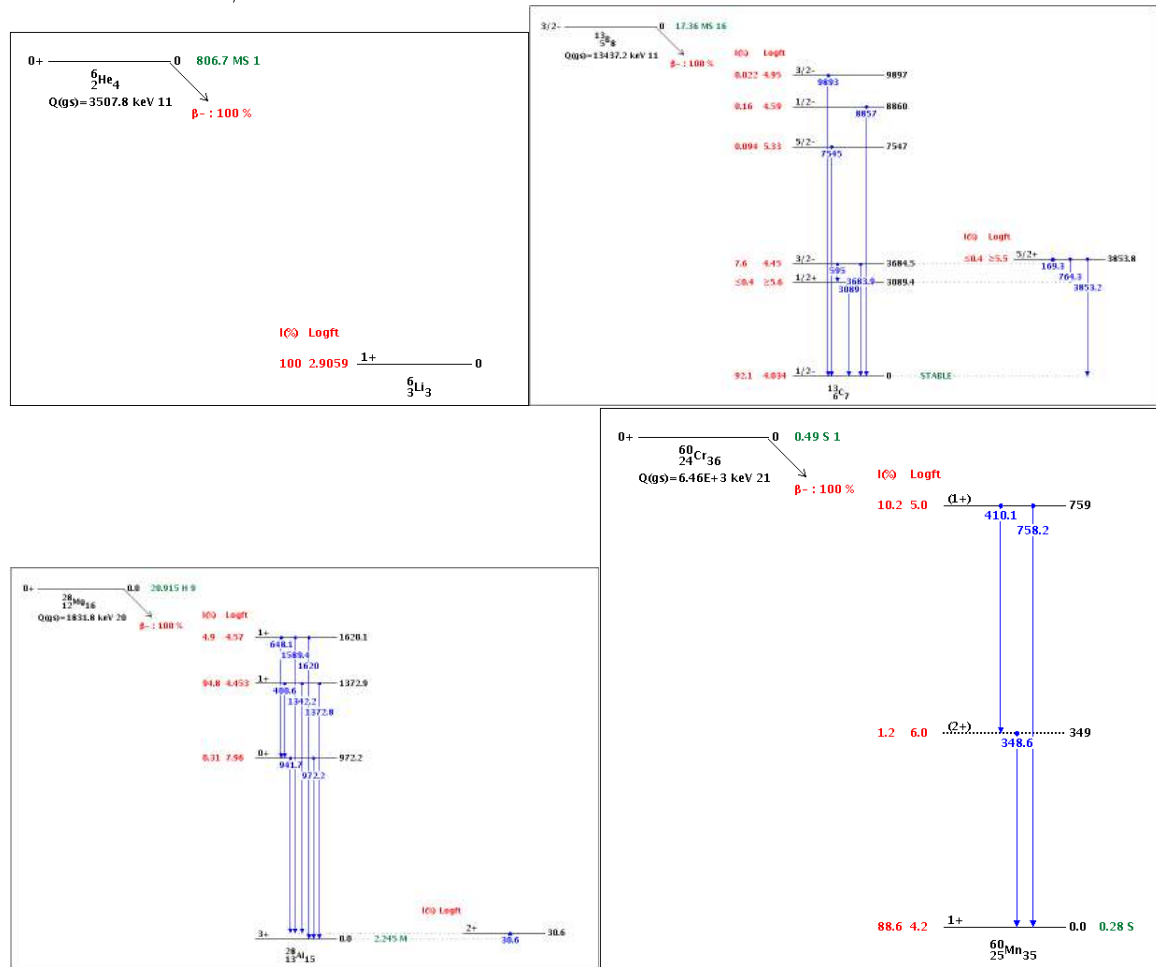


Figure 3.20: The scheme plots for the allowed β -decays of the Gamow-Teller type. The half-lives are shown as $\log_{10}(fT_{1/2})$. From IAEA database NuDat 2.6 at "<http://www.nndc.bnl.gov/nudat2/>".



where M_{fi} is dimensionless. So after integration M_{fi} is replaced by its average value, the decay rate or constant is then

$$\lambda_{\text{EC}} = \frac{G^2}{\pi^2} (Ze^2 m_e)^3 |\bar{M}_{\text{fi}}|^2 E_\nu^2.$$

We have taken into account that there are two 1s electrons in the K-shell. We see that the decay constant is proportional to Z^3 .

Now we calculate the cross section of the inverse beta decay processes described by

$$\begin{aligned} \frac{A}{Z}X + \nu_e &\rightarrow \frac{A}{Z+1}Y + e^-, \\ \frac{A}{Z}X + \bar{\nu}_e &\rightarrow \frac{A}{Z-1}Y + e^+. \end{aligned} \quad (3.124)$$

The simplest inverse beta decays are

$$\begin{aligned} \text{p} + \bar{\nu}_e &\rightarrow \text{n} + e^+, \\ \text{n} + \nu_e &\rightarrow \text{p} + e^-. \end{aligned} \quad (3.125)$$

The transition rate for the inverse reaction is given by

$$d\lambda_{\text{inv-b}} = 2\pi |\mathcal{M}_{\text{fi}}|^2 \delta(E_e - \Delta E) \frac{dn}{dE_e} dE_e \quad (3.126)$$

where $\Delta E = E_i + E_\nu - E_f$, and

$$\frac{dn}{dE_e} = \frac{V}{2\pi^2} k_e E_e \quad (3.127)$$

After integration, we obtain

$$\begin{aligned} \lambda_{\text{inv-b}} &= 2\pi G^2 \frac{1}{V^2} |\bar{M}_{\text{fi}}|^2 \frac{dn}{dE_e} = \frac{1}{\pi V} G^2 p_e E_e |\bar{M}_{\text{fi}}|^2 \\ &= \frac{1}{\pi V} G^2 m_e^2 |\bar{M}_{\text{fi}}|^2 w \sqrt{w^2 - 1} \end{aligned} \quad (3.128)$$

where the dimensionless nuclear matrix element M_{fi} is defined by

$$M_{\text{fi}} = \int d^3\mathbf{x} u_f^*(\mathbf{x}) u_i(\mathbf{x}) e^{i(\mathbf{k}_\nu - \mathbf{k}_e) \cdot \mathbf{x}} \quad (3.129)$$

In general both Fermi-type and Gamow-Teller type reactions are present,

$$|\bar{M}_{\text{fi}}|^2 = |\bar{M}_{\text{fi}}(F)|^2 + \frac{G_{\text{GT}}^2}{G_{\text{F}}^2} |\bar{M}_{\text{fi}}(\text{GT})|^2 \quad (3.130)$$

Note that $G_{\text{F}} \approx G$. The cross section is then given by

$$\begin{aligned} \sigma_{\text{inv-b}} &= \frac{\lambda_{\text{inv-b}}}{E_\nu} = \lambda_{\text{inv-b}} V/c \\ &= \frac{1}{\pi} G^2 m_e^2 w \sqrt{w^2 - 1} |\bar{M}_{fi}|^2 \end{aligned} \quad (3.131)$$

Using the value $|\bar{M}_{\text{fi}}|^2 \approx 5$, we can estimate the magnitude of $\sigma_{\text{inv-b}}$ for e.g. $w = 3$: $\sigma_{\text{inv-b}} \sim 20 \times 10^{-44} \text{ cm}^2$.

In real situations we have to determine the electron energy from energy-momentum conservation. We assume the inverse beta decay only affect the nucleon inside the nucleus. Then we have following equations from energy-momentum conservation in the center-of-mass frame,

$$\begin{aligned} p_{c\nu} &= p_{ci} \\ p_{ce} &= p_{cf} \\ E_{c\nu} + \sqrt{p_{ci}^2 + m_p^2} &= \sqrt{p_{ce}^2 + m_e^2} + \sqrt{p_{cf}^2 + m_n^2} \end{aligned} \quad (3.132)$$

We can express E_{ce} as a function of $p_{c\nu}$

$$E_{ce} = \frac{(p_{c\nu} + \sqrt{p_{c\nu}^2 + m_p^2})^2 + m_e^2 - m_n^2}{2(p_{c\nu} + \sqrt{p_{c\nu}^2 + m_p^2})} \quad (3.133)$$

The neutrino energy in the c.m.s. is related to that in the lab frame,

$$p_{c\nu} = \gamma_c(p_\nu - \beta_c E_\nu) = \frac{1 - \beta_c}{\sqrt{1 - \beta_c^2}} p_\nu \quad (3.134)$$

where $\gamma_c = \frac{1}{\sqrt{1 - \beta_c^2}}$ and $\beta_c = \frac{p_\nu}{p_\nu + m_p}$. Then we transform to the lab frame where the initial state nucleon is static,

$$E_e = \gamma_c(E_{ec} + \beta_c p_{ec} \cos \theta_{ce}) \quad (3.135)$$

We can take average over θ_{ce} for E_e , so we get the average electron energy in the lab frame, $E_e = \gamma_c E_{ce}$, or explicitly,

$$\langle E_e \rangle = \gamma_c \frac{(p_{c\nu} + \sqrt{p_{c\nu}^2 + m_p^2})^2 + m_e^2 - m_n^2}{2(p_{c\nu} + \sqrt{p_{c\nu}^2 + m_p^2})} \quad (3.136)$$

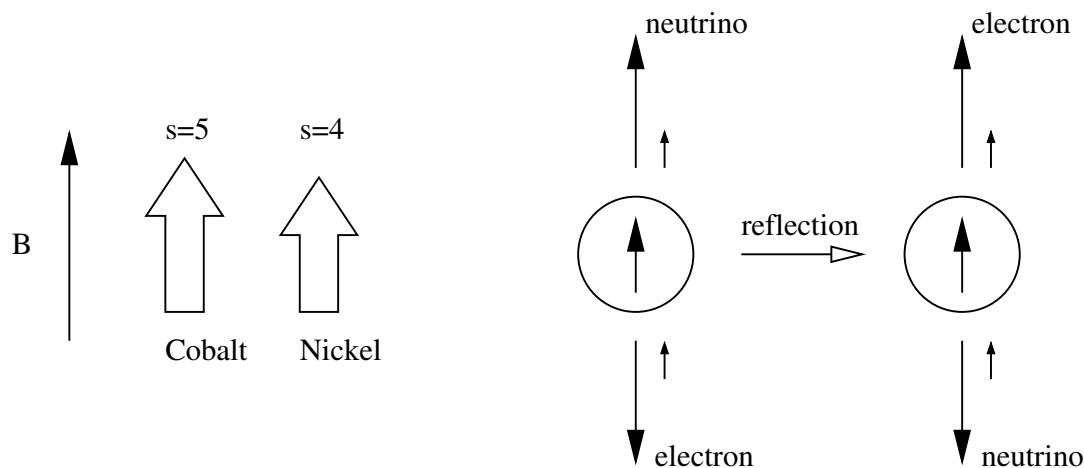
Substituting $w = \langle E_e \rangle / m_e$ into Eq. (3.131), we can obtain the cross section as a function of the neutrino energy.

Exercise 21. *When the neutrino has a mass, what happens to the electron energy spectra $\frac{d\lambda}{dE_e}$ as $E_e \rightarrow \Delta E$.*

Exercise 22. *Calculate the cross section of the inverse beta decay $p + \bar{\nu}_e \rightarrow n + e^+$ and $n + \nu_e \rightarrow p + e^-$ for $p_\nu = [0, 10]m_e$. One should use exact masses for proton and neutron, i.e. take the mass difference into account.*

Exercise 23. *Read the article about solar neutrino problem in Ref. [36]. Write a report about it in 2000 chinese words.*

Exercise 24. *Find as many as possible the super-allowed and unique Gamow-Teller β decays and in the IAEA database NuDat. For each decay, please list the decay reaction formula and the quantity $\log(ft)$ for the half life.*

Figure 3.21: The parity violation in the β decay.

Exercise 25. The half-life of the beta decay is given by

$$T_{1/2} = \frac{\ln 2}{\lambda} = \frac{2\pi^3 \ln 2}{G^2 m_e^5 f(Z, w_0) |M_{fi}|^2}$$

where $G = 0.88 \times 10^{-4} \text{ MeV} \cdot \text{fm}^3 = 1.15 \times 10^{-5} \text{ GeV}^{-2}$, $w_0 = \Delta E/m_e$ with the decay energy ΔE and electron mass $m_e = 0.511 \text{ MeV}$. For $w_0 \gg 1$, we can approximate $f(Z, w_0) \sim w_0^5/5$. For a pure Fermi transition ($L = 0, S_{e\nu} = 0$), we have $|M_{fi}|^2 = 1$. For a pure Gamow-Teller transition ($L = 0, S_{e\nu} = 1$), we have $|M_{fi}|^2 = 3$, because there are three spin states. For super-allowed transition ($0^+ \rightarrow 0^+$), we have $|M_{fi}|^2 = 2$ due to two pairing nucleons outside the shell in the initial 0^+ state. See Fig. 3.19 for super-allowed transition of ${}^{14}_8\text{O} \rightarrow {}^{14}_7\text{N}^*$. Calculate $T_{1/2}$ for such a beta decay in the unit of second.

3.4.2 Parity violation in β decay

In 1950s there was a $\tau - \theta$ puzzle that seemingly identical strange mesons θ^+ and τ^+ can decay into two and three pions respectively,

$$\begin{aligned} \theta^+ &\rightarrow \pi^+ + \pi^0 \\ \tau^+ &\rightarrow \pi^+ + \pi^+ + \pi^- \end{aligned}$$

Considering a pion has negative parity and the decay occurs in s-wave, it seems that θ^+ and τ^+ are different particles with opposite parity. But actually they are all kaons and parity is violated in weak decays.

In 1957 C.S. Wu and her collaborators measured the electron distribution in the β decay of polarized cobalt ,



They found that electrons are predominantly emitted opposite to the nuclear spin. Under the parity transformation $\mathbf{r} \rightarrow -\mathbf{r}$, the magnetic field and the spin are invariant while the momentum changes

the direction, i.e.

$$\begin{aligned}\mathbf{B} &\rightarrow \mathbf{B} \\ \mathbf{s} &\rightarrow \mathbf{s} \\ \mathbf{p} &\rightarrow -\mathbf{p}\end{aligned}\tag{3.138}$$

Along the direction of the magnetic field, a cobalt nucleus carries a spin of $5\hbar$ while a nickel nucleus carries a spin of $4\hbar$. The difference in spin is compensated by the emitted electron and anti-neutrino. Since the anti-neutrino is right-handed (the spin of the anti-neutrino is along its momentum), the electron is predominantly emitted opposite to the direction of the nuclear spin, see the left panel of Fig. 3.21.

Exercise 26. *Wu and her collaborators measured the electron distribution in the β decay of polarized cobalt, ${}^{60}_{27}\text{Co} \rightarrow {}^{60}_{28}\text{Ni} + e^- + \bar{\nu}_e$. Describe the main result of the experiment and explain why the result indicates that the parity is violated.*

3.5 γ decay: electromagnetic interaction at work

Nuclei are many body systems of nucleons which interact via nuclear force or strong interaction. A nucleus can stay in some quantum states with specific energies. By external perturbation a nucleus can be excited to higher energetic states and can jump onto its ground state by radiating photons (for example, the nuclei normally stay in their excited states right after the α and β decay).

3.5.1 Classical electrodynamics for radiation field

Classical electrodynamics can be summarized by Maxwell equations,

$$\begin{aligned}\nabla \cdot \mathbf{E} &= 4\pi\rho, \\ \nabla \times \mathbf{B} &= \frac{4\pi}{c}\mathbf{j} + \frac{1}{c}\frac{\partial \mathbf{E}}{\partial t}, \\ \nabla \cdot \mathbf{B} &= 0, \\ \nabla \times \mathbf{E} &= -\frac{1}{c}\frac{\partial \mathbf{B}}{\partial t}.\end{aligned}\tag{3.139}$$

From the last two equations, we can define scalar and vector potential $\phi(t, \mathbf{x})$ and $\mathbf{A}(t, \mathbf{x})$,

$$\begin{aligned}\mathbf{B} &= \nabla \times \mathbf{A} \\ \mathbf{E} &= -\nabla\phi - \frac{1}{c}\frac{\partial \mathbf{A}}{\partial t}\end{aligned}\tag{3.140}$$

The above equations are invariant under gauge transformation

$$\begin{aligned}\phi' &= \phi + \frac{1}{c}\frac{\partial f}{\partial t} \\ \mathbf{A}' &= \mathbf{A} - \nabla f\end{aligned}\tag{3.141}$$

where $f(t, \mathbf{x})$ is a function of space and time. Eq. (3.140) satisfies the last two equations of (3.139) automatically. Then inserting Eq. (3.140) into the first two equations of (3.139), we obtain

$$\begin{aligned}-\nabla^2\phi - \frac{1}{c}\frac{\partial}{\partial t}\nabla \cdot \mathbf{A} &= 4\pi\rho \\ \frac{1}{c^2}\frac{\partial^2 \mathbf{A}}{\partial t^2} - \nabla^2 \mathbf{A} + \nabla(\nabla \cdot \mathbf{A}) + \frac{1}{c}\frac{\partial}{\partial t}\nabla\phi &= \frac{4\pi}{c}\mathbf{j},\end{aligned}\tag{3.142}$$

We choose the Coulomb gauge,

$$\nabla \cdot \mathbf{A} = 0 \quad (3.143)$$

and consider the free space where $\rho = 0$ and $\mathbf{j} = 0$. Then Eq. (3.143) becomes

$$\begin{aligned} \nabla^2 \phi &= 0 \\ \frac{1}{c^2} \frac{\partial^2 \mathbf{A}}{\partial t^2} - \nabla^2 \mathbf{A} + \frac{1}{c} \frac{\partial}{\partial t} \nabla \phi &= \frac{4\pi}{c} \mathbf{j}, \end{aligned} \quad (3.144)$$

We can further set $\phi = 0$ as a solution to Poisson equation $\nabla^2 \phi = 0$ in free space with boundary condition $\phi|_{\mathbf{x} \rightarrow \infty} = 0$. Then we obtain the wave equation for radiation

$$\frac{1}{c^2} \frac{\partial^2 \mathbf{A}}{\partial t^2} - \nabla^2 \mathbf{A} = 0 \quad (3.145)$$

A vector field satisfying the Coulomb gauge is called a transverse field. We consider a solution to the wave equation (3.145)

$$\mathbf{A}(t, \mathbf{x}) = \mathbf{A}_0 e^{i(\mathbf{k} \cdot \mathbf{x} - \omega t)} \quad (3.146)$$

with $k^2 = \omega^2/c^2$. The Coulomb gauge gives transverse condition

$$\mathbf{k} \cdot \mathbf{A} = 0 \quad (3.147)$$

Such waves satisfying transverse condition are called radiation fields. Now we collect all equations we need for describing radiation,

$$\begin{aligned} \mathbf{B} &= \nabla \times \mathbf{A} \\ \mathbf{E}_T &= -\frac{1}{c} \frac{\partial \mathbf{A}}{\partial t} \\ \nabla \cdot \mathbf{A} &= 0 \\ \frac{1}{c^2} \frac{\partial^2 \mathbf{A}}{\partial t^2} - \nabla^2 \mathbf{A} &= 0 \end{aligned} \quad (3.148)$$

where we have denoted \mathbf{E}_T as the transverse electric field. The Hamiltonian for radiation field is

$$H_{\text{rad}} = \frac{1}{8\pi} \int d^3x (\mathbf{E}_T^2 + \mathbf{B}^2) \quad (3.149)$$

In order to quantize the radiation field, we consider a box of length L and volume $V = L^3$. The periodic condition reads

$$\mathbf{A}(t, \mathbf{x} \in \text{boundary}) = \text{constant} \quad (3.150)$$

We choose the following complete set of transverse orthonormal vectors which satisfy the above periodic boundary condition,

$$\frac{1}{\sqrt{V}} \boldsymbol{\epsilon}(r, \mathbf{k}) e^{i\mathbf{k} \cdot \mathbf{x}} \quad (3.151)$$

where $\boldsymbol{\epsilon}(r, \mathbf{k})$ with $r = 1, 2$ are two perpendicular real unit vectors and

$$\mathbf{k} = \frac{2\pi}{L} (n_1, n_2, n_3), \quad n_1, n_2, n_3 = 0, \pm 1, \pm 2, \dots \quad (3.152)$$

The polarization vectors $\boldsymbol{\epsilon}(r, \mathbf{k})$ satisfy following orthogonal and transverse conditions

$$\boldsymbol{\epsilon}(r, \mathbf{k}) \cdot \boldsymbol{\epsilon}(s, \mathbf{k}) = \delta_{rs}, \quad \mathbf{k} \cdot \boldsymbol{\epsilon}(r, \mathbf{k}) = 0 \quad (3.153)$$

Then the vector potential can be expanded in this complete set of transverse orthonormal vectors as Fourier series,

$$\mathbf{A}(t, \mathbf{x}) = \sum_{\mathbf{k}, s} \left(\frac{2\pi}{V\omega_{\mathbf{k}}} \right)^{1/2} \boldsymbol{\epsilon}(s, \mathbf{k}) [a(t, s, \mathbf{k}) e^{i\mathbf{k} \cdot \mathbf{x}} + a^*(t, s, \mathbf{k}) e^{-i\mathbf{k} \cdot \mathbf{x}}] \quad (3.154)$$

where $\omega_k = k$. We see that $\mathbf{A}(t, \mathbf{x})$ in the above form is real. Substituting Eq. (3.154) into Eq. (3.145), we get

$$\frac{\partial^2 a(t, s, \mathbf{k})}{\partial t^2} + \omega_k^2 a(t, s, \mathbf{k}) = 0 \quad (3.155)$$

So we can determine the time dependent part as

$$a(t, s, \mathbf{k}) = a(s, \mathbf{k})e^{-i\omega_k t} \quad (3.156)$$

Then the vector potential in (3.154) becomes

$$\mathbf{A}(t, \mathbf{x}) = \sum_{\mathbf{k}, s} \left(\frac{2\pi}{V\omega_k} \right)^{1/2} \boldsymbol{\epsilon}(s, \mathbf{k}) [a(s, \mathbf{k})e^{-i\omega_k t + i\mathbf{k}\cdot\mathbf{x}} + a^*(s, \mathbf{k})e^{i\omega_k t - i\mathbf{k}\cdot\mathbf{x}}] \quad (3.157)$$

The Hamiltonian (3.149) can be evaluated as

$$\begin{aligned} H_{\text{rad}} &= \frac{1}{8\pi} \int d^3x \left[\left(\frac{\partial \mathbf{A}}{\partial t} \right)^2 + (\nabla \times \mathbf{A})^2 \right] \\ &= \sum_{\mathbf{k}, s} \omega_k a(s, \mathbf{k}) a^*(s, \mathbf{k}) \end{aligned} \quad (3.158)$$

The first term $\left(\frac{\partial \mathbf{A}}{\partial t} \right)^2$ is evaluated as

$$\begin{aligned} \frac{\partial \mathbf{A}}{\partial t} &= -i \sum_{\mathbf{k}, s} \left(\frac{2\pi}{V\omega_k} \right)^{1/2} \boldsymbol{\epsilon}(s, \mathbf{k}) \omega_k [a(s, \mathbf{k})e^{-i\omega_k t + i\mathbf{k}\cdot\mathbf{x}} - a^*(s, \mathbf{k})e^{i\omega_k t - i\mathbf{k}\cdot\mathbf{x}}] \\ \left(\frac{\partial \mathbf{A}}{\partial t} \right)^2 &= -i \sum_{\mathbf{k}, s} \sum_{\mathbf{k}_1, s_1} \frac{2\pi}{V} (\omega_k \omega_{k_1})^{1/2} \boldsymbol{\epsilon}(s, \mathbf{k}) \cdot \boldsymbol{\epsilon}(s_1, \mathbf{k}_1) \\ &\quad \times [a(s, \mathbf{k})e^{-i\omega_k t + i\mathbf{k}\cdot\mathbf{x}} - a^*(s, \mathbf{k})e^{i\omega_k t - i\mathbf{k}\cdot\mathbf{x}}] \\ &\quad \times [a(s_1, \mathbf{k}_1)e^{-i\omega_{k_1} t + i\mathbf{k}_1\cdot\mathbf{x}} - a^*(s_1, \mathbf{k}_1)e^{i\omega_{k_1} t - i\mathbf{k}_1\cdot\mathbf{x}}] \\ \int d^3x \left(\frac{\partial \mathbf{A}}{\partial t} \right)^2 &= - \sum_{\mathbf{k}, s} \sum_{\mathbf{k}_1, s_1} \frac{2\pi}{V} (\omega_k \omega_{k_1})^{1/2} \boldsymbol{\epsilon}(s, \mathbf{k}) \cdot \boldsymbol{\epsilon}(s_1, \mathbf{k}_1) \\ &\quad \times [a(s, \mathbf{k})a(s_1, \mathbf{k}_1)e^{-i\omega_k t - i\omega_{k_1} t} \int d^3x e^{i(\mathbf{k} + \mathbf{k}_1)\cdot\mathbf{x}} \\ &\quad - a(s, \mathbf{k})a^*(s_1, \mathbf{k}_1)e^{-i\omega_k t + i\omega_{k_1} t} \int d^3x e^{i(\mathbf{k} - \mathbf{k}_1)\cdot\mathbf{x}} \\ &\quad - a^*(s, \mathbf{k})a(s_1, \mathbf{k}_1)e^{i\omega_k t - i\omega_{k_1} t} \int d^3x e^{-i(\mathbf{k} - \mathbf{k}_1)\cdot\mathbf{x}} \\ &\quad + a^*(s, \mathbf{k})a^*(s_1, \mathbf{k}_1)e^{i\omega_k t + i\omega_{k_1} t} \int d^3x e^{-i(\mathbf{k} + \mathbf{k}_1)\cdot\mathbf{x}}] \\ &= \sum_{\mathbf{k}, s} 4\pi\omega_k a(s, \mathbf{k}) a^*(s, \mathbf{k}) + I_1 \end{aligned} \quad (3.159)$$

where we have used $\int d^3x e^{i\mathbf{k}\cdot\mathbf{x}} = V\delta_{\mathbf{k},0}$, and I_1 denotes the oscillating terms $\sim e^{\pm 2i\omega_k t}$,

$$\begin{aligned} I_1 &= - \sum_{\mathbf{k}, s} \sum_{s_1} 2\pi\omega_k \boldsymbol{\epsilon}(s, \mathbf{k}) \cdot \boldsymbol{\epsilon}(s_1, -\mathbf{k}) \\ &\quad \times [a(s, \mathbf{k})a(s_1, -\mathbf{k})e^{-2i\omega_k t} + a^*(s, \mathbf{k})a^*(s_1, -\mathbf{k})e^{2i\omega_k t}] \end{aligned} \quad (3.160)$$

we will see it will cancel the same term in $(\nabla \times \mathbf{A})^2$. The second term $(\nabla \times \mathbf{A})^2$ is evaluated as

$$\begin{aligned}
\nabla \times \mathbf{A} &= i \sum_{\mathbf{k}, s} \left(\frac{2\pi}{V\omega_k} \right)^{1/2} \mathbf{k} \times \boldsymbol{\epsilon}(s, \mathbf{k}) [a(s, \mathbf{k})e^{-i\omega_k t + i\mathbf{k} \cdot \mathbf{x}} - a^*(s, \mathbf{k})e^{i\omega_k t - i\mathbf{k} \cdot \mathbf{x}}] \\
(\nabla \times \mathbf{A})^2 &= - \sum_{\mathbf{k}, s} \sum_{\mathbf{k}_1, s_1} \frac{2\pi}{V} (\omega_k \omega_{k_1})^{-1/2} [\mathbf{k} \times \boldsymbol{\epsilon}(s, \mathbf{k})] \cdot [\mathbf{k}_1 \times \boldsymbol{\epsilon}(s_1, \mathbf{k}_1)] \\
&\quad \times [a(s, \mathbf{k})e^{-i\omega_k t + i\mathbf{k} \cdot \mathbf{x}} - a^*(s, \mathbf{k})e^{i\omega_k t - i\mathbf{k} \cdot \mathbf{x}}] \\
&\quad \times [a(s_1, \mathbf{k}_1)e^{-i\omega_{k_1} t + i\mathbf{k}_1 \cdot \mathbf{x}} - a^*(s_1, \mathbf{k}_1)e^{i\omega_{k_1} t - i\mathbf{k}_1 \cdot \mathbf{x}}] \\
\int d^3x (\nabla \times \mathbf{A})^2 &= - \sum_{\mathbf{k}, s} \sum_{\mathbf{k}_1, s_1} \frac{2\pi}{V} (\omega_k \omega_{k_1})^{-1/2} [\mathbf{k} \times \boldsymbol{\epsilon}(s, \mathbf{k})] \cdot [\mathbf{k}_1 \times \boldsymbol{\epsilon}(s_1, \mathbf{k}_1)] \\
&\quad \times [a(s, \mathbf{k})a(s_1, \mathbf{k}_1)e^{-i\omega_k t - i\omega_{k_1} t} \int d^3x e^{i(\mathbf{k} + \mathbf{k}_1) \cdot \mathbf{x}} \\
&\quad - a(s, \mathbf{k})a^*(s_1, \mathbf{k}_1)e^{-i\omega_k t + i\omega_{k_1} t} \int d^3x e^{i(\mathbf{k} - \mathbf{k}_1) \cdot \mathbf{x}} \\
&\quad - a^*(s, \mathbf{k})a(s_1, \mathbf{k}_1)e^{i\omega_k t - i\omega_{k_1} t} \int d^3x e^{-i(\mathbf{k} - \mathbf{k}_1) \cdot \mathbf{x}} \\
&\quad + a^*(s, \mathbf{k})a^*(s_1, \mathbf{k}_1)e^{i\omega_k t + i\omega_{k_1} t} \int d^3x e^{-i(\mathbf{k} + \mathbf{k}_1) \cdot \mathbf{x}}] \\
&= \sum_{\mathbf{k}, s} 4\pi\omega_k a(s, \mathbf{k})a^*(s, \mathbf{k}) - I_1 \tag{3.161}
\end{aligned}$$

where we have used

$$\begin{aligned}
[\mathbf{k} \times \boldsymbol{\epsilon}(s, \mathbf{k})] \cdot [\mathbf{k}_1 \times \boldsymbol{\epsilon}(s_1, \mathbf{k}_1)] &= -\{\mathbf{k}_1 \times [\mathbf{k} \times \boldsymbol{\epsilon}(s, \mathbf{k})]\} \cdot \boldsymbol{\epsilon}(s_1, \mathbf{k}_1) \\
&= -[\mathbf{k}_1 \cdot \boldsymbol{\epsilon}(s, \mathbf{k})][\mathbf{k} \cdot \boldsymbol{\epsilon}(s_1, \mathbf{k}_1)] \\
&\quad + [\mathbf{k} \cdot \mathbf{k}_1][\boldsymbol{\epsilon}(s, \mathbf{k}) \cdot \boldsymbol{\epsilon}(s_1, \mathbf{k}_1)] \tag{3.162}
\end{aligned}$$

The combining Eq. (3.159) and (3.161), we get Eq. (3.158).

Exercise 27. Derive the classical Hamiltonian in Eq. (3.158) using the momentum decomposition for the classical field in Eq. (3.157).

3.5.2 Quantization of radiation field

The quantization of radiation field can be done by treating $a(s, \mathbf{k})$ and $a^*(s, \mathbf{k})$ as creation and destruction operator. Then we impose following commutation relations

$$\begin{aligned}
[a(s, \mathbf{k}), a^\dagger(s_1, \mathbf{k}_1)] &= \delta_{s, s_1} \delta_{\mathbf{k}, \mathbf{k}_1} \\
[a(s, \mathbf{k}), a(s_1, \mathbf{k}_1)] &= [a^\dagger(s, \mathbf{k}), a^\dagger(s_1, \mathbf{k}_1)] = 0 \tag{3.163}
\end{aligned}$$

The vector potential is then an operator,

$$\mathbf{A}(t, \mathbf{x}) = \sum_{\mathbf{k}, s} \left(\frac{2\pi}{V\omega_k} \right)^{1/2} \boldsymbol{\epsilon}(s, \mathbf{k}) [a(s, \mathbf{k})e^{-i\omega_k t + i\mathbf{k} \cdot \mathbf{x}} + a^\dagger(s, \mathbf{k})e^{i\omega_k t - i\mathbf{k} \cdot \mathbf{x}}] \tag{3.164}$$

The Hamiltonian as an operator is written in the form

$$H_{\text{rad}} = \sum_{\mathbf{k}, s} \omega_k [a^\dagger(s, \mathbf{k})a(s, \mathbf{k}) + \frac{1}{2}] \tag{3.165}$$

The number operator for mode (s, \mathbf{k}) is given by

$$N(s, \mathbf{k}) = a^\dagger(s, \mathbf{k})a(s, \mathbf{k}) \quad (3.166)$$

Its eigenstate is then

$$|n(s, \mathbf{k})\rangle = \frac{[a^\dagger(s, \mathbf{k})]^{n(s, \mathbf{k})}}{\sqrt{n(s, \mathbf{k})!}} |0\rangle \quad (3.167)$$

One can check

$$\begin{aligned} a(s, \mathbf{k}) |n(s, \mathbf{k})\rangle &= \sqrt{n(s, \mathbf{k})} |n(s, \mathbf{k}) - 1\rangle \\ a^\dagger(s, \mathbf{k}) |n(s, \mathbf{k})\rangle &= \sqrt{n(s, \mathbf{k}) + 1} |n(s, \mathbf{k}) + 1\rangle \\ a^\dagger(s, \mathbf{k})a(s, \mathbf{k}) |n(s, \mathbf{k})\rangle &= n(s, \mathbf{k}) |n(s, \mathbf{k})\rangle \end{aligned}$$

The eigenfunction of radiation Hamiltonian H_{rad} is then a product of such states for a set of modes,

$$|\mathcal{A}\rangle = \prod_{\mathbf{k}_i, s_i} |n(s_i, \mathbf{k}_i)\rangle \quad (3.168)$$

The energy is then

$$E = \langle \mathcal{A} | H_{\text{rad}} | \mathcal{A} \rangle = \sum_{\mathbf{k}, s} \omega_{\mathbf{k}} [n(s, \mathbf{k}) + \frac{1}{2}] \quad (3.169)$$

Now we can use creation and destruction operators to express the momentum of electromagnetic field,

$$\begin{aligned} \mathbf{P} &= \frac{1}{4\pi} \int d^3x \mathbf{E}_T \times \mathbf{B} \\ &= -\frac{1}{4\pi} \int d^3x \frac{\partial \mathbf{A}}{\partial t} \times (\nabla \times \mathbf{A}) \\ &= -\frac{1}{4\pi} \sum_{\mathbf{k}, s} \sum_{\mathbf{k}_1, s_1} \frac{2\pi}{V} \left(\frac{1}{\omega_{\mathbf{k}} \omega_{\mathbf{k}_1}} \right)^{1/2} \omega_{\mathbf{k}} \mathbf{k}_1 [\boldsymbol{\epsilon}(s, \mathbf{k}) \cdot \boldsymbol{\epsilon}(s_1, \mathbf{k}_1)] \\ &\quad \times \int d^3x [a(s, \mathbf{k}) e^{-i\omega_{\mathbf{k}} t + i\mathbf{k} \cdot \mathbf{x}} - a^\dagger(s, \mathbf{k}) e^{i\omega_{\mathbf{k}} t - i\mathbf{k} \cdot \mathbf{x}}] \\ &\quad \times [a(s_1, \mathbf{k}_1) e^{-i\omega_{\mathbf{k}_1} t + i\mathbf{k}_1 \cdot \mathbf{x}} - a^\dagger(s_1, \mathbf{k}_1) e^{i\omega_{\mathbf{k}_1} t - i\mathbf{k}_1 \cdot \mathbf{x}}] \\ &= \frac{1}{4\pi} \sum_{\mathbf{k}, s} \sum_{\mathbf{k}_1, s_1} \frac{2\pi}{V} \left(\frac{1}{\omega_{\mathbf{k}} \omega_{\mathbf{k}_1}} \right)^{1/2} \omega_{\mathbf{k}} \mathbf{k}_1 [\boldsymbol{\epsilon}(s, \mathbf{k}) \cdot \boldsymbol{\epsilon}(s_1, \mathbf{k}_1)] \\ &\quad \times \int d^3x [a(s, \mathbf{k}) a^\dagger(s_1, \mathbf{k}_1) e^{-i(\omega_{\mathbf{k}} - \omega_{\mathbf{k}_1}) t + i(\mathbf{k} - \mathbf{k}_1) \cdot \mathbf{x}} \\ &\quad + a^\dagger(s, \mathbf{k}) a(s_1, \mathbf{k}_1) e^{i(\omega_{\mathbf{k}} - \omega_{\mathbf{k}_1}) t - i(\mathbf{k} - \mathbf{k}_1) \cdot \mathbf{x}}] \\ &= \sum_{\mathbf{k}, s} \mathbf{k} [a^\dagger(s, \mathbf{k}) a(s, \mathbf{k}) + 1/2] = \sum_{\mathbf{k}, s} \mathbf{k} [N(s, \mathbf{k}) + \frac{1}{2}] \end{aligned} \quad (3.170)$$

Exercise 28. Derive the quantized energy momentum of the radiating EM system in Eqs. (3.165, 3.170) using the quantized field in Eq. (3.164).

3.5.3 Interaction of radiation with matter

Now we can add matter and matter-field interaction part of Hamiltonian. Consider a system of point charged particles with mass m_i and charge q_i , the matter part of Hamiltonian reads,

$$\begin{aligned}
 H_m &= \sum_i \frac{1}{2m_i} (\mathbf{p}_i - q_i \mathbf{A}_i)^2 \\
 &= \sum_i \frac{1}{2m_i} \mathbf{p}_i^2 - \sum_i \frac{q_i}{2m_i} (\mathbf{p}_i \cdot \mathbf{A}_i + \mathbf{A}_i \cdot \mathbf{p}_i) + \sum_i \frac{q_i^2}{2m_i} \mathbf{A}_i^2 \\
 &= \sum_i \frac{1}{2m_i} \mathbf{p}_i^2 - \sum_i \frac{q_i}{m_i} \mathbf{A}_i \cdot \mathbf{p}_i + \sum_i \frac{q_i^2}{2m_i} \mathbf{A}_i^2 \\
 &\equiv H_0 + H_I
 \end{aligned} \tag{3.171}$$

where H_0 is the free part and H_I is the interaction part of particles and fields. Here we have used

$$\mathbf{p}_i \cdot \mathbf{A}_i + \mathbf{A}_i \cdot \mathbf{p}_i = -i\nabla_i \cdot \mathbf{A}_i - i\mathbf{A}_i \cdot \nabla_i = -2i\mathbf{A}_i \cdot \nabla_i - i(\nabla_i \cdot \mathbf{A}_i) = -2i\mathbf{A}_i \cdot \nabla_i \tag{3.172}$$

under the Coulomb gauge condition. Here we have denoted $\mathbf{A}_i = \mathbf{A}(\mathbf{x}_i)$ and $\mathbf{B}_i = \mathbf{B}(\mathbf{x}_i)$. We can look at the term $\mathbf{A}_i \cdot \mathbf{p}_i$, with $\mathbf{A} = \frac{1}{2}\mathbf{B} \times \mathbf{r}$, we have $\frac{q_i}{2m_i} \mathbf{A}_i \cdot \mathbf{p}_i = \frac{q_i}{2m_i} \mathbf{B}_i \cdot \mathbf{L}_i$ with $\mathbf{L}_i = \mathbf{r}_i \times \mathbf{p}_i$ is the orbital angular momentum of particle i . So this term is actually the interaction energy of the magnetic moment from the orbital angular momentum in a magnetic field. Similarly there should also be a term $g_i \frac{q_i}{2m_i} \boldsymbol{\sigma} \cdot \mathbf{B}_i$ for spin angular momentum $\boldsymbol{\sigma}$ if the particle has spin, where g_i is the g-factor of the particle's spin magnetic moment. For neutrons with $q_i = 0$, the spin magnetic moment would be vanishing which is not true, in order to avoid this problem, we can write the spin magnetic moment term as $g_i \frac{e}{2m_i} \boldsymbol{\sigma} \cdot \mathbf{B}_i$ where e is the absolute value of the electron charge, all information of the magnetic moment is contained in g_i .

The electromagnetic energy is denoted as H_{em} ,

$$H_{\text{em}} = \frac{1}{8\pi} \int d^3x (\mathbf{E}^2 + \mathbf{B}^2) \tag{3.173}$$

where $\mathbf{E} = \mathbf{E}_L + \mathbf{E}_T$ is the full electric field. The electric part of the electromagnetic is

$$\begin{aligned}
 \frac{1}{8\pi} \int d^3x \mathbf{E}^2 &= \frac{1}{8\pi} \int d^3x (\mathbf{E}_L + \mathbf{E}_T)^2 \\
 &= \frac{1}{8\pi} \int d^3x (\mathbf{E}_L^2 + \mathbf{E}_T^2) \\
 &= \frac{1}{2} \int d^3x d^3x' \frac{\rho(t, \mathbf{x})\rho(t, \mathbf{x}')}{|\mathbf{x} - \mathbf{x}'|} + \frac{1}{8\pi} \int d^3x \mathbf{E}_T^2
 \end{aligned} \tag{3.174}$$

In order to prove the above equation, we can use

$$\mathbf{E}_L = -\nabla\phi, \quad \mathbf{E}_T = -\frac{\partial \mathbf{A}}{\partial t} \tag{3.175}$$

and the Coulomb gauge condition $\nabla \cdot \mathbf{A} = 0$. The mixed electric energy term for transverse and longitudinal electric fields can be proved to be vanishing,

$$\begin{aligned}
 \int d^3x \mathbf{E}_L \cdot \mathbf{E}_T &= \int d^3x (\nabla\phi) \cdot \frac{\partial \mathbf{A}}{\partial t} \\
 &= \int d^3x \nabla \cdot \left(\phi \frac{\partial \mathbf{A}}{\partial t} \right) - \int d^3x \phi \nabla \cdot \left(\frac{\partial \mathbf{A}}{\partial t} \right) \\
 &= \phi \frac{\partial \mathbf{A}}{\partial t} \Big|_{\text{boundary}} - \int d^3x \phi \frac{\partial}{\partial t} \nabla \cdot \mathbf{A} = 0
 \end{aligned} \tag{3.176}$$

using the Coulomb gauge condition. The longitudinal electric energy becomes

$$\begin{aligned}\int d^3x \mathbf{E}_L^2 &= \int d^3x (\nabla\phi)^2 = - \int d^3x \phi \nabla^2 \phi = 4\pi \int d^3x \phi \rho \\ &= 4\pi \int d^3x d^3x' \frac{1}{|\mathbf{x} - \mathbf{x}'|} \rho(t, \mathbf{x}) \rho(t, \mathbf{x}')\end{aligned}$$

where we have used

$$\phi(t, \mathbf{x}) = \int d^3x' \frac{\rho(t, \mathbf{x}')}{|\mathbf{x} - \mathbf{x}'|} \quad (3.177)$$

For discrete system of charged particles, we can further derive

$$\begin{aligned}\int d^3x \mathbf{E}_L^2 &= 4\pi \int d^3x d^3x' \frac{1}{|\mathbf{x} - \mathbf{x}'|} \sum_i q_i \delta(\mathbf{x} - \mathbf{x}_i) \sum_j q_j \delta(\mathbf{x}' - \mathbf{x}_j) \\ &= 4\pi \sum_{i \neq j} \frac{q_i q_j}{|\mathbf{x}_i - \mathbf{x}_j|}\end{aligned} \quad (3.178)$$

where we have used

$$\rho(t, \mathbf{x}) = \sum_i q_i \delta(\mathbf{x} - \mathbf{x}_i) \quad (3.179)$$

So we can define the Coulomb part of electric energy H_C which comes from the longitudinal electric field,

$$H_C = \frac{1}{2} \sum_{i \neq j} \frac{q_i q_j}{|\mathbf{x}_i - \mathbf{x}_j|} \quad (3.180)$$

Therefore, we can summarize the total Hamiltonian as

$$H = H_m + H_{em} = H_0 + H_I + H_C + H_{rad} \quad (3.181)$$

where

$$\begin{aligned}H_0 &= \sum_i \frac{1}{2m_i} \mathbf{p}_i^2 \\ H_I &= - \sum_i \frac{q_i}{m_i} \mathbf{A}_i \cdot \mathbf{p}_i + \sum_i \frac{q_i^2}{2m_i} \mathbf{A}_i^2 - \sum_i g_i \frac{e}{2m_i} \boldsymbol{\sigma} \cdot \mathbf{B}_i \\ H_C &= \frac{1}{2} \sum_{i \neq j} \frac{q_i q_j}{|\mathbf{x}_i - \mathbf{x}_j|} \\ H_{rad} &= \frac{1}{8\pi} \int d^3x (\mathbf{E}_T^2 + \mathbf{B}^2)\end{aligned} \quad (3.182)$$

Here we have added a spin-magnetic-field coupling term into H_I .

Let us calculate the transition amplitude of an atom or a nucleus between two energy states of electrons or nuclear by absorption or emission of one photon, $a \rightarrow b + \gamma$, through the coupling $\mathbf{A}_i \cdot \mathbf{p}_i$. The initial/final states for atom or nucleus and photons are as follows

$$\begin{aligned}\text{initial} &= |a\rangle |n(s, \mathbf{k})\rangle \\ \text{final} &= |b\rangle |n(s, \mathbf{k}) \pm 1\rangle\end{aligned} \quad (3.183)$$

The transition amplitude is then

$$\begin{aligned}M_{fi} &= \langle b, n(s, \mathbf{k}) \pm 1 | H_I | a, n(s, \mathbf{k}) \rangle \\ &= i \sum_i \frac{q_i}{m_i} \langle b, n(s, \mathbf{k}) \pm 1 | \mathbf{A}_i \cdot \nabla_i | a, n(s, \mathbf{k}) \rangle\end{aligned} \quad (3.184)$$

Note that we have neglected \mathbf{A}^2 term since it is of quadratic order in the electric charge.

First we consider the photon emission case. Inserting Eq. (3.164) into Eq. (3.184), we obtain the amplitude for photon emission,

$$\begin{aligned}
 M_{fi} &= i \sum_{\mathbf{k}_1, s_1} \left(\frac{2\pi}{V\omega_{k_1}} \right)^{1/2} \langle n(s, \mathbf{k}) + 1 | a^\dagger(s_1, \mathbf{k}_1) | n(s, \mathbf{k}) \rangle \\
 &\quad \times \boldsymbol{\epsilon}(s_1, \mathbf{k}_1) \cdot \langle b | \sum_i \frac{q_i}{m_i} e^{i\omega_{k_1}t - i\mathbf{k}_1 \cdot \mathbf{x}_i} \nabla_i | a \rangle \\
 &= i \left(\frac{2\pi}{V\omega_k} \right)^{1/2} \sqrt{n(s, \mathbf{k}) + 1} \boldsymbol{\epsilon}(s, \mathbf{k}) \cdot \langle b | \sum_i \frac{q_i}{m_i} e^{i\omega_k t - i\mathbf{k} \cdot \mathbf{x}_i} \nabla_i | a \rangle
 \end{aligned} \tag{3.185}$$

Following the Fermi golden rule, we obtain the transition rate by taking an integral over the photon momentum and a sum over the photon spin state,

$$\begin{aligned}
 \lambda_{a \rightarrow b + \gamma} &= 2\pi \int \frac{V d^3 k}{(2\pi)^3} \delta(E_b + \omega_k - E_a) \sum_{s=\pm} |M_{fi}|^2 \\
 &= \frac{1}{2\pi} \int d\Omega_k dk \delta(E_b + \omega_k - E_a) \omega_k \sum_{s=\pm} [n(s, \mathbf{k}) + 1] \\
 &\quad \times \left| \boldsymbol{\epsilon}(s, \mathbf{k}) \cdot \langle b | \sum_i \frac{q_i}{m_i} e^{-i\mathbf{k} \cdot \mathbf{x}_i} \nabla_i | a \rangle \right|^2
 \end{aligned} \tag{3.186}$$

After completing the integration over the photon energy to remove the energy conservation delta function, we arrive at

$$\begin{aligned}
 \lambda_{a \rightarrow b + \gamma} &= \frac{\omega_k}{2\pi} [\bar{n}(\mathbf{k}) + 1] \sum_{s=\pm 1} \int d\Omega_k \\
 &\quad \times \left| \boldsymbol{\epsilon}(s, \mathbf{k}) \cdot \langle b | \sum_i \frac{q_i}{m_i} e^{-i\mathbf{k} \cdot \mathbf{x}_i} \nabla_i | a \rangle \right|^2
 \end{aligned} \tag{3.187}$$

where we have used $\omega_k = E_a - E_b = |\mathbf{k}|$ and $\bar{n}(\mathbf{k}) = (1/2) \sum_{s=\pm} n(s, \mathbf{k})$.

For photon absorption $b + \gamma \rightarrow a$, we derive a similar formula

$$\begin{aligned}
 M_{fi} &= i \sum_{\mathbf{k}_1, s_1} \left(\frac{2\pi}{V\omega_{k_1}} \right)^{1/2} \langle n(s, \mathbf{k}) - 1 | a(s_1, \mathbf{k}_1) | n(s, \mathbf{k}) \rangle \\
 &\quad \times \boldsymbol{\epsilon}(s_1, \mathbf{k}_1) \cdot \langle a | \sum_i \frac{q_i}{m_i} e^{-i\omega_{k_1}t + i\mathbf{k}_1 \cdot \mathbf{x}_i} \nabla_i | b \rangle \\
 &= i \left(\frac{2\pi}{V\omega_k} \right)^{1/2} \sqrt{n(s, \mathbf{k})} \boldsymbol{\epsilon}(s, \mathbf{k}) \cdot \langle a | \sum_i \frac{q_i}{m_i} e^{-i\omega_k t + i\mathbf{k} \cdot \mathbf{x}_i} \nabla_i | b \rangle
 \end{aligned} \tag{3.188}$$

The transition rate reads,

$$\begin{aligned}
 \lambda_{b + \gamma \rightarrow a} &= 2\pi \int \frac{V d^3 k}{(2\pi)^3} \delta(E_b + \omega_k - E_a) \sum_{s=\pm} |M_{fi}|^2 \\
 &= \frac{1}{2\pi} d\Omega_k dk \delta(E_b + \omega_k - E_a) \omega_k \bar{n}(\mathbf{k}) \\
 &\quad \times \sum_{s=\pm 1} \left| \boldsymbol{\epsilon}(s, \mathbf{k}) \cdot \langle a | \sum_i \frac{q_i}{m_i} e^{i\mathbf{k} \cdot \mathbf{x}_i} \nabla_i | b \rangle \right|^2
 \end{aligned} \tag{3.189}$$

which has the following form after completing the integration over the photon energy

$$\lambda_{b+\gamma\rightarrow a} = \frac{\omega_k}{2\pi} \bar{n}(\mathbf{k}) \sum_{s=\pm 1} \int d\Omega_k \times \left| \boldsymbol{\epsilon}(s, \mathbf{k}) \cdot \langle a | \sum_i \frac{q_i}{m_i} e^{i\mathbf{k}\cdot\mathbf{x}_i} \nabla_i | b \rangle \right|^2 \quad (3.190)$$

Now we look at the simplest case, the electric dipole radiation at the long wave length limit. At this limit the wavelength of radiation is much larger than the size of the atom or the nucleus, so we can approximate $\mathbf{k}\cdot\mathbf{x} \approx 0$ or $e^{-i\mathbf{k}\cdot\mathbf{x}} \approx 1$. Then the matrix element in Eq. (3.187) can be put into the form,

$$\langle b | \sum_i \frac{q_i}{m_i} \nabla_i | a \rangle = \omega_k \langle b | \sum_i q_i \mathbf{x}_i | a \rangle \equiv \omega_k \mathbf{D}_{ba} \quad (3.191)$$

where we have defined the electric dipole moment $\mathbf{D}_{ba} = \langle b | \sum_i q_i \mathbf{x}_i | a \rangle$. Here we have used

$$\nabla = i\mathbf{p} = im \frac{d\mathbf{x}}{dt} = m[\mathbf{x}, \hat{H}_0] \quad (3.192)$$

Then the photon emission/absorption rate in Eqs. (3.187,3.190) becomes

$$\begin{aligned} \lambda_{a\rightarrow b+\gamma} &= \frac{\omega_k^3}{2\pi} [\bar{n}(\mathbf{k}) + 1] \sum_{s=\pm 1} \int d\Omega_k |\boldsymbol{\epsilon}(s, \mathbf{k}) \cdot \mathbf{D}_{ba}|^2 \\ \lambda_{b+\gamma\rightarrow a} &= \frac{\omega_k^3}{2\pi} \bar{n}(\mathbf{k}) \sum_{s=\pm 1} \int d\Omega_k |\boldsymbol{\epsilon}(s, \mathbf{k}) \cdot \mathbf{D}_{ab}|^2 \end{aligned} \quad (3.193)$$

Note that we have $|\mathbf{D}_{ab}|^2 = |\mathbf{D}_{ba}^*|^2$. If there is no other photons in the environment, we can set $\bar{n}(\mathbf{k}) = 0(1)$ for the process $a \rightarrow b + \gamma$ ($b + \gamma \rightarrow a$), the above rates become

$$\lambda_{a\rightarrow b+\gamma} = \lambda_{b+\gamma\rightarrow a} = \frac{\omega_k^3}{2\pi} \sum_{s=\pm 1} \int d\Omega_k |\boldsymbol{\epsilon}(s, \mathbf{k}) \cdot \mathbf{D}_{ba}|^2 \quad (3.194)$$

The power of radiation is given by,

$$I_\omega = \lambda_{a\rightarrow b+\gamma} \omega_k = \frac{\omega_k^4}{2\pi} \sum_{s=\pm 1} \int d\Omega_k |\boldsymbol{\epsilon}(s, \mathbf{k}) \cdot \mathbf{D}_{ba}|^2 \quad (3.195)$$

Suppose the photon is emitted along the z-axis (\mathbf{k} is along the z-axis) and \mathbf{D}_{ba} is in the plane of $\boldsymbol{\epsilon}(1, \mathbf{k})$ and \mathbf{k} , so \mathbf{D}_{ba} is perpendicular to $\boldsymbol{\epsilon}(2, \mathbf{k})$. Suppose the angle between \mathbf{D}_{ba} and \mathbf{k} is θ , the above integral of matrix element becomes

$$\begin{aligned} \sum_{s=\pm 1} \int d\Omega_k |\boldsymbol{\epsilon}(s, \mathbf{k}) \cdot \mathbf{D}_{ba}|^2 &= \int d\Omega_k |\boldsymbol{\epsilon}(1, \mathbf{k}) \cdot \mathbf{D}_{ba}|^2 \\ &= \int d\Omega_k |\mathbf{D}_{ba}|^2 \sin^2 \theta = \frac{8\pi}{3} |\mathbf{D}_{ba}|^2 \end{aligned} \quad (3.196)$$

So the radiation power turns out to be

$$I_\omega = \frac{4}{3} \omega_k^4 |\mathbf{D}_{ba}|^2 \quad (3.197)$$

which is consistent to the result of classical electrodynamics.

We now look at the electric quadrupole radiation by considering the linear order term $\sim \mathbf{k} \cdot \mathbf{x}$ in the phase factor $e^{-i\mathbf{k} \cdot \mathbf{x}}$ in Eq. (3.187). For simplicity of notation, we suppress the subscript i which labels the charged particles, and we have

$$\frac{q}{m}(\mathbf{k} \cdot \mathbf{x})(\boldsymbol{\epsilon} \cdot \mathbf{p}) = C_+ + C_- \quad (3.198)$$

where C_{\pm} is defined by

$$C_{\pm} \equiv \frac{q}{2m}[(\mathbf{k} \cdot \mathbf{x})(\boldsymbol{\epsilon} \cdot \mathbf{p}) \pm (\mathbf{k} \cdot \mathbf{p})(\boldsymbol{\epsilon} \cdot \mathbf{x})] \quad (3.199)$$

We focus on C_+ which corresponds to quadrupole radiation,

$$\begin{aligned} C_+ &= \frac{q}{2m}[(\mathbf{k} \cdot \mathbf{x})(\boldsymbol{\epsilon} \cdot \mathbf{p}) + (\mathbf{k} \cdot \mathbf{p})(\boldsymbol{\epsilon} \cdot \mathbf{x})] \\ &= \frac{q}{2}[(\mathbf{k} \cdot \mathbf{x})\boldsymbol{\epsilon} \cdot \frac{d\mathbf{x}}{dt} + (\mathbf{k} \cdot \frac{d\mathbf{x}}{dt})(\boldsymbol{\epsilon} \cdot \mathbf{x})] \\ &= \frac{1}{6}q \frac{d}{dt}[3(\mathbf{k} \cdot \mathbf{x})(\boldsymbol{\epsilon} \cdot \mathbf{x}) - \mathbf{x}^2(\boldsymbol{\epsilon} \cdot \mathbf{k})] \\ &= \frac{1}{6}\epsilon_i k_j \frac{d}{dt} Q_{ij} = -i \frac{1}{6}\epsilon_i k_j [Q_{ij}, \hat{H}_0] \end{aligned} \quad (3.200)$$

where we used $\boldsymbol{\epsilon} \cdot \mathbf{k} = 0$ and we have defined $Q_{ij} = q(3x_i x_j - x^2 \delta_{ij})$. We have also used the Schrodinger equation for the operator O , $i \frac{d}{dt} O = [O, \hat{H}_0]$. Substituting Eq. (3.200) into Eq. (3.187) and setting $\bar{n}(\mathbf{k}) = 0$, we obtain the emission rate

$$\begin{aligned} \lambda_{\mathbf{a} \rightarrow \mathbf{b} + \gamma} &= \frac{\omega_k}{72\pi} \sum_{s=\pm 1} \int d\Omega_k \left| \epsilon_i(\mathbf{k}, s) k_j \langle \mathbf{b} | \sum_n [Q_{ij}^{(n)}, H_0] | \mathbf{a} \rangle \right|^2 \\ &= \frac{\omega_k^3}{72\pi} \sum_{s=\pm 1} \int d\Omega_k \left| \epsilon_i(\mathbf{k}, s) k_j \langle \mathbf{b} | \sum_n Q_{ij}^{(n)} | \mathbf{a} \rangle \right|^2 \end{aligned} \quad (3.201)$$

where n labels all charged particles in the system. This gives the electric quadrupole transition rate. The absorption rate can be similarly derived from Eq. (3.190).

Let us look at the C_- term in Eq. (3.199),

$$\begin{aligned} C_- &= \frac{q}{2m}[(\mathbf{k} \cdot \mathbf{x})(\boldsymbol{\epsilon} \cdot \mathbf{p}) - (\mathbf{k} \cdot \mathbf{p})(\boldsymbol{\epsilon} \cdot \mathbf{x})] = \frac{q}{2m}(\mathbf{k} \times \boldsymbol{\epsilon}) \cdot (\mathbf{x} \times \mathbf{p}) \\ &= (\mathbf{k} \times \boldsymbol{\epsilon}) \cdot \boldsymbol{\mu}_L \end{aligned}$$

Note that $\mathbf{k} \times \boldsymbol{\epsilon}$ comes from $\mathbf{B} = \nabla \times \mathbf{A}$, so $C_- \sim -\boldsymbol{\mu}_L \cdot \mathbf{B}$ is from the interaction of magnetic moment in magnetic field. So this term corresponds to the magnetic dipole transition. If the particle has spin, there is also a term $(\mathbf{k} \times \boldsymbol{\epsilon}) \cdot \boldsymbol{\mu}_S$. So we can combine $\boldsymbol{\mu}_S$ and $\boldsymbol{\mu}_L$ and write the term as

$$C_- \rightarrow (\mathbf{k} \times \boldsymbol{\epsilon}) \cdot (\boldsymbol{\mu}_L + \boldsymbol{\mu}_S) \quad (3.202)$$

We then obtain the magnetic dipole transition rate from

$$\lambda_{\mathbf{a} \rightarrow \mathbf{b} + \gamma} = \frac{\omega_k^3}{2\pi} \sum_{s=\pm 1} \int d\Omega_k \left| [\hat{\mathbf{k}} \times \boldsymbol{\epsilon}(\mathbf{k}, s)] \cdot \langle \mathbf{b} | \sum_n (\boldsymbol{\mu}_L^{(n)} + \boldsymbol{\mu}_S^{(n)}) | \mathbf{a} \rangle \right|^2 \quad (3.203)$$

where n labels all charged particles in the system.

From Eq. (3.193) we further obtain

$$\frac{\lambda_{\mathbf{a} \rightarrow \mathbf{b} + \gamma}}{\lambda_{\mathbf{b} + \gamma \rightarrow \mathbf{a}}} = \frac{\bar{n}(\mathbf{k}) + 1}{\bar{n}(\mathbf{k})} \quad (3.204)$$

If we assume equilibrium,

$$N(A)\lambda_{a\rightarrow b} = N(B)\lambda_{b\rightarrow a} \quad (3.205)$$

then we have $N(a) \propto e^{-E_a/T}$ and $N(b) \propto e^{-E_b/T}$,

$$\begin{aligned} \frac{N(a)}{N(b)} &= \frac{\bar{n}(\mathbf{k})}{\bar{n}(\mathbf{k}) + 1} = e^{-\omega_k/T} \\ \bar{n}(\mathbf{k}) &= \frac{1}{e^{\omega_k/T} - 1} \end{aligned} \quad (3.206)$$

which is Bose-Einstein distribution.

3.5.4 Multipole expansion

Let's first look at electric and magnetic dipole radiation. A static electric dipole is made up of two opposite charges ($q, -q$) separated by a distance d along the z -axis. The electric dipole moment is $D_E = qd$. Suppose it is oscillating in time, $D_E = qd \cos(\omega t)$, it will induce an electric current I in the z -direction which produces a magnetic field tangent to the circle parallel to the xy -plane and centered along the z -axis. So the magnetic field is perpendicular to the coordinate vector \mathbf{x} , i.e. $\mathbf{x} \cdot \mathbf{B}_{(E)} = 0$. The electric field is determined by $\mathbf{E}_{(E)} = \mathbf{B}_{(E)} \times \hat{\mathbf{k}}$ with \mathbf{k} the wave vector. An oscillating magnetic moment is expressed as $D_M = Ia \cos(\omega t)$ where I and a denote the electric current density and the area of a coil. Similarly it will induce a circular electric field perpendicular to the coordinate vector \mathbf{x} , i.e. $\mathbf{x} \cdot \mathbf{E}_{(M)} = 0$. The magnetic field is determined by $\mathbf{B}_{(M)} = \hat{\mathbf{k}} \times \mathbf{E}_{(M)}$. See Fig. 3.22.

Both electric and magnetic dipole radiation give the same power distribution but radiation fields have opposite parity under the transformation $\mathbf{x} \rightarrow -\mathbf{x}$. The electric dipole moment is odd under the transformation, therefore the magnetic field it induces changes sign, i.e. $\mathbf{B}_{(E)}(-\mathbf{x}) = -\mathbf{B}_{(E)}(\mathbf{x})$, $\mathbf{E}_{(E)}(-\mathbf{x}) = -\mathbf{E}_{(E)}(\mathbf{x})$. The magnetic dipole moment is even under the transformation $\mathbf{x} \rightarrow -\mathbf{x}$, so the fields do not change sign, i.e. $\mathbf{B}_{(M)}(-\mathbf{x}) = \mathbf{B}_{(M)}(\mathbf{x})$, $\mathbf{E}_{(M)}(-\mathbf{x}) = \mathbf{E}_{(M)}(\mathbf{x})$.

The wave equation for the vector potential in free space reads

$$\frac{1}{c^2} \frac{\partial^2 \mathbf{A}}{\partial t^2} - \nabla^2 \mathbf{A} = 0 \quad (3.207)$$

Let us assume that the vector potential has an oscillating part of the form of $e^{-i\omega t}$. The wave equation becomes

$$(\nabla^2 + k^2)\mathbf{A}(k, \mathbf{x}) = 0 \quad (3.208)$$

where $k \equiv |\mathbf{k}| = \omega$ and ∇^2 is given by

$$\begin{aligned} \nabla^2 &= \frac{1}{r^2} \frac{\partial}{\partial r} \left(r^2 \frac{\partial}{\partial r} \right) - \frac{1}{r^2} \hat{L}^2 \\ \hat{L} &= -i\mathbf{x} \times \nabla \\ \hat{L}^2 &= - \left[\frac{1}{\sin \theta} \frac{\partial}{\partial \theta} \left(\sin \theta \frac{\partial}{\partial \theta} \right) + \frac{1}{\sin^2 \theta} \frac{\partial^2}{\partial \phi^2} \right] \end{aligned}$$

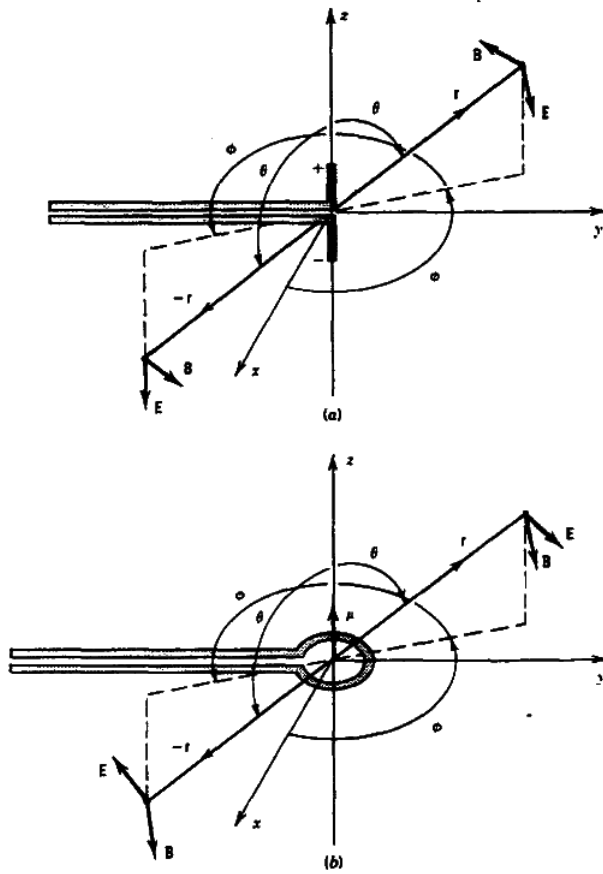
Here \hat{L} is the angular momentum operator and can be written as

$$\hat{L} = \sum_{n=0, \pm 1} \hat{L}_n \mathbf{e}_{-n} \quad (3.209)$$

where $\hat{L}_{\pm} = (\hat{L}_x \pm i\hat{L}_y)/\sqrt{2}$ are operator that can raise or lower the magnetic quantum number,

$$\hat{L}_{\pm} Y_{LM} = \frac{1}{\sqrt{2}} \sqrt{(L \mp M)(L \pm M + 1)} Y_{L, M \pm 1} \quad (3.210)$$

Figure 3.22: Electric and magnetic dipole radiation. Taken from page 329 of Ref. [4].



and $\mathbf{e}_{\pm 1} = \frac{1}{\sqrt{2}}(\mathbf{e}_x \pm i\mathbf{e}_y)$, $\mathbf{e}_0 = \mathbf{e}_z$ and $\hat{L}_0 = \hat{L}_z$. So we obtain

$$\begin{aligned}
\hat{\mathbf{L}}Y_{LM} &= \sum_{n=0,\pm 1} \hat{L}_n Y_{LM} \mathbf{e}_{-n} \\
&= \frac{1}{\sqrt{2}} \sqrt{(L-M)(L+M+1)} Y_{L,M+1} \mathbf{e}_{-1} \\
&\quad - \frac{1}{\sqrt{2}} \sqrt{(L+M)(L-M+1)} Y_{L,M-1} \mathbf{e}_1 + M Y_{L,M} \mathbf{e}_z \\
&= \sqrt{L(L+1)} \sum_{n=0,\pm 1} C_{L,M+n;1,-n}^{LM} Y_{L,M+n} \mathbf{e}_{-n}
\end{aligned} \tag{3.211}$$

Any function can be expanded as,

$$F(\mathbf{x}) = \sum_{L,M} f_L(r) Y_{LM}(\theta, \phi) \tag{3.212}$$

The radial part $f_L(r)$ satisfies the following equation

$$\left[\frac{d^2}{dr^2} + \frac{2}{r} \frac{d}{dr} + k^2 - \frac{L(L+1)}{r^2} \right] f_L(r) = 0$$

Using the replacement $f_L(r) = u_L(r)/r^{1/2}$, the above equation can be simplified as

$$\left[\frac{d^2}{dr^2} + \frac{1}{r} \frac{d}{dr} + k^2 - \frac{(L+1/2)^2}{r^2} \right] u_L(r) = 0 \tag{3.213}$$

Its solution is the Bessel function with $\nu = 1 + 1/2$. Then the radial part $f_L(r)$ has the following solution

$$\begin{aligned}
f_L(r) &= C_{LM}^{(1)} h_L^{(1)}(r) + C_{LM}^{(2)} h_L^{(2)}(r) \\
&= (C_{LM}^{(1)} + C_{LM}^{(2)}) j_L(r) + i(C_{LM}^{(1)} - C_{LM}^{(2)}) n_L(r)
\end{aligned} \tag{3.214}$$

where the coefficients $C_{LM}^{(i)}$ ($i = 1, 2$) can be determined by the boundary condition, and $h_L^{(1)}(x)$ and $h_L^{(2)}(x)$ are spherical Bessel functions of the third kind, see Appenix B.

Let us look at the multipole radiation in electrodynamics. Let us assume that all fields are oscillating in the form of $e^{-i\omega t}$. The Maxwell equations in vacuum read,

$$\begin{aligned}
\nabla \times \mathbf{E} &= ik\mathbf{B}, \\
\nabla \times \mathbf{B} &= -ik\mathbf{E}, \\
\nabla \cdot \mathbf{E} &= 0, \\
\nabla \cdot \mathbf{B} &= 0,
\end{aligned} \tag{3.215}$$

where $k = \omega$. We can derive the equations for \mathbf{E} and \mathbf{B} respectively,

$$\begin{aligned}
(\nabla^2 + k^2)\mathbf{B} &= 0, \quad \nabla \cdot \mathbf{B} = 0, \\
\text{with } \mathbf{E} &= \frac{i}{k} \nabla \times \mathbf{B}, \\
(\nabla^2 + k^2)\mathbf{E} &= 0, \quad \nabla \cdot \mathbf{E} = 0, \\
\text{with } \mathbf{B} &= -\frac{i}{k} \nabla \times \mathbf{E}.
\end{aligned} \tag{3.216}$$

The electric and magnetic fields are related to the vector potential,

$$\mathbf{B} = \nabla \times \mathbf{A}, \quad \mathbf{E} = -\frac{\partial \mathbf{A}}{\partial t} \tag{3.217}$$

We can solve the vector potential and obtain all radiation fields from above. One way of solving Eq. (3.216) is to solve the wave equation for each component of \mathbf{E} or \mathbf{B} first and then insert all components into the transverse condition $\nabla \cdot \mathbf{E}$ or $\nabla \cdot \mathbf{B}$ respectively and select the final solution.

We will solve \mathbf{E} and \mathbf{B} in a different way. We have the following relations

$$\begin{aligned}(\nabla^2 + k^2)(\mathbf{x} \cdot \mathbf{B}) &= 0 \\ (\nabla^2 + k^2)(\mathbf{x} \cdot \mathbf{E}) &= 0\end{aligned}\quad (3.218)$$

where we have used

$$\begin{aligned}\nabla^2(\mathbf{x} \cdot \mathbf{B}) &= \partial_i[\partial_i(x_j B_j)] = \partial_i[(\partial_i x_j)B_j + (\partial_i B_j)x_j] \\ &= 2\partial_i B_i + (\partial_i \partial_i B_j)x_j = 2\nabla \cdot \mathbf{B} + \mathbf{x} \cdot \nabla^2 \mathbf{B}\end{aligned}\quad (3.219)$$

This combines the wave function and the transverse condition. We can define the magnetic multipole mode, or the transverse electric (TE) mode, of order (L, M) as follows

$$\begin{aligned}\mathbf{x} \cdot \mathbf{B}_{LM}^{(M)} &= \frac{L(L+1)}{k} g_L(kr) Y_{LM}(\theta, \phi) \\ \mathbf{x} \cdot \mathbf{E}_{LM}^{(M)} &= 0\end{aligned}\quad (3.220)$$

where $g_L(kr) = C_L^{(1)} h_L^{(1)}(kr) + C_L^{(2)} h_L^{(2)}(kr)$. From the last line of Eq. (3.216), we obtain the relation for the electric field,

$$\begin{aligned}\mathbf{x} \cdot \mathbf{B}_{LM}^{(M)} &= -\frac{i}{k} \mathbf{x} \cdot \nabla \times \mathbf{E}_{LM}^{(M)} = \frac{1}{k} \hat{\mathbf{L}} \cdot \mathbf{E}_{LM}^{(M)} \\ \hat{\mathbf{L}} \cdot \mathbf{E}_{LM}^{(M)} &= L(L+1) g_L(kr) Y_{LM}(\theta, \phi)\end{aligned}\quad (3.221)$$

Then we obtain the field of the TE or magnetic multipole mode,

$$\begin{aligned}\mathbf{E}_{LM}^{(M)} &= g_L(kr) \hat{\mathbf{L}} Y_{LM}(\theta, \phi) \\ \mathbf{B}_{LM}^{(M)} &= -\frac{i}{k} \nabla \times \mathbf{E}_{LM}^{(M)}\end{aligned}\quad (3.222)$$

Similarly the electric multipole mode, or the transverse magnetic (TM) mode, of order (L, M) satisfies the condition

$$\begin{aligned}\mathbf{x} \cdot \mathbf{E}_{LM}^{(E)} &= \frac{i}{k} \mathbf{x} \cdot \nabla \times \mathbf{B}_{LM}^{(E)} = -\frac{1}{k} \hat{\mathbf{L}} \cdot \mathbf{B}_{LM}^{(E)} \\ &\equiv -\frac{L(L+1)}{k} f_L(kr) Y_{LM}(\theta, \phi) \\ \mathbf{x} \cdot \mathbf{B}_{LM}^{(E)} &= 0\end{aligned}\quad (3.223)$$

The fields of the TM mode are given by

$$\begin{aligned}\mathbf{B}_{LM}^{(E)} &= f_L(kr) \hat{\mathbf{L}} Y_{LM}(\theta, \phi) \\ \mathbf{E}_{LM}^{(E)} &= \frac{i}{k} \nabla \times \mathbf{B}_{LM}^{(E)}\end{aligned}\quad (3.224)$$

It is convenient to use following normalized vector functions

$$\mathbf{X}_{LM}(\theta, \phi) = \frac{1}{\sqrt{L(L+1)}} \hat{\mathbf{L}} Y_{LM}(\theta, \phi)\quad (3.225)$$

which satisfy the normalization and orthogonality conditions

$$\begin{aligned}\int d\Omega \mathbf{X}_{L'M'}^* \cdot \mathbf{X}_{LM} &= \delta_{LL'} \delta_{MM'} \\ \int d\Omega \mathbf{X}_{L'M'}^* \cdot (\mathbf{r} \times \mathbf{X}_{LM}) &= 0\end{aligned}\quad (3.226)$$

So general solutions to Maxwell's equations in multipole expansion can be expressed by

$$\begin{aligned}\mathbf{E} &= \sum_{L,M} \left[\frac{i}{k} c_{(E)}(L, M) \nabla \times f_L(kr) \mathbf{X}_{LM} + c_{(M)}(L, M) g_L(kr) \mathbf{X}_{LM} \right] \\ \mathbf{B} &= \sum_{L,M} \left[c_{(E)}(L, M) f_L(kr) \mathbf{X}_{LM} - \frac{i}{k} c_{(M)}(L, M) \nabla \times g_L(kr) \mathbf{X}_{LM} \right]\end{aligned}\quad (3.227)$$

The vector potential can be obtained by $\mathbf{E} = -\partial \mathbf{A} / \partial t = ik \mathbf{A}$,

$$\begin{aligned}\mathbf{A} &= \sum_{L,M} \left[\frac{1}{k^2} c_{(E)}(L, M) \nabla \times f_L(kr) \mathbf{X}_{LM} - \frac{i}{k} c_{(M)}(L, M) g_L(kr) \mathbf{X}_{LM} \right] \\ &= \sum_{L,M} [a_{(E)}(L, M) \mathbf{A}_{LM}^{(E)}(k, \mathbf{x}) + a_{(M)}(L, M) \mathbf{A}_{LM}^{(M)}(k, \mathbf{x})]\end{aligned}\quad (3.228)$$

In Eqs. (3.227, 3.228) $a_{(E),(M)}$ and $c_{(E),(M)}$ are all expansion coefficients. We can verify that the above vector potential really satisfies $\mathbf{B} = \nabla \times \mathbf{A}$. We can check this. The second term does obviously obey $\mathbf{B} = \nabla \times \mathbf{A}$, so does the first term since

$$\begin{aligned}\nabla \times \{\nabla \times [f_L(kr) \mathbf{X}_{LM}]\} &= \nabla(\nabla \cdot [f_L(kr) \mathbf{X}_{LM}]) - \nabla^2 [f_L(kr) \mathbf{X}_{LM}] \\ &= k^2 f_L(kr) \mathbf{X}_{LM}\end{aligned}\quad (3.229)$$

where we have used $(\nabla^2 + k^2)[f_L(kr) \mathbf{X}_{LM}] = 0$. We can choose $f_L(kr) = g_L(kr)$ by re-defining $c_{(E)}$ and $c_{(M)}$, then we have

$$\mathbf{A}_{LM}^{(E)}(k, \mathbf{x}) = \frac{i}{k} \nabla \times \mathbf{A}_{LM}^{(M)}(k, \mathbf{x}) \quad (3.230)$$

In proper normalization, the vector potential of a TE mode is given by

$$\mathbf{A}_{LM}^{(M)} = k \sqrt{\frac{8\pi}{R_0}} \mathbf{X}_{LM}(\theta, \phi) j_L(kr) \quad (3.231)$$

where we have chosen $j_L(kr)$ for it fulfills the boundary condition $\mathbf{A}_{LM}^{(M)}(r=0)$ should be finite and $\mathbf{A}_{LM}^{(M)}(r \rightarrow \infty) = 0$. The parity of the magnetic multipole field is $(-1)^L$. Due to $\mathbf{x} \cdot \hat{\mathbf{L}} = 0$, we see that $\mathbf{A}_{LM}^{(M)}$ is perpendicular to \mathbf{x} . The normalization constant can be determined from

$$\begin{aligned}\int d^3x \mathbf{A}_{LM}^{(M)*} \cdot \mathbf{A}_{L'M'}^{(M)} &= \frac{8\pi k k'}{R_0} \int d\Omega \mathbf{X}_{LM}^* \cdot \mathbf{X}_{L'M'} \int dr r^2 j_L(kr) j_{L'}(k'r) \\ &= 4\pi \delta_{LL'} \delta_{MM'} \delta_{k,k'}\end{aligned}\quad (3.232)$$

where we have assumed for $kR_0 > kr \gg L$,

$$j_L(kr) \approx \frac{1}{kr} \sin(kr - \frac{\pi}{2}L) \quad (3.233)$$

The boundary condition

$$j_L(kR_0) = 0, \quad k_n R_0 - \frac{\pi}{2}L = n\pi \quad (3.234)$$

So we have

$$\begin{aligned} k^3 \int_0^{R_0} dr r^2 j_L^2(kr) &= \int_0^{kR_0} dy y^2 j_L^2(y) \\ &\approx \int_0^{kR_0} dy \sin^2(y - \frac{\pi}{2}L) = \frac{1}{2}kR_0 \end{aligned} \quad (3.235)$$

The the vector potential of a TM mode is obtained by Eq. (3.230),

$$\mathbf{A}_{LM}^{(E)}(k, \mathbf{x}) = \frac{i}{k} \nabla \times \mathbf{A}_{LM}^{(M)}(k, \mathbf{x}) = i \sqrt{\frac{8\pi}{R_0}} \nabla \times \mathbf{X}_{LM}(\theta, \phi) j_L(kr)$$

The parity of the electric multipole field is $(-1)^{L+1}$. The TE and TM modes are dual to each other,

$$\mathbf{E}_{LM}^{(E)} = \mathbf{B}_{LM}^{(M)}, \quad \mathbf{B}_{LM}^{(E)} = -\mathbf{E}_{LM}^{(M)} \quad (3.236)$$

The energy flows of both TE and TM modes are along \mathbf{x} .

Having the transverse radiation fields $\mathbf{A}_{LM}^{(E),(M)}$, we can write down the general solution by expansion and quantize it,

$$\begin{aligned} \mathbf{A}(t, \mathbf{x}) &= \sum_{L,M,k} \sum_{\sigma=(E),(M)} \frac{1}{\sqrt{2\omega}} [a_\sigma(k, L, M) \mathbf{A}_{LM}^\sigma(k, \mathbf{x}) e^{-i\omega t} \\ &\quad + a_\sigma^\dagger(k, L, M) \mathbf{A}_{LM}^{\sigma*}(k, \mathbf{x}) e^{i\omega t}] \end{aligned} \quad (3.237)$$

where a_σ and a_σ^\dagger are destruction and creation operators,

$$\begin{aligned} [a_\sigma(k, L, M), a_{\sigma'}^\dagger(k', L', M')] &= \delta_{\sigma,\sigma'} \delta_{LL'} \delta_{MM'} \delta_{kk'} \\ \text{all others} &= 0 \end{aligned} \quad (3.238)$$

The Hamiltonian for the radiation field is

$$\begin{aligned} H_{\text{rad}} &= \frac{1}{8\pi} \int d^3x (\mathbf{E}^2 + \mathbf{B}^2) = \frac{1}{8\pi} \int d^3x \left[\left(\frac{\partial \mathbf{A}}{\partial t} \right)^2 + (\nabla \times \mathbf{A})^2 \right] \\ &= \sum_{L,M,k,\sigma} k \left[a_\sigma^\dagger(k, L, M) a_\sigma(k, L, M) + \frac{1}{2} \right] \end{aligned} \quad (3.239)$$

Here we treat the nucleus as a single identity. The transition amplitude from the initial state to the final state is

$$\lambda = 2\pi |\langle b, 1 | H_I | a, 0 \rangle|^2 \rho(E_f) \quad (3.240)$$

where H_I is given by Eq. (3.182). Here $\rho(E_f)$ is the density of final states,

$$\rho(E_f) = \frac{dn}{dE_f} = \frac{R_0}{\pi} \quad (3.241)$$

where we have used Eq. (3.234).

For electric multipole radiation or TM mode the non-vanishing term in the matrix element $\langle b, 1 | H_I | a, 0 \rangle$ comes from the creation operator term in the vector field $\mathbf{A}(t, \mathbf{x})$ and magnetic field $\mathbf{B}(t, \mathbf{x})$,

$$\begin{aligned} \frac{1}{\sqrt{2\omega}} a_{(E)}^\dagger(k, L, M) \mathbf{A}_{LM}^{(E)*}(k, \mathbf{r}) &= -i a_{(E)}^\dagger(k, L, M) \sqrt{\frac{4\pi}{R_0\omega}} \nabla \times [\mathbf{X}_{LM}^*(\theta, \phi) j_L(kr)] \\ \frac{1}{\sqrt{2\omega}} a_{(E)}^\dagger(k, L, M) \mathbf{B}_{LM}^{(E)*}(k, \mathbf{r}) &= -i a_{(E)}^\dagger(k, L, M) \sqrt{\frac{4\pi}{R_0\omega}} \nabla \times \nabla \times [\mathbf{X}_{LM}^*(\theta, \phi) j_L(kr)] \end{aligned} \quad (3.242)$$

where

$$\begin{aligned}\mathbf{A}_{LM}^{(E)*}(k, \mathbf{r}) &= -i\sqrt{\frac{8\pi}{R_0}}\nabla \times [\mathbf{X}_{LM}^*(\theta, \phi)j_L(kr)] \\ \mathbf{B}_{LM}^{(E)*}(k, \mathbf{r}) &= \nabla \times \mathbf{A}_{LM}^{(E)*}(k, \mathbf{r})\end{aligned}\quad (3.243)$$

Substituting Eq. (3.242) into H_I in Eq. (3.182) and using Eq. (3.240), we obtain the amplitude for one charged particle (we suppressed the particle label in the charge and g-factor),

$$\begin{aligned}\langle b, 1 | H_I | a, 0 \rangle &= i\frac{1}{2m}\sqrt{\frac{4\pi}{R_0\omega L(L+1)}} \\ &\quad \times \left\{ eq \langle b | [\nabla \times (\hat{\mathbf{L}}^* Y_{LM}^* j_L)] \cdot (-i\nabla) + (-i\nabla) \cdot [\nabla \times (\hat{\mathbf{L}}^* Y_{LM}^* j_L)] | a \rangle \right. \\ &\quad \left. + eg \langle b | \boldsymbol{\sigma} \cdot \nabla \times [\nabla \times (\hat{\mathbf{L}}^* Y_{LM}^* j_L)] | a \rangle \right\} \\ &= i\frac{1}{2m}\sqrt{\frac{4\pi}{R_0\omega L(L+1)}} \\ &\quad \times \left\{ eq \langle b | [\nabla \times (\mathbf{x} \times \nabla Y_{LM}^* j_L)] \cdot \nabla + \nabla \cdot [\nabla \times (\mathbf{x} \times \nabla Y_{LM}^* j_L)] | a \rangle \right. \\ &\quad \left. + eg \langle b | \boldsymbol{\sigma} \cdot \nabla \times [\nabla \times (\hat{\mathbf{L}}^* Y_{LM}^* j_L)] | a \rangle \right\} \\ &= -i\sqrt{\frac{4\pi(L+1)}{R_0\omega L}} \frac{k^{L+1}}{(2L+1)!!} \\ &\quad \times \left\{ eq \langle b | r^L Y_{LM}^* | a \rangle + kg \frac{e}{2m} \frac{1}{L+1} \langle b | [\boldsymbol{\sigma} \cdot \hat{\mathbf{L}}(r^L Y_{LM}^*)] | a \rangle \right\} \\ &= -i\sqrt{\frac{4\pi(L+1)}{R_0\omega L}} \frac{k^{L+1}}{(2L+1)!!} (Q_{1,LM} + Q_{2,LM})\end{aligned}\quad (3.244)$$

Here we have assumed that there is only one charged particle in the system, we will add a sum over all particles in the end. We also assume that kr is very small, i.e. the photon wavelength is much smaller than nucleus size. We have defined

$$\begin{aligned}Q_{1,LM} &= eq \langle b | r^L Y_{LM}^* | a \rangle \\ Q_{2,LM} &= g \frac{e}{2m} \frac{k}{L+1} \langle b | [\boldsymbol{\sigma} \cdot \hat{\mathbf{L}}(r^L Y_{LM}^*)] | a \rangle\end{aligned}\quad (3.245)$$

We have used

$$\begin{aligned}&\psi_b^* [\nabla \times (\mathbf{x} \times \nabla Y_{LM}^* j_L)] \cdot \nabla \psi_a + \psi_b^* \nabla \cdot [\nabla \times (\mathbf{x} \times \nabla Y_{LM}^* j_L)] \psi_a \\ &= 2m \frac{(L+1)k^L}{(2L+1)!!} \psi_b^* \left\{ -\frac{\nabla^2}{2m} (r^L Y_{LM}^* \psi_a) - r^L Y_{LM}^* \left(-\frac{\nabla^2}{2m}\right) \psi_a \right\} \\ &= 2m \frac{(L+1)k^L}{(2L+1)!!} \psi_b^* \left\{ \left[-\frac{\nabla^2}{2m} + V(r)\right] r^L Y_{LM}^* - r^L Y_{LM}^* \left[-\frac{\nabla^2}{2m} + V(r)\right] \right\} \psi_a \\ &= -2m \frac{(L+1)k^L}{(2L+1)!!} (E_a - E_b) \psi_b^* r^L Y_{LM}^* \psi_a \\ &= -2m \frac{(L+1)k^{L+1}}{(2L+1)!!} \psi_b^* r^L Y_{LM}^* \psi_a\end{aligned}\quad (3.246)$$

and

$$\begin{aligned}
\boldsymbol{\sigma} \cdot \nabla \times [\nabla \times (\hat{\mathbf{L}}^* Y_{LM}^* j_L)] &= i\boldsymbol{\sigma} \cdot \nabla \times [\nabla \times (\mathbf{x} \times \nabla Y_{LM}^* j_L)] \\
&= i\boldsymbol{\sigma} \cdot \nabla \times [\mathbf{x} \nabla^2 (Y_{LM}^* j_L)] \\
&= -ik^2 \boldsymbol{\sigma} \cdot \nabla \times (\mathbf{x} Y_{LM}^* j_L) = ik^2 \boldsymbol{\sigma} \cdot [\mathbf{x} \times \nabla (Y_{LM}^* j_L)] \\
&\approx i \frac{k^{L+2}}{(2L+1)!!} (\boldsymbol{\sigma} \times \mathbf{x}) \cdot \nabla (r^L Y_{LM}^*) \\
&= -\frac{k^{L+2}}{(2L+1)!!} \boldsymbol{\sigma} \cdot \hat{\mathbf{L}} (r^L Y_{LM}^*)
\end{aligned} \tag{3.247}$$

Here in deriving the above two formula we have used

$$\begin{aligned}
&\psi_b^* [\nabla \times (\mathbf{x} \times \nabla Y_{LM}^* j_L)] \cdot \nabla \psi_a + \psi_b^* \nabla \cdot [\nabla \times (\mathbf{x} \times \nabla Y_{LM}^* j_L)] \psi_a \\
&\approx -\frac{(L+1)k^L}{(2L+1)!!} \{\psi_b^* [\nabla (r^L Y_{LM}^*)] \cdot \nabla \psi_a + \psi_b^* \nabla \cdot [\nabla (r^L Y_{LM}^*) \psi_a]\} \\
&= -\frac{(L+1)k^L}{(2L+1)!!} \{\psi_b^* [\nabla (r^L Y_{LM}^*)] \cdot \nabla \psi_a + \psi_b^* \nabla \cdot [\nabla (r^L Y_{LM}^* \psi_a) - r^L Y_{LM}^* \nabla \psi_a]\} \\
&= -\frac{(L+1)k^L}{(2L+1)!!} \{\psi_b^* [\nabla (r^L Y_{LM}^*)] \cdot \nabla \psi_a \\
&\quad + \psi_b^* [\nabla^2 (r^L Y_{LM}^* \psi_a) - \nabla (r^L Y_{LM}^*) \cdot \nabla \psi_a - r^L Y_{LM}^* \nabla^2 \psi_a]\} \\
&\quad - \frac{(L+1)k^L}{(2L+1)!!} \psi_b^* \{\nabla^2 r^L Y_{LM}^* - r^L Y_{LM}^* \nabla^2\} \psi_a
\end{aligned} \tag{3.248}$$

and

$$\begin{aligned}
j_L(kr) &\approx \frac{(kr)^L}{(2L+1)!!}, \quad \text{for } kr \ll 1 \\
x_j \partial_j \partial_h &= \partial_h x_j \partial_j - \partial_h \\
\nabla \times (\mathbf{x} \times \nabla Y_{LM}^* j_L) &= \mathbf{e}_h \epsilon_{hni} \epsilon_{ijk} \partial_n (x_j \partial_k Y_{LM}^* j_L) \\
&= \mathbf{e}_h \epsilon_{hni} \epsilon_{ijk} (\delta_{nj} \partial_k + x_j \partial_n \partial_k) Y_{LM}^* j_L \\
&= \mathbf{e}_h (\delta_{hj} \delta_{nk} - \delta_{hk} \delta_{nj}) (\delta_{nj} \partial_k + x_j \partial_n \partial_k) Y_{LM}^* j_L \\
&= \mathbf{e}_h (x_h \partial^2 - 2\partial_h - x_j \partial_j \partial_h) Y_{LM}^* j_L \\
&= \mathbf{e}_h [x_h \partial^2 - \partial_h (1 + x_j \partial_j)] Y_{LM}^* j_L \\
&= [\mathbf{x} \nabla^2 - \nabla (1 + r \partial_r)] Y_{LM}^* j_L \\
&= -\mathbf{x} k^2 Y_{LM}^* j_L - [\nabla (1 + r \partial_r) Y_{LM}^* j_L] \\
&\approx -\mathbf{x} \frac{k^2 (kr)^L}{(2L+1)!!} - \frac{(L+1)k^L}{(2L+1)!!} \nabla (r^L Y_{LM}^*) \\
&\approx -\frac{(L+1)k^L}{(2L+1)!!} \nabla (r^L Y_{LM}^*)
\end{aligned} \tag{3.249}$$

So the transition rate from the electric multipole field is

$$\begin{aligned}
\lambda_{(E)} &= 2\pi |\langle b, 1 | H_I | a, 0 \rangle|^2 \rho(E_f) \\
&= \frac{8\pi(L+1)}{L[(2L+1)!!]^2} k^{2L+1} \sum_{M_a, M_b, M} \frac{1}{2J_a + 1} |Q_{1,LM} + Q_{2,LM}|^2
\end{aligned} \tag{3.250}$$

where we have taken average over the initial states and sum over the final states. When we recover

the sum over all charged particles, $Q_{1(2),LM}$ are given by

$$\begin{aligned} Q_{1,LM} &= e \sum_i q_i \langle \mathbf{b} | r_i^L Y_{LM}^*(i) | \mathbf{a} \rangle \\ Q_{2,LM} &= \frac{k}{L+1} \sum_i g_i \frac{e}{2m_i} \langle \mathbf{b} | (\boldsymbol{\sigma}_i \cdot \hat{\mathbf{L}}_i) [r_i^L Y_{LM}^*(i)] | \mathbf{a} \rangle \end{aligned} \quad (3.251)$$

From spherical harmonics, $Y_{1,\pm 1}(\theta, \phi) = \mp \sqrt{3/8\pi} \sin \theta e^{\pm i\phi}$, $Y_{1,0}(\theta, \phi) = \sqrt{3/4\pi} \cos \theta$, we have

$$\begin{aligned} Q_{1;1,\pm 1} &= \mp \sqrt{\frac{3}{8\pi}} \left\langle \mathbf{b} \left| e \sum_i q_i (x_i \pm iy_i) \right| \mathbf{a} \right\rangle \\ Q_{1;1,0} &= \sqrt{\frac{3}{4\pi}} \left\langle \mathbf{b} \left| e \sum_i q_i z_i \right| \mathbf{a} \right\rangle \end{aligned} \quad (3.252)$$

If we neglect $Q_{2,LM}$, Eq. (3.250) becomes

$$\lambda_{(E1)} = \frac{4}{3} \omega_k^3 \sum_{M_a, M_b} \frac{1}{2J_a + 1} |\mathbf{D}_{ba}(M_b, M_a)|^2 \quad (3.253)$$

The power of radiation is then

$$I_{(E1)} = \frac{4}{3} \omega_k^4 \sum_{M_a, M_b} \frac{1}{2J_a + 1} |\mathbf{D}_{ba}(M_b, M_a)|^2 \quad (3.254)$$

which is the same as Eq. (3.197). From Eq. (3.251) we have $Q_1 = Q_2 = 0$ when $L = 0$, so there is no E0 transition.

Now we consider the magnetic multipole transition. The vector potential and magnetic fields for a L, M mode which appear in the creation operator term are given by

$$\begin{aligned} \mathbf{A}_{LM}^{(M)*}(k, \mathbf{r}) &= k \sqrt{\frac{8\pi}{R_0}} \mathbf{X}_{LM}^*(\theta, \phi) j_L(kr) \\ \mathbf{B}_{LM}^{(M)*}(k, \mathbf{r}) &= \nabla \times \mathbf{A}_{LM}^{(M)*}(k, \mathbf{r}) \end{aligned} \quad (3.255)$$

Then the creation operator terms in $\mathbf{A}(t, \mathbf{x})$ and magnetic field $\mathbf{B}(t, \mathbf{x})$ are given by

$$\begin{aligned} \frac{1}{\sqrt{2\omega}} a_{(M)}^\dagger(k, L, M) \mathbf{A}_{LM}^{(M)*}(k, \mathbf{r}) &= a_{(M)}^\dagger(k, L, M) \sqrt{\frac{4\pi}{R_0\omega}} \mathbf{X}_{LM}^*(\theta, \phi) j_L(kr) \\ \frac{1}{\sqrt{2\omega}} a_{(M)}^\dagger(k, L, M) \mathbf{B}_{LM}^{(M)*}(k, \mathbf{r}) &= a_{(M)}^\dagger(k, L, M) \sqrt{\frac{4\pi}{R_0\omega}} \nabla \times [\mathbf{X}_{LM}^*(\theta, \phi) j_L(kr)] \end{aligned} \quad (3.256)$$

Substituting the above into Eq. (3.240), we get the transition amplitude,

$$\begin{aligned}
\langle b, 1 | H_I | a, 0 \rangle &= -\frac{k}{2m} \sqrt{\frac{4\pi}{R_0 \omega L(L+1)}} \\
&\times \left\{ e q \langle b | (\hat{\mathbf{L}}^* Y_{LM}^* j_L) \cdot (-i\nabla) + (-i\nabla) \cdot (\hat{\mathbf{L}}^* Y_{LM}^* j_L) | a \rangle \right. \\
&\left. + e g \langle b | \boldsymbol{\sigma} \cdot [\nabla \times (\hat{\mathbf{L}}^* Y_{LM}^* j_L)] | a \rangle \right\} \\
&= -\frac{k}{2m} \sqrt{\frac{4\pi}{R_0 \omega L(L+1)}} \\
&\times \left\{ e q \langle b | (\mathbf{x} \times \nabla Y_{LM}^* j_L) \cdot \nabla + \nabla \cdot (\mathbf{x} \times \nabla Y_{LM}^* j_L) | a \rangle \right. \\
&\left. + e g \langle b | \boldsymbol{\sigma} \cdot [\nabla \times (\hat{\mathbf{L}}^* Y_{LM}^* j_L)] | a \rangle \right\} \\
&= -\frac{k}{2m} \sqrt{\frac{4\pi}{R_0 \omega L(L+1)}} \frac{k^L}{(2L+1)!!} \\
&\times \left\{ -2ieq \langle b | \hat{\mathbf{L}} \cdot \nabla (r^L Y_{LM}^*) | a \rangle - ieg(L+1) \langle b | \boldsymbol{\sigma} \cdot \nabla (r^L Y_{LM}^*) | a \rangle \right\} \\
&= i \sqrt{\frac{4\pi(L+1)}{R_0 \omega L}} \frac{k^{L+1}}{(2L+1)!!} (M_{1,LM} + M_{2,LM}) \tag{3.257}
\end{aligned}$$

Here we have used

$$\begin{aligned}
&\psi_b^* (\mathbf{x} \times \nabla Y_{LM}^* j_L) \cdot \nabla \psi_a + \psi_b^* \nabla \cdot (\mathbf{x} \times \nabla Y_{LM}^* j_L) \psi_a \\
&= 2\psi_b^* (\mathbf{x} \times \nabla Y_{LM}^* j_L) \cdot \nabla \psi_a = -2\psi_b^* (\nabla Y_{LM}^* j_L) \cdot (\mathbf{x} \times \nabla \psi_a) \\
&= 2\psi_b^* \nabla \cdot (\mathbf{x} \times \nabla Y_{LM}^* j_L) \psi_a \\
&= -2\psi_b^* \mathbf{x} \times \nabla \cdot [\nabla (Y_{LM}^* j_L) \psi_a] \tag{3.258}
\end{aligned}$$

$$\begin{aligned}
\boldsymbol{\sigma} \cdot [\nabla \times (\hat{\mathbf{L}}^* Y_{LM}^* j_L)] &= i\boldsymbol{\sigma} \cdot \{ \nabla \times [\mathbf{x} \times \nabla (Y_{LM}^* j_L)] \} \\
&\approx -i \frac{(L+1)k^L}{(2L+1)!!} \boldsymbol{\sigma} \cdot \nabla (r^L Y_{LM}^*) \tag{3.259}
\end{aligned}$$

The transition rate from the magnetic multipole field or TE mode is

$$\lambda_{(M)} = \frac{8\pi(L+1)}{L[(2L+1)!!]^2} k^{2L+1} \sum_{M_a, M_b, M} \frac{1}{2J_a+1} |M_{1,LM} + M_{2,LM}|^2 \tag{3.260}$$

where $M_{1,LM}$ and $M_{2,LM}$ are defined by

$$\begin{aligned}
M_{1,LM} &= \frac{1}{L+1} \sum_i \frac{eq_i}{m_i} \langle b | \hat{\mathbf{L}}_i \cdot \nabla_i [r_i^L Y_{LM}^*(i)] | a \rangle \\
&= \frac{1}{L+1} \sum_i \frac{eq_i}{m_i} \langle b | \{ \nabla_i [r_i^L Y_{LM}^*(i)] \} \cdot \hat{\mathbf{L}}_i | a \rangle \\
M_{2,LM} &= \sum_i g_i \frac{e}{2m_i} \langle b | \boldsymbol{\sigma}_i \cdot \nabla_i [r_i^L Y_{LM}^*(i)] | a \rangle \tag{3.261}
\end{aligned}$$

where we have recovered the sum over all charged particles. From Eq. (3.261) we have $M_1 = M_2 = 0$ for $L = 0$, so there is no M0 transition.

Let us estimate the magnitude of the transition. For the electric multipole field,

$$\begin{aligned}
Q_{1,LM} &= eq \langle b | r^L Y_{LM}^* | a \rangle \sim e \langle r^L \rangle \sim e \frac{\int dr r^{L+2}}{\int dr r^2} \sim e \frac{3}{L+3} R^L \\
Q_{2,LM} &= g \frac{e}{2m} \frac{k}{L+1} \langle b | (\boldsymbol{\sigma} \cdot \hat{\mathbf{L}}) (r^L Y_{LM}^*) | a \rangle \sim \frac{e\omega}{m} \frac{3}{2(L+1)(L+3)} R^L \tag{3.262}
\end{aligned}$$

For the nuclear γ decay, the ratio becomes

$$\frac{Q_{2,LM}}{Q_{1,LM}} \sim \frac{\omega}{m} \sim 10^{-3} \quad (3.263)$$

So we can neglect $Q_{2,LM}$ relative to $Q_{1,LM}$. For the magnetic multipole field, $M_{1,LM}$ and $M_{2,LM}$ are of the same order,

$$M_{1,LM} \sim M_{2,LM} \sim \frac{e}{m} R^{L-1} \quad (3.264)$$

The transitions of the higher order are much suppressed relative to the lower order,

$$\frac{\lambda_{(E)}(L+1)}{\lambda_{(E)}(L)} \sim \frac{\lambda_{(M)}(L+1)}{\lambda_{(M)}(L)} \sim k^2 R^2 \sim (\text{MeV} \cdot 10 \text{ fm})^2 \sim 2.5 \times 10^{-3} \quad (3.265)$$

The magnitude of the magnetic transition is suppressed relative to that of electric one of the same order,

$$\frac{\lambda_{(M)}(L)}{\lambda_{(E)}(L)} \sim \frac{1}{m^2 R^2} \sim \frac{1}{(1 \text{ GeV} \cdot 10 \text{ fm})^2} \sim 4 \times 10^{-4} \quad (3.266)$$

Then we can roughly have the relation $\lambda_{(E)}(L+1) \sim \lambda_{(M)}(L)$, i.e. E(L+1) radiation is comparable to ML one in magnitude.

Selection rules for parity are given as follows. The parity of the operators are know as

$$\begin{aligned} P(r^L Y_{LM}^*) &= (-1)^L \\ P[\mathbf{L} \cdot \nabla(r^L Y_{LM}^*)] &= P[\boldsymbol{\sigma} \cdot \nabla(r^L Y_{LM}^*)] = (-1)^{L-1} \end{aligned} \quad (3.267)$$

For EL and ML transitions

$$\begin{aligned} P_i P_f &= (-1)^L, \quad \text{EL} \\ P_i P_f &= (-1)^{L+1}, \quad \text{ML} \end{aligned} \quad (3.268)$$

where $P_{i,f}$ are parities for the initial and final states.

Selection rules for angular momentum. Following the Wigner-Eckart theorem,

$$\langle J_f, M_f | T_{LM} | J_i, M_i \rangle = C_{J_i M_i, LM}^{J_f M_f} \langle J_f || T_{LM} || J_i \rangle \quad (3.269)$$

where

$$T_{LM} = r^L Y_{LM}^*, \hat{\mathbf{L}} \cdot \nabla(r^L Y_{LM}^*), \boldsymbol{\sigma} \cdot \nabla(r^L Y_{LM}^*) \quad (3.270)$$

and $L \neq 0$ obeys that $\mathbf{J}_f, \mathbf{J}_i, \mathbf{L}$ form a vector triangle,

$$\begin{aligned} \mathbf{J}_f &= \mathbf{J}_i + \mathbf{L} \\ |J_i - J_f| &\leq L \leq |J_i + J_f| \end{aligned} \quad (3.271)$$

There is no transition with $J_i = J_f$ and $L = 0$ since there is no monopole transition. Note that the transition with $L = |J_i - J_f|$ is dominant.

The mixing only takes place between E(2L) and E(2L'), M(2L) and M(2L') or ML and E(L+1) [but not EL and M(L+1) due to the disparity of the two transition strengths]. For example, a transition $2^+ \rightarrow 1^+$ can be M1 or E2. From the parity conservation $(-1)^L / (-1)^{L+1}$ must be 1 for electric/magnetic field, so L must be even/odd for the electric/magnetic field. For angular momentum conservation, we have $L = 1, 2, 3$. So the possible transitions are M1, E2 or M3. The dominant transitions are M1 or E2.

Table 3.4: Selection rules for parity and angular momentum. Note that when

$ J_i - J_f $	0,1	2	3	4	5
$P_i P_f = +$	$M1(E2)$	$E2$	$M3(E4)$	$E4$	$M5(E6)$
$P_i P_f = -$	$E1$	$M2(E3)$	$E3$	$M4(E5)$	$E5$

Figure 3.23: Energy spectra of electrons from beta decay and internal conversion of radioactive nuclei. The peaks on top of continuous the spectrum are from internal conversion.

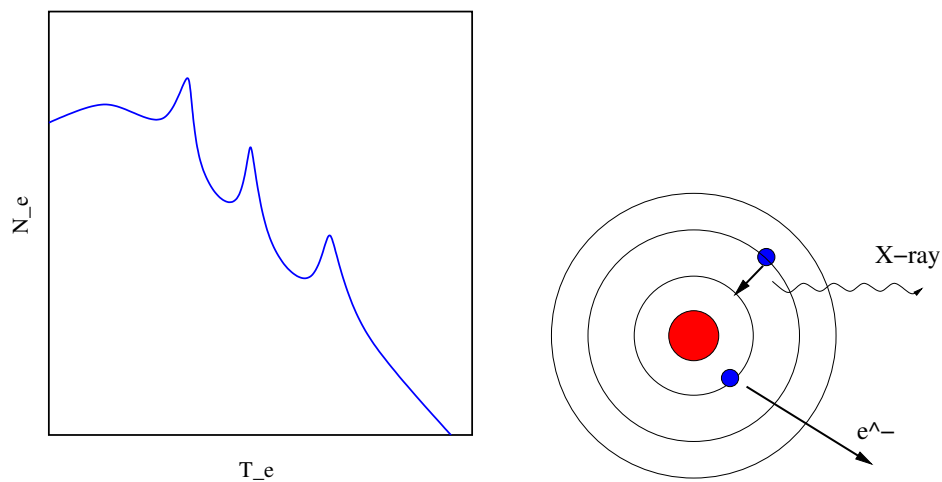
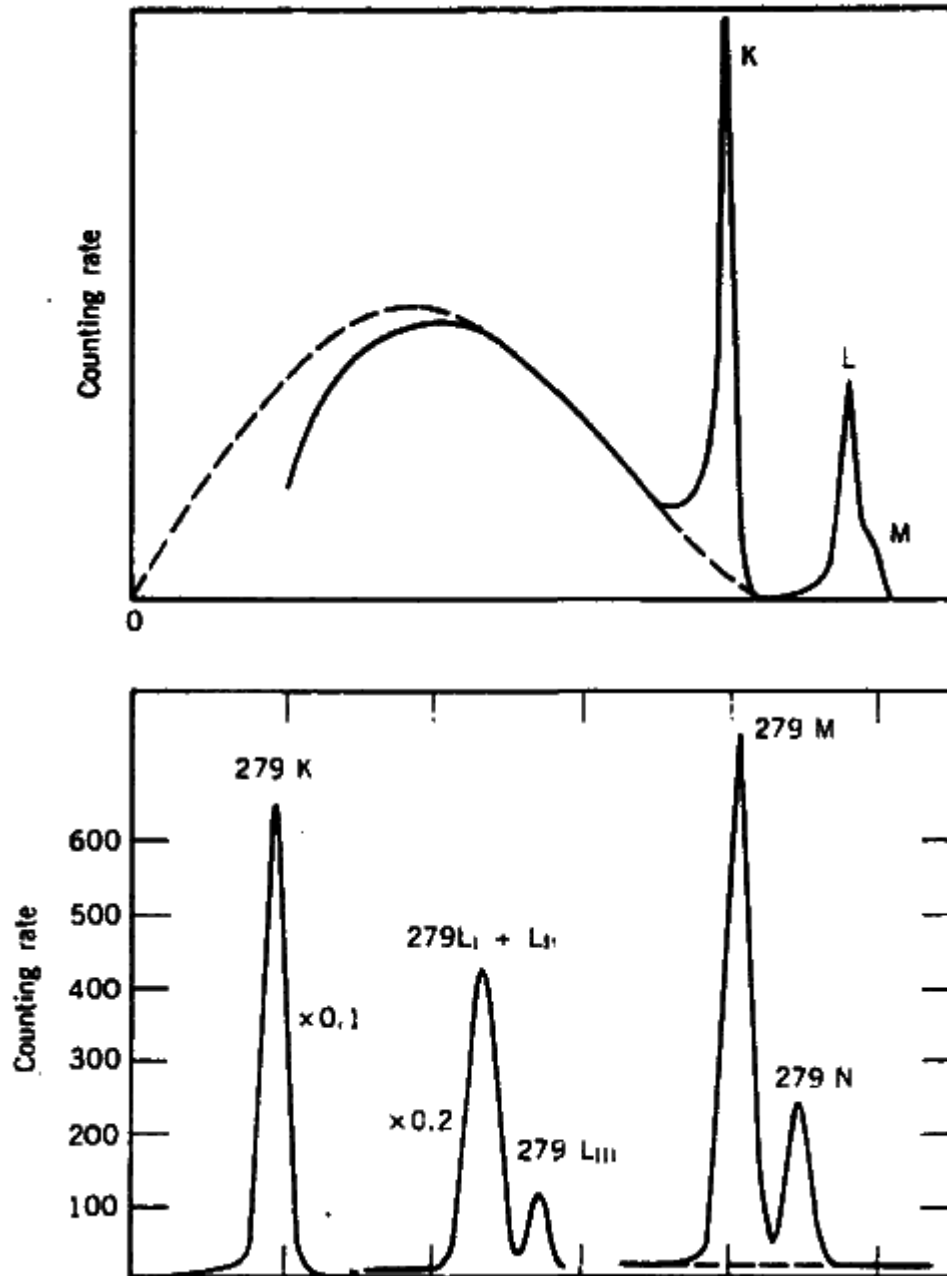


Figure 3.24: The electron spectrum in the β -decay $^{203}\text{Hg} \rightarrow ^{203}\text{Tl}$ with internal conversion of ^{203}Tl .

There are no $0^+ \rightarrow 0^+$ transition, since this would need a monopole radiation with $L = 0$ which does not exist. These decay processes can happen through internal conversion. Internal conversion is a radioactive decay where a transition of an excited nucleus to its lower energy level takes place and the energy is transferred to an electron on the inner atomic shell which is kicked out. Internal conversion is not photo-electric effect since there is no photon involved. The electrons emitted from internal conversion can be distinguished from those from the β -decay. The electron energy is continuous in the β -decay, while it is discrete in the internal conversion. See Fig. 3.23.

The electron energy in internal conversion can be expressed by $T_e = E_\gamma - W$, where E_γ is the transition energy and W is the binding energy of the electron in the atomic shell. Normally an electron in the K-shell ($n = 1$) is kicked out, so from the K-shell binding energy W_K and the electron energy T_e we can determine the transition energy or the difference of the two energy levels. For the L-shell ($n = 2$) electrons, there are atomic orbitals $2s_{1/2}$, $2p_{1/2}$ and $2p_{3/2}$, which are also called L_I , L_{II} and L_{III} shells. The vacancy left by the knocked out electron is instantly filled by the electron from an outer shell. This results in accompanying X-ray.

As an example we consider the β decay of ${}^{203}_{80}\text{Hg} \rightarrow {}^{203}_{81}\text{Tl}$ followed by a γ -decay of energy 279.19 keV. We need to know the electron binding energies of the Tl (Thallium) atom whose lower shells are [4],

$$\begin{aligned} B(K) &= 85.529 \text{ keV} \\ B(L_I) &= 15.347 \text{ keV} \\ B(L_{II}) &= 14.698 \text{ keV} \\ B(L_{III}) &= 12.657 \text{ keV} \\ B(M_I) &= 3.704 \text{ keV} \end{aligned} \quad (3.272)$$

So the conversion electrons have energies as follows,

$$\begin{aligned} T_e(K) &= (279.19 - 85.529) \text{ keV} = 193.661 \text{ keV} \\ T_e(L_I) &= (279.19 - 15.347) \text{ keV} = 263.843 \text{ keV} \\ T_e(L_{II}) &= (279.19 - 14.698) \text{ keV} = 264.492 \text{ keV} \\ T_e(L_{III}) &= (279.19 - 12.657) \text{ keV} = 266.533 \text{ keV} \\ T_e(M_I) &= (279.19 - 3.704) \text{ keV} = 275.486 \text{ keV} \end{aligned} \quad (3.273)$$

See Fig. 3.24 for the electron spectrum of ${}^{203}\text{Hg}$. One can see the peaks on the continuous background of the β -decay. The intensities of internal conversion varies from β decays. In some cases internal conversion is favored over the γ emission, in others, it is opposite. We can define the ratio of the internal conversion rate (decay constant) to the γ -emission rate, $\alpha = \lambda_e/\lambda_\gamma$. Then the total decay constant can be put in the form $\lambda_t = \lambda_\gamma(1 + \alpha)$.

Let us take the γ -emission of Se-72 for an example. The energy level of Se-72 is shown in Fig. 3.25. We notice that the 937-MeV transition must be an internal conversion since it is a $0^+ \rightarrow 0^+$ transition. Let us look at the energy level of 1317 keV. The half life of the level 1317 keV is 8.7 ps, whose total decay rate is

$$\lambda_t = \frac{\ln 2}{t_{1/2}} = \frac{0.693}{8.7 \times 10^{-12} \text{ s}} = 7.97 \times 10^{10} \text{ s}^{-1} \quad (3.274)$$

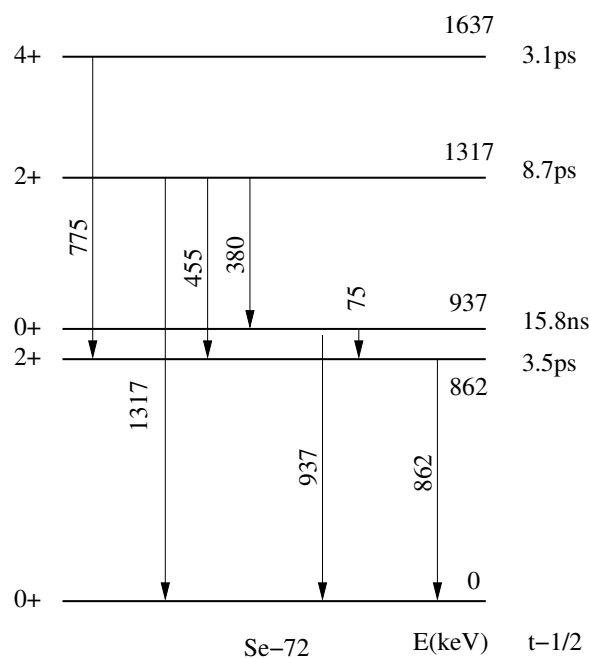
The total decay rate is the sum of the rates for three transitions, 1317 keV, 455 keV and 380 keV,

$$\begin{aligned} \lambda_t &= \lambda_{1317} + \lambda_{455} + \lambda_{380} \\ &= \lambda_{\gamma,1317}(1 + \alpha_{1317}) + \lambda_{\gamma,455}(1 + \alpha_{455}) + \lambda_{\gamma,380}(1 + \alpha_{380}) \\ &\approx \lambda_{\gamma,1317} + \lambda_{\gamma,455} + \lambda_{\gamma,380} \end{aligned} \quad (3.275)$$

The relative intensities for these γ -decays are

$$\lambda_{\gamma,1317} : \lambda_{\gamma,455} : \lambda_{\gamma,380} = 51 : 39 : 10 \quad (3.276)$$

Figure 3.25: Energy level of Se-72.



Then we obtain

$$\begin{aligned}
 \lambda_{\gamma,1317} &= 0.51\lambda_t = 4.1 \times 10^{10} \text{ s}^{-1} \\
 \lambda_{\gamma,455} &= 0.39\lambda_t = 3.1 \times 10^{10} \text{ s}^{-1} \\
 \lambda_{\gamma,380} &= 0.1\lambda_t = 8 \times 10^9 \text{ s}^{-1}
 \end{aligned}
 \tag{3.277}$$

We can compare these partial rates to the values from Eqs. (3.245,3.250). Let us assume an E2 transition, then we get

$$\begin{aligned}
 \lambda_{E2,1317} &\approx \frac{8\pi(L+1)}{L[(2L+1)!!!]^2} k^{2L+1} e^2 \left(\frac{3}{L+3}\right)^2 R^{2L} \\
 &\sim \frac{4\pi}{75 \times 137} \times (1.317 \times 5/197)^4 \times 1.317/197 \text{ fm}^{-1} \\
 &\approx 3.67 \times 10^{-12} \text{ c/fm} \sim 1.1 \times 10^{12} \text{ s}^{-1}
 \end{aligned}
 \tag{3.278}$$

where we have used $R \approx A^{1/3}r_0 \approx 5 \text{ fm}$. We can obtain the rates of other E2 transitions as

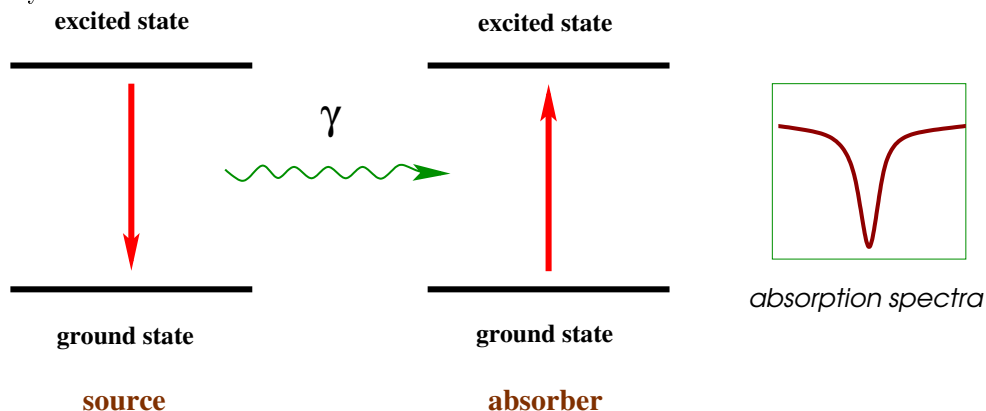
$$\begin{aligned}
 \lambda_{E2,455} &= (455/1317)^5 \lambda_{E2,1317} = 5.4 \times 10^9 \text{ s}^{-1} \\
 \lambda_{E2,380} &= (380/1317)^5 \lambda_{E2,1317} = 2.2 \times 10^9 \text{ s}^{-1}
 \end{aligned}
 \tag{3.279}$$

We can see that there is difference between Eqs. (3.245,3.250) and from Eq. (3.277), which is within a factor of 10. In real applications, Eqs. (3.245,3.250) have to be improved.

Exercise 29. Which is larger $E(L+1)$ and EL radiation? Why?

Exercise 30. Write down the parity selection rules for EL and ML radiation.

Figure 3.26: The Mössbauer effect: recoil-free nuclear resonance emission and absorption of gamma-ray.



Exercise 31. For the γ -decay from the transition $2^+ \rightarrow 1^-$, what are the possible types of multipole radiations? why?

Exercise 32. The ratio of the transition rate of $E(L+1)$ to EL and $M(L+1)$ to ML transition can be estimated as

$$r_1 = \frac{\lambda_{(E)}(L+1)}{\lambda_{(E)}(L)} \sim \frac{\lambda_{(M)}(L+1)}{\lambda_{(M)}(L)} \sim k^2 R^2$$

where k is the wave number (momentum) of the Gamma ray and R is the typical radius of the nucleus. The ratio of the transition rate of magnetic to electric transition can be estimated as

$$r_2 = \frac{\lambda_{(M)}(L)}{\lambda_{(E)}(L)} \sim \frac{1}{m^2 R^2}$$

where m is the nucleon mass. (1) Try to estimate r_1 and r_2 for typical values of $k = 1 \text{ MeV}$ and $R = 10 \text{ fm}$. (2) Given the initial and final state's parities P_i and P_f for Gamma decay, write down the parity selection rule for EL and ML transition. (3) What is the angular selection rule for the Gamma decay? (4) ${}^{167}_{68}\text{Er}$ has the following energy levels starting from the ground state,

$$\begin{array}{ccccc} 7^+ & 3^+ & 1^- & 3^- & 5^- \\ \frac{1}{2} & \frac{1}{2} & \frac{1}{2} & \frac{1}{2} & \frac{1}{2} \end{array}$$

give the dominant Gamma transitions for each excited states.

3.6 Mössbauer effect

Mössbauer discovered the recoil-free emission and absorption of gamma rays by nuclei in 1958 and was awarded the Nobel prize in physics for this effect name after him. See Fig. 3.26. Using the Mössbauer effect one can make very high precision measurement of the energy to observe the fine structure.

The transition rate of an energy level is inversely proportional to its life and proportional to its

width. In the γ decay, the ratio of its width to its energy is normally 10^{-8} , which requires very high precision measurement. One usually measure the width of a γ transition by the resonant absorption. This emission and subsequent absorption is called resonant fluorescence. But the recoil of the mother nuclei will take off a lot of energy making the resonant absorption very difficult. Mössbauer was the first physicist who tackled this difficulty.

Take the gamma decay 14.4 KeV of $^{57}_{26}\text{Fe}^*$ as example. The momentum of the photon is

$$p \equiv |\mathbf{p}| = 0.0144 \text{ MeV} \quad (3.280)$$

The recoil energy of the nucleus is

$$E_R = \frac{p^2}{2m} = \frac{(0.0144)^2}{2 \times 57 \times 931} \approx 2 \times 10^{-3} \text{ eV} \quad (3.281)$$

The lifetime of the excited state of $^{57}_{26}\text{Fe}^*$ is $\tau \sim 10^{-7}$ s. The width of $^{57}_{26}\text{Fe}^*$ is then

$$\begin{aligned} \Gamma &= \frac{1}{\tau} \approx \frac{1}{10^{-7} \times 3 \times 10^8 \times 10^{15}} \text{ fm}^{-1} \approx 3.3 \times 10^{-17} \text{ fm}^{-1} \\ &\approx 197 \times 3.3 \times 10^{-17} \text{ MeV} \approx 6 \times 10^{-9} \text{ eV} \end{aligned} \quad (3.282)$$

One sees

$$E_R \gg \Gamma \quad (3.283)$$

In this case the resonant absorption cannot take place. For the resonant absorption to occur, one should have

$$\begin{aligned} E_{\gamma,\text{em}} &= E_0 - E_R \\ E_{\gamma,\text{ab}} &= E_0 + E_R \\ E_{\gamma,\text{ab}} - E_{\gamma,\text{em}} &= 2E_R < 2\Gamma \end{aligned} \quad (3.284)$$

It was a great breakthrough to realize that one could get resonance absorption of gamma rays by putting the source nuclei in a crystal in low temperature. To see how many iron nuclei would have to recoil together to keep the gamma within the natural linewidth:

$$\begin{aligned} E_R &= \frac{p^2}{2mN} = \Gamma, \\ N &= \frac{p^2}{2m\Gamma} \approx \frac{2 \times 10^{-3}}{6 \times 10^{-9}} \approx 3.3 \times 10^5 \end{aligned} \quad (3.285)$$

which is many orders of magnitude smaller than the macroscopic scale 10^{23} .

Exercise 33. *The resonant absorption without recoil is observed in the γ -decay of $^{191}_{77}\text{Ir}_{114}$. The energy of the photon is 120 KeV and the width of the spectrum is given by its life $\tau \approx 1.4 \times 10^{-10}$ s. Estimate the recoil energy of the nucleus if the nucleus is put in free space. In order for the resonant absorption to take place, what is the least mass of the crystal in which the nuclei are embeded in order for the resonant absorption to take place.*

Chapter 4

Nuclear models

A nucleus is a many body system of nucleons. Nucleons interact with each other via nuclear force. Besides two-body forces, there are many-body forces like three-body forces etc.. Nuclear models are simplified descriptions of some of nuclear properties.

4.1 The shell model

4.1.1 Phenomena related to shell structure

It is found that a nucleus is stable when the neutron or proton number is 2,8,20,28,50,82, and the neutron number is 126. These numbers are called the magic numbers. A nucleus can be singly magic with proton or neutron number being a magic number, or doubly magic with both proton and neutron numbers being magic numbers. Several evidences about the magic numbers are as follows.

(1) Abundance. (a) On the earth, the following nuclei are more abundant than their neighbors:

$$\begin{aligned} & {}^4_2\text{He}_2, {}^{16}_8\text{O}_8, {}^{40}_{20}\text{Ca}_{20}, {}^{60}_{28}\text{Ni}_{32}, {}^{88}_{38}\text{Sr}_{50}, {}^{90}_{40}\text{Zr}_{50}, \\ & {}^{120}_{50}\text{Sn}_{70}, {}^{128}_{56}\text{Ba}_{82}, {}^{140}_{58}\text{Ce}_{82}, {}^{208}_{82}\text{Pb}_{126} \end{aligned} \quad (4.1)$$

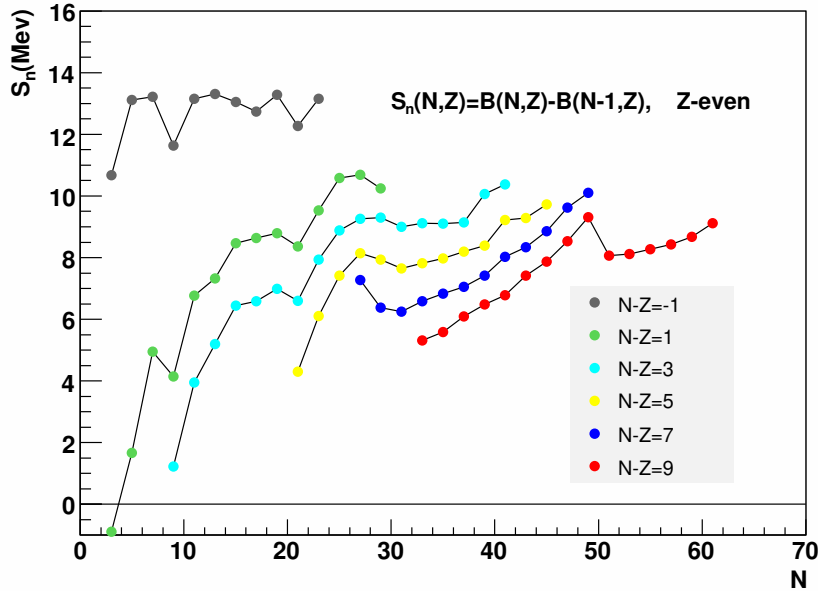
In nuclei with even proton numbers (even Z), it is less likely that their abundances are more than 50%. There are exceptions: the abundances of ${}^{88}_{38}\text{Sr}_{50}$, ${}^{138}_{56}\text{Ba}_{82}$ and ${}^{140}_{58}\text{Ce}_{82}$ are 82.56%, 71.66% and 88.48%. One can see that when the neutron number is 50 or 82 the nucleus is much more stable than a normal one. (b) In all stable elements, those with neutron number 20, 28, 50, 82 have more number of isotones than their neighbors. Elements with $N = 20, 28$ have 5 isotones, $N = 50$ have 6, $N = 82$ have 7. (c) When the proton number $Z = 8, 20, 28, 50, 82$, the number of stable isotopes are much larger than their neighbors. (d) The presence of pairing energy shows that even-even nuclei are more stable than odd-odd ones, see Table 2.2. (e) The average excitation energy of the first excited state in even-even nuclei show a maximum when the neutron number is a magic one.

(2) The binding or separation energies of the last nucleon for nuclei are defined by

$$\begin{aligned} S_n &= B(Z, A) - B(Z, A - 1) = M(Z, A - 1) - M(Z, A) + m_n \\ S_p &= B(Z, A) - B(Z - 1, A - 1) = M(Z - 1, A - 1) - M(Z, A) + m_p \end{aligned} \quad (4.2)$$

They are much smaller for nuclei with $Z - 1$ or $N - 1$ being magic numbers than others, which indicates that the nuclei with magic number are more tightly bound. The neutron binding energy is small for nuclei with $N = 8, 20$, implying that it is relatively hard for them to capture a neutron. The empirical formula for the nuclear binding energy per nucleon deviates from data strongly when N or Z are magic numbers. The neutron capture cross sections are much smaller for nuclei whose neutron numbers are magic numbers. See Fig. 4.1.

(3) There are sudden changes of nucleus radius for nuclei whose neutron numbers are magic numbers.

Figure 4.1: Neutron separation energy S_n as a function of the neutron number of final nucleus.

4.1.2 Main points of the shell model

The shell model was mainly developed in 1949 by several physicists independently, mainly by Wigner, Mayer and Jensen, who was awarded by Nobel prize in physics in 1963. Every nucleon can be regarded as moving in the mean field of other nucleons. For spherical shape, the mean field provides a central force. Such a picture is called the independent particle model. Pauli exclusion principle limits the maximum number of nucleons in one energy level. The mean free path of nucleon is large since a lot of collision is forbidden if the final state is an occupied state.

There are mainly three kinds of single nucleon potentials, the square well, the Woods-Saxon and the harmonic oscillator. The real potential is between the square well and the harmonic oscillator. The Woods-Saxon nuclear potential is

$$V(r) = -\frac{V_0}{\exp\left(\frac{r-R}{a}\right) + 1} \quad (4.3)$$

where $V_0 > 0$, and R and a are the radius and the width of the potential. The potential for harmonic oscillator is

$$V(r) = \frac{1}{2}m\omega^2 r^2 \quad (4.4)$$

Let us first consider harmonic oscillator. The wave function can be factorized into a radial part and an angular part, $\psi = R_L(r)Y_{LM}(\theta, \phi)$. The radial part of the wave function $R_L(r)$ satisfies the following radial part of the Schrodinger equation

$$\left[\frac{d^2}{dr^2} + \frac{2}{r} \frac{d}{dr} + 2m \left(E - \frac{1}{2}m\omega^2 r^2 \right) - \frac{L(L+1)}{r^2} \right] R_L(r) = 0 \quad (4.5)$$

We can first look at the solution with $E = 0$. Two possible divergent points are at $r = 0, \infty$. We first look at $r = 0$, where the equation becomes

$$\left[\frac{d^2}{dr^2} + \frac{2}{r} \frac{d}{dr} - \frac{L(L+1)}{r^2} \right] R_L(r) = 0 \quad (4.6)$$

which has two solutions,

$$R_L \sim r^L, \frac{1}{r^{L+1}} \quad (4.7)$$

The solution is $R_L \sim r^L$ is physical. Then we look at the case for $r = \infty$,

$$\left(\frac{d^2}{dr^2} - m^2 \omega^2 r^2 \right) R_l(r) = 0 \quad (4.8)$$

The solutions are

$$R_L(r) \sim \exp(\pm m\omega r^2/2) \quad (4.9)$$

where we only the solution with the minus sign is physical at infinity. So we can assume a general solution $R_L(r)$ for non-vanishing E has the following form

$$R_L(r) \sim r^L \exp(-m\omega r^2/2) u_L(r) \quad (4.10)$$

Changing the variable r to a dimensionless $\xi = m\omega r^2$, we arrive at the equation for the confluent hypergeometric function for $u_L(\xi)$,

$$\xi \frac{d^2 u_L}{d\xi^2} + \left[\left(L + \frac{3}{2} \right) - \xi \right] \frac{du_L}{d\xi} - \left(\frac{L + 3/2}{2} - \frac{E}{2\omega} \right) u_L = 0 \quad (4.11)$$

whose physical solution is

$$u(r) \sim F(-n_r, L + \frac{3}{2}, \xi) \quad (4.12)$$

with the radial quantum number n_r given by

$$n_r = \frac{E}{2\omega} - \frac{L + 3/2}{2}$$

The wave functions of a harmonic oscillator can be written in a compact and analytic form,

$$\begin{aligned} \psi_{n_r L M}(r, \theta, \phi) &= R_{n_r L}(r) Y_{LM}(\theta, \phi) \\ R_{n_r L}(r) &= \alpha^{3/2} \left[\frac{2^{L+2-n_r} (2L + 2n_r + 1)!!}{\sqrt{\pi} n_r! [(2L + 1)!!]^2} \right]^{1/2} \\ &\quad \times (\alpha r)^L \exp\left(-\frac{1}{2} \alpha^2 r^2\right) F(-n_r, L + 3/2, \alpha^2 r^2) \end{aligned} \quad (4.13)$$

where F is the confluent hypergeometrical function and $\alpha \equiv \sqrt{m\omega}$. The energy level is,

$$\begin{aligned} E &= (N + 3/2)\omega \\ N &= 2n_r + L \end{aligned} \quad (4.14)$$

Some lowest levels and their quantum numbers are illustrated in Fig. 4.1. The degeneracy for the energy level N is

$$\begin{aligned} d_N &= 2 \sum_{n_r=0}^{[N/2]} [2(N - 2n_r) + 1] \\ &= (N + 1)(N + 2) \end{aligned} \quad (4.15)$$

where we have included two spin states of nucleons.

Another example is the square well with depth $-V_0$ in the range $r \in [0, R]$. The Schoedinger equation for the radial part becomes the equation for spherical Bessel functions,

$$\left[\frac{d^2}{dr^2} + \frac{2}{r} \frac{d}{dr} + k^2 - \frac{L(L+1)}{r^2} \right] R_L(r) = 0 \quad (4.16)$$

Table 4.1: Some energy levels of the harmonic oscillator. The quantum numbers for the orbital angular momentum are $L = 0(s), 1(p), 2(d), 3(f), 4(g), 5(h)$.

$E_{n_r L}(\omega)$ (N)	n_r	state (n_r, L)	nucleon number	accumulation number
0	0	$0s$	2	2
1	0	$0p$	6	8
2	0,1	$1s, 0d$	12	20
3	0,1	$1p, 0f$	20	40
4	0,1,2	$2s, 1d, 0g$	30	70
5	0,1,2	$2p, 1f, 0h$	42	112
6	0,1,2,3	$3s, 2d, 1g, 0i$	56	168

Table 4.2: The energy levels of the square well potential. Here n denotes the n -th zero point of $J_{l+1/2}(x)$.

nL	x_{nL}	d_n	$\sum_n d_n$
1s	3.1416	2	2
1p	4.4934	6	8
1d	5.7635	10	18
2s	6.2832	2	20
1f	6.9879	14	34
2p	7.7253	6	40
1g	8.1826	18	58
2d	9.0950	10	68
1h	9.3558	22	90
3s	9.4248	2	92

where $k = \sqrt{2m(E + V_0)}$ with energy $E < 0$. Assuming $R_L = u_L/\sqrt{r}$, the above equation becomes,

$$\left[\frac{d^2}{dr^2} + \frac{1}{r} \frac{d}{dr} + k^2 - \frac{(L + 1/2)^2}{r^2} \right] u_L(r) = 0 \quad (4.17)$$

The solution which satisfies the boundary condition is

$$\begin{aligned} R_L &= C j_L(kr) \\ R_L|_{r=0} &= \text{finite} \\ R_L|_{r=R} &= C j_L(kR) = 0, \end{aligned} \quad (4.18)$$

where $j_L(x) = \sqrt{\pi/(2x)} J_{L+1/2}(x)$ is the spherical Bessel function. The wave vectors k at zero points are denoted as $k_{nL} = x_{nL}/R$, where x_{nL} is the n -th zero point of $j_L(x)$. The energy is then

$$E_{nL} = -V_0 + \frac{x_{nL}^2}{2mR^2} \quad (4.19)$$

The degeneracy factor is

$$d_n = 2L + 1 \quad (4.20)$$

When applying to a nucleon system, one has to include two spin states in d_n . See Table 4.2 for the energy levels of the square well potential.

We consider a charged particle with magnetic moment moving in a magnetic field. In the rest frame of the moving particle, the interaction energy is

$$\Delta H = -\boldsymbol{\mu} \cdot \mathbf{B}' \quad (4.21)$$

with magnetic moment $\boldsymbol{\mu} = \frac{gq}{2m} \mathbf{S}$. Here the magnetic field \mathbf{B}' is related to \mathbf{B} in the lab frame by

$$\mathbf{B}' = \mathbf{B} - \mathbf{v} \times \mathbf{E} \quad (4.22)$$

where \mathbf{E} is the electric field in the lab frame felt by the moving particle. In the central potential we have

$$q\mathbf{E} = -\frac{\mathbf{r}}{r} \frac{dV(r)}{dr} \quad (4.23)$$

Then the interaction becomes

$$\Delta H = -\frac{gq}{2m} \mathbf{S} \cdot \mathbf{B} + \frac{g}{2m^2} (\mathbf{S} \cdot \mathbf{L}) \frac{1}{r} \frac{dV(r)}{dr} \quad (4.24)$$

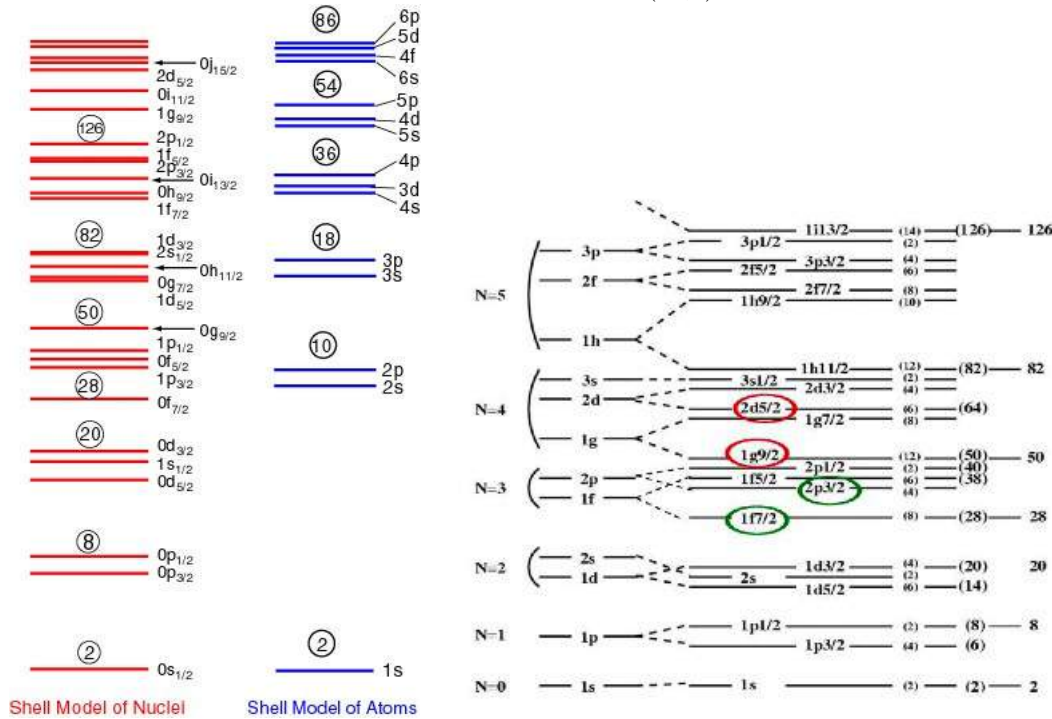
where $\mathbf{L} = m(\mathbf{r} \times \mathbf{v})$ is the orbital angular momentum. The second term is just the spin-orbital coupling. Actually one can show that the spin-orbital coupling arises from the meson exchange in the nuclear potential.

Mayer and Jensen introduced the spin-orbital coupling to nuclei for a nucleon moving in the mean field of other nucleons,

$$\begin{aligned} \Delta V(r) &= -C \mathbf{L} \cdot \mathbf{S} = -\frac{C}{2} [(\mathbf{L} + \mathbf{S})^2 - \mathbf{L}^2 - \mathbf{S}^2] \\ &= -\frac{C}{2} \left[J(J+1) - L(L+1) - \frac{3}{4} \right] \\ &= \begin{cases} -\frac{C}{2} L, & J = L + 1/2 \\ \frac{C}{2} (L+1), & J = L - 1/2 \end{cases} \end{aligned} \quad (4.25)$$

One sees that there is splitting between the levels with $J = L + 1/2$ and $J = L - 1/2$. The energy level can be labeled by (n_r, L, J) .

Figure 4.2: Nuclear shell model versus atomic shell model. For 3-d harmonic oscillator the energy eigenvalue is controlled by $N = 2n_r + l$ and while for hydrogen atom it is controlled by $N = n_r + l + 1$. The energy levels for nuclei are labeled by (n_r, l, j) (left panel) or $(n_r + 1, l, j)$ (right panel). The 3-d harmonic oscillator and hydrogen atom are labeled by (n_r, l) .



The applications of the Mayer-Jensen shell models are given in following examples.

(1) The spins and parities (J^P) of the nuclei in ground states can be explained by the model. For even-even nuclei, $J^P = 0^+$. Following the Racah seniority principle a pair of identical particles are in the lowest energy if their coupling angular momentum is zero. This is because the wave functions have largest overlap if the total angular momentum is zero. For even-even nuclei every two protons or neutrons pair, so that the total angular momentum is vanishing. The J^P of even-odd nuclei are determined by the unpaired nucleon. For example, the J^P of $^{13}_6\text{C}$ and $^{13}_7\text{N}$ are $(1/2)^-$, the spin and parity are determined by the nucleon outside the fully occupied shell. Another example, an even-odd nucleus Niobium, $^{93}_{41}\text{Nb}_{52}$, there are two neutrons outside the full shell (50) which are in the $0g_{7/2}$ state. But their pair has $J = 0$. The spin of the nucleus is determined by the 41-th proton which is in the $0g_{9/2}$ state. So the spin and parity of $^{93}_{41}\text{Nb}_{52}$ are $(9/2)^+$.

(2) The shell model can explain the J^P of nuclei of the lowest excited states. An excited state with the filled shell plus or minus one nucleon shows single particle property and its J^P is given by that of the nucleon outside the shell.

(3) The magnetic moments of nuclei can be described by the shell model. The magnetic moment of an odd-A nucleus is determined by the last unpaired nucleon. The magnetic moment of the unpaired nucleon is

$$\boldsymbol{\mu}_J = \boldsymbol{\mu}_L + \boldsymbol{\mu}_S = g_L \mathbf{L} + g_S \mathbf{S} = g_J \mathbf{J} \quad (4.26)$$

where \mathbf{J} , \mathbf{L} and \mathbf{S} are the total, orbital and spin momenta. $g_{i=J,L,S}$ are their g-factors. We have

$$\begin{aligned} g_J \mathbf{J} \cdot \mathbf{J} &= g_L \mathbf{L} \cdot \mathbf{J} + g_S \mathbf{S} \cdot \mathbf{J} \\ g_J J &= g_L \frac{J(J+1) + L(L+1) - S(S+1)}{2(J+1)} + g_S \frac{J(J+1) + S(S+1) - L(L+1)}{2(J+1)} \end{aligned} \quad (4.27)$$

For an odd-A nucleus, its magnetic moment μ_J is

$$\begin{aligned} \mu_J = g_J J &= g_L \frac{J(J+1) + L(L+1) - S(S+1)}{2(J+1)} + g_S \frac{J(J+1) + S(S+1) - L(L+1)}{2(J+1)} \\ &= \begin{cases} g_L(J-1/2) + g_S/2, & J = L + 1/2 \\ [J/(J+1)][g_L(J+3/2) - g_S/2], & J = L - 1/2 \end{cases} \end{aligned} \quad (4.28)$$

For an odd-N and even-Z nucleus, the last nucleon is a neutron which has $g_L = 0$ and $g_S = -3.82$,

$$\mu_J = \begin{cases} -1.91, & J = L + 1/2 \\ 1.91 \frac{J}{J+1}, & J = L - 1/2 \end{cases} \quad (4.29)$$

For an even-N and odd-Z nucleus, the last nucleon is a proton which has $g_L = 1$ and $g_S = 5.58$,

$$\mu_J = \begin{cases} J + 2.29, & J = L + 1/2 \\ J - 2.29 \frac{J}{J+1}, & J = L - 1/2 \end{cases} \quad (4.30)$$

The experiments partially verify the above behavior for odd-A nuclei.

(4) Electric quadrupole moments. The electric quadrupole moment of a nucleus is defined by

$$Q = \frac{1}{e} \int d^3r (3z^2 - r^2) \rho_e(\mathbf{r}) = \frac{q}{e} (2 \langle z^2 \rangle - \langle x^2 \rangle - \langle y^2 \rangle) \quad (4.31)$$

where $\rho_e(\mathbf{r})$ is the electric charge density and $q = \int d^3r \rho_e(\mathbf{r})$ the total charge. If the charge distribution is spherical, $Q = 0$. For long/short ellipsoid, $Q > 0$ and $Q < 0$. Following the shell model, the electric quadrupole moment is determined by the protons outside the filled shell. For odd-Z and even-N nucleus, there are n_p protons outside the filled shell and have angular momentum J , the quadrupole moment is given by

$$Q = -\langle r^2 \rangle \frac{2J-1}{2(J+1)} \left[1 - \frac{2(n_p-1)}{2J-1} \right] \quad (4.32)$$

We see that when $n_p < J + 1/2$, i.e. the number of protons is less than half the number of levels, $Q < 0$, otherwise $Q > 0$. So for an odd-A nucleus with number of protons being a magic number ± 1 , we have $Q < 0/Q > 0$. The shell model can well describe the electric quadrupole moments with only a few protons away from the magic numbers, but it can not describe those of other nuclei.

Exercise 34. For a square well potential with depth $V(r) = -V_0$ for $r \in [0, R]$ and $V(r) = 0$ for $r > R$. Calculate the lowest 15 energy levels.

Exercise 35. The magnetic moments of an odd-A nucleus is determined by the last unpaired nucleon. Write down its formula with respect to the nuclear spin J .

Exercise 36. Give J^P of ^{13}C , ^{13}N and $^{93}_{41}\text{Nb}_{52}$.

Exercise 37. The electric quadrupole moment of a nucleus is given by

$$Q = \frac{1}{e} \int d^3r \rho_e (3z^2 - r^2) = \frac{q}{e} (2\langle z^2 \rangle - \langle x^2 \rangle - \langle y^2 \rangle)$$

For an ellipsoid which is symmetric with respect to rotation along the z -axis (symmetric for x and y coordinates), give a simple explanation why $Q > 0$ and $Q < 0$ correspond to the long and short ellipsoid.

Exercise 38. The ground states of nuclei can be treated as a many body system of identical fermions where protons and neutrons are isospin doublets. A nucleon is moving in the mean field of other nucleons. As a simple model, people use harmonic oscillator to simulate the mean field potential. Then nucleons fill in the single particle energy levels. The eigen-energy reads,

$$E_N = N\omega = (2n_r + L)\omega$$

For a fixed N or eigen-energy, (1) calculate the degeneracy of the states, or how many states are there having the same energy; (2) write down the states in terms of $(n_r + 1)L$ for $N = 3$ using the notation s, p, d, f, g, h and i for $L = 0, 1, 2, 3, 4, 5, 6$. For example, $1s$ or $2f$ etc.. (3) When the number of protons or neutrons is the magic number 2, 8, 20, 28, 50, 82, and 126, the nuclei are most stable. But the harmonic spectra can only reproduce the first three magic numbers corresponding to $N = 0, 1, 2$. In order to explain all magic numbers, Mayer and Jensen introduced the coupling $-C\mathbf{L} \cdot \mathbf{S}$. How to explain the magic number 28 and 50? (4) The introduction of the $\mathbf{L} \cdot \mathbf{S}$ coupling term shift the energy level for $J = L + 1/2$ and $J = L - 1/2$. What the energy difference between the two levels? Which one is shifted higher? (5) As an application of the shell model, what's the spin and parity of ^{13}C and ^{13}N ?

4.2 Collective models

For even-even nuclei, to form an excited state, it will cost much more energy to break a pair of nucleons and excite one nucleon to higher level than in collective motion. There are three groups of nuclei. (1) One group is around the double magic number which can be described by the shell model. This is called single particle energy levels. (2) Even-even nuclei far away from magic numbers with ($60 < A < 150$ or $190 < A < 220$) whose lower excitations show the harmonic oscillation feature. (3) Even-even nuclei far away from magic numbers with ($150 < A < 190$ or $A > 220$) whose energy levels are like spectra of rotation.

The shape of nuclei with double magic numbers is sphere. With increase of nucleons outside the filled shell, the shape gradually turns into ellipsoid. See Fig. 4.3. This arises from the filling of nucleons in the energy state above the full shell in such a way that makes the binding energy larger. The nuclear deformation can be described by a multipole expansion of a position on the nuclear surface

$$R(\theta, \phi) = R_0 \left[1 + \sum_{LM} \alpha_{LM} Y_{LM}(\theta, \phi) \right] \quad (4.33)$$

where α_{LM} are coefficients characterizing the magnitudes of the deformation. Since $Y_{LM}^*(\theta, \phi) = (-1)^M Y_{L, L-M}(\theta, \phi)$, the coefficients satisfy $\alpha_{LM}^* = (-1)^M \alpha_{L, L-M}$. We can remove the $L = 0$ term, which corresponds to the volume change. The dipole component with $L = 1$ of an nucleus corresponds to displacement of nucleus, which has nothing to do with internal motion of nucleons. The lowest non-vanishing component deviating from sphere is the quadrupole deformation with $L = 2$. A deformed nuclei have non-zero electric quadrupole moments.

We now look at the lowest deformation, the quadrupole with $L = 2$. We now list spherical harmonic functions $Y_{2M}(\theta, \phi)$ with $M = -2, -1, 0, 1, 2$ as follows

$$\begin{aligned} Y_{20}(\theta, \phi) &= \frac{1}{2} \sqrt{\frac{5}{4\pi}} (3 \cos^2 \theta - 1), \\ Y_{2, \pm 1}(\theta, \phi) &= \mp \sqrt{\frac{15}{8\pi}} \sin \theta \cos \theta e^{\pm i\varphi}, \\ Y_{2, \pm 2}(\theta, \phi) &= \frac{1}{2} \sqrt{\frac{15}{8\pi}} \sin^2 \theta e^{\pm 2i\varphi}. \end{aligned} \quad (4.34)$$

We define a unit vector $\mathbf{n} = (\sin \theta \cos \varphi, \sin \theta \sin \varphi, \cos \theta)$ and $Y_{2M}(\theta, \phi)$ can be rewritten as

$$\begin{aligned} Y_{20} &= \frac{1}{2} \sqrt{\frac{5}{4\pi}} (2n_z^2 - n_x^2 - n_y^2), \\ Y_{2, \pm 1} &= \mp \sqrt{\frac{15}{8\pi}} n_z (n_x \pm i n_y), \\ Y_{2, \pm 2} &= \frac{1}{2} \sqrt{\frac{15}{8\pi}} (n_x^2 - n_y^2 \pm i 2n_x n_y). \end{aligned} \quad (4.35)$$

So we see that (a) α_{20} describes the stretching or contraction along the z axis; (b) $\alpha_{2, \pm 1}$ describe the oblique deformation along the the z axis; (c) $\alpha_{2, \pm 2}$ describe the length difference between the x axis and y axis and the oblique deformation in the xy plane.

An ellipsoid satisfies $R(\theta, \phi) = R(\pi - \theta, \phi) = R(\theta, -\phi)$, so we have $\alpha_{21} = \alpha_{2, -1} = 0$, $\alpha_{22} = \alpha_{2, -2}$. Then Eq. (4.33) becomes

$$\begin{aligned} R(\theta, \phi) &= R_0 [1 + \alpha_{20} Y_{20}(\theta, \phi) + \alpha_{22} Y_{22}(\theta, \phi) + \alpha_{22} Y_{2, -2}(\theta, \phi)] \\ &= R_0 \left[1 + \alpha_{20} \frac{1}{2} \sqrt{\frac{5}{4\pi}} (3 \cos^2 \theta - 1) + \alpha_{22} \sqrt{\frac{15}{8\pi}} \sin^2 \theta \cos(2\varphi) \right] \end{aligned} \quad (4.36)$$

We can also use (β, γ) to replace $(\alpha_{20}, \alpha_{22})$,

$$\begin{aligned}\alpha_{20} &= \beta \cos \gamma \\ \alpha_{22} &= \frac{1}{\sqrt{2}}\beta \sin \gamma\end{aligned}\quad (4.37)$$

The deformed values of lengths of three axis from that of the sphere are

$$\begin{aligned}\delta R_x &= R_x - R_0 = \sqrt{\frac{5}{4\pi}}\beta R_0 \cos(\gamma - \frac{2}{3}\pi) \\ \delta R_y &= R_y - R_0 = \sqrt{\frac{5}{4\pi}}\beta R_0 \cos(\gamma - \frac{4}{3}\pi) \\ \delta R_z &= R_z - R_0 = \sqrt{\frac{5}{4\pi}}\beta R_0 \cos \gamma\end{aligned}\quad (4.38)$$

A symmetric ellipsoid with respect to the z-axis corresponds to $\gamma = 0$, i.e. $\alpha_{22} = 0$, this corresponds to

$$\begin{aligned}R(\theta) &= R_0[1 + \alpha_{20}Y_{20}(\theta, \phi)] \\ &= R_0 \left[1 + \alpha_{20} \frac{1}{2} \sqrt{\frac{5}{4\pi}} (3 \cos^2 \theta - 1) \right]\end{aligned}\quad (4.39)$$

and we have

$$\begin{aligned}R_x &= R_y = R_0 \left(1 - \frac{1}{2} \sqrt{\frac{5}{4\pi}} \beta \right) \\ R_z &= R_0 \left(1 + \sqrt{\frac{5}{4\pi}} \beta \right)\end{aligned}\quad (4.40)$$

A long/flat ellipsoid or prolate/oblate is described by $\beta > 0/\beta < 0$, see Fig. 4.3.

The Lagrangian for nuclear vibration is given by

$$L = \frac{1}{2} \sum_{LM} \left[B_L \dot{R}_{LM}^2(t) + C_L R_{LM}^2 \right]\quad (4.41)$$

The canonical conjugated momentum of X_{LM} is given by $P_{LM} = B_L \dot{R}_{LM}$. The Hamiltonian is given by

$$H = \frac{1}{2} \sum_{LM} \left[\frac{1}{B_L} P_{LM}^2 + C_L R_{LM}^2 \right]\quad (4.42)$$

which is a sum of harmonic oscillators with the frequency $\omega_L = \sqrt{C_L/B_L}$.

The ground state is 0^+ and the lowest excited state is 2^+ which corresponds to quadrupole deformation, whose excitation is called phonon. The next-lowest excited state with two phonon excitations are $J^P = 0^+, 2^+, 4^+$. The total angular of momentum of two phonons with $L = 2$ can be determined by $J = (L_1, m_1) \oplus (L_2, m_2) = 0 \oplus 2 \oplus 4$ with $L_1 = L_2 = 2$ and $m_1, m_2 = (\pm 2, \pm 1, 0)$. We can verify that $J \neq 1, 3$. The energy level of an oscillator has equal distance feature,

$$E = (N + 5/2)\omega\quad (4.43)$$

For quadrupole vibration mode, there are N phonons each of which contributes to 2 units angular momentum. All states have positive parity. The oscillation spectra manifest themselves in nuclei with filled shells. The main form is quadrupole oscillation where β fluctuates around zero.

The rotation of an ellipsoid even-even nucleus along an axis perpendicular to the symmetry axis has observable effect. Rotation spectra can be described by

$$E_J = \frac{1}{2I} J(J+1) \quad (4.44)$$

where I is the inertial moment and J the total momentum. It can be proved that J must be even and the parity must be positive. Eq. (4.44) is valid for small I . For larger I , a correction is needed due to large centrifugal force which makes more deformation and less kinetic energy,

$$E_J = \frac{1}{2I} J(J+1) - BJ^2(J+1)^2 \quad (4.45)$$

For deformed odd-A nuclei, there exists one energy band for every single particle energy level,

$$E_I = \frac{1}{2I} [J(J+1) - K(K+1)] \quad (4.46)$$

for $K > 1/2$. When $K = 1/2$,

$$E_I = \frac{1}{2I} \left[J(J+1) - \frac{3}{4} + a + a(-1)^{J+1/2}(J+1/2) \right] \quad (4.47)$$

The states in the same band have the same parity. For $K > 1/2$ we have,

$$E_{K+1} : E_{K+2} : E_{K+3} : \dots = (K+1) : (2K+3) : (3K+6) : \dots \quad (4.48)$$

4.3 Hartree-Fock self-consistent method

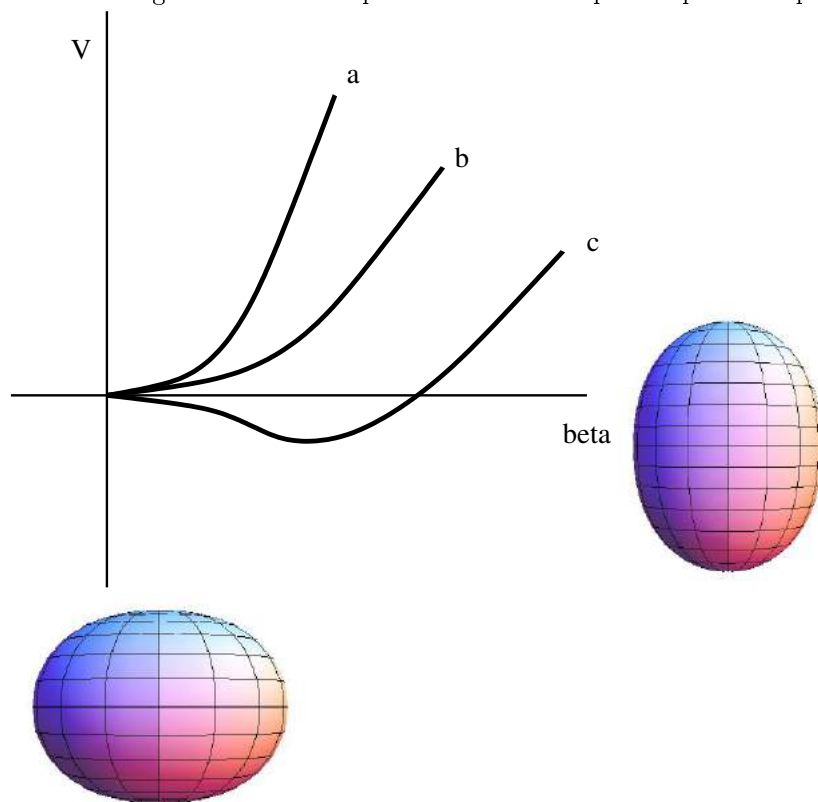
In a nucleus composed of A nucleons, a particular nucleon can be regarded as moving in a mean field of other $A-1$ nucleons. But this is a very rough picture because it neglects the correlation or interaction between nucleons beyond the mean field. The Hamiltonian can be written by

$$H = \sum_i \frac{\mathbf{p}_i^2}{2m} + \frac{1}{2} \sum_{i \neq j} V(\mathbf{r}_i, \mathbf{r}_j) \quad (4.49)$$

and the trial wave function can be expressed by a Slater determinant of A single particle wave functions,

$$\begin{aligned} \Psi(1, 2, \dots, A) &= \frac{1}{\sqrt{A!}} \begin{vmatrix} \psi_1(\mathbf{r}_1) & \psi_1(\mathbf{r}_2) & \dots & \psi_A(\mathbf{r}_A) \\ \psi_2(\mathbf{r}_1) & \psi_2(\mathbf{r}_2) & \dots & \psi_A(\mathbf{r}_A) \\ \dots & \dots & \dots & \dots \\ \psi_A(\mathbf{r}_1) & \psi_A(\mathbf{r}_2) & \dots & \psi_A(\mathbf{r}_A) \end{vmatrix} \\ &= \frac{1}{\sqrt{A!}} \sum_P (-1)^P \psi_{P(1)}(\mathbf{r}_1) \psi_{P(2)}(\mathbf{r}_2) \dots \psi_{P(A)}(\mathbf{r}_A) \end{aligned} \quad (4.50)$$

Figure 4.3: Nuclear potential versus shape. Shapes with quadrupole moments.



where P denotes the permutation of $(1, 2, \dots, A)$. Now we evaluate the expectation value of the Hamiltonian, where the kinetic energy is

$$\begin{aligned}
\int [dr] \Psi^\dagger \sum_i \frac{\mathbf{p}_i^2}{2m} \Psi &= \frac{1}{A!} \sum_i \sum_{P, P'} (-1)^{P+P'} \int [dr] \prod_{k=1}^A \psi_{P'(k)}^\dagger(\mathbf{r}_k) \left(-\frac{\nabla_i^2}{2m} \right) \prod_{l=1}^A \psi_{P'(l)}(\mathbf{r}_l) \\
&= \frac{1}{A!} \int [dr] \prod_{k \neq i}^A \psi_{P'(k)}^\dagger(\mathbf{r}_k) \prod_{l \neq i}^A \psi_{P'(l)}(\mathbf{r}_l) \sum_i \int dr_i \psi_{P'(i)}^\dagger(\mathbf{r}_i) \left(-\frac{\nabla_i^2}{2m} \right) \psi_{P'(i)}(\mathbf{r}_i) \\
&= \frac{1}{A} \sum_i \int dr_i \psi_{P'(i)}^\dagger(\mathbf{r}_i) \left(-\frac{\nabla_i^2}{2m} \right) \psi_{P'(i)}(\mathbf{r}_i) \\
&= \sum_j \int dr \psi_j^\dagger(\mathbf{r}) \left(-\frac{\nabla^2}{2m} \right) \psi_j(\mathbf{r})
\end{aligned} \tag{4.51}$$

where $[dr] \equiv dr_1 dr_2 \dots dr_A$ and we have used the orthogonality condition for each spatial integral that $P(k) = P'(k)$ for $k \neq i$ which gives $(A-1)!$ identical terms. The potential part is

$$\begin{aligned}
\int [dr] \Psi^\dagger \frac{1}{2} \sum_{i \neq j} V(\mathbf{r}_i, \mathbf{r}_j) \Psi &= \frac{1}{2} \frac{1}{A!} \sum_{i \neq j} \sum_{P, P'} (-1)^{P+P'} \int [dr] \prod_{k=1}^A \psi_{P'(k)}^\dagger(\mathbf{r}_k) V(\mathbf{r}_i, \mathbf{r}_j) \prod_{l=1}^A \psi_{P'(l)}(\mathbf{r}_l) \\
&= \frac{1}{2} \frac{1}{A!} \sum_{P, P'} (-1)^{P+P'} \int [dr] \prod_{k \neq i, j}^A \psi_{P'(k)}^\dagger(\mathbf{r}_k) \prod_{l \neq i, j}^A \psi_{P'(l)}(\mathbf{r}_l) \\
&\quad \times \sum_{i \neq j} \int dr_i dr_j \psi_{P'(i)}^\dagger(\mathbf{r}_i) \psi_{P'(j)}^\dagger(\mathbf{r}_j) V(\mathbf{r}_i, \mathbf{r}_j) \psi_{P'(i)}(\mathbf{r}_i) \psi_{P'(j)}(\mathbf{r}_j) \\
&= \frac{1}{2} \frac{1}{A(A-1)} \sum_{i \neq j} (-1)^{P+P'} \int dr_i dr_j \psi_{P'(i)}^\dagger(\mathbf{r}_i) \psi_{P'(j)}^\dagger(\mathbf{r}_j) \\
&\quad \times V(\mathbf{r}_i, \mathbf{r}_j) \psi_{P'(i)}(\mathbf{r}_i) \psi_{P'(j)}(\mathbf{r}_j) \\
&= \frac{1}{2} \sum_{k, l} \int dr dr' \left[\psi_k^\dagger(\mathbf{r}) \psi_l^\dagger(\mathbf{r}') V(\mathbf{r}, \mathbf{r}') \psi_k(\mathbf{r}) \psi_l(\mathbf{r}') \right. \\
&\quad \left. - \psi_k^\dagger(\mathbf{r}) \psi_l^\dagger(\mathbf{r}') V(\mathbf{r}, \mathbf{r}') \psi_k(\mathbf{r}') \psi_l(\mathbf{r}) \right]
\end{aligned} \tag{4.52}$$

So the expectation value of the Hamiltonian is

$$\begin{aligned}
\bar{E} &= \sum_j \int dr \psi_j^\dagger(\mathbf{r}) \left(-\frac{\nabla^2}{2m} \right) \psi_j(\mathbf{r}) \\
&\quad + \frac{1}{2} \sum_{k, l} \int dr dr' \left[\psi_k^\dagger(\mathbf{r}) \psi_l^\dagger(\mathbf{r}') V(\mathbf{r}, \mathbf{r}') \psi_k(\mathbf{r}) \psi_l(\mathbf{r}') \right. \\
&\quad \left. - \psi_k^\dagger(\mathbf{r}) \psi_l^\dagger(\mathbf{r}') V(\mathbf{r}, \mathbf{r}') \psi_k(\mathbf{r}') \psi_l(\mathbf{r}) \right]
\end{aligned} \tag{4.53}$$

We can solve the eigenstates through the variational method. The requirement is to make the expectation value of the Hamiltonian stable with the variance of the wave function under the normalization condition of the wave function,

$$\begin{aligned}
\delta \int [dr] \Psi^\dagger H \Psi &= 0 \\
\int [dr] \Psi^\dagger \Psi &= 1
\end{aligned} \tag{4.54}$$

which is equivalent to

$$\delta \int [dr] \Psi^\dagger H \Psi - \epsilon \delta \int [dr] \Psi^\dagger \Psi \quad (4.55)$$

where ϵ is a Lagrange multiplier. The variances of the expectation values of the kinetic and interaction energy are,

$$\begin{aligned} \delta \int [dr] \Psi^\dagger \sum_i \frac{\mathbf{p}_i^2}{2m} \Psi &= \sum_j \int dr \delta \psi_j^\dagger(\mathbf{r}) \left(-\frac{\nabla^2}{2m} \right) \psi_j(\mathbf{r}) \\ &\quad + \sum_j \int dr \psi_j^\dagger(\mathbf{r}) \left(-\frac{\nabla^2}{2m} \right) \delta \psi_j(\mathbf{r}) \end{aligned} \quad (4.56)$$

and

$$\begin{aligned} \delta \int [dr] \Psi^\dagger \frac{1}{2} \sum_{i \neq j} V(\mathbf{r}_i, \mathbf{r}_j) \Psi &= \frac{1}{2} \sum_{k,l} \int dr dr' \left\{ \left[(\delta \psi_k^\dagger(\mathbf{r}) \psi_l^\dagger(\mathbf{r}') + \psi_k^\dagger(\mathbf{r}) \delta \psi_l^\dagger(\mathbf{r}')) \right] \right. \\ &\quad \times V(\mathbf{r}, \mathbf{r}') \psi_k(\mathbf{r}) \psi_l(\mathbf{r}') \\ &\quad \left. - \left[\delta \psi_k^\dagger(\mathbf{r}) \psi_l^\dagger(\mathbf{r}') + \psi_k^\dagger(\mathbf{r}) \delta \psi_l^\dagger(\mathbf{r}') \right] V(\mathbf{r}, \mathbf{r}') \psi_k(\mathbf{r}') \psi_l(\mathbf{r}) \right\} \\ &\quad + H.c. \\ &= \sum_{k,l} \int dr dr' \left\{ \delta \psi_k^\dagger(\mathbf{r}) \psi_l^\dagger(\mathbf{r}') V(\mathbf{r}, \mathbf{r}') \psi_k(\mathbf{r}) \psi_l(\mathbf{r}') \right. \\ &\quad \left. - \delta \psi_k^\dagger(\mathbf{r}) \psi_l^\dagger(\mathbf{r}') V(\mathbf{r}', \mathbf{r}) \psi_l(\mathbf{r}) \psi_k(\mathbf{r}') \right\} \\ &\quad + H.c. \end{aligned} \quad (4.57)$$

where we have used $V(\mathbf{r}, \mathbf{r}') = V(\mathbf{r}', \mathbf{r})$. Then the requirement of Eq. (4.55) becomes

$$\begin{aligned} \left(-\frac{\nabla^2}{2m} \right) \psi_k(\mathbf{r}) + \sum_l \int dr' V(\mathbf{r}, \mathbf{r}') |\psi_l(\mathbf{r}')|^2 \psi_k(\mathbf{r}) \\ - \sum_l \int dr' \psi_l^\dagger(\mathbf{r}') V(\mathbf{r}', \mathbf{r}) \psi_l(\mathbf{r}) \psi_k(\mathbf{r}') = \epsilon \psi_k(\mathbf{r}) \end{aligned} \quad (4.58)$$

The above equation is called the Hartree-Fock equation.

The above method is too complicated for the many body problems. A better method is to use occupation number representation and the second quantization. Similar to the expectation value of energy in Eq. (4.53), we can write down the Hamiltonian operator in terms of quantum fields of nucleons,

$$\begin{aligned} H &= \int dx \psi^\dagger(\mathbf{x}) \left(-\frac{\nabla^2}{2m} \right) \psi(\mathbf{x}) \\ &\quad + \frac{1}{2} \int dx dx' \psi^\dagger(\mathbf{x}) \psi^\dagger(\mathbf{x}') V(\mathbf{x}, \mathbf{x}') \psi(\mathbf{x}') \psi(\mathbf{x}) \end{aligned} \quad (4.59)$$

where the quantum fields are

$$\begin{aligned} \psi(\mathbf{x}) &= \sum_s \psi_s(\mathbf{x}) \eta_s = \frac{1}{\sqrt{\Omega}} \sum_{k,s} e^{i\mathbf{k}\cdot\mathbf{x}} \eta_s a_{k,s} \\ \psi^\dagger(\mathbf{x}) &= \sum_s \psi_s^\dagger(\mathbf{x}) \eta_s = \frac{1}{\sqrt{\Omega}} \sum_{k,s} e^{-i\mathbf{k}\cdot\mathbf{x}} \eta_s a_{k,s}^\dagger \end{aligned} \quad (4.60)$$

where $s = \pm 1$ denote the spin orientation and $\eta_+ = \begin{pmatrix} 1 \\ 0 \end{pmatrix}$ and $\eta_- = \begin{pmatrix} 0 \\ 1 \end{pmatrix}$. Note that the quantum field has the same dimension as the wave function, so the creation and destruction operators are dimensionless. One can check that the ordering of the second term in Eq. (4.59) would lead to the Hermitian property of the Hamiltonian. They satisfy the following anti-commutator relations,

$$\begin{aligned} \{\psi_s(\mathbf{x}), \psi_t(\mathbf{x}')\} &= \{\psi_s^\dagger(\mathbf{x}), \psi_t^\dagger(\mathbf{x}')\} = 0 \\ \{\psi_s(\mathbf{x}), \psi_t^\dagger(\mathbf{x}')\} &= \frac{1}{\Omega} \sum_{k,k'} e^{i\mathbf{k}\cdot\mathbf{x}} e^{-i\mathbf{k}'\cdot\mathbf{x}'} \{a_{k,s}, a_{k',t}^\dagger\} \\ &= \delta_{st} \frac{1}{\Omega} \sum_k e^{i\mathbf{k}\cdot(\mathbf{x}-\mathbf{x}')} = \delta_{st} \delta(\mathbf{x}-\mathbf{x}') \end{aligned} \quad (4.61)$$

where

$$\{a_{k,s}, a_{k',t}^\dagger\} = \delta_{st} \delta_{k,k'}, \quad \{a_{k,s}, a_{k',t}\} = \{a_{k,s}^\dagger, a_{k',t}^\dagger\} = 0 \quad (4.62)$$

Then using Eq. (4.59) and (4.62), the Hamiltonian (4.59) becomes

$$\begin{aligned} H &= \frac{1}{\Omega} \sum_{k,k',s,t} \int dx e^{i(\mathbf{k}-\mathbf{k}')\cdot\mathbf{x}} \eta_t^\dagger \eta_s \frac{\mathbf{k}^2}{2m} a_{k',t}^\dagger a_{k,s} \\ &\quad + \frac{1}{\Omega^2} \sum_{k_1-4, s_1-4} \int dx dx' e^{-i\mathbf{k}_1\cdot\mathbf{x}} e^{-i\mathbf{k}_2\cdot\mathbf{x}'} e^{i\mathbf{k}_3\cdot\mathbf{x}} e^{i\mathbf{k}_4\cdot\mathbf{x}'} V(\mathbf{x}, \mathbf{x}') \\ &\quad \times \eta_{s_1}^\dagger \eta_{s_2}^\dagger \eta_{s_3} \eta_{s_4} a_{k_1, s_1}^\dagger a_{k_2, s_2}^\dagger a_{k_3, s_3} a_{k_4, s_4} \\ &= \sum_{k,s} \frac{\mathbf{k}^2}{2m} a_{k,s}^\dagger a_{k,s} + \frac{1}{\Omega^2} \sum_{k_1-4, s_1, 2} \int dx dx' e^{-i(\mathbf{k}_1-\mathbf{k}_4)\cdot\mathbf{x}} e^{-i(\mathbf{k}_2-\mathbf{k}_3)\cdot\mathbf{x}'} V(\mathbf{x}, \mathbf{x}') \\ &\quad \times a_{k_1, s_1}^\dagger a_{k_2, s_2}^\dagger a_{k_3, s_2} a_{k_4, s_1} \\ &= \sum_{k,s} \frac{\mathbf{k}^2}{2m} a_{k,s}^\dagger a_{k,s} + \frac{1}{\Omega^2} \sum_{k_1-4, s_1, 2} \int dX dy \exp[i(\mathbf{k}_4 + \mathbf{k}_3 - \mathbf{k}_1 - \mathbf{k}_2) \cdot \mathbf{X}] \\ &\quad \exp[i(\mathbf{k}_2 - \mathbf{k}_3 - \mathbf{k}_1 + \mathbf{k}_4) \cdot \mathbf{y}/2] V(\mathbf{y}) a_{k_1, s_1}^\dagger a_{k_2, s_2}^\dagger a_{k_3, s_2} a_{k_4, s_1} \\ &= \sum_{k,s} \frac{\mathbf{k}^2}{2m} a_{k,s}^\dagger a_{k,s} + \sum_{p,k,q,s_1,2} \tilde{V}(\mathbf{q}) a_{k-q, s_1}^\dagger a_{p+q, s_2}^\dagger a_{p, s_2} a_{k, s_1} \end{aligned} \quad (4.63)$$

where we have assumed $V(\mathbf{x}, \mathbf{x}') = V(\mathbf{X}, \mathbf{y}) = V(\mathbf{y})$ with $\mathbf{X} = (\mathbf{x} + \mathbf{x}')/2$ and $\mathbf{y} = \mathbf{x} - \mathbf{x}'$. We also used $\tilde{V}(\mathbf{q}) = \frac{1}{\Omega} \int dx e^{i\mathbf{q}\cdot\mathbf{x}} V(\mathbf{x})$. We will assume that $\tilde{V}(\mathbf{q})$ only depends on $|\mathbf{q}|$.

Now we can calculate the expectation value of the ground state energy. The ground state is a state that all states below the Fermi momentum $k_F = |\mathbf{k}_F|$ is occupied and those above it are empty,

$$|F\rangle = \prod_{r, |\mathbf{k}| < k_F} a_{k,r}^\dagger |0\rangle \quad (4.64)$$

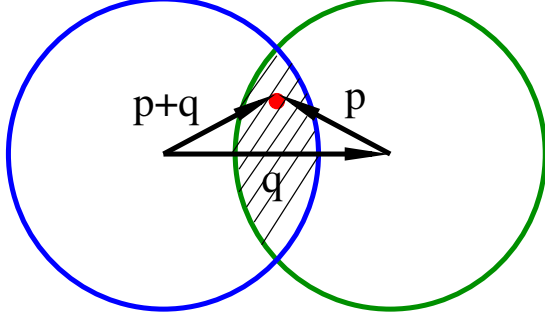
Then the kinetic energy is

$$\begin{aligned} \bar{E}_0 &= \sum_{k,s} \frac{\mathbf{k}^2}{2m} \langle F | a_{k,s}^\dagger a_{k,s} | F \rangle = 2 \sum_k \frac{\mathbf{k}^2}{2m} \theta(|\mathbf{k}| < k_F) \\ &= 2\Omega \int \frac{d^3k}{(2\pi)^3} \frac{k^2}{2m} \theta(|\mathbf{k}| < k_F) = \frac{3}{5} \frac{k_F^3}{2m} N \end{aligned} \quad (4.65)$$

where N the total number of the fermions and is given by $N = \Omega \frac{1}{3\pi^2} k_F^3$. The expectation value of the interaction energy is

$$\bar{E}_1 = \sum_{p,k,q,s_1,2} \tilde{V}(\mathbf{q}) \langle F | a_{k-q, s_1}^\dagger a_{p+q, s_2}^\dagger a_{p, s_2} a_{k, s_1} | F \rangle \quad (4.66)$$

Figure 4.4: The overlapping of Fermi surface in evaluating the potential energy of a fermionic system at zero temperature.



From two destruction operators acting on $|F\rangle$ we see that both \mathbf{p} and \mathbf{k} must be below the Fermi surface. Similarly from two creation operators acting on $\langle F|$ we see that both $\mathbf{k} - \mathbf{q}$ and $\mathbf{p} + \mathbf{q}$ must be below the Fermi surface. And the two groups of momenta must be the same otherwise there is overlapping,

$$[(\mathbf{p}, s_2), (\mathbf{k}, s_1)] = [(\mathbf{k} - \mathbf{q}, s_1), (\mathbf{p} + \mathbf{q}, s_2)] \quad (4.67)$$

Note that another order for the pair of momenta is not valid because \mathbf{p} cannot be $\mathbf{p} + \mathbf{q}$. So the potential energy (4.66) is evaluated as

$$\begin{aligned} E_1 &= \sum_{p,k,q,s_1,s_2} \tilde{V}(\mathbf{q}) \langle F| a_{k-q,s_1}^\dagger a_{p+q,s_2}^\dagger a_{p,s_2} a_{k,s_1} |F\rangle \\ &= \sum_{p,q,s_1} \tilde{V}(\mathbf{q}) \langle F| a_{p,s_1}^\dagger a_{p+q,s_1}^\dagger a_{p,s_1} a_{p+q,s_1} |F\rangle \\ &= - \sum_{p,q,s_1} \tilde{V}(\mathbf{q}) \langle F| n_{p,s_1} n_{p+q,s_1} |F\rangle \\ &= -2\Omega^2 \int \frac{d^3p}{(2\pi)^3} \frac{d^3q}{(2\pi)^3} \tilde{V}(\mathbf{q}) \theta(|\mathbf{p}| < k_F) \theta(|\mathbf{p} + \mathbf{q}| < k_F) \end{aligned}$$

The two step functions give the overlapping area of the Fermi surface if $|\mathbf{q}| < 2k_F$. We can first integrate over \mathbf{p} while fixing $|\mathbf{q}|$,

$$\begin{aligned} &\int d^3p \theta(|\mathbf{p}| < k_F) \theta(|\mathbf{p} + \mathbf{q}| < k_F) \\ &= 2 \left[\frac{2\pi}{3} (1-x) k_F^3 - \frac{\pi}{3} k_F^3 x (1-x^2) \right] \theta(x < 1) \\ &= \frac{2\pi}{3} (2-3x+x^3) k_F^3 \theta(x < 1) \end{aligned}$$

Then we carry out the integral over \mathbf{q} ,

$$\begin{aligned} E_1 &= -\frac{2}{3\pi^4} \Omega^2 k_F^6 \int_0^1 dx \tilde{V}(2k_F x) x^2 (2-3x+x^3) \\ &= -6N^2 \int_0^1 dx \tilde{V}(2k_F x) x^2 (2-3x+x^3) \end{aligned}$$

Chapter 5

Nuclear reaction

Like chemical reaction, in nuclear reaction some nuclei or particles and nuclei collide and give rise to different particles or nuclei in the final state. There are many type of nuclear reactions which can be characterized by the type and energy of incoming particles and the target nuclei. The natural decay processes can be regarded as without incoming particles but with $Q > 0$. In accelerator reactions, charged particles, e.g. electrons, protons, alpha-particles or even heavier nuclei (heavy ions), are accelerated to hit the target nuclei. Beams of neutrons can thus be obtained in nuclear reactors as fragments in collisions of charged particles and target nuclei. Bombardment of leptons like electrons, muons and neutrinos on target nuclei are also nuclear reactions. Here are notable examples of nuclear reactions: nuclear fusion, fission, spallation, induced gamma emission etc.. The spallation is a kind of nuclear reaction that a nucleus is hit by a lighter particle with sufficient energy and momentum to knock out several small fragments or break into many fragments. Induced gamma emission is a process that a nucleus absorbs a photon of a specific energy to be excited to a higher energy level, and then emits fluorescent gamma rays often with a delay after absorption.

A two-to-two nuclear reaction can be written as $a + X \rightarrow b + Y$ or the shorthand notation $X(a, b)Y$ where X and Y are the target and outgoing nuclei and 'a' denotes the lighter projectile and 'b' the fragment particle.

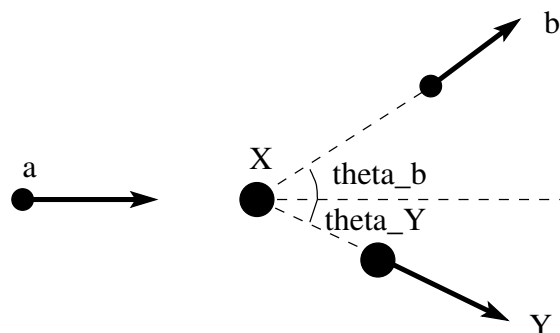
We can classify the reaction by the reaction energy. Low energy nuclear reaction is characterized by the order of 10 MeV per nucleon or less. The medium energy nuclear reaction is in the range 100 MeV to 1 GeV, where mesons can be produced and protons and neutrons can transform into each other. In high energy nuclear reaction, all particles can be produced including quarks and gluons, the constituents of nucleons.

We can classify the reaction by incident and outgoing particles. If the incident and outgoing particles are the same, i.e. $a + X \rightarrow a + X$, we call the reaction the elastic scattering process. Sometimes 'b' is the same as 'a' but there is another nucleon being ejected, this reaction is called a knockout reaction.

The reaction can also be classified by the mechanism involved. In direct reactions, very few nucleons take part in the reactions, while other nucleons serve as spectators. Such reactions can be used to explore the inner structure of nuclei. In contrast, compound nucleus can be formed in some types of reactions, where incoming and outgoing nuclei merge in very short time and sharing the energy among all nucleons before ejecting a few nucleons. The resonance reactions are between the direct and compound nuclear reactions, in which the incoming and outgoing particle form quasi-bound state before emitting outgoing particles.

Here are examples of nuclear reactions [5],

Figure 5.1: Momentum configuration in the two-to-two nuclear reaction in the lab frame.



- (1) $\alpha + {}^{14}_7\text{N} \rightarrow {}^{17}_8\text{O} + \text{p}$
- (2) $\text{p} + {}^{14}_7\text{N} \rightarrow {}^7_4\text{Be} + 2\alpha$
- (3) $\text{p} + {}^{27}_{13}\text{Al} \rightarrow {}^{28}_{14}\text{Si}^*$
- (4) $3\alpha \rightarrow {}^{12}_6\text{C}$
- (5) $\gamma + {}^{63}_{29}\text{Cu} \rightarrow {}^{62}_{28}\text{Ni} + \text{p}$
- (6) $\gamma + {}^{233}_{92}\text{U} \rightarrow {}^{90}_{37}\text{Rb} + {}^{141}_{55}\text{Cs} + 2\text{n}$

The reaction (1) was the first nuclear reaction made in laboratory by Rutherford in 1919. The first three reactions are induced by lighter projectiles the α particle and proton on heavier nuclei. In the reactions (3) there is only one product in the final state. The reaction (4) takes place in the star interior at high temperature and density. The reactions (5) and (6) are radiative capture or photo-nuclear reactions.

5.1 Conservation laws and kinematics

Here are the conservation laws for nuclear reactions: (a) Conservation of energy momentum; (b) Conservation of total angular momentum; (c) Conservation of charge and baryon number; (d) Conservation of parity. At low energy, the conservation of baryon number in (c) becomes that of proton and neutron number in which the energy is not enough to produce mesons. Note that we neglect all weak processes because the time scale of weak interaction is much longer than that of nuclear reactions.

We consider a two-to-two nuclear reaction $a + X \rightarrow b + Y$ or $X(a,b)Y$, see Fig. 5.1. The conservation of energy requires that the total energy of incoming particles should be equal to the outgoing particles. We have

$$T_X + m_X + T_a + m_a = T_Y + m_Y + T_b + m_b \quad (5.1)$$

where $T_i = \frac{1}{2}m_i v_i^2$ denote the kinetic energy. The Q-value of a reaction is defined by

$$Q = m_X + m_a - m_Y - m_b = T_Y + T_b - T_X - T_a \quad (5.2)$$

In the lab and center-of-mass frames, the velocities for all particles are

$$\begin{aligned} \text{Lab: } & \mathbf{v}_X = 0, \mathbf{v}_a, \mathbf{v}_b, \mathbf{v}_Y \\ \text{CM: } & \mathbf{v}'_X, \mathbf{v}'_a, \mathbf{v}'_b, \mathbf{v}'_Y \end{aligned} \quad (5.3)$$

We can express the velocities in the center of mass frame in terms of those in the lab frame,

$$\mathbf{v}'_X = -\mathbf{v}_{CM}, \mathbf{v}'_a = \mathbf{v}_a - \mathbf{v}_{CM}, \mathbf{v}'_b = \mathbf{v}_b - \mathbf{v}_{CM}, \mathbf{v}'_Y = \mathbf{v}_Y - \mathbf{v}_{CM} \quad (5.4)$$

where \mathbf{v}_{CM} is the velocity of the center of mass frame in the lab frame and given by

$$\mathbf{v}_{CM} = \frac{m_a \mathbf{v}_a}{m_a + m_X} \quad (5.5)$$

According to momentum conservation we have

$$m_a \mathbf{v}_a = m_b \mathbf{v}_b + m_Y \mathbf{v}_Y \quad (5.6)$$

Suppose we choose the direction of \mathbf{v}_a (same as \mathbf{v}_{CM}) as the z-axis, and denote the angles between the direction of \mathbf{v}_b and the z-axis as θ_b and θ'_b in the lab and center of mass frame respectively. We decompose the total momentum into parallel and transverse directions, the momentum conservation becomes

$$\begin{aligned} m_a v_a &= m_b v_b \cos \theta_b + m_Y v_Y \cos \theta_Y \\ 0 &= m_b v_b \sin \theta_b - m_Y v_Y \sin \theta_Y \end{aligned} \quad (5.7)$$

Once the initial state is fixed there are six variables, \mathbf{v}_b and \mathbf{v}_Y , in the final state. There are four energy-momentum conservation relations. The two-to-two scattering is on a plane so there is freedom to fix the orientation of the plane. Therefore there is only one free variable, we can choose it to be the angle θ_b or the scalar velocity v_b .

Now we can determine the Q-value, which is frame independent. We can eliminate v_Y and θ_Y since it is hard to measure in experiments from Eq. (5.7),

$$\begin{aligned} m_Y^2 v_Y^2 &= (m_b v_b \sin \theta_b)^2 + (m_a v_a - m_b v_b \cos \theta_b)^2 \\ &= m_b^2 v_b^2 + m_a^2 v_a^2 - 2m_a m_b v_a v_b \cos \theta_b \end{aligned} \quad (5.8)$$

Then the Q-value is

$$\begin{aligned} Q &= T_Y + T_b - T_X - T_a \\ &= \frac{1}{2m_Y} [m_b^2 v_b^2 + m_a^2 v_a^2 - 2m_a m_b v_a v_b \cos \theta_b] + T_b - T_X - T_a \\ &= \left(1 + \frac{m_b}{m_Y}\right) T_b + \left(-1 + \frac{m_a}{m_Y}\right) T_a - T_X - \frac{m_a m_b}{m_Y} v_a v_b \cos \theta_b \end{aligned} \quad (5.9)$$

If we let θ_b be the free variable, we can determine v_b from the above energy conservation equation. Then from Eqs. (5.7,5.8) we can determine v_Y and θ_Y .

We obtain the relation between θ_b and θ'_b ,

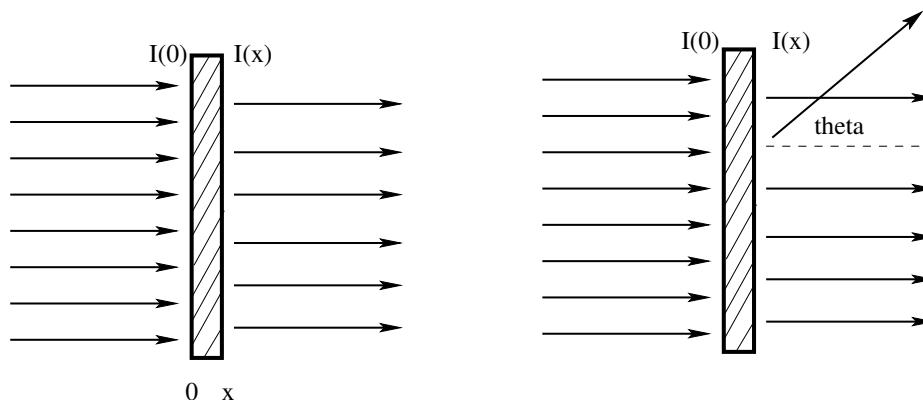
$$\begin{aligned} v'_b \sin \theta'_b &= v_b \sin \theta_b, \\ v'_b \cos \theta'_b &= v_b \cos \theta_b - v_{CM}, \\ \tan \theta'_b &= \frac{v_b \sin \theta_b}{v_b \cos \theta_b - v_{CM}}. \end{aligned} \quad (5.10)$$

Here v'_b is given by $(v'_b)^2 = v_b^2 + v_{CM}^2 - 2v_b v_{CM} \cos \theta_b$. In the center of mass frame, we have $m_Y \mathbf{v}'_Y = -m_b \mathbf{v}'_b$, then we can determine $v'_Y = (m_b/m_Y)v'_b$.

The reaction rate depends on the energies of participating particles, the particle flux and the cross section of the reaction. The cross section is used to describe the probability for a type of nuclear reaction to take place. The cross section is defined as,

$$\sigma = \frac{R}{I_0 N_S}, \quad (5.11)$$

Figure 5.2: The cross section.



where R is the number of reactions per unit time or the reaction rate, N_S the number of nuclei per unit area, and I_0 the incident particles per unit time. Consider a sheet of target material with width x in Fig. 5.2. We have $N_S = N_V x$, where N_V is the number of nuclei per unit volume in the target. Then the number of incident particles per unit time which are through the target without collisions is

$$I(x) = I_0 - R = I_0(1 - \sigma N_V x) \approx I_0 e^{-\sigma N_V x} \quad (5.12)$$

We can see that $I(x)$ decays with x exponentially. The mean free path is given by $1/(\sigma N_V)$.

The cross section means the reaction rate of one particle hitting one target nucleus per unit area. The unit for the cross section is barn (b), milli-barn (mb) and micro-barn (μb),

$$\begin{aligned} 1 \text{ b} &= 10^{-28} \text{ m}^2, \\ 1 \text{ mb} &= 10^{-31} \text{ m}^2, \\ 1 \mu\text{b} &= 10^{-34} \text{ m}^2. \end{aligned} \quad (5.13)$$

The differential cross section is defined as,

$$\frac{d\sigma}{d\Omega}(\theta, \phi) = \frac{\Delta R}{I_0 N_S \Delta\Omega}, \quad (5.14)$$

where ΔR is the number of scatterings in the solid angle $\Delta\Omega$ per unit time.

The differential cross section depends on the frame since the polar angle θ is different in different frame. Suppose the differential cross section is independent of the azimuthal angle, we have the relation between the lab and center of mass frame,

$$\frac{d\sigma}{d\Omega}(\theta) \sin\theta d\theta = \frac{d\sigma}{d\Omega}(\theta') \sin\theta' d\theta', \quad (5.15)$$

and we obtain from the first line of Eq. (5.10),

$$\frac{d\sigma}{d\Omega}(\theta) = \frac{d \cos\theta'}{d \cos\theta} \frac{d\sigma}{d\Omega}(\theta') = \left(\frac{v}{v'} + \frac{v v_{CM} \cos\theta'}{v'^2} \right) \frac{d\sigma}{d\Omega}(\theta'). \quad (5.16)$$

Exercise 39. Consider the reaction $d + {}^6\text{Li} \rightarrow \alpha + \alpha$ with $T_d = 2 \text{ MeV}$ in the lab frame, calculate the emission angle θ of one α -particle in the lab frame as function of the velocity of one alpha particle v_α .

Exercise 40. Derive Eq. (5.16).

5.2 Partial wave analysis and optical potential

The elastic, inelastic and total cross section are

$$\begin{aligned}\sigma_{\text{el}} &= \frac{\pi}{k^2} \sum_{l=0}^{\infty} (2l+1) |1 - S_l|^2 \\ \sigma_{\text{in}} &= \frac{\pi}{k^2} \sum_{l=0}^{\infty} (2l+1) (1 - |S_l|^2) \\ \sigma_{\text{tot}} &= \frac{2\pi}{k^2} \sum_{l=0}^{\infty} (2l+1) (1 - \text{Re}S_l)\end{aligned}\quad (5.17)$$

where $S_l = |S_l|e^{2i\delta_l(k)}$ and $\delta_l(k)$ is the phase shift. Having $|1 - S_l|^2 = 1 - 2\text{Re}S_l + |S_l|^2$, we can verify

$$\sigma_{\text{tot}} = \sigma_{\text{el}} + \sigma_{\text{in}} \quad (5.18)$$

In nuclear reaction, the elastic scattering can be further divided into potential and resonance scatterings

$$\sigma_{\text{el}} = \sigma_{\text{pot}} + \sigma_{\text{res}} \quad (5.19)$$

So the total cross section can be decomposed in several different ways,

$$\begin{aligned}\sigma_{\text{tot}} &= \sigma_{\text{el}} + \sigma_{\text{in}} \\ &= \sigma_{\text{pot}} + \sigma_{\text{res}} + \sigma_{\text{in}} \\ &= \sigma_{\text{pot}} + \sigma_{\text{a}} \\ &= \sigma_{\text{pot}} + \sigma_{\text{CN}} + \sigma_{\text{D}}\end{aligned}\quad (5.20)$$

where $\sigma_{\text{a}} = \sigma_{\text{res}} + \sigma_{\text{in}} = \sigma_{\text{CN}} + \sigma_{\text{D}}$, with $\sigma_{\text{CN}}, \sigma_{\text{D}}$ the formation cross sections of compound nuclei and direct reaction respectively.

The idea of the optical potential is to treat a nucleus as a semi-opaque ball. When incident particle hits the nucleus part of it is reflected or scattered, the other part of it is absorbed. It is convenient to introduce the optical potential,

$$V_{\text{eff}}(r) = \begin{cases} -(V_0 + iU), & r \leq R \\ 0, & r > R \end{cases} \quad (5.21)$$

with the nuclear radius R . The wave function is in the form,

$$\psi = Ae^{ik_c x} \quad (5.22)$$

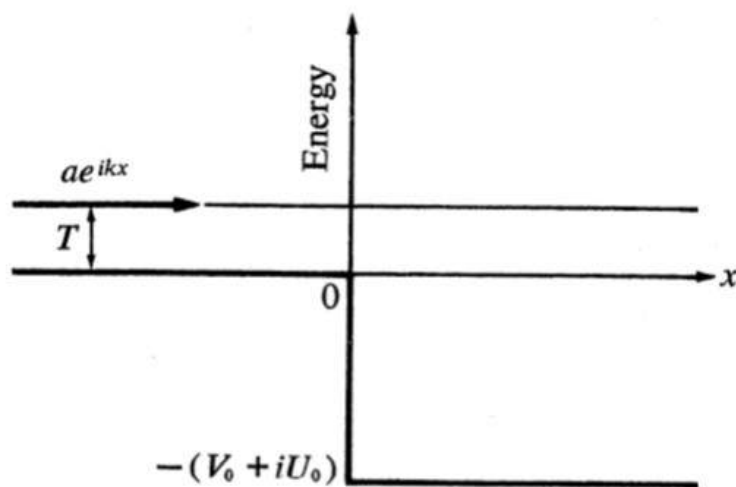
where

$$\begin{aligned}k_c &= \sqrt{2m(T + V_0 + iU)} \\ &\approx \sqrt{2m(T + V_0)} + iU \sqrt{\frac{m}{T + V_0}} \\ &= k + ik'\end{aligned}\quad (5.23)$$

where T is the kinetic energy of the incident particle. So the wave function have a damping part,

$$\psi = Ae^{ik_c x} = Ae^{ikx} e^{-k'x} \quad (5.24)$$

Figure 5.3: Optical potential [4].



(a)



(b)

The absorption rate is proportional to $e^{-2k'x}$. The typical attenuation length is given by

$$l = \frac{1}{2k'} = \frac{1}{2U} \sqrt{\frac{T + V_0}{m}} \quad (5.25)$$

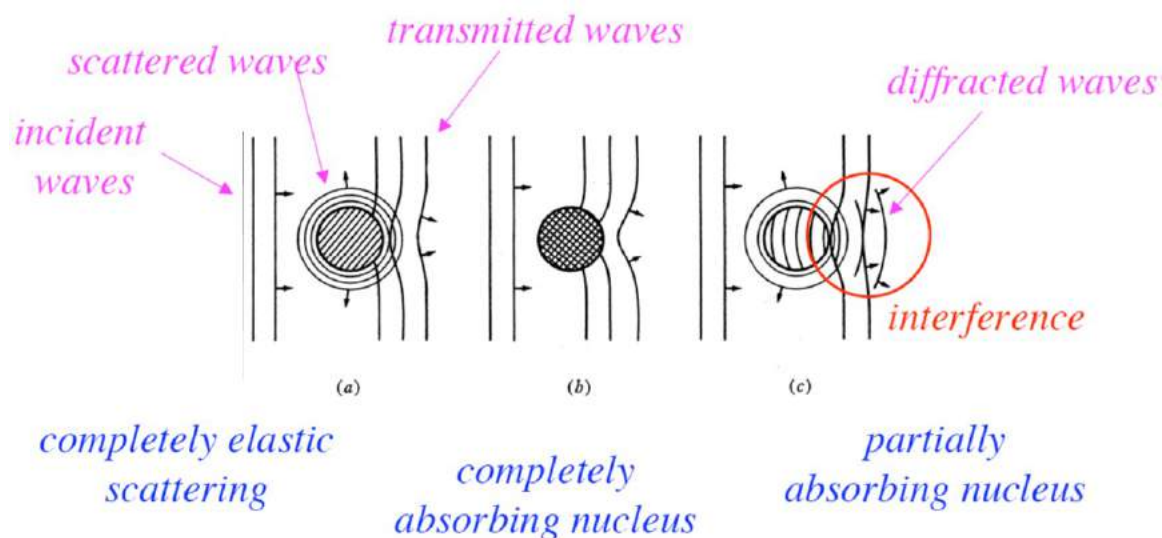
We can estimate the mean free path when a neutron with energy $T = 10$ MeV hits a nucleus with potential $V_0 = 40$ MeV and $U = 1$ MeV. We obtain $l \approx 23$ fm, which is much larger than nuclear size. We conclude that such a neutron can go through the nucleus almost without collisions.

More precisely the square well potential can be replaced by Woods-Saxon potential as

$$V_{\text{eff}}(r) = -\frac{V_0(V_0 + iU)}{1 + e^{(r-R)/a}} \quad (5.26)$$

where a is the width of the nuclear surface. For nuclear reaction induced by neutron and proton, the spin-orbital term can be included into the potential.

Figure 5.4: Types of scatterings [4].



5.3 Resonance and compound nuclear reaction

Compound nuclear reaction is one of low energy nuclear reaction and was first proposed by N. Bohr in 1936. It can be written as



where C^* denotes the compound nucleus. The cross section for the above reaction is

$$\sigma_{ab} = \sigma_a \frac{\Gamma_b}{\Gamma} \quad (5.28)$$

where σ_a is the formation cross section for the compound nucleus C^* , Γ is the total decay width of the compound nucleus C^* , and Γ_b is the decay width for the b-channel. When the incident particle (nucleus or nucleon) enters the nucleus X it strongly interacts with surrounding nucleons inside X and quickly loses its energy to the surrounding nucleons to reach equilibrium and then form the excited compound nucleus C^* . The excitation energy levels are well discretized for low excitations. So the cross section has a resonance feature. For higher excitations, the energy levels are continuous so the cross section varies slowly with energy, which is called continuum region. The transition from resonance to continuum depends on the energy and nucleus atomic number. The compound nucleus in the excited state will decay by emitting a number of nucleons or a nucleus.

We can derive the resonance cross section. The total cross section is

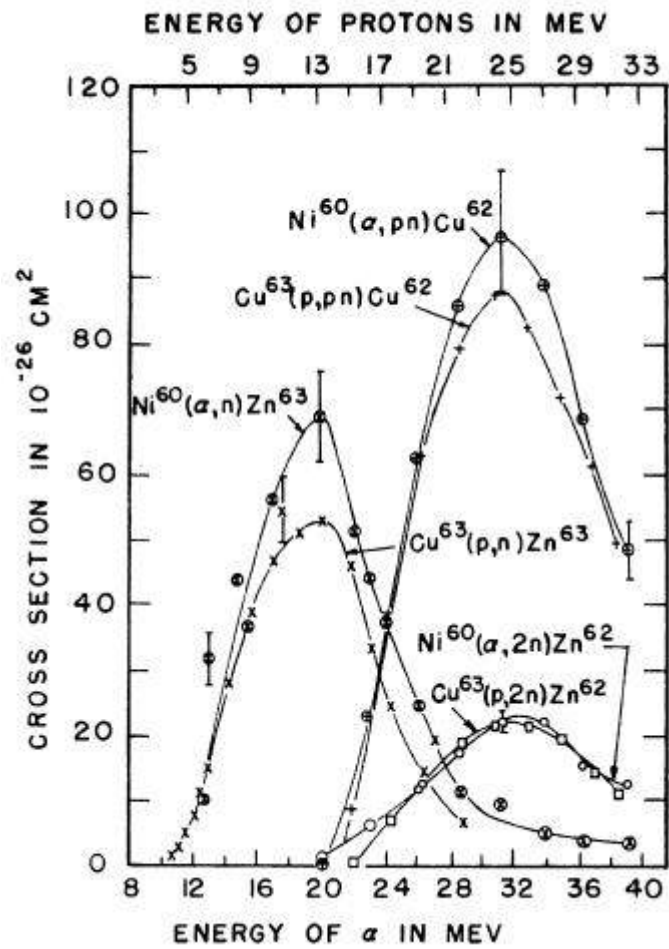
$$\begin{aligned} \sigma_{\text{tot}} &= \frac{4\pi}{k} \sum_{l=0}^{\infty} (2l+1) \text{Im} f_l(0) \\ &= \frac{4\pi}{k^2} \sum_{l=0}^{\infty} (2l+1) \sin^2 \delta_l(E) \end{aligned} \quad (5.29)$$

where is $f_l = (S_l - 1)/(2ik)$ with $S_l = e^{2i\delta_l(k)}$. When $\delta_l(E)$ satisfy

$$\delta_l(E) \sim (n + 1/2)\pi, \text{ or } \sin^2 \delta_l(E) \sim 1 \quad (5.30)$$

the partial wave cross section reaches maximum and the resonant states occur. We can expand near

Figure 5.5: Test the compound nuclear reaction model. See "An Experimental Verification of the Theory of Compound Nucleus", *Phy. Rev.* 80, 939(1950).



the resonant energy $E = E_0$ as

$$\begin{aligned}\sin \delta_l(E) &\approx \sin \delta_l(E_0) + \left[\cos \delta_l(E) \frac{d\delta_l}{dE} \right]_{E_0} (E - E_0) \approx 1 \\ \cos \delta_l(E) &\approx \cos \delta_l(E_0) - \left[\sin \delta_l(E) \frac{d\delta_l}{dE} \right]_{E_0} (E - E_0) \\ &= - \frac{d\delta_l}{dE} \Big|_{E_0} (E - E_0) = -\frac{2}{\Gamma} (E - E_0)\end{aligned}\quad (5.31)$$

where we have defined

$$\Gamma = 2 \left/ \frac{d\delta_l}{dE} \right|_{E_0} \quad (5.32)$$

So the partial wave amplitude The we have

$$\begin{aligned}f_l &= \frac{1}{k} \exp[i\delta_l(k)] \sin \delta_l(k) \\ &= \frac{1}{k} \frac{\sin \delta_l(k)}{\cos \delta_l(k) - i \sin \delta_l(k)} \\ &\approx \frac{1}{k} \frac{1}{-\frac{2}{\Gamma}(E - E_0) - i} = \frac{1}{k} \frac{-\Gamma/2}{(E - E_0) + i\Gamma/2} \\ \text{Im} f_l &= \frac{1}{k} \frac{\Gamma^2/4}{(E - E_0)^2 + \Gamma^2/4}\end{aligned}\quad (5.33)$$

If at $E \sim E_0$, the partial wave l is dominant, the cross section is then

$$\sigma_l^{\text{tot}} = \frac{\pi}{k^2} (2l + 1) \frac{\Gamma^2}{(E - E_0)^2 + \Gamma^2/4} \quad (5.34)$$

We can extend the above formula into the compound nuclear reaction $a + X \rightarrow C^*$ and choose the lowest partial wave. The cross section is then

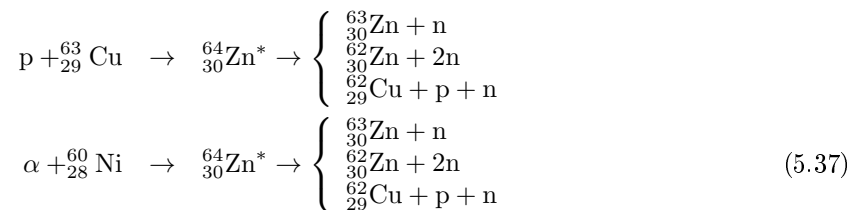
$$\sigma_a = \frac{\pi}{k^2} \frac{\Gamma_a \Gamma}{(E - E_0)^2 + \Gamma^2/4} \quad (5.35)$$

where Γ is the total width and Γ_a is the partial width for the a-channel. So the cross section for reaction (5.27) is then

$$\sigma_{ab} = \frac{\pi}{k^2} \frac{\Gamma_a \Gamma_b}{(E - E_0)^2 + \Gamma^2/4} \quad (5.36)$$

For incident nuclei with spins and resonance with non-zero spin, we should also include a spin counting factor $g = (2I_C + 1)/[(2I_a + 1)(2I_X + 1)]$, where I_C , I_a and I_X are spins of the resonance, incident particle and target nucleus respectively.

To test the compound nuclear reaction model, Ghoshal measured $p + {}^{63}_{29}\text{Cu}$ and $\alpha + {}^{60}_{28}\text{Ni}$ to form ${}^{64}_{30}\text{Zn}^*$,



The data show that

$$\sigma_{p,n} : \sigma_{p,2n} : \sigma_{p,pn} = \sigma_{\alpha,n} : \sigma_{\alpha,2n} : \sigma_{\alpha,pn} = \Gamma_n : \Gamma_{2n} : \Gamma_{pn} \quad (5.38)$$

which predicted by the model.

The angular distribution of nucleon emitted by compound nuclei is almost isotropic without preferable direction, i.e. the compound nuclei lose the memory of the incident particle's direction. The emission of outgoing particles is like evaporation. This is not surprising since the energy of the incident particle is distributed among all nucleons in the nucleus. The more energy is pumped into the nuclei, more particles are likely to evaporate.

Exercise 41. *The Breit-Wigner formula for the single-level compound cross section in the nuclear reaction $a + X \rightarrow C^*$ is*

$$\sigma_{ab} = g \frac{\pi}{k^2} \frac{\Gamma_a \Gamma_b}{(E - E_0)^2 + \Gamma^2/4}$$

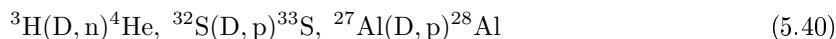
where $g = (2I_C + 1)/[(2I_a + 1)(2I_X + 1)]$, I_C , I_a and I_X are spins of the compound nucleus or resonance, incident particle and target nucleus respectively. Consider the compound nucleus (resonance) reaction $n + {}_{92}^{235}\text{U} \rightarrow C^*$ with $I_U = 7/2$ and $I_n = 1/2$. At neutron energies below 0.5 eV, the cross section is dominated by one resonance with $I_C = 3$ at a kinetic energy of 0.29 eV with a width of 0.135 eV. There are three channels, which allow the compound state to decay by neutron emission, photon emission, or fission. At resonance the contributions to the neutron cross sections are (a) elastic and resonant scattering ($\ll 1$ barn); (b) radiative capture (70 barns); (c) fission (200 barns). The questions: (1) Calculate the partial widths for the three channels. (2) How many fissions per second will there be in a sheet of U-235 of thickness 1mg/cm^{-2} , traversed by normally by a neutron beam of 10^5 per second with a kinetic energy of 0.29 eV?

5.4 Direct reaction

Stripping reaction is one kind of direct reaction, where the projectile nucleus loses some of its constituents to the target nucleus and the rest of it pass through as final nucleus. Stripping reaction for deuteron is a normal type and can be denoted as



For example, we have



Nuclear fission and fusion are also direct reactions.

Knock-out reaction is another type of direct reaction, where the projectile nucleus knocks out some constituents of the target and stays in the target or emits with less energy. For example,



The transfer reaction is a reaction type where a number of protons or neutrons of the projectile leave in the target or the projectile grab a number of protons or neutrons from the target nuclear. For example,

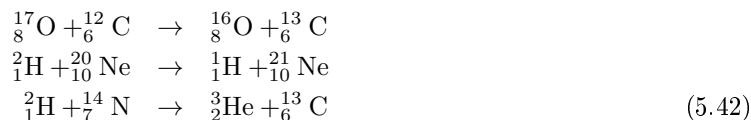
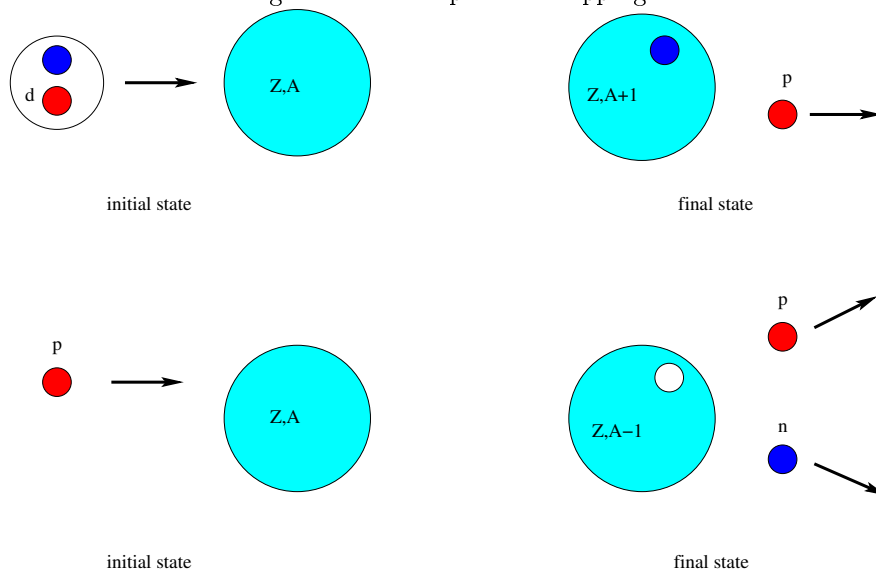


Figure 5.6: Examples for stripping and knock-out reactions.

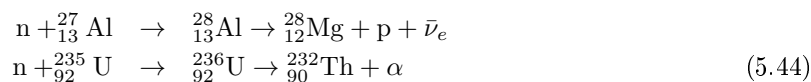


Another example is the reaction in which the neutron was first discovered by Chadwick in 1932,



It is also used for generating neutrons in the lab. The helium-4 particles come from radioactive americium, and the beryllium is just a piece of metal.

Neutron absorption is a reaction where a neutron is absorbed by a nucleus, for example,



Note that aluminum-28 and uranium-236 are very unstable and decay very quickly through β and α decay respectively.

Another important nuclear reaction is the heavy ion collisions, where two heavy nuclei collide each other.

5.5 Nuclear fission

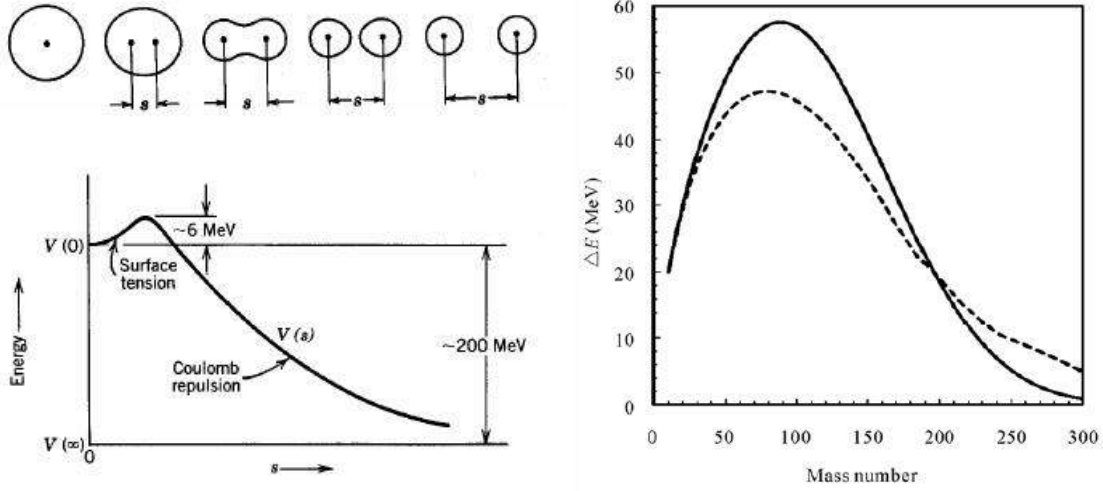
Nuclear fission is phenomenon where a nucleus split to two fragments of approximately equal mass. The nuclear fission was discovered in 1939 by Hahn and Strassmann when they found the uranium atom, when bombarded by neutrons, can produce barium, a much lighter element than uranium.

There are two types of nuclear fissions: the spontaneous fission and induced fission. The spontaneous fission happens without any outside perturbations. The induced fission needs an absorption of additional particles, e.g. a slow neutron, to excite the nucleus and fragment into smaller pieces. Induced fission takes place in nuclear reactors.

5.5.1 Spontaneous fission

In order for the spontaneous fission to take place, fissile nuclei must overcome the Coulomb barrier, see Fig. 5.7(a). We take U-238 for example. We assume it split into two equal daughter nuclei

Figure 5.7: (a) Droplet model for fission. Fission barrier is about 6 MeV. (b) The fission barrier as a function of mass number.



whose surface touch. Then the distance between two daughter nuclei can be approximated as $R = 2 \times 1.2 \times (238/2)^{1/3} \approx 14.9$ fm. We can estimate the Coulomb potential as follows,

$$V = \frac{(Z/2)^2 e^2}{R} = \frac{46^2 \times 197}{14.9 \times 137} \approx 204 \text{ MeV.} \quad (5.45)$$

This is roughly the energy released in fission. The fission barrier or the activation energy as a function of mass number can be shown in Fig. 5.7(b).

Now we first discuss about the spontaneous fission in detail. We take a very simple example, a mother nucleus splits into two daughters,



where $A = A_1 + A_2$ and $Z = Z_1 + Z_2$. The Q-value is

$$\begin{aligned} Q &= a_S(A^{2/3} - A_1^{2/3} - A_2^{2/3}) + a_C(Z^2 A^{-1/3} - Z_1^2 A_1^{-1/3} - Z_2^2 A_2^{-1/3}) \\ &= a_S[A^{2/3} - A_1^{2/3} - (A - A_1)^{2/3}] \\ &\quad + a_C[Z^2 A^{-1/3} - Z_1^2 A_1^{-1/3} - (Z - Z_1)^2 (A - A_1)^{-1/3}] \end{aligned} \quad (5.47)$$

We require that Q is stable with respect to varying A_1 and Z_1 , i.e.

$$\begin{aligned} \frac{\partial Q}{\partial A_1} &= \frac{2}{3} a_S [-A_1^{-1/3} + (A - A_1)^{-1/3}] \\ &\quad + \frac{1}{3} a_C [Z_1^2 A_1^{-4/3} - (Z - Z_1)^2 (A - A_1)^{-4/3}] = 0 \\ \frac{\partial Q}{\partial Z_1} &= 2 a_C [-Z_1 A_1^{-1/3} + (Z - Z_1)(A - A_1)^{-1/3}] = 0 \end{aligned} \quad (5.48)$$

which gives $A = 2A_1$ and $Z = 2Z_1$. The stability of the nucleus with respect to the fission is that the Q-value is less than zero, with $A = 2A_1$ and $Z = 2Z_1$, the threshold condition is then

$$Q(A_1 = A/2, Z_1 = Z/2) = a_S(1 - 2^{1/3})A^{2/3} + a_C(1 - 2^{-2/3})\frac{Z^2}{A^{1/3}} = 0 \quad (5.49)$$

whose solution is

$$\frac{Z^2}{A} = \frac{a_S(2^{1/3} - 1)}{a_C(1 - 2^{-2/3})} \approx 0.7 \frac{a_S}{a_C} \approx 18 \quad (5.50)$$

where we have used $a_S \approx 17.8$ MeV and $a_C \approx 0.71$ MeV. Note that Q is an increasing function of A , then we conclude that nuclei with $A \lesssim 70$ are stable with respect to spontaneous fission.

Like alpha decay, the spontaneous fission is also a quantum tunneling effect. For the spontaneous fission to take place the Q -value must be equal to the Coulomb barrier at the distance of scission for two daughter nuclei or at $2R_1$,

$$a_S(1 - 2^{1/3})A^{2/3} + a_C(1 - 2^{-2/3})\frac{Z^2}{A^{1/3}} = \frac{Z_1^2 e^2}{2R_1} \quad (5.51)$$

where $R_1 \approx r_0 A_1^{1/3} \approx r_0 2^{-1/3} A^{1/3}$ and $Z_1 \approx Z/2$. Then the solution is

$$\begin{aligned} \frac{Z^2}{A} &= \frac{a_S(1 - 2^{1/3})}{e^2/(r_0 2^{8/3}) - a_C(1 - 2^{-2/3})} \\ &\approx \frac{0.26a_S}{0.37a_C - 0.16e^2 r_0^{-1}} \approx 2.25 \frac{a_S}{a_C} \approx 56 \end{aligned} \quad (5.52)$$

where we have used $r_0 = 1.25$ fm, $e^2 = 1/137$, $e^2/r_0 \approx 1.62a_C$ with $a_C = 0.71$ MeV and $a_S = 17.8$ MeV. The stability condition for spontaneous fission is $Z^2/A \lesssim 56$. So we find a heavy nucleus with $A \approx 226$ and $Z \approx 113$ cannot have spontaneous fission. Of course this is a very rough estimation.

Bohr explained the spontaneous fission using the nuclear droplet model, see Fig. 5.7. The deformation is assumed to be the reason for the fission. Nuclear density or volume is almost constant under small deformations. A sphere has the smallest ratio of surface area to volume. If the sphere is deformed to ellipsoid at constant density its surface area and surface energy will increase. Since the deformation makes charges separate, the Coulomb energy will decrease. The surface tension tends to make the deformed nucleus recover to sphere, while the Coulomb potential tends to make the nucleus be even more deformed. That the nucleus will be stable or unstable for a small deformation depends on whether the increase of surface energy outperforms the decrease of Coulomb energy. The deformation can be described by a long ellipsoid with the half lengths of the long axis and short axis are $r_1 = R(1 + a)$ and $r_2 = R/\sqrt{1 + a}$ respectively. The Coulomb and surface energies are

$$\begin{aligned} E_C(a) &= \frac{1}{2} \int dV dV' \frac{1}{|\mathbf{r} - \mathbf{r}'|} \rho(\mathbf{r}) \rho(\mathbf{r}') = \frac{3}{5} \frac{Q^2}{R} \left(1 - \frac{a^2}{5}\right) = a_C Z^2 A^{-1/3} \left(1 - \frac{a^2}{5}\right) \\ E_S(a) &= 4\pi R^2 \sigma \left(1 + \frac{2a^2}{5}\right) = a_S A^{2/3} \left(1 + \frac{2a^2}{5}\right) \end{aligned} \quad (5.53)$$

where we have used

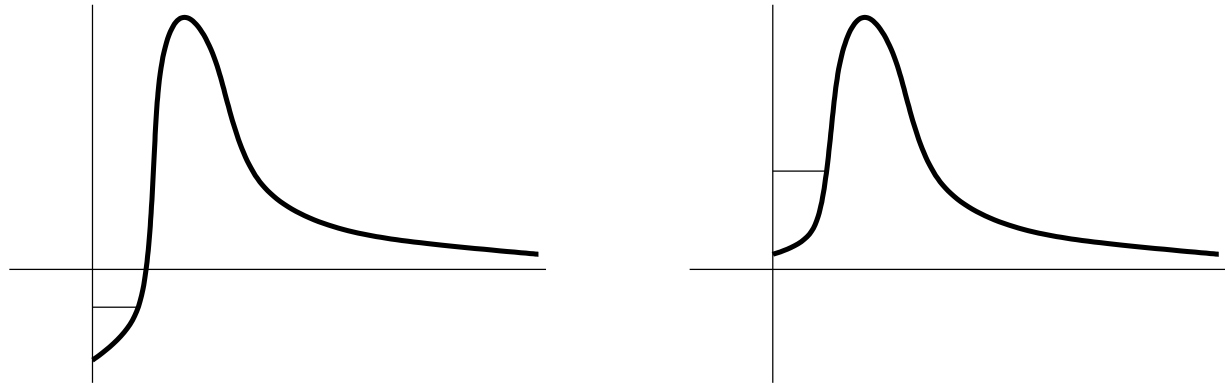
$$\begin{aligned} V &= \frac{4\pi}{3} r_1 r_2^2 = \frac{4\pi}{3} R^3 \\ S &= 2\pi \left[r_2^2 + \frac{r_1 r_2 \sin^{-1} e}{e} \right] \end{aligned} \quad (5.54)$$

where $e = \sqrt{1 - (r_2/r_1)^2}$. The change in the binding energy of the deformed nucleus is from the Coulomb and surface energy,

$$\begin{aligned} \Delta E &= E_C(a) + E_S(a) - E_C(0) - E_S(0) \\ &= -a_C Z^2 A^{-1/3} \frac{a^2}{5} + a_S A^{2/3} \frac{2a^2}{5} = a_S A^{2/3} \frac{2a^2}{5} (1 - x) \end{aligned} \quad (5.55)$$

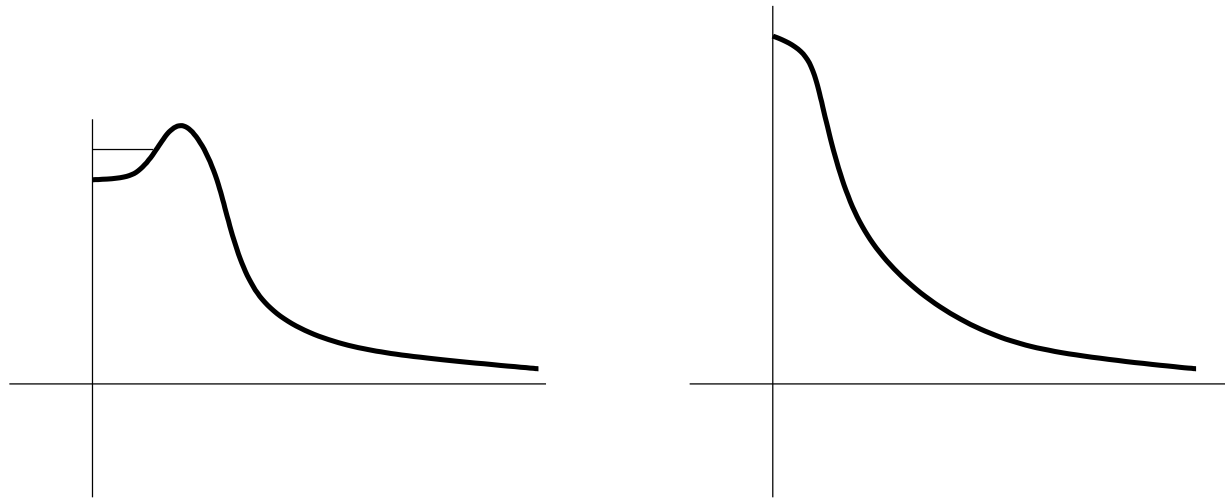
where $x = \frac{a_C}{2a_S} \frac{Z^2}{A}$. Here we have used $\frac{3}{5} \frac{Q^2}{R} = a_C \frac{Z^2}{A^{1/3}}$ and $4\pi R^2 \sigma = a_S A^{2/3}$. When $x < 1$, the binding gets positive correction, so the nucleus is stable against the spontaneous fission, when $x > 1$, the binding gets negative correction, the nucleus is unstable against the fission.

Figure 5.8: The potential energy of a nucleus as a function of deformation parameter Z^2/A . (a) $Z^2/A \ll 0.7 \frac{a_S}{a_C}$; (b) $Z^2/A \gtrsim 0.7 \frac{a_S}{a_C}$; (c) $Z^2/A \lesssim 2.6 \frac{a_S}{a_C}$; (d) $Z^2/A > 2.6 \frac{a_S}{a_C}$.



(a)

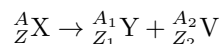
(b)



(c)

(d)

Exercise 42. Suppose a mother nucleus splits into two equal daughters,



where $A_1 = A_2 = A/2$ and $Z_1 = Z_2 = Z/2$. The coefficients in the nuclear binding energy are: $a_V \approx 15.75$ MeV (volume energy term), $a_S \approx 17.8$ MeV (surface energy term), $a_C \approx 0.71$ MeV (Coulomb energy term), $a_{\text{sym}} \approx 23.3$ MeV (symmetric energy term), $a_P \approx 12$ MeV (pairing energy term). (1) Express the Q -value of the above fission reaction. (2) In order for the fission to take place, Q value must be no less than the Coulomb barrier $Z_1^2 e^2 / (2R_1)$, try to estimate the critical value of Z^2/A at which fission can take place. Here $R_1 = r_0 A_1^{1/3}$ and $r_0 = 1.2$ fm. (3) If we further assume $Z = A/2$, what would A be for fissionable nuclei?

5.5.2 Induced fission

The uranium nucleus ${}^{235}_{92}\text{U}$ can have fission when absorbing a slow neutron which makes ${}^{236}_{92}\text{U}$ in an excited state with excitation energy obtained by,

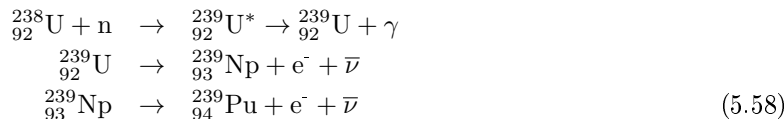
$$\begin{aligned} S_n({}^{236}\text{U}) &= m({}^{235}\text{U}) + m_n - m({}^{236}\text{U}) \\ &= \Delta({}^{235}\text{U}) + \Delta m_n - \Delta({}^{236}\text{U}) \\ &= 40.91 + 8.07 - 42.44 \approx 6.54 \text{ MeV} \end{aligned} \quad (5.56)$$

where Δ denotes the nuclear mass excess relative to atomic mass unit (931.5 MeV) times the atomic number. We see that $S_n({}^{236}\text{U}) \approx 6.54$ MeV is larger than its fission barrier 5.9 MeV.

But ${}^{238}\text{U}$ cannot undergo fission with a slow neutron. The difference is that ${}^{236}\text{U}$ is an even-even nucleus whose binding energy is larger with full pairings of neutrons while ${}^{239}\text{U}$ is an even-odd nucleus whose binding energy is smaller. The uranium nucleus ${}^{239}\text{U}$ tends to decay to its ground state through emitting a γ photon. Since ${}^{236}\text{U}$ is tightly bound, so it tends to split into nearly equally massive fragments. By capturing a slow neutron, the excitation energy of ${}^{239}\text{U}$ is

$$\begin{aligned} S_n({}^{239}\text{U}) &= m({}^{238}\text{U}) + m_n - m({}^{239}\text{U}) \\ &= \Delta({}^{238}\text{U}) + \Delta m_n - \Delta({}^{239}\text{U}) \\ &= 47.3 + 8.07 - 50.6 \approx 4.8 \text{ MeV} \end{aligned} \quad (5.57)$$

which is not enough to overcome the fission barrier 6.2 MeV. Here are reactions of ${}^{238}\text{U}$ when capturing a slow neutron,



Here ${}^{239}_{94}\text{Pu}$ is fissionable element since it is an even-odd nucleus. The abundances of ${}^{235}\text{U}$ and ${}^{238}\text{U}$ are 0.7% and 99.3% on the earth. ${}^{239}\text{U}$ and ${}^{239}\text{Pu}$ do not exist on the earth.

The fission cross sections for ${}^{235}\text{U}/{}^{238}\text{U}$ or ${}^{235}\text{U}(n, f)/{}^{238}\text{U}(n, f)$ are shown in Figs. 5.9 and 5.11. In the thermal region, the cross section has $1/v$ behavior. In the energy range 1-100 eV there are many resonances produced. For U-235, the cross section for fission induced by thermal neutrons is 3 orders of magnitude larger than by fast neutrons. For U-238, fission cannot occur in the thermal region.

As we have shown before that the fissionable nuclei are heavy nuclei, the heavier the nuclei are the more neutrons they have because the number of neutron increases with the mass number. Therefore the fragments have more neutrons and away from beta-stable line. These neutrons are called prompt

Figure 5.9: The cross sections of the neutron induced fissions for ^{235}U and ^{238}U . The data are from Neutron Cross-section Standards 2006 [<http://www-nds.iaea.org/>].

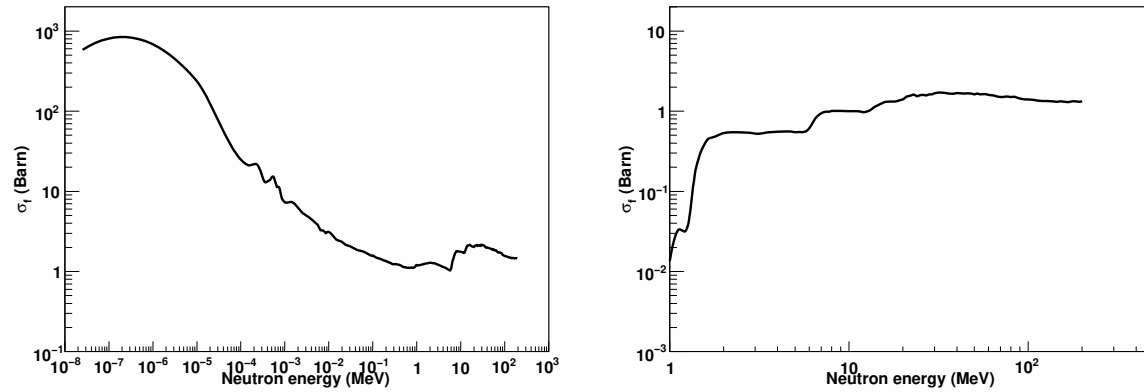


Figure 5.10: The energy spectra of fission neutron. (a) Fission neutron spectrum for the system $^{238}\text{U}(n, f)$ measured with the FIGARO setup [32]. Data are for incident neutron energies from 2.1 to 4.0 MeV and are compared to a precision measurement at 2.9 MeV incident neutron energy [33]. (b) Prompt fission neutron spectrum of Neptunium-237 for 0.62 MeV incident neutrons.

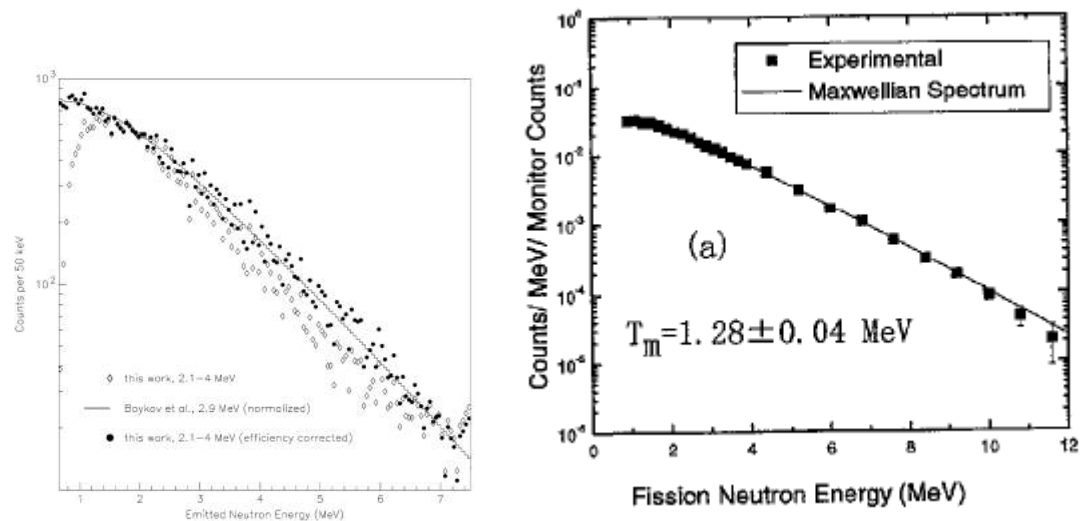


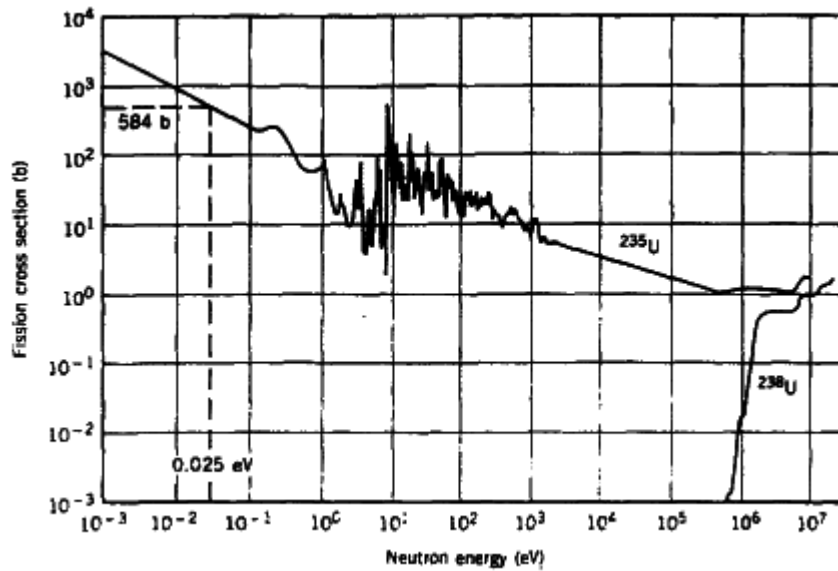
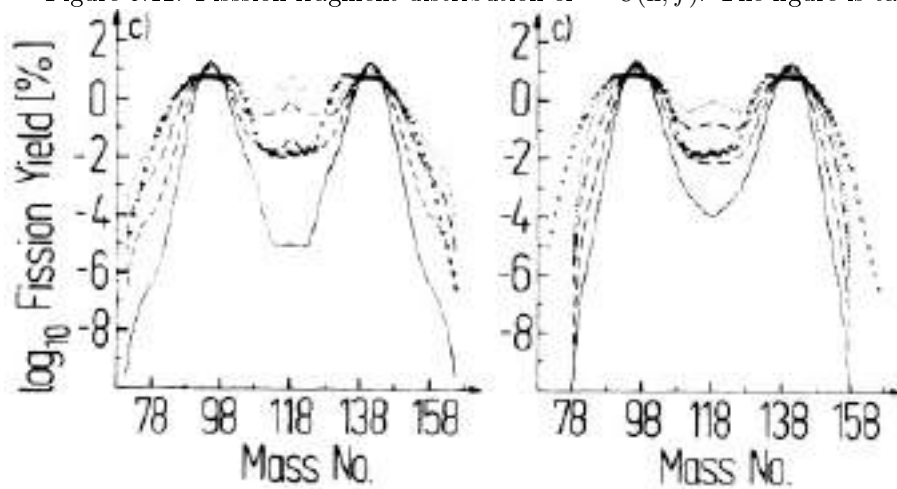
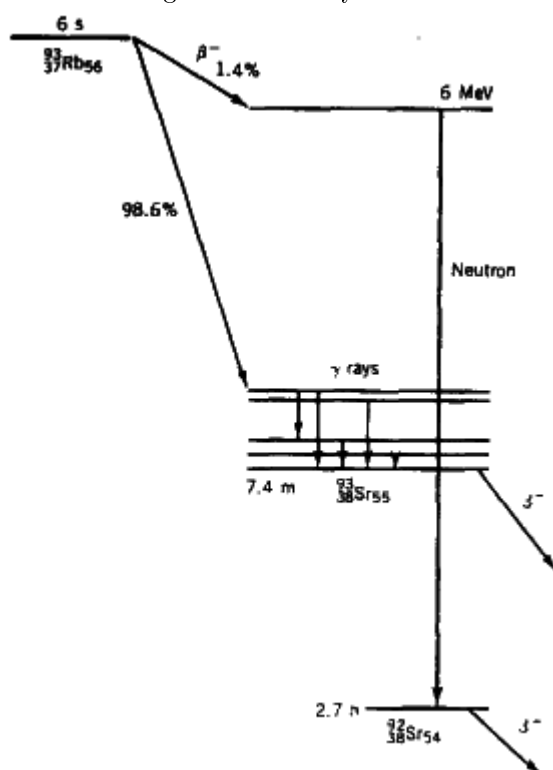
Figure 5.11: Cross sections for neutron induced fission of ^{235}U and ^{238}U . Taken from Ref. [4].Figure 5.12: Fission fragment distribution of $^{235}\text{U}(n, f)$. The figure is taken from Ref. [30].

Figure 5.13: Delayed neutron emission from Rb-93. Taken from Ref. [4].



neutrons because they emitted in less than 10^{-15} s. Their distribution is isotropic. The fission fragments normally undergo beta decay and followed by more neutron emission. These neutrons are called delayed neutron. The delay time is of order of a few seconds. For example, following the 6-seconds beta decay of $^{93}_{37}\text{Rb} \rightarrow ^{93}_{38}\text{Sr}^* + e^- + \bar{\nu}_e$, the excited state $^{93}_{38}\text{Sr}^*$ has a larger enough energy than neutron separation energy, so it can decay by neutron emission in competition with Gamma emission, $^{93}_{38}\text{Sr}^* \rightarrow ^{92}_{38}\text{Sr} + n$. The delay neutrons are normally used to control chain reactions in fission reactors. See Fig. 5.13 for the scheme plot of the above beta decay and delayed neutron emission.

The energy spectra of the prompt neutrons follows Maxwell distribution

$$f(E) \sim \sqrt{E} \exp(-E/T_m) \quad (5.59)$$

where T_M is called Maxwell temperature of about one or two MeV, see Fig. 5.10. The example for the neutron energy spectra are those in the spontaneous fission of $^{252}_{98}\text{Cf}$ and in the induced fission of $^{235}_{92}\text{U}$ with thermal neutrons, where T_m are

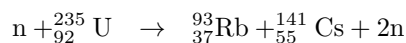
$$\begin{aligned} T_m[^{252}_{98}\text{Cf}] &= 1.453 \pm 0.017 \text{ MeV} \\ T_m[^{235}_{92}\text{U} + n_{\text{th}}] &= 1.319 \pm 0.019 \text{ MeV} \end{aligned} \quad (5.60)$$

The average energy of neutrons is $3T_m/2$. The number of neutrons follows the Gauss distribution

$$P(\lambda) = \frac{1}{\sqrt{2\pi\sigma}} \exp\left[-\frac{(\lambda - \bar{\lambda})^2}{2\sigma^2}\right] \quad (5.61)$$

where $\bar{\lambda}$ is the average number of neutrons including prompt and delayed neutrons, which is about 2 to 4 for most nuclei. For thermal induced fission of ^{233}U , ^{235}U and ^{238}U , the average numbers of prompt neutrons are 2.48, 2.42, 2.86 respectively.

The probability for a fissionable nucleus to split to two equal fragments is very small. Normally there is a distribution of fission fragments as a function of mass number, for example the fragments of $^{235}\text{U}(n, f)$ follow the distribution as shown in Fig. 5.12. The most probable fragments for induced fission reaction $^{235}\text{U}(n, f)$ are around $A_1 = 95$ and $A_2 = 140$. This is a typical example for induced fission,



5.5.3 Self-sustaining nuclear fissions and fission reactor

A nucleus of ^{235}U absorb a slow neutron and undergoes fission and release on average 193 MeV of energy. For example, the fission reaction



has the Q-value

$$\begin{aligned} Q &= m({}^{235}_{92}\text{U}) - m({}^{92}_{36}\text{Kr}) - m({}^{142}_{56}\text{Ba}) - m_n \\ &= [235.04 - (91.93 + 141.92) - 1.0] \text{ u} \\ &= 0.19 \text{ u} \approx 177 \text{ MeV} \end{aligned} \quad (5.63)$$

Most of them is converted to thermal energy. On average 2.5 prompt neutrons and 0.018 delayed neutrons are produced in each fission process. If at least one neutron is captured by the ^{235}U nuclei the nuclear fission is then self-sustaining with constant output of energy.

In natural uranium material on the earth the self-sustaining fission can not take place since 99.28% of ingredients are ^{238}U . The fissions of ^{238}U rely on higher energy neutrons of above 1 MeV but the neutrons quickly lose their energies via inelastic scatterings. In the 1 MeV region the cross section of $^{238}\text{U}(n, \gamma)^{239}\text{U}$ is 1/10 of $^{235}\text{U}(n, f)$ but the abundance of ^{238}U is 138 times that of ^{235}U . So in natural uranium most neutrons produced in fissions of ^{235}U are absorbed by ^{238}U which stop further fissions. There are two methods to solve this problem: either to enrich ^{235}U or to change the energy spectra of neutrons to enhance the cross section of $^{235}\text{U}(n, f)$ over $^{238}\text{U}(n, \gamma)^{239}\text{U}$. The latter method can be realized by thermalization of neutrons. Note that the fission cross section of ^{235}U follows a $1/v = \sqrt{m_n/2E}$ law, the smaller v the larger the cross section.

Through elastic scattering of light nuclei, fast neutrons of about 1 MeV can lose their energies very quickly. Now we can estimate how much energy a neutron would lose in each collision. Suppose in the lab frame a neutron with velocity v_n collides with a nucleus of mass M which is still, the scattered neutron moves in the direction θ in the center-of-mass frame. The center-of-mass frame has a velocity $v_{\text{CM}} = m_n v_n / (m_n + M)$ in the lab frame. So in the lab frame the energy is

$$\begin{aligned} E_L &= \frac{1}{2} m_n [(v_n - v_{\text{CM}}) \cos \theta + v_{\text{CM}}]^2 + (v_n - v_{\text{CM}})^2 \sin^2 \theta \\ &= \frac{1}{2} m_n [(v_n - v_{\text{CM}})^2 + v_{\text{CM}}^2 + 2(v_n - v_{\text{CM}})v_{\text{CM}} \cos \theta] \end{aligned} \quad (5.64)$$

The average energy over angle θ is then

$$\begin{aligned} \bar{E}_L &= \frac{\frac{1}{2} m_n \int d \cos \theta [(v_n - v_{\text{CM}})^2 + v_{\text{CM}}^2 + 2(v_n - v_{\text{CM}})v_{\text{CM}} \cos \theta]}{\int d \cos \theta} \\ &= \frac{1}{2} m_n [(v_n - v_{\text{CM}})^2 + v_{\text{CM}}^2] = \frac{1}{2} m_n \frac{m_n^2 + M^2}{(m_n + M)^2} v_n^2 \end{aligned} \quad (5.65)$$

So the fraction of \bar{E}_L in the incident energy E_{in} becomes

$$\frac{\bar{E}_L}{E_{\text{in}}} = \frac{M_n^2 + M^2}{(M_n + M)^2} \quad (5.66)$$

If $M \rightarrow \infty$, the lab frame coincides with the center-of-mass frame, so the neutron would not lose energy by elastic scatterings. If we use carbon as a moderator with mass $M \approx 12M_n$, the fraction becomes $\bar{E}_L/E_{in} = 145/169 \approx 0.86$, i.e. the neutron loses 14% of its energy per scattering. For a neutron of 1 MeV it will undergo $6 \ln(10)/\ln(1/0.86) \approx 91$ collisions to reach 1 eV. One would think that hydrogen would be best choice for the moderator but the cross section of $p(n, \gamma)d$ is very large so that it is not suitable. But hydrogen in the form of heavy water D_2O or some compound can be used as the moderator in the reactor with enriched uranium. Graphite is the material used as a moderator in natural uranium because ^{12}C is a light nucleus and all nucleons are in pairs so the nucleus is tightly bound.

5.5.4 Time constant of a fission reactor

The neutron number distribution in a reactor is a function of the time, position and energy of the neutron. For an ideal case, we consider a homogeneous number density n for neutrons. Due to the capture processes for these neutrons, the number of neutrons will decrease as follows $dn/dt = -n/\tau$ whose solution is $n = n_0 e^{-t/\tau}$. Here τ is the time constant and given by

$$\frac{1}{\tau} = \sum_i \sigma_i v N_i \quad (5.67)$$

where σ_i and N_i are the cross section and particle number density for the i -th process and nucleus i respectively. For a neutron with energy 1/40 eV, the cross sections are $^{238}U(n, \gamma)^{239}U$: 2.73 barns, $^{235}U(n, f)$: 577 barns, $^{235}U(n, \gamma)^{236}U$: 101 barns.

If we include the production of neutrons, the rate equation becomes

$$\frac{dn}{dt} = (k - 1) \frac{n}{\tau} \quad (5.68)$$

where k is the neutron reproduction or multiplication factor and defined as the ratio of the number of neutrons in one generation to the that in proceeding generations. It reflects the net change in the thermal neutron number between two generations. The solution to the above equation is then

$$n = n_0 e^{(k-1)t/\tau} \quad (5.69)$$

Only if $k \geq 1$, will the number density of neutrons increase, and then the fission is self-sustaining. If $k > 1$, we call it super-critical. If $k = 1$, we call it critical. If $k < 1$, we call it sub-critical. The neutron reproduction factor k is defined by

$$k = \eta f \epsilon p \quad (5.70)$$

This is known as four-factor formula. Here f is the thermal fuel utilization factor for neutrons which gives the fraction of neutrons available to U-235 and U-238. It is defined by

$$f = \frac{N_U \sigma_a(U)}{\sum_i N_i \sigma_a(i) + N_U \sigma_a(U)} \quad (5.71)$$

where $\sigma_a(i)$ is the absorption (including fission) cross section for nuclide i . The factor η is defined as the mean number of fission neutrons produced per thermal neutron in the last generation, which is given by

$$\eta(U) = \bar{\lambda} \frac{\sigma_f(U)}{\sigma_f(U) + \sigma_a(U)} \quad (5.72)$$

where $\sigma_a(U)$ is the absorption cross section by uranium. For example, for natural uranium and 1/40 eV neutrons, we have $\sigma_f(^{235}U) = 577$ b, $\sigma_a(^{235}U) = 101$ b, $\sigma_f(^{238}U) = 0$ b and $\sigma_a(^{238}U) = 2.73$ b, then we can obtain

$$\begin{aligned} \sigma_f(U) &= 0.0072 \sigma_f(^{235}U) + 0.9928 \sigma_f(^{238}U) = 4.15 \text{ b} \\ \sigma_a(U) &= 0.0072 \sigma_a(^{235}U) + 0.9928 \sigma_a(^{238}U) = 3.43 \text{ b} \end{aligned}$$

With $\bar{\lambda} = 2.5$, we get the factor $\eta(U) = 1.37$. One way to increase $\eta(U)$ is to enrich uranium.

For natural uranium, a fast neutron can induce ^{238}U to undergo fission which will also produce neutrons, so ϵ is the factor for induced fission by fast neutrons (fast-fission factor) and defined by

$$\epsilon = \frac{N_{\text{fast}} + N_{\text{thermal}}}{N_{\text{thermal}}} \quad (5.73)$$

where N_{fast} and N_{thermal} are neutron numbers from induced fission by fast and thermal neutrons respectively. In natural uranium before cooled down to thermal energy resonant absorption takes place for some neutrons.

The escape rate from such resonance absorption is denoted by resonance escape probability p . Here ϵ and p depend on the geometric shape of the reactor.

5.6 Accelerator-Driven System

5.6.1 Spallation neutron source

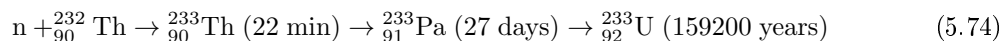
Neutrons have many properties that make them an ideal tool for certain types of research. Neutrons are neutral and are highly penetrating. So they can be used as clean and non-destructive probe to materials. Neutrons are very sensitive to hydrogen, they can locate hydrogen atoms and then to determine the structure of molecules or materials. Neutrons are also sensitive to light atoms among heavy ones. This properties have been used to locate light oxygen atoms in yttrium-barium-copper oxide (YBCO), a high-Tc superconducting ceramic, whose positions in the ceramic are crucial to the superconducting properties. Neutrons have spin and magnetic moment. Such a property makes neutron act like a compass needle to detect the magnetic structure of materials and help develop new magnetic materials. The energies of thermal neutrons almost match those of atoms in motion, or in other words, the neutron wavelength is close to the atomic spacing, so neutrons can be used to track molecular vibrations, movements of atoms during catalytic reactions, and crystal structures and atomic spacings, etc..

Neutron sources have been built to meet the needs in many fields. The Spallation Neutron Source (SNS) is an accelerator-based neutron source in Oak Ridge, Tennessee, USA, at the site of Oak Ridge National Laboratory by the U.S. Department of Energy (DOE). Spallation is a process in which fragments of material (spall) are ejected from a body due to impact or stress. In nuclear physics is the process in which a heavy nucleus emits a large number of nucleons as a result of being hit by a high-energy particle. The SNS uses high-energy protons to bombard a target made of heavy particles to produce many neutrons. For each collision 20 to 30 neutrons are ejected. The neutron energies are about 30 MeV for proton beam with 1 GeV. For more about SNS, see "<http://www.sns.gov/>".

These neutrons can be used to bombard nuclear fuel to make sustainable nuclear fission. This is called the Accelerator-Driven system (ADS). The neutrons produced by spallation act as a trigger to ignite the fission which will continue by additional neutrons produced in the course of fission. There is an advantage for the ADS system is that the fission will stop immediately once the proton beam is switched off, therefore an ADS is safer than conventional reactor. For more information about ADS, see, e.g., "<http://www.world-nuclear.org/>".

5.6.2 Thorium as fission fuel

Thorium reservation on the earth is 3 to 5 times that of uranium. Thorium can be used as fission fuel by capturing a neutron,



which is analogous to

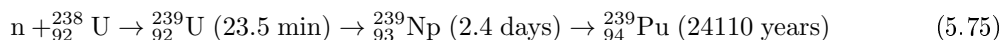
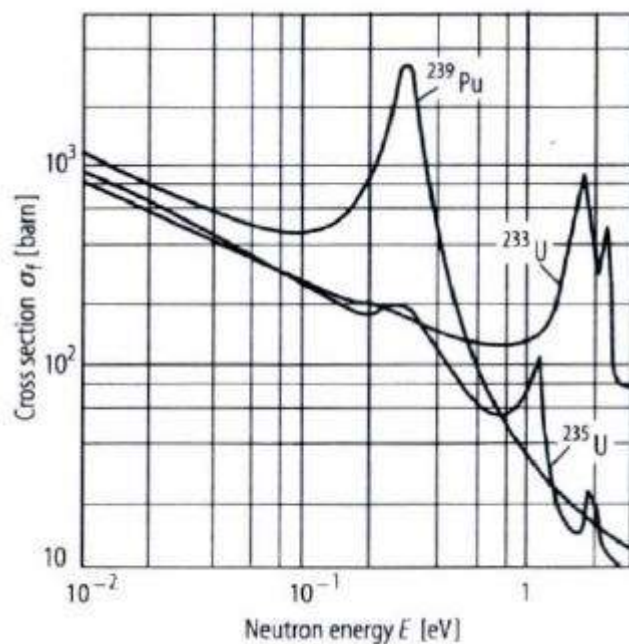


Figure 5.14: Fission cross section of Uranium-233.



The process of converting fertile isotopes to fissile ones is called breeding. Uranium-233 needs enough neutrons to undergo sustainable fission. Carlo Rubbia first proposed to use ADS to produce enough neutrons to ignite sustainable fission of Thorium-232.

5.6.3 Nuclear waste incinerator

Used nuclear fuel in conventional reactors normally contain a lot of long-lived heavy isotopes, particularly actinides. Among nuclides heavier than Th-232, those with odd atomic number can most probably absorb a neutron to undergo fission, while those with even atomic number will first undergo beta-decay and then fission. ADS can be used to transmute these long-lived isotopes into short-lived ones. ADS can also be used to destroy long-lived fission product such as Tc-99 and I-129.

5.7 Nuclear fusion

As can be seen in the behavior of the binding energy per nucleon versus the mass number, two light nuclei lower than iron in mass merge into a middle sized nucleus can release energy. This process is called fusion. There are many types of nuclear fusion, among which are thermonuclear fusion, inertial confinement fusion, beam-beam and beam-target fusion etc.. Nuclear fusion have been known to power the stars. H. Bethe found the main cycle of nuclear fusion in stars in 1930s. The hydrogen bomb was successful in 1952 as part of the Manhattan Project. Civilian use of fusion power is not successful until now because for the fusion to take place two light nuclei have to overcome the Coulomb barrier which needs extremely high temperature environment.

The Coulomb barrier is shown in Fig. 5.15 and is given by

$$E_B = \frac{Z_1 Z_2 e^2}{R} \quad (5.76)$$

where $R = r_0(A_1^{1/3} + A_2^{1/3})$, and Z_1 and Z_2 are proton numbers for incident nuclei. The turning point

is

$$R_{\text{tp}} = \frac{Z_1 Z_2 e^2}{E} \quad (5.77)$$

where $E = \frac{1}{2}m_r v^2$ with the reduced mass $m_r = m_1 m_2 / (m_1 + m_2)$ of two incident nuclei and their relative velocity v . The barrier transparency factor T is given by,

$$T \approx e^{-G} \approx e^{-\sqrt{E_G/E}} = e^{-2\pi Z_1 Z_2 e^2 / v} \quad (5.78)$$

where $E_G = 2m_r(Z_1 Z_2 e^2 \pi)^2$ is called the Gamow energy. The above is valid for $E_G \gg E$. The tunneling factor G can be evaluated as,

$$\begin{aligned} G &= 2\sqrt{2m_r} \int_R^{R_{\text{tp}}} dr \sqrt{V(r) - E} \\ &= 4\sqrt{2m_r E} R_{\text{tp}} \int_{y_0}^1 dy \sqrt{1 - y^2} \\ &\approx \sqrt{\frac{E_G}{E}}, \quad \text{for } R \ll R_{\text{tp}} \end{aligned} \quad (5.79)$$

where $V(r) = Z_1 Z_2 e^2 / r$, $y = \sqrt{r/R_{\text{tp}}}$ and $y_0 = \sqrt{R/R_{\text{tp}}}$. We see that the Coulomb barrier is extremely sensitive to $Z_1 Z_2$. The less $Z_1 Z_2$, the most probably the fusion reaction can take place. The barrier is the lowest for hydrogen isotopes, $E_B \sim e^2 / R \sim 100/137 \sim 0.7$ MeV. This is still much larger than typical kinetic energy of a few KeV.

The fusion cross section is normally parameterized as

$$\sigma \approx \sigma_{\text{geom}} T F \quad (5.80)$$

where σ_{geom} is the geometrical cross section and F is the reaction characteristic factor and depends on the nature of the reaction. The geometrical cross section σ_{geom} is given by the wavelength of the induced mass,

$$\sigma_{\text{geom}} \sim \lambda^2 \sim \frac{1}{(m_r v)^2} \sim \frac{1}{m_r E} \quad (5.81)$$

So the fusion cross section can be finally written as

$$\sigma(E) = \frac{S(E)}{E} e^{-\sqrt{E_G/E}} \quad (5.82)$$

where $S(E)$ is called astrophysical S-factor, a weakly energy dependent function for non-resonant reactions.

The reaction rate per unit volume for two collision particles is given by

$$R_{12} = \frac{n_1 n_2}{1 + \delta_{12}} \langle \sigma v \rangle \quad (5.83)$$

where σ is the cross section for the reaction, v is the relative velocity, n_1 and n_2 are number densities. If two colliding particles are identical $\delta_{12} = 1$, otherwise $\delta_{12} = 0$. In thermal environment, the velocity obeys Boltzmann-Maxwell distribution, then $\langle \sigma v \rangle$ is evaluated as

$$\begin{aligned} \langle \sigma v \rangle &= N^{-1} \int dv v^2 \sigma v \exp(-\beta m_r v^2 / 2) \\ &= 2N^{-1} m_r^{-2} \int_0^\infty dE S(E) \exp \left[- \left(\sqrt{E_G/E} + \beta E \right) \right] \end{aligned} \quad (5.84)$$

where $\beta = (k_B T)^{-1}$ and

$$\begin{aligned}
 N &= \int_0^\infty dv v^2 e^{-m_r v^2 / (2k_B T)} = \frac{\sqrt{2}}{m_r^{3/2}} \int dE \sqrt{E} e^{-\beta E} \\
 &= \sqrt{2} \left(\frac{k_B T}{m_r} \right)^{3/2} \int_0^\infty dx \sqrt{x} e^{-x} = \sqrt{2} \left(\frac{k_B T}{m_r} \right)^{3/2} \frac{1}{2} \Gamma\left(\frac{1}{2}\right) \\
 &= \sqrt{\frac{\pi}{2}} \left(\frac{k_B T}{m_r} \right)^{3/2}
 \end{aligned} \tag{5.85}$$

is the normalization constant. Inserting the above into Eq. (5.83), we obtain the reaction rate. Here we have used the cross section formula in Eq. (5.82). The energy integral in Eq. (5.84) is dominated by the minimum value of the function $f(E) = \sqrt{\frac{E_G}{E}} + \beta E$ in the exponent at E_0 ,

$$\begin{aligned}
 \frac{df(E)}{dE} &= -\frac{1}{2} \sqrt{E_G} E_0^{-3/2} + \beta = 0 \\
 E_0 &= E_G^{1/3} \left(\frac{k_B T}{2} \right)^{2/3}
 \end{aligned} \tag{5.86}$$

So we can expand $f(E) = \sqrt{\frac{E_G}{E}} + \beta E$ at $E = E_0$ and keep the quadratic term,

$$\begin{aligned}
 f(E) &\approx f(E_0) + \frac{1}{2} \left. \frac{d^2 f(E)}{dE^2} \right|_{E=E_0} (E - E_0)^2 \\
 &= f(E_0) + \frac{3}{8} E_G^{1/2} E_0^{-5/2} (E - E_0)^2
 \end{aligned} \tag{5.87}$$

So Eq. (5.84) becomes

$$\begin{aligned}
 \langle \sigma v \rangle &\approx 2N^{-1} m_r^{-2} S(E_0) \exp \left[- \left(\sqrt{E_G/E_0} + \beta E_0 \right) \right] \\
 &\int_0^\infty dE \exp \left[- \frac{3}{8} E_G^{1/2} E_0^{-5/2} (E - E_0)^2 \right] \\
 &\approx \frac{2^{4/3}}{\sqrt{3\pi}} (Z_1 Z_2 e^2 \pi)^{1/3} (k_B T)^{-2/3} m_r^{-1/3} S(E_0) \exp \left[- \frac{3}{2^{2/3}} \left(\frac{E_G}{k_B T} \right)^{1/3} \right]
 \end{aligned} \tag{5.88}$$

The Sun is a perfect prototype of self-sustaining thermonuclear fusion reactor. The basic fusion process in the sun is the hydrogen burning process into helium. Hydrogen is the most abundant material in the universe, almost 90% of elements in the universe are hydrogens. The temperature in the center of the Sun is about 1.6×10^7 K (about 1.38 KeV with $1 \text{ eV} = 1.1604 \times 10^4$ K). Most fusion reactions occur within 25% of the Sun's radius ($R_\odot = 6.95 \times 10^5$ km). Most of the sun energy comes from the proton-proton chain reaction. The reaction rate in the center is about 9.2×10^{37} times per second. In each reaction four protons are converted into alpha particles or Helium-4. So about 3.7×10^{38} proton out of 10^{57} protons are converted to Helium-4 per second. Each fusion releases the energy of about 25.7 MeV (or 27.8 MeV if including electron-positron annihilation), see below. Thus the energy power is about $(3 - 4) \times 10^{26}$ W ($1 \text{ W} = 1 \text{ J} \cdot \text{s}^{-1} = 10^7 \text{ erg} \cdot \text{s}^{-1}$).

The proton-proton chain reaction of type-I (pp-I chain) is,

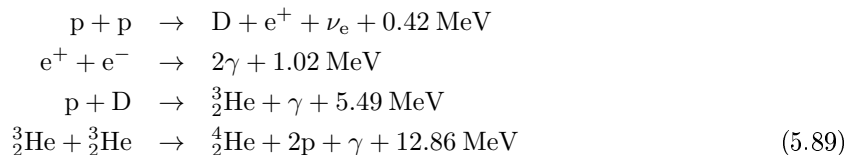
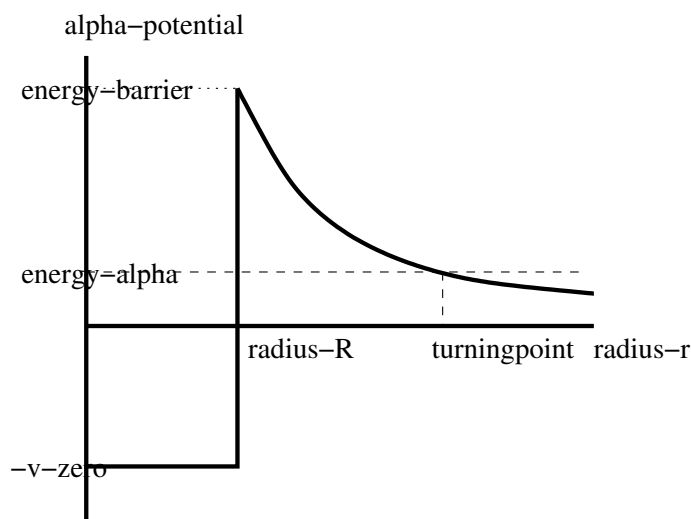
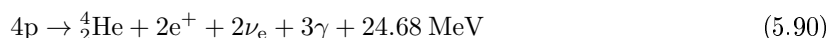


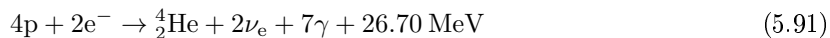
Figure 5.15: Coulomb barrier for fusion.



Note that in definition of the Q-value we did not count the electron in the final state. If we do not take the second reaction for electron-positron annihilation into account, the net reaction is

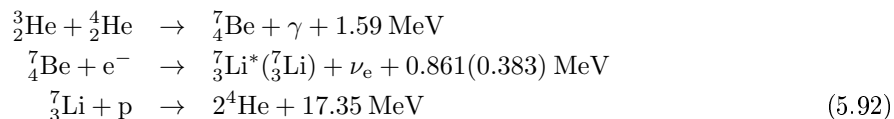


when including electron-positron annihilation, the net reaction becomes

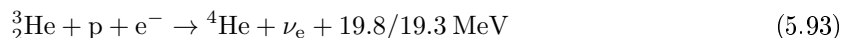


The pp-I branch is dominant at temperatures of 10 to 14 megakelvins ($\text{MK} = 10^6 \text{ K}$). Below 10 MK, the ${}^4_2\text{He}$ yield is suppressed. Since in the first reaction a proton must be converted to a neutron in the weak interaction. The rate is controlled by the first reaction since the time scale for weak interaction is much longer than the strong interaction. The cross section is of order 10^{-33} b and 10^{-23} b at KeV and MeV respectively. The proton number density of the core of the Sun is about $7.5 \times 10^{25} \text{ cm}^{-3}$, and the temperature is about 16 MK. Given these parameters, we can estimate the rate of the first reaction, which is actually the rate of the pp-chain.

The pp-II chain is more important for temperatures of 14 to 23 MK. The pp-II chain reaction is



whose net reaction is



90% of the neutrinos produced in the reaction ${}^7_4\text{Be}(e^-, \nu_e){}^7_3\text{Li}^*$ carry an energy of 0.861 MeV (Lithium-7 in the excited state), while the remaining 10% carry 0.383 MeV (Lithium-7 in the ground state).

If the temperature is above 23 MK, there is pp-III chain reaction as follows,

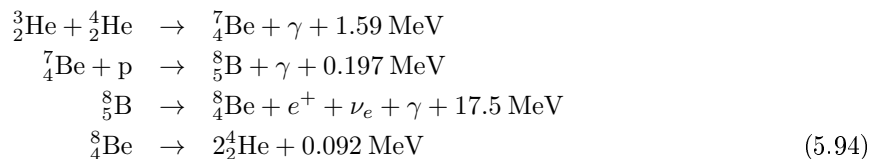
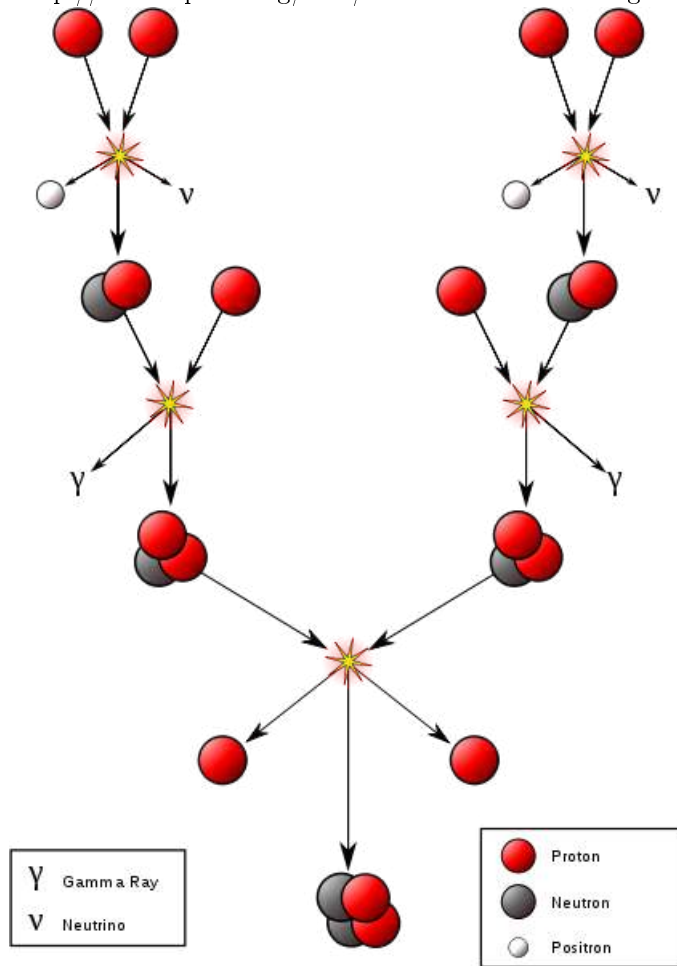


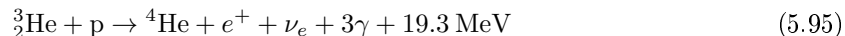
Figure 5.16: Parameters for some fusions. The Q-value is only from nuclear mass difference. The table is from S. Atzeni and J. Meyer-Ter-Vehn, “The Physics of Inertial Fusion: Beam Plasma Interaction, Hydrodynamics, Hot Dense Matter”, Oxford University Press, 2009. The data is from C. Angulo et al., Nucl. Phys. A656 (1999)3-187. [http://pntpm.ulb.ac.be/Nacre/nacre_d.htm]

	Q (MeV)	$\langle Q_\nu \rangle$ (MeV)	$S(0)$ (keV barn)	$\epsilon_G^{1/2}$ (keV ^{1/2})
<i>Main controlled fusion fuels</i>				
$D + T \rightarrow \alpha + n$	17.59		1.2×10^4	34.38
$D + D \rightarrow \begin{cases} T + p \\ {}^3\text{He} + n \\ \alpha + \gamma \end{cases}$	4.04 3.27 23.85		56 54 4.2×10^{-3}	31.40 31.40 31.40
$T + T \rightarrow \alpha + 2n$	11.33		138	38.45
<i>Advanced fusion fuels</i>				
$D + {}^3\text{He} \rightarrow \alpha + p$	18.35		5.9×10^3	68.75
$p + {}^6\text{Li} \rightarrow \alpha + {}^3\text{He}$	4.02		5.5×10^3	87.20
$p + {}^7\text{Li} \rightarrow 2\alpha$	17.35		80	88.11
$p + {}^{11}\text{B} \rightarrow 3\alpha$	8.68		2×10^5	150.3
<i>The p-p cycle</i>				
$p + p \rightarrow D + e^+ + \nu$	1.44	0.27	4.0×10^{-22}	22.20
$D + p \rightarrow {}^3\text{He} + \gamma$	5.49		2.5×10^{-4}	25.64
${}^3\text{He} + {}^3\text{He} \rightarrow \alpha + 2p$	12.86		5.4×10^3	153.8
<i>CNO cycle</i>				
$p + {}^{12}\text{C} \rightarrow {}^{13}\text{N} + \gamma$	1.94		1.34	181.0
$[{}^{13}\text{N} \rightarrow {}^{13}\text{C} + e^+ + \nu + \gamma]$	2.22	0.71	—	—
$p + {}^{13}\text{C} \rightarrow {}^{14}\text{N} + \gamma$	7.55		7.6	181.5
$p + {}^{14}\text{N} \rightarrow {}^{15}\text{O} + \gamma$	7.29		3.5	212.3
$[{}^{15}\text{O} \rightarrow {}^{15}\text{N} + e^+ + \nu + \gamma]$	2.76	1.00	—	—
$p + {}^{15}\text{N} \rightarrow {}^{12}\text{C} + \alpha$	4.97		6.75×10^4	212.8
<i>Carbon burn</i>				
${}^{12}\text{C} + {}^{12}\text{C} \rightarrow \begin{cases} {}^{23}\text{Na} + p \\ {}^{20}\text{Ne} + \alpha \\ {}^{24}\text{Mg} + \gamma \end{cases}$	2.24 4.62 13.93		8.83×10^{19}	2769

Figure 5.17: The pp chain reaction in the sun. From <http://en.wikipedia.org/wiki/File:FusionintheSun.svg>.

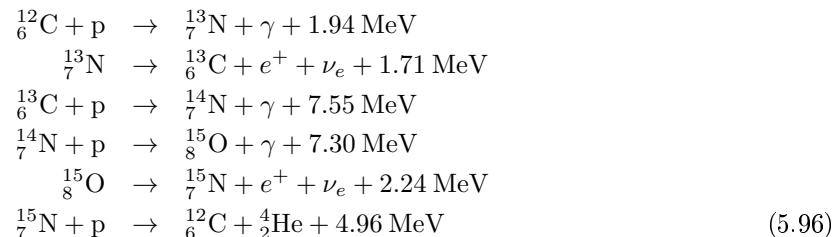


whose net reaction is

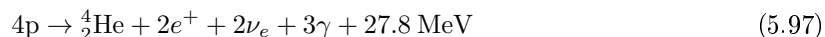


The pp III chain is not a major source of energy for the Sun (only 0.11%), but was very important in the solar neutrino problem because it generates very high energy neutrinos (up to 14.06 MeV).

The CNO cycle is more important for heavier stars and higher temperatures (called CNO-I),

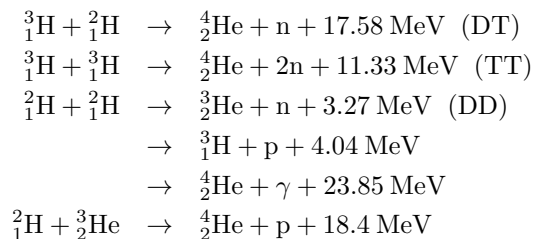


The net reaction is



Note that the Carbon, Nitrogen and Oxygen nuclei do not really participate the net reaction but play as catalyst. The net reaction is still Eq. (5.91). There are also another chain reactions called CNO-II involving ${}^{16}_8\text{O}$ and ${}^{17}_9\text{O}$.

The pp-chain and CNO cycle are not feasible on the earth because there is anything that can confine the matter at such high temperatures in such a long time. The fusion reactions which can be used on the earth are those with large cross sections at moderate temperatures. For example, here are a few such reactions,



Because of large energy release, the DT reaction is chosen for controlled fusion reaction in reactors.

Figure 5.18: The cross sections for DD and DT fusion reactions. Also shown is the fusion reaction of He-3 and deuteron. Taken from [4].

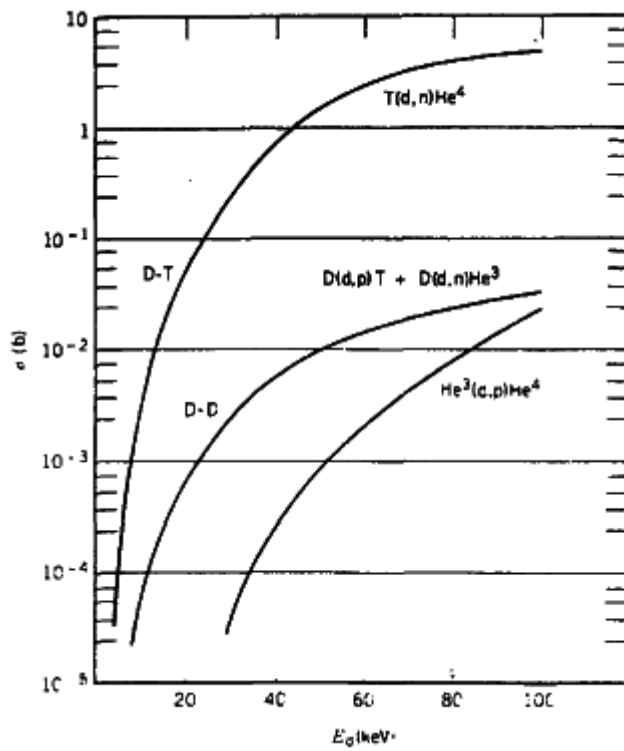
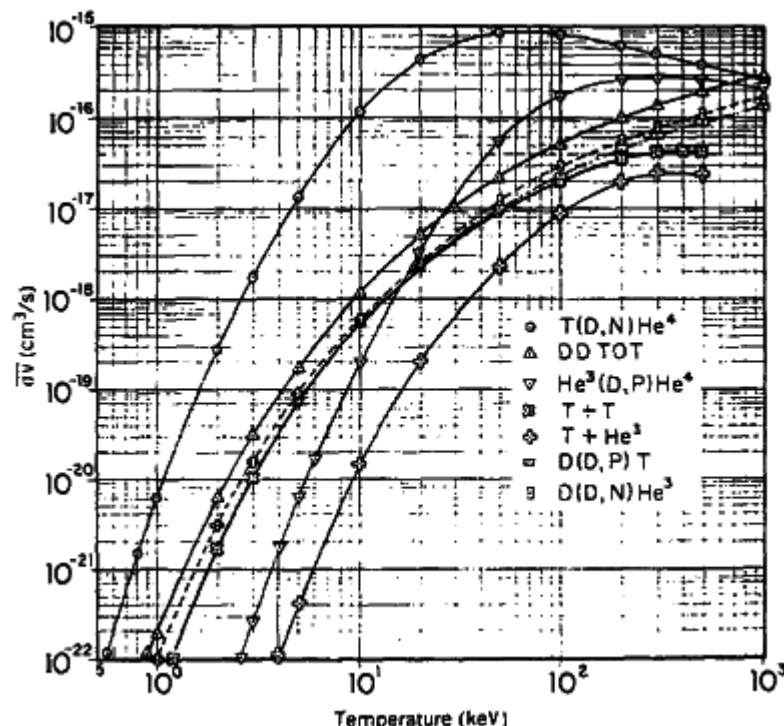
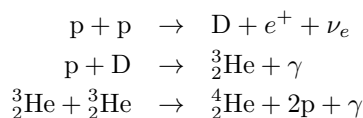


Figure 5.19: The cross sections for DD and DT fusion reactions averaged over Boltzmann-Maxwell distribution. Also shown is the fusion reaction of He-3 and deuteron. Taken from [4].



Exercise 43. *The Sun is a perfect prototype of self-sustaining thermonuclear fusion reactor. The basic fusion process in the sun is the hydrogen burning process into helium. The proton-proton chain reaction of type-I (pp-I chain) is dominant one,*



Given the atomic masses (not nuclear mass, given by mass excess relative to atomic mass unit) of nuclides $M_D = 12.628 \text{ MeV}$, $M_{\text{He}3} = 14.931 \text{ MeV}$, $M_{\text{He}4} = 2.425 \text{ MeV}$. The proton and neutron masses (mass excess) are $m_p = 0.007276 \text{ u}$, $m_n = 0.008665 \text{ u}$ with $1 \text{ u} = 931.494 \text{ MeV}/c^2$. The electron mass is $m_e = 0.511 \text{ MeV}$. (1) Calculate the Q -value of each reaction. The Q -value is defined as the mass surplus of initial state nuclei relative to final state nuclei. (2) Write the net reaction and the Q -value. (3) Among the three reactions, which one is dominant to control the total reaction rate? Why? (4) The fusion cross section of the first reaction $p + p \rightarrow D + e^+ + \nu_e$ can be written as

$$\sigma(E) = \frac{S(E)}{E} e^{-\sqrt{E_G/E}}$$

where $E = m_r v^2/2$ is the kinetic energy with reduced mass of two incident nuclei $m_r = m_1 m_2 / (m_1 + m_2)$, and $E_G = 2m_r (Z_1 Z_2 e^2 \pi)^2$, $S(E) = S(0) + (dS(0)/dE)E$ with $S(0) = 3.8 \times 10^{-22} \text{ KeV-barn}$ and $dS(0)/dE = 4.2 \times 10^{-24} \text{ barn}$. We note that the fusion takes place within 25% of the Sun's radius ($R_\odot = 6.95 \times 10^5 \text{ km}$) and the proton mass density is about 100 g/cm^3 . We can approximate that the kinetic energy E is given $3T/2$ with $T = 1.6 \times 10^7 \text{ K}$. For reference we list following constants here: $1 \text{ MeV} = 1.16 \times 10^{10} \text{ K}$, Avogadro's constant $N_A = 6.022 \times 10^{23} / \text{mol}$, $\text{barn} = 10^{-24} \text{ cm}^2$. Try to calculate the rate of the fusion reaction per unit volume.

[Solution: $E = 3T/2 = 2.07 \text{ KeV}$, $S(E)/E \approx 1.9 \times 10^{-22} \text{ barn}$, $E_G \approx 940 \times 10^3 \times \pi^2/137^2 \approx 494 \text{ KeV}$, $\sqrt{E_G/E} \approx 15.4$, $e^{-\sqrt{E_G/E}} = 1.95 \times 10^{-7}$. $\sigma = 3.6 \times 10^{-29} \text{ barn} = 3.6 \times 10^{-53} \text{ cm}^2$. $v = \sqrt{2E/m_r} = \sqrt{4.14 \times 10^{-3}/940} = 2.09 \times 10^{-3} \rightarrow 6.3 \times 10^7 \text{ cm/s}$. $\sigma v = 2.3 \times 10^{-45} \text{ cm}^3/\text{s}$. $n_H = 100 \times 6.022 \times 10^{23} = 6 \times 10^{25} / \text{cm}^3$. $R/V = n_H^2 \sigma v / 2 = 5.76 \times 10^6 \text{ s}^{-1} \text{cm}^{-3}$. $R = 1.92 \times 10^{-19} / \text{s}$, $\tau = 1/R = 5.2 \times 10^{18} \text{ s} = 1.65 \times 10^{11} \text{ y}$.]

Chapter 6

Nuclear force and nucleon-nucleon interaction

6.1 Properties of nucleons

The proton and neutron are nucleons, the building blocks of nuclei. The properties of nucleons are summarized in Table 6.1. The main difference between the proton and the neutron is that the mass of the neutron is 1.29 MeV larger than that of the proton and that the proton is stable but the neutron is not. The dominant decay mode for the neutron is $n \rightarrow p + e^- + \bar{\nu}_e$.

6.2 General properties of nuclear force

The human knowledge about nuclear force started from 1934, shortly after neutron was discovered in 1932 by J. Chadwick. Then H. Yukawa proposed that nuclear force was mediated by meson which was discovered in 1947. From modern perspective nuclear force can be understood as a residual force of strong interaction whose elementary particles are quarks and gluons. Mesons are actually composite particles made of quarks and gluons. Nuclear force is like a Van der Waals force among atoms which is a short range force much weaker than electromagnetic force. The Van der Waals force originates from separation of charges (electric polarization) in atoms which are electrically neutral. Similarly, quarks and gluons are bound together into a nucleon which is a color singlet object (color neutral). When quarks and gluons with colors fluctuate inside the nucleon they produce a short range force felt by a neighboring nucleon. Therefore the nuclear force is a residual force of quarks and gluons.

1. *Saturation and short distance.* The forces which bind the nucleons together in nuclei are very

Table 6.1: Properties of nucleons.

	proton	neutron
quark content	uud	udd
$I(J^P)$	$\frac{1}{2} (\frac{1}{2})^+$	$-\frac{1}{2} (\frac{1}{2})^+$
mass	938.27203 ± 0.00008 MeV	939.56536 ± 0.00008 MeV
Magnetic moment	$2.792847351 \pm 0.000000028$ μ_N	-1.9130427 ± 0.0000005 μ_N
Charge radius	0.875 ± 0.007 fm	-0.1161 ± 0.0022 fm
Mean life	$> 2.1 \times 10^{29}$ years	885.7 ± 0.8 s

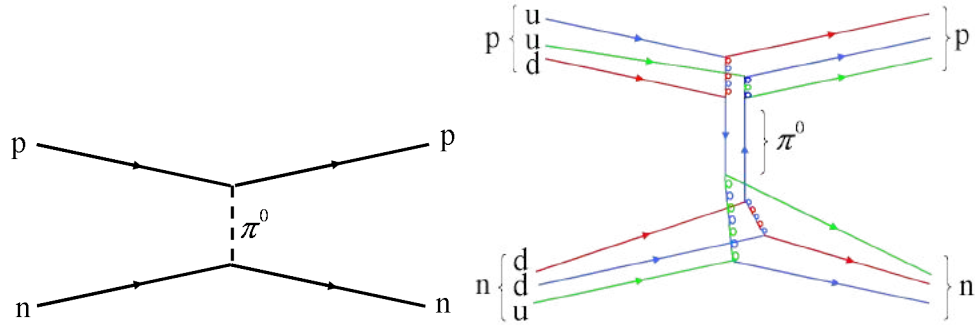
Figure 6.1: Nuclear force mediated by meson. From "http://en.wikipedia.org/wiki/Nuclear_force".

Figure 6.2: The nuclear force.

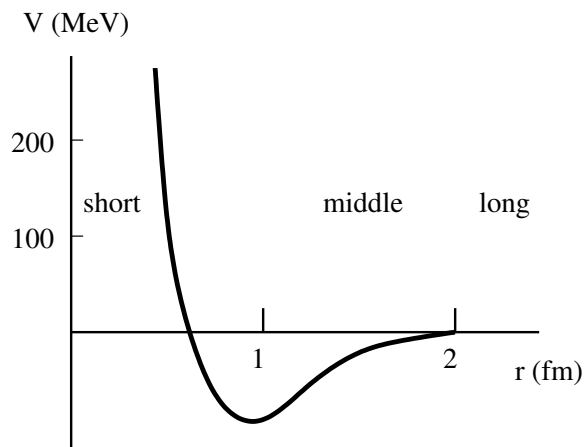


Table 6.2: The states of NN system denoted by the symbol ${}^{2S+1}L$. B, H, M and W mean Bartlett, Heisenberg, Majorana and Wigner force.

NN	state	L	S	I	$\sigma_1 \cdot \sigma_2$	$\tau_1 \cdot \tau_2$	B	H	M	W
pp,np,nn	1S	0	0	1	-3	1	1	1	-1	-1
np	3S	0	1	0	1	-3	-1	-1	-1	-1
np	1P	1	0	0	-3	-3	1	-1	1	-1
pp,np,nn	3P	1	1	1	1	1	-1	1	1	-1

strong because they can at least overcome the Coulomb repulsion among protons. The nuclear forces have one property which we call the saturation: a nucleon can only interact with nucleons surrounding it in a nucleus because it is an attractive force at short distances. This is why the binding energy is proportional to the number of nucleons in a nucleus or the atomic number A . We can easily understand it. Suppose the nuclear forces in the nucleus would be attractive between all pairs of nucleons, then the total potential exerted on one nucleon by other $A - 1$ nucleons is proportional to $(A - 1)$. There are A nucleons, so the total potential energy is proportional to A^2 , which is not the real case. There must be some other effects to keep the nucleons apart when the inter-nucleon distance is larger than a threshold value. It turns out to be that the nuclear force is attractive in the intermediate short range $r \in [1, 2]$ fm and repulsive at very short distance $r \in [0, 1]$ fm, where r is the distance between two nucleons. In some sense the nuclear force is like Van der Waals force of molecules, which arises from inhomogeneous distributions of electric charges though the molecule does not carry net charges or is electric neutral. The nuclear force is illustrated in Fig. 6.2.

2. *Exchange property.* Nuclear force is mediated by mesons (pions and others) like the covalent bonding in molecules. The force is attractive or repulsive depending on if the pair of nucleons is in a symmetric or an anti-symmetric state in their separation. This counts in part for the saturation of the forces. If we regard the proton and nucleon as an isospin doublet, we can extend the Pauli principle by including the isospin. For a NN system, the total wavefunction must be anti-symmetric with respect to exchange of two nucleons, which requires

$$(-1)^{L+S+I} = -1 \quad (6.1)$$

Assume $\psi(\mathbf{r}_1, \sigma_1, \tau_1; \mathbf{r}_2, \sigma_2, \tau_2)$ is the wavefunction of the NN system, where σ_i and τ_i ($i = 1, 2$) label the spin and isospin states. We introduce three exchange operators P_r , P_σ and P_τ which exchange the spatial positions, spins and isospins of two nucleons,

$$\begin{aligned} P_r \psi(\mathbf{r}_1, \sigma_1, \tau_1; \mathbf{r}_2, \sigma_2, \tau_2) &= \psi(\mathbf{r}_2, \sigma_1, \tau_1; \mathbf{r}_1, \sigma_2, \tau_2) \\ P_\sigma \psi(\mathbf{r}_1, \sigma_1, \tau_1; \mathbf{r}_2, \sigma_2, \tau_2) &= \psi(\mathbf{r}_1, \sigma_2, \tau_1; \mathbf{r}_2, \sigma_1, \tau_2) \\ P_\tau \psi(\mathbf{r}_1, \sigma_1, \tau_1; \mathbf{r}_2, \sigma_2, \tau_2) &= \psi(\mathbf{r}_1, \sigma_1, \tau_2; \mathbf{r}_2, \sigma_2, \tau_1) \end{aligned} \quad (6.2)$$

These operators satisfy

$$P_r^2 = P_\sigma^2 = P_\tau^2 = 1 \quad (6.3)$$

So the eigenvalues of the above operators must be ± 1 . Considering the properties under the exchange of positions, spins and isospins for a NN state with the angular momentum, spin and isospin quantum number L , S and I ,

$$\begin{aligned} P_r &= (-1)^L \\ P_\sigma &= (-1)^{S+1} \\ P_\tau &= (-1)^{I+1} \end{aligned} \quad (6.4)$$

According to Eq. (6.1), we have

$$P_r P_\sigma P_\tau = -1 \quad (6.5)$$

These operators can be expressed in terms of Pauli matrices for spins and isospins $\sigma_{1,2}$ and $\tau_{1,2}$,

$$\begin{aligned} P_\sigma &= (1 + \boldsymbol{\sigma}_1 \cdot \boldsymbol{\sigma}_2)/2 = S(S+1) - 1 \\ P_\tau &= (1 + \boldsymbol{\tau}_1 \cdot \boldsymbol{\tau}_2)/2 = I(I+1) - 1 \\ P_r &= -(1 + \boldsymbol{\sigma}_1 \cdot \boldsymbol{\sigma}_2)(1 + \boldsymbol{\tau}_1 \cdot \boldsymbol{\tau}_2)/4 \end{aligned} \quad (6.6)$$

One can check $S(S+1) - 1 = (-1)^{S+1}$ for $S = 0, 1$.

In nucleon-nucleon interaction, the nuclear force can be modeled by nuclear potential in Schroedinger equation. The most widely used nucleon-nucleon potentials are the Paris potential, the Argonne potential, the Bonn potential and the Nijmegen potentials. The parameters of these potentials are fixed by fitting experimental data, such as the deuteron binding energy, nucleon-nucleon elastic scattering cross sections, etc.. A recent development is to systematically derive the nucleon-nucleon potential from chiral effective field theory. Nuclear potential can be classified into four kinds, they are attractive or repulsive depends on the quantum state of the nucleon-nucleon system. In the following, $v_W(r)$, $v_M(r)$, $v_H(r)$ and $v_B(r)$ are all positive functions.

- Spin exchange potential (Bartlett force),

$$V_B = -\frac{1}{2}(1 + \boldsymbol{\sigma}_1 \cdot \boldsymbol{\sigma}_2)v_B(r) \quad (6.7)$$

The spin exchange potential is attractive for the spin triplet state $S = 1$ and repulsive for the singlet $S = 0$.

- Isospin exchange potential (Heisenberg force),

$$V_H = \frac{1}{2}(1 + \boldsymbol{\tau}_1 \cdot \boldsymbol{\tau}_2)v_H(r) \quad (6.8)$$

The isospin exchange potential is attractive for the isospin singlet state $I = 0$ and repulsive for the triplet $I = 1$.

- Space exchange potential (Majorana force),

$$V_M = \frac{1}{4}(1 + \boldsymbol{\sigma}_1 \cdot \boldsymbol{\sigma}_2)(1 + \boldsymbol{\tau}_1 \cdot \boldsymbol{\tau}_2)v_M(r) \quad (6.9)$$

- Non-exchange potential (Wigner force),

$$V_W = -v_W(r) \quad (6.10)$$

We see that the non-exchange potential is always attractive.

In the above we note that $v_W(r)$, $v_M(r)$, $v_H(r)$ and $v_B(r)$ are all positive functions. As shown in Table 6.2, the above four forces are all attractive for the state 3S .

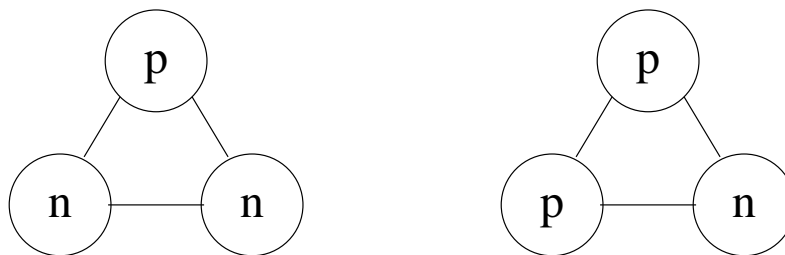
3. *Charge independence or isospin invariance.* The nuclear force between two nucleons is equal irrelevant of if they are proton-proton, neutron-neutron or proton-neutron,

$$V_{pp} \approx V_{nn} \approx V_{pn} \quad (6.11)$$

This property was verified in the NN scattering experiments and in the presence of isospin multiplets in nuclear structure. A good example is the mirror nuclei ${}^3\text{H}$ and ${}^3\text{He}$ (see Fig. 6.3). It is found that the difference in binding energies of ${}^3\text{H}$ and ${}^3\text{He}$ only comes from the Coulomb energy of proton-proton in ${}^3\text{He}$.

4. *Momentum dependence.* The nuclear force nontrivially depends on the relative momentum due to the fact that it is mediated by meson exchange. The most important force that is momentum dependent is the LS coupling,

$$(\mathbf{L} \cdot \mathbf{S})V(r) \quad (6.12)$$

Figure 6.3: Mirror nuclei: ${}^3\text{H}$ and ${}^3\text{He}$.

which is essential to explain the shell structure of in nuclei.

5. *Spin dependent.* Apart from the spin exchange force listed in Eq. (6.7), there is also tensor force formed by three vectors $\boldsymbol{\sigma}_1$, $\boldsymbol{\sigma}_2$ and $\hat{\mathbf{r}} = \mathbf{r}/|\mathbf{r}|$,

$$\begin{aligned} S_{12} &= 3(\hat{\mathbf{r}} \cdot \boldsymbol{\sigma}_1)(\hat{\mathbf{r}} \cdot \boldsymbol{\sigma}_2) - (\boldsymbol{\sigma}_1 \cdot \boldsymbol{\sigma}_2) = (3\hat{r}_i\hat{r}_j - \delta_{ij})\sigma_{1i}\sigma_{2j} \\ &= 6(\mathbf{S} \cdot \hat{\mathbf{r}})^2 - 2\mathbf{S}^2 \end{aligned} \quad (6.13)$$

The tensor force violates the angular momentum conservation.

In summary, the nuclear force has the following general form,

$$\begin{aligned} V &= V_c(r) + V_\sigma(r)(\boldsymbol{\sigma}_1 \cdot \boldsymbol{\sigma}_2) + V_\tau(r)(\boldsymbol{\tau}_1 \cdot \boldsymbol{\tau}_2) + V_{\sigma\tau}(r)(\boldsymbol{\sigma}_1 \cdot \boldsymbol{\sigma}_2)(\boldsymbol{\tau}_1 \cdot \boldsymbol{\tau}_2) \\ &\quad + V_I(r)S_{12} + V_{I\tau}(r)S_{12}(\boldsymbol{\tau}_1 \cdot \boldsymbol{\tau}_2) \end{aligned} \quad (6.14)$$

One sees that the potential conserves the total isospin since it is commutable with

$$I^2 = \frac{1}{4}(\boldsymbol{\tau}_1 + \boldsymbol{\tau}_2)^2 = \frac{1}{2}(3 + \boldsymbol{\tau}_1 \cdot \boldsymbol{\tau}_2) \quad (6.15)$$

The potential does not depend on I_3 , i.e. it does not discriminate protons and neutrons.

NN potentials have the following properties,

- A scalar, because it is an energy;
- Only depends on the relative distance between two nucleons r and $\boldsymbol{\sigma} \cdot \mathbf{r}$ - locality and momentum conservation;
- Invariant under the spatial reflection - parity invariance;
- Invariant under rotation - angular momentum conservation;
- Invariant under the time reflection;
- Invariant under the exchange of proton and neutron;
- Not dependent on velocity - static;

Exercise 44. What is general Pauli exclusive principle? From this principle, fill the empty space of the following table,

NN	state	L	S	I	$\sigma_1 \cdot \sigma_2$	$\tau_1 \cdot \tau_2$	B	H	M	W
pp, np, nn	1S						1	1	-1	-1
np	3S						-1	-1	-1	-1
np	1P						1	-1	1	-1
pp, np, nn	3P						-1	1	1	-1

Table 6.3: Static properties of the deuteron nucleus ($J^P = 1^+$).

observables	data
binding energy B_D (MeV)	2.224
magnetic moment μ_D/μ_N	0.857
electric quadrupole Q_D (fm ²)	0.286
average square root radius $\langle\sqrt{r^2}\rangle$ (fm)	1.964
ratio of D to S states $\eta = A_D/A_S$	0.026

Exercise 45. *What is the saturation property of nuclear force?*

Exercise 46. *Assume $\psi(\mathbf{r}_1, \sigma_1, \tau_1; \mathbf{r}_2, \sigma_2, \tau_2)$ is the wavefunction of the nucleon-nucleon system, where σ_i and τ_i ($i = 1, 2$) label the spin and isospin states. We introduce operators P_σ and P_τ which exchange the spins and isospins of two nucleons,*

$$\begin{aligned} P_\sigma \psi(\mathbf{r}_1, \sigma_1, \tau_1; \mathbf{r}_2, \sigma_2, \tau_2) &= \psi(\mathbf{r}_1, \sigma_2, \tau_1; \mathbf{r}_2, \sigma_1, \tau_2) \\ P_\tau \psi(\mathbf{r}_1, \sigma_1, \tau_1; \mathbf{r}_2, \sigma_2, \tau_2) &= \psi(\mathbf{r}_1, \sigma_1, \tau_2; \mathbf{r}_2, \sigma_2, \tau_1) \end{aligned}$$

Considering that the nucleon-nucleon state can be in spin and isospin singlet and triplet, write down the formula for P_σ and P_τ using σ_i and τ_i .

6.3 Deuteron nucleus

The Deuteron nucleus is the second most simple nuclei and made of one proton and one neutron. Following the Pauli principle 6.1, the total wave function must be anti-symmetric with the exchange of two nucleons. The Deuteron nucleus is an isospin singlet and has spin-parity $J^P = 1^+$. The interaction inside the deuteron is purely nuclear force without Coulomb contribution. Since $S = 1$ gives a stronger nuclear attraction, the deuterium ground state is in the $S = 1, L = 0$ state. As we know from the positive parity and total angular momentum 1 of the deuteron, it must be in the states with relative orbital angular momentum $L = 0, 2, \dots$, where two lowest states are ${}^{2S+1}L_J = {}^3S_1, {}^3D_1$.

6.3.1 S-state

For the 3S_1 state, the relative motion of neutron and proton can be described by Schrödinger equation with a square well potential,

$$\left[-\frac{1}{m_N} \nabla^2 + V(r) - E \right] \psi(\mathbf{r}) = 0 \quad (6.16)$$

Here the reduced mass is $m_N/2$. The square well potential is defined by,

$$V(r) = \begin{cases} -V_0, & (r \leq a) \\ 0, & (r > a) \end{cases} \quad (6.17)$$

Since the deuteron nucleus is in the S-state, the wave function only depends on the radius r ,

$$\psi(r) = u(r)/r \quad (6.18)$$

Then the Schrödinger equation becomes

$$\left[-\frac{1}{m_N} \frac{1}{r^2} \frac{d}{dr} r^2 \frac{d}{dr} + V(r) - E \right] \frac{u(r)}{r} = 0 \quad (6.19)$$

Using

$$\begin{aligned} \frac{1}{r^2} \frac{d}{dr} r^2 \frac{d}{dr} &= \frac{d^2}{dr^2} + \frac{2}{r} \frac{d}{dr} \\ \frac{d^2}{dr^2} \frac{u(r)}{r} &= \frac{u''(r)}{r} - \frac{2}{r^3} (ru' - u) \\ \frac{2}{r} \frac{d}{dr} \frac{u(r)}{r} &= \frac{2}{r^3} (ru' - u) \end{aligned} \quad (6.20)$$

the the Schrödinger equation can be simplified as

$$-\frac{1}{m_N} u''(r) + [V(r) - E]u(r) = 0 \quad (6.21)$$

and further as

$$\begin{aligned} u''(r) + m_N[E + V_0]u &= 0, \quad (r \leq a) \\ u''(r) + m_N E u &= 0, \quad (r > a) \end{aligned} \quad (6.22)$$

where the energy is chosen to be the binding energy $E = B_D = -2.224$ MeV. Using the boundary condition, $u(0) = u(\infty) = 0$, we get the solution

$$u(r) = \begin{cases} A \sin(\sqrt{m_N(E + V_0)}r), & (r \leq a) \\ B \exp(-\sqrt{m_N|E|r}), & (r > a) \end{cases} \quad (6.23)$$

At $r = a$, $u(r)$ and $u'(r)$ must be continuous. So we get

$$\begin{aligned} A \sin(\sqrt{m_N(E + V_0)}a) &= B \exp(-\sqrt{m_N|E|}a) \\ A \sqrt{m_N(E + V_0)} \cos(\sqrt{m_N(E + V_0)}a) &= -B \sqrt{m_N|E|} \exp(-\sqrt{m_N|E|}a) \end{aligned} \quad (6.24)$$

and then

$$\frac{1}{\sqrt{m_N(E + V_0)}} \tan(\sqrt{m_N(E + V_0)}a) = -\frac{1}{\sqrt{m_N|E|}} \quad (6.25)$$

which gives the relation between V_0 and a . We can choose $a = 2$ fm. Define $ka = \sqrt{m_N|E|}a \approx \sqrt{938 \times 2.224} \times 2/197 \approx 0.465$ and $k_0a \equiv \sqrt{m_N V_0}a$, with $k < k_0$, the above equation is rewritten as

$$\tan(\sqrt{(k_0a)^2 - (ka)^2}) = -\frac{\sqrt{(k_0a)^2 - (ka)^2}}{ka} \quad (6.26)$$

In order for the above equation to have solutions, k_0a must be within $[(2n + 1/2)\pi, (2n + 1)\pi]$ so that two functions $y = \tan \sqrt{x_0^2 - x^2}$ and $y = -x^{-1} \sqrt{x_0^2 - x^2}$ ($x_0 \equiv k_0a$, $x \equiv ka$) have intersections. For $ka \approx 0.465$, we can find the smallest value $k_0a \approx 1.87$ which is about 1.19 times $\pi/2$ and within $[\pi/2, \pi]$. In this case, the potential depth is $V_0 = 36.5$ MeV.

The electric dipole moment of the deuteron is zero. Its magnetic moment is

$$\boldsymbol{\mu}_J = \boldsymbol{\mu}_L + \boldsymbol{\mu}_S = g_L \mu_N \mathbf{L} + g_S \mu_N \mathbf{S} = g_J \mu_N \mathbf{J} \quad (6.27)$$

where \mathbf{J} , \mathbf{L} and \mathbf{S} are the total, orbital and spin momenta. $g_{i=J,L,S}$ are their g-factors, and we have $g_L = (g_L^p + g_L^n)/2 = g_L^p/2 = 1/2$ and $g_S = (g_S^p + g_S^n)/2$. The g-factor of deuteron for orbital

angular momentum can be easily understood by the fact that only proton contributes with half of total orbital angular momentum: $\boldsymbol{\mu}_L = g_L^p \mu_N \mathbf{L}_p = g_L^p \mu_N \mathbf{L}/2$. The g-factor of deuteron for spin can also be derived:

$$\begin{aligned}\boldsymbol{\mu}_S &= g_S \mu_N \mathbf{S} = \frac{1}{2} \mu_N (g_S^p \boldsymbol{\sigma}_1 + g_S^n \boldsymbol{\sigma}_2) \\ g_S \mathbf{S} \cdot \mathbf{S} &= \frac{1}{4} (g_S^p \boldsymbol{\sigma}_1 \cdot \mathbf{S} + g_S^n \boldsymbol{\sigma}_2 \cdot \mathbf{S}) \\ &= \frac{3}{4} (g_S^p + g_S^n) + \frac{1}{4} (g_S^p + g_S^n) \boldsymbol{\sigma}_1 \cdot \boldsymbol{\sigma}_2\end{aligned}\quad (6.28)$$

where we have used $\mathbf{S} = \frac{1}{2}(\boldsymbol{\sigma}_1 + \boldsymbol{\sigma}_2)$. We see that for $S = 1$, $g_S = (g_S^p + g_S^n)/2$.

We multiply \mathbf{J} to both sides of Eq. (6.27) and obtain

$$\begin{aligned}g_J \mathbf{J} \cdot \mathbf{J} &= \frac{1}{2} g_L^p (\mathbf{L} \cdot \mathbf{J}) + \frac{1}{2} (g_S^p + g_S^n) (\mathbf{S} \cdot \mathbf{J}) \\ g_J J &= g_L^p \frac{J(J+1) + L(L+1) - S(S+1)}{4(J+1)} \\ &\quad + (g_S^p + g_S^n) \frac{J(J+1) + S(S+1) - L(L+1)}{4(J+1)}\end{aligned}\quad (6.29)$$

Then the magnetic moments of the deuteron states 3S_1 ($S = 1$, $J = 1$ and $L = 0$) and 3D_1 ($S = 1$, $J = 1$ and $L = 2$) are

$$\begin{aligned}\mu_J({}^3S_1) &= g_J J = \frac{1}{2} (g_S^p + g_S^n) = 0.879 \\ \mu_J({}^3D_1) &= g_J J = \frac{3}{4} g_L^p - \frac{1}{4} (g_S^p + g_S^n) = 0.31\end{aligned}\quad (6.30)$$

We can see we can reproduce the magnetic moment of deuteron nucleus in such a simple model.

6.3.2 S and D states

Data show that the deuteron has non-zero quadrupole moment, indicating that one should take non-central potential into account. The most simple non-central potential is the tensor one, then the total potential of the deuteron can be written as

$$V(r) = V_c(r) + S_{12} V_T(r) \quad (6.31)$$

where the tensor operator S_{12} is given in Eq. (6.13). As we have mentioned in the last subsection that the lowest ground states of the deuteron are states 3S_1 and 3D_1 . Let us denote ϕ_S and ϕ_D as the spin and angular part of the S- and D-state wavefunction,

$$\begin{aligned}\phi_S^{1M} &= \chi_{1M} Y_{00}(\theta, \phi) \\ \phi_D^{1M} &= \sum_{M_1, M_2} c(M; M_1, M_2) Y_{2M_1}(\theta, \phi) \chi_{1M_2}\end{aligned}\quad (6.32)$$

where the Clebsch-Gordon coefficients $c(m; m_1, m_2)$ can be taken from [19] and are listed below,

$$\begin{aligned}c(1; 2, -1) &= \sqrt{3/5}, \quad c(1; 1, 0) = -\sqrt{3/10}, \quad c(1; 0, 1) = \sqrt{1/10} \\ c(0; 1, -1) &= \sqrt{3/10}, \quad c(0; 0, 0) = -\sqrt{2/5}, \quad c(0; -1, 1) = \sqrt{3/10} \\ c(-1; 0, -1) &= \sqrt{1/10}, \quad c(-1; -1, 0) = -\sqrt{3/10}, \quad c(-1; -2, 1) = \sqrt{3/5}\end{aligned}\quad (6.33)$$

The spin wave functions are

$$\begin{aligned}\chi_{1,1} &= \uparrow\uparrow \\ \chi_{1,0} &= \frac{1}{\sqrt{2}}(\uparrow\downarrow + \downarrow\uparrow) \\ \chi_{1,-1} &= \downarrow\downarrow\end{aligned}\tag{6.34}$$

and angular momentum ones are

$$\begin{aligned}Y_{2,2}(\theta, \phi) &= \frac{1}{4}\sqrt{\frac{15}{2\pi}}\sin^2\theta e^{2i\phi} = \frac{1}{4}\sqrt{\frac{15}{2\pi}}\frac{1}{3}(T^{11} - T^{22} + i2T^{12}) \\ Y_{2,1}(\theta, \phi) &= -\sqrt{\frac{15}{8\pi}}\sin\theta\cos\theta e^{i\phi} = -\sqrt{\frac{15}{8\pi}}\frac{1}{3}(T^{13} + iT^{23}) \\ Y_{2,0}(\theta, \phi) &= \sqrt{\frac{5}{4\pi}}\left(\frac{3}{2}\cos^2\theta - \frac{1}{2}\right) = \frac{1}{2}\sqrt{\frac{5}{4\pi}}T^{33} \\ Y_{2,-m}(\theta, \phi) &= (-1)^m Y_{2,m}^*(\theta, \phi)\end{aligned}\tag{6.35}$$

where the rank-2 tensor is defined by $T^{ij} = 3\hat{r}_i\hat{r}_j - \delta_{ij}$. With Eq. (6.13), one can prove

$$\begin{aligned}S_{12}\phi_S^{1M} &= \sqrt{8}\phi_D^{1M} \\ S_{12}\phi_D^{1M} &= \sqrt{8}\phi_S^{1M} - 2\phi_D^{1M}\end{aligned}\tag{6.36}$$

Now we can introduce the D wavefunction into the ground state of the deuteron,

$$\begin{aligned}\psi(\mathbf{r}) &= \sqrt{P_S}\psi_S(\mathbf{r}) + \sqrt{P_D}\psi_D(\mathbf{r}) \\ &= \frac{u(r)}{r}\phi_S^{1M} + \frac{w(r)}{r}\phi_D^{1M}\end{aligned}\tag{6.37}$$

Then P_S and P_D are given by

$$\begin{aligned}P_S &= \int_0^\infty \left|\frac{u(r)}{r}\right|^2 r^2 dr = \int_0^\infty u^2(r) dr \\ P_D &= \int_0^\infty \left|\frac{w(r)}{r}\right|^2 r^2 dr = \int_0^\infty w^2(r) dr \\ P_S + P_D &= \int_0^\infty [u^2(r) + w^2(r)] dr = 1\end{aligned}\tag{6.38}$$

The Schrödinger equation becomes

$$\left[-\frac{1}{m_N}\nabla^2 + V_c(r) + S_{12}V_T(r) - E\right]\psi(\mathbf{r}) = 0\tag{6.39}$$

We can simplify it by

$$\begin{aligned}
& \left[-\frac{1}{m_N} \nabla^2 + V_c(r) + S_{12} V_T(r) - E \right] \left(\frac{u(r)}{r} \phi_S^{1M} + \frac{w(r)}{r} \phi_D^{1M} \right) \\
= & \left[-\frac{1}{m_N} \nabla^2 + V_c(r) - E \right] \left(\frac{u(r)}{r} \phi_S^{1M} + \frac{w(r)}{r} \phi_D^{1M} \right) \\
& + S_{12} V_T(r) \left(\frac{u(r)}{r} \phi_S^{1M} + \frac{w(r)}{r} \phi_D^{1M} \right) \\
= & \left[-\frac{1}{m_N} \nabla^2 + V_c(r) - E \right] \left(\frac{u(r)}{r} \phi_S^{1M} + \frac{w(r)}{r} \phi_D^{1M} \right) \\
& + V_T(r) \left(\frac{u(r)}{r} \sqrt{8} \phi_D^{1M} + \frac{w(r)}{r} \sqrt{8} \phi_S^{1M} - \frac{w(r)}{r} 2 \phi_D^{1M} \right) \\
= & \left[-\frac{1}{m_N} \nabla^2 + V_c(r) - E \right] \frac{u(r)}{r} \phi_S^{1M} + \frac{w(r)}{r} \sqrt{8} V_T(r) \phi_S^{1M} \\
& + \left[-\frac{1}{m_N} \nabla^2 + V_c(r) - E \right] \frac{w(r)}{r} \phi_D^{1M} + V_T(r) \left(\sqrt{8} \frac{u(r)}{r} - 2 \frac{w(r)}{r} \right) \phi_D^{1M} = 0 \quad (6.40)
\end{aligned}$$

The we get

$$\begin{aligned}
\left[-\frac{1}{m_N} \nabla^2 + V_c(r) - E \right] u(r) + w(r) \sqrt{8} V_T(r) &= 0 \\
\left[-\frac{1}{m_N} \nabla^2 + V_c(r) - 2V_T(r) - E \right] w(r) + \sqrt{8} V_T(r) u(r) &= 0 \quad (6.41)
\end{aligned}$$

The boundary conditions are

$$u(r), w(r) = 0, \quad r = 0, \infty$$

The coupled equations can be solved numerically. The solutions have to be adjusted to fit the data. These equations can be decoupled outside the range of nuclear force, the asymptotic behaviors are

$$\begin{aligned}
u(r) &= A_S e^{-kr} \\
w(r) &= A_D \left[1 + \frac{3}{kr} + \frac{3}{(kr)^2} \right] e^{-kr} \quad (6.42)
\end{aligned}$$

with $k = \sqrt{m_N |E|}$. The ratio of D to S state is

$$\eta = A_D / A_S \approx 0.025 \quad (6.43)$$

The electric quadrupole moment is

$$Q_D = \langle \psi | \hat{Q} | \psi \rangle = P_S \langle \psi_S | \hat{Q} | \psi_S \rangle + P_D \langle \psi_D | \hat{Q} | \psi_D \rangle + 2\sqrt{P_S P_D} \langle \psi_S | \hat{Q} | \psi_D \rangle \quad (6.44)$$

where the quadrupole operator is defined as

$$\hat{Q} = \frac{1}{4} (3z^2 - r^2) = \sqrt{\frac{\pi}{5}} r^2 Y_{20}(\theta) \quad (6.45)$$

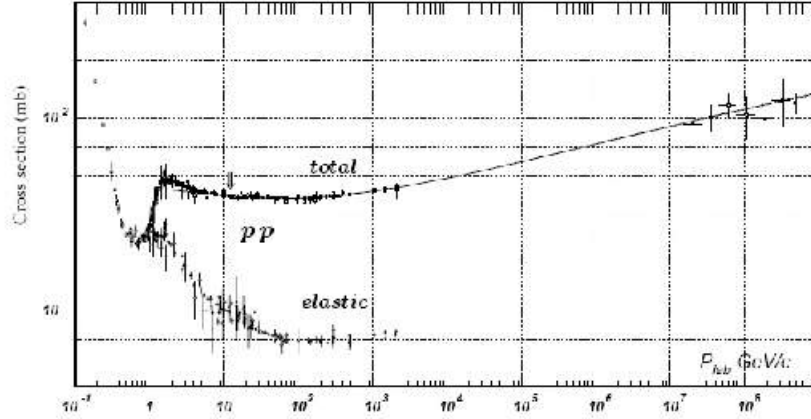
Note that the first term in Eq. (2.39) does not contribute following the Wigner-Eckart theorem, i.e. there is no $[1]$ in $[5] \otimes [1] = [5]$. Then we can derive

$$Q_D = \frac{\sqrt{2}}{10} \int_0^\infty dr r^2 u(r) w(r) - \frac{1}{20} \int_0^\infty dr r^2 w^2(r) \quad (6.46)$$

Exercise 47. *The spin-parity of deuteron is $J^P = 1^+$. What are two lowest states for deuteron? Express the states using the optical spectrum symbol $^{2S+1}L_J$ with S, P, D, G, F, \dots for $L = 1, 2, 3, 4, 5, \dots$.*

Exercise 48. *Prove Eq. (6.36).*

Exercise 49. *Prove Eq. (6.46).*

Figure 6.4: pp cross sections

6.4 Low energy nucleon-nucleon scatterings

When considering nucleon-nucleon scatterings, we have spin-orbit and spin-spin interactions in addition to the central potential. Neither spins nor orbital angular momenta are conserved in the scatterings. Only the total angular momentum, its third component and the parity are conserved. For a general two-to-two scattering $a + b \rightarrow c + d$, the selection rules for the interaction are

$$\begin{aligned}
 (1) \quad & P_a P_b (-1)^L = P_c P_d (-1)^{L'} \\
 (2) \quad & m_a + m_b + m_L = m_c + m_d + m_{L'} \\
 (3) \quad & J = J'
 \end{aligned} \tag{6.47}$$

where P_i are intrinsic parities for particles $i = a, b, c, d$; m_i are the third components of the spins; m_L and $m_{L'}$ are the third components of the relative angular momenta of initial and final states; J and J' are the total angular momenta of initial and final states.

Nucleon-nucleon scatterings include np, pp and nn scatterings. One can measure the cross sections, differential cross sections or angular distributions with or without polarizations. For low energy scatterings $ka \ll 1$, s-wave is dominant. We can estimate the incident energy for which $ka < 1$ holds, $ka \approx \sqrt{m_n E a} \approx \sqrt{m_n E_L / 2a}$ where E_L is the energy in the lab frame. When $E_L \sim 10$ MeV and $a \sim 2$ fm, $ka \sim 0.7$, so for $E_L < 10$ MeV, we can safely consider only the s-wave. In this case the total cross section is

$$\sigma_{\text{tot}} \sim 4\pi \frac{1}{k^2} (P_1 \sin^2 \delta_1 + P_3 \sin^2 \delta_3) \approx \pi (a_{s1}^2 + 3a_{s3}^2) \tag{6.48}$$

where δ_i and a_{si} for $i = 1, 3$ are phase shifts and scattering lengths for the spin singlet and triplet. The total cross section is obtained by summing over all the final states and taking average over the initial states for which $P_{1,3} = 1/4, 3/4$ are degeneracy weights from spin counting. Since the total angular momentum is conserved, there is no mixing of the singlet and triplet in the amplitude. From Eq. (??) and (A.62), we have

$$\begin{aligned}
 k \coth \delta_1 &= -\frac{1}{a_{s1}} + \frac{1}{2} r_{\text{eff},1} k^2 \\
 k \coth \delta_3 &= -\frac{1}{a_{s3}} + \frac{1}{2} r_{\text{eff},3} k^2
 \end{aligned} \tag{6.49}$$

where $r_{\text{eff},1,3}$ are effective force distances for the singlet and triplet. For neutron-proton scatterings, their values are given by

$$\begin{aligned} a_{s1} &\approx 23.7 \text{ fm} \\ r_{\text{eff},1} &\approx 2.5 \text{ fm} \\ a_{s3} &\approx -5.4 \text{ fm} \\ r_{\text{eff},3} &\approx 1.7 \text{ fm} \end{aligned} \tag{6.50}$$

Note that the triplet/singlet channel is attractive/repulsive since a_{s3}/a_{s1} is negative/positive. From the scattering length we can determine the depth of the potential provided the potential width a is known following Eq. (A.63). If we set $a = 3$ fm, we have the potential depths for singlet and triplet channels are 311 and 96 MeV respectively, corresponding to $k_0 a = 1.51\pi, 0.46\pi$. The total cross section is then about 20.4 barns (10^{-24} cm²), where those for the singlet and the triplet are 71 and 3.7 barns. From these value we can determine the potential depth and width from Eqs. (A.65,A.63). At low energy the phase shift as function of wave number are independent of potential shape because the wave length is much larger than the force distance. The scattering length for the triplet is negative means the phase shift is positive and the force is attractive.

6.5 Nucleon-Nucleon scatterings in moderate energy

To gain knowledge about the deep structure of the nuclear force, one has to use high energy scatterings. When the nucleon incident energy in the lab frame $E_L > 400$ GeV, the internal mesonic degree of freedoms can be excited and the relativistic effects enter the play. New particles can be produced by transforming part of the kinetic energy into the masses.

Suppose the incident protons are moving along the z-axis in proton-neutron scatterings. The differential cross section $d\sigma/d\Omega$ of neutron-proton scatterings in moderate energies has a feature that there are peaks at $\theta = 0, \pi$ and the peak at $\theta = \pi$ is higher than that at $\theta = 0$. There is a valley at $\theta = \pi/2$. The large peak at $\theta = \pi$ is understood as the signal for the exchange character of the nuclear force. The protons can exchange a pion with the neutrons and turn to neutrons which emit at small angles, while the protons transformed from the incident neutron absorbing the pions move out along the negative z-axis.

In proton-proton scatterings the differential cross section shows an isotropic feature with respect to polar angles except $\theta < \pi/8$. This is a result of coherence effect among a variety of partial waves.

6.6 Meson exchange model for NN potentials

Yukawa first proposed in 1934 that in analogy to the scalar potential of the electromagnetic field there is also a potential between the proton and the neutron. The potential has an additional exponential factor besides the Coulomb potential,

$$V(r) = g \frac{e^{-\lambda r}}{r}$$

where g is the coupling constant and λ characterizes the distance of the nuclear force. He argued that λ is actually the mass of one kind of particle which mediate the nuclear force which was later called the pion.

Fig. 6.5 shows the central force, one can see that the repulsive part of the nucleon-nucleon potential in short distance is from the vector meson exchange ω and ρ . For intermediate distance the potential is dominated by the σ meson exchange. The long distance part is from the pion exchange. The tensor force is provided by the pion and the ρ meson, while the spin-orbital force is from the σ and ω mesons.

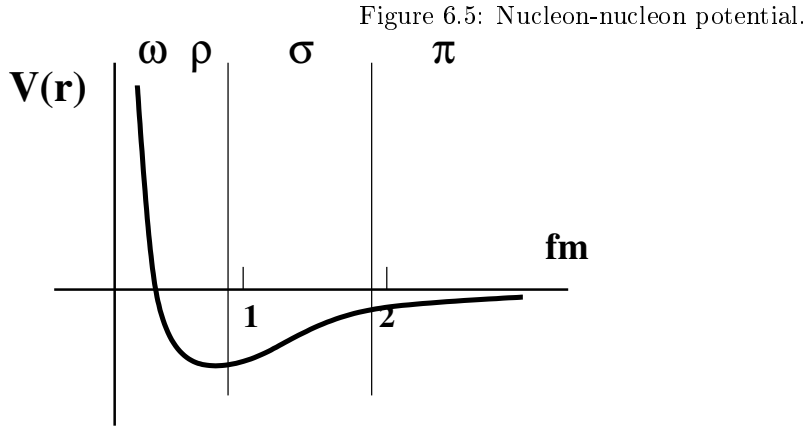
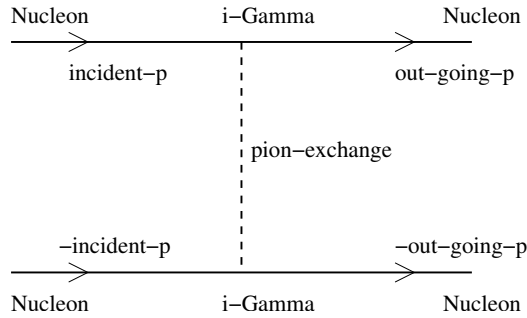


Figure 6.6: NN interaction through pion exchange.



6.6.1 One pion exchange potential (OPEP)

The interaction potential via one pion exchange can be obtained from the Lagrangian by the scattering amplitude of two nucleons. This can be translated into the Yukawa coupling $ig_{\text{PS}}\bar{\psi}\gamma_5\tau_j\psi\phi_{\text{PS}}^j$ in the Lagrangian where ϕ_{PS}^j ($j = 1, 2, 3$ are isospin indices) denote the pseudoscalar pion fields and τ_j are Pauli matrices in isospin space. The coupling vertex is $i\Gamma_j = -g_{\text{PS}}\gamma_5\tau_j$. It is easy to introduce the pion propagator, i.e. the Green function in momentum space,

$$iG_{ij}(q) = \frac{i}{q^2 - m_\pi^2} \delta_{ij} \quad (6.51)$$

where q is the four-momentum and m_π the pion mass. An incoming nucleon is denoted by $u_{\text{N}}(p) = (u_p, u_n)^T$, an outgoing nucleon by $\bar{u}_{\text{N}}(p) = u_{\text{N}}^\dagger \gamma_0$. Here γ_0 and γ_5 are Dirac matrices given by

$$\gamma_0 = \begin{pmatrix} 1 & 0 \\ 0 & -1 \end{pmatrix}, \quad \gamma_5 = \begin{pmatrix} 0 & 1 \\ 1 & 0 \end{pmatrix} \quad (6.52)$$

We write down the T-matrix,

$$\begin{aligned} i \langle p', h'_1, h'_2 | T | p, h_1, h_2 \rangle &= -\bar{u}_{\text{N}}(-p', h'_2) i\Gamma_i u_{\text{N}}(-p, h_2) \\ &\quad \times \frac{i}{q^2 - m_\pi^2} \delta_{ij} \bar{u}_{\text{N}}(p', h'_1) i\Gamma_j u_{\text{N}}(p, h_1) \end{aligned} \quad (6.53)$$

where $q = p - p'$ is the four-momentum transfer in nucleon-nucleon scattering and $h = \uparrow, \downarrow$ denote the spin states. At low energies we can transform all quantities to non-relativistic (NR) ones $q^2 \rightarrow -\mathbf{q}^2$,

$E_N \rightarrow m_N$ and

$$u_N(p, h) = \left(\begin{array}{c} \chi(h) \\ \frac{\boldsymbol{\sigma} \cdot \mathbf{p}}{E + m_N} \chi(h) \end{array} \right) \rightarrow \left(\begin{array}{c} \chi(h) \\ \frac{\boldsymbol{\sigma} \cdot \mathbf{p}}{2m_N} \chi(h) \end{array} \right) \quad (6.54)$$

where $\chi = (\chi_p, \chi_n)^T$ with $\chi_{p,n} = |\uparrow\rangle, |\downarrow\rangle$ are Pauli spinors for spin states. We obtain

$$\begin{aligned} \bar{u}_N(p', h'_1) \gamma_5 \tau_j u_N(p, h_1) &= \langle \chi(1') | \left(1, \frac{\boldsymbol{\sigma} \cdot \mathbf{p}'}{2m_N} \right) \begin{pmatrix} 1 & 0 \\ 0 & -1 \end{pmatrix} \begin{pmatrix} 0 & 1 \\ 1 & 0 \end{pmatrix} \tau_j \begin{pmatrix} 1 \\ \frac{\boldsymbol{\sigma} \cdot \mathbf{p}}{2m_N} \end{pmatrix} | \chi(1) \rangle \\ &= \frac{1}{2m_N} \langle \chi(1') | \boldsymbol{\sigma} \cdot (\mathbf{p} - \mathbf{p}') \tau_j | \chi(1) \rangle \\ \bar{u}_N(-p', h'_2) \gamma_5 \tau_i u_N(-p, h_2) &= -\frac{1}{2m_N} \langle \chi(2') | \boldsymbol{\sigma} \cdot (\mathbf{p} - \mathbf{p}') \tau_i | \chi(2) \rangle \end{aligned} \quad (6.55)$$

Then the T-matrix element in the non-relativistic limit can be simplified by

$$\begin{aligned} &\langle p', h'_1, h'_2 | T | p, h_1, h_2 \rangle_{\text{NR}} \\ &= -\frac{g_{\text{PS}}^2}{4m_N^2 (\mathbf{q}^2 + m^2)} \langle \chi(1') | (\boldsymbol{\sigma} \cdot \mathbf{q}) \tau_i | \chi(1) \rangle \langle \chi(2') | (\boldsymbol{\sigma} \cdot \mathbf{q}) \tau_i | \chi(2) \rangle \end{aligned} \quad (6.56)$$

which give rise to the effective potential in the Born approximation,

$$V_\pi(\mathbf{q}) = -\frac{g_{\text{PS}}^2}{4m_N^2} \frac{1}{\mathbf{q}^2 + m_\pi^2} (\boldsymbol{\tau}_1 \cdot \boldsymbol{\tau}_2) (\boldsymbol{\sigma}_1 \cdot \mathbf{q}) (\boldsymbol{\sigma}_2 \cdot \mathbf{q}) \quad (6.57)$$

The potential in coordinate space can be obtained by Fourier transformation,

$$\begin{aligned} V_\pi(r) &= \int \frac{d^3 \mathbf{q}}{(2\pi)^3} e^{i\mathbf{q} \cdot \mathbf{r}} V(\mathbf{q}) \\ &= \frac{g_{\text{PS}}^2}{4m_N^2} (\boldsymbol{\tau}_1 \cdot \boldsymbol{\tau}_2) (\boldsymbol{\sigma}_1 \cdot \nabla) (\boldsymbol{\sigma}_2 \cdot \nabla) \int \frac{d^3 \mathbf{q}}{(2\pi)^3} e^{i\mathbf{q} \cdot \mathbf{r}} \frac{1}{\mathbf{q}^2 + m_\pi^2} \\ &= \frac{g_{\text{PS}}^2}{4m_N^2} (\boldsymbol{\tau}_1 \cdot \boldsymbol{\tau}_2) (\boldsymbol{\sigma}_1 \cdot \nabla) (\boldsymbol{\sigma}_2 \cdot \nabla) \frac{e^{-m_\pi r}}{4\pi r} \end{aligned} \quad (6.58)$$

where we have used

$$\begin{aligned} \int \frac{d^3 \mathbf{q}}{(2\pi)^3} e^{i\mathbf{q} \cdot \mathbf{r}} \frac{1}{\mathbf{q}^2 + m_\pi^2} &= \frac{1}{(2\pi)^2} \int_0^\infty dq q^2 \int_{-1}^1 d \cos \theta \frac{e^{iqr \cos \theta}}{q^2 + m_\pi^2} \\ &= \frac{1}{(2\pi)^2} \int_0^\infty dq q^2 \int_{-1}^1 d \cos \theta \frac{e^{iqr \cos \theta}}{q^2 + m_\pi^2} \\ &= \frac{-i}{(2\pi)^2 r} \int_0^\infty dq q \frac{e^{iqr} - e^{-iqr}}{q^2 + m_\pi^2} = \frac{-i}{(2\pi)^2 r} \int_{-\infty}^\infty dq q \frac{e^{iqr}}{q^2 + m_\pi^2} \\ &= \frac{-i}{2(2\pi)^2 r} \int_C dq e^{iqr} \left(\frac{1}{q - im_\pi} + \frac{1}{q + im_\pi} \right) = \frac{1}{4\pi r} e^{-m_\pi r} \end{aligned} \quad (6.59)$$

where the contour C is in the upper half plane. The OPEP potential then becomes

$$V_\pi(r) = \frac{g_{\text{PS}}^2}{16\pi m_N^2} \boldsymbol{\tau}_1 \cdot \boldsymbol{\tau}_2 \left[\left(\frac{1}{r^2} + \frac{m_\pi}{r} + \frac{m_\pi^2}{3} \right) S_{12} + \frac{m_\pi^2}{3} \boldsymbol{\sigma}_1 \cdot \boldsymbol{\sigma}_2 \right] \frac{e^{-m_\pi r}}{r} \quad (6.60)$$

where S_{12} is defined by

$$S_{12} = 3(\boldsymbol{\sigma}_1 \cdot \hat{\mathbf{r}})(\boldsymbol{\sigma}_2 \cdot \hat{\mathbf{r}}) - \boldsymbol{\sigma}_1 \cdot \boldsymbol{\sigma}_2 \quad (6.61)$$

Table 6.4: Exchanged bosons in OBEP.

bosons	spin, parity J^P	isospin I	mass (MeV)	coupling	type
π^\pm	0^-	1	139.57	14.24	isovector, pseudoscalar
π^0	0^-	1	134.98	14.24	isovector, pseudoscalar
σ	0^+	0	(550)	3.16	isoscalar, scalar
η	0^-	0	548.7	5.77	isoscalar, pseudoscalar
ρ	1^-	1	759.9	0.71	isovector, vector
ω	1^-	0	781.9	10.06	isoscalar, vector

Table 6.5: Lagrangian density for boson-nucleon couplings. For isospin multiplet like pions, we should replace $\psi \rightarrow (\psi_p, \psi_n)^T$, $\phi \rightarrow \phi_i$ and $\Gamma \tau_i$.

Boson type	Lagrangian term ($g\bar{\psi}\Gamma\psi\phi$)	coupling term ($i\Gamma$)
scalar (S)	$g_S\bar{\psi}\psi\phi_S$	$i g_S$
pseudoscalar (PS)	$i g_{PS}\bar{\psi}\gamma_5\psi\phi_{PS}$	$-g_{PS}\gamma_5$
pseudoscalar vector-type (PV)	$\frac{g_{PV}}{m}\bar{\psi}\gamma_5\gamma^\mu\psi\partial_\mu\phi_{PV}$	$-\frac{g_{PV}}{m}\gamma_5\gamma^\mu q_\mu$
vector (V)	$g_V\bar{\psi}\gamma_\mu\psi\phi_V^\mu$	$i g_V\gamma_\mu$
vector (T)	$\frac{g_T}{2m}\bar{\psi}\sigma_{\mu\nu}\psi\partial^\mu\phi_V^\nu$	$-\frac{g_T}{2m}\sigma_{\mu\nu}q^\nu$

and we have used

$$\begin{aligned}
\nabla_j \frac{e^{-m_\pi r}}{r} &= \left(-\frac{r_j}{r^3} - m_\pi \frac{r_j}{r^2} \right) e^{-m_\pi r} \\
\nabla_i \nabla_j \frac{e^{-m_\pi r}}{r} &= -\nabla_i \left[\left(\frac{r_j}{r^3} + m_\pi \frac{r_j}{r^2} \right) e^{-m_\pi r} \right] \\
&= \left(3 \frac{r_i r_j}{r^5} - \frac{\delta_{ij}}{r^3} + 2m_\pi \frac{r_i r_j}{r^4} - m_\pi \frac{\delta_{ij}}{r^2} \right) e^{-m_\pi r} \\
&\quad + m_\pi \left(\frac{r_i r_j}{r^4} + m_\pi \frac{r_i r_j}{r^3} \right) e^{-m_\pi r} \\
&= \left[\left(\frac{3}{r^3} + \frac{3m_\pi}{r^2} + \frac{m_\pi^2}{r} \right) \frac{r_i r_j}{r^2} - \left(\frac{1}{r^3} + \frac{m_\pi}{r^2} \right) \delta_{ij} \right] e^{-m_\pi r} \\
&= \left[\left(\frac{1}{r^2} + \frac{m_\pi}{r} + \frac{m_\pi^2}{3} \right) \left(\frac{3r_i r_j}{r^2} - \delta_{ij} \right) + \frac{m_\pi^2}{3} \delta_{ij} \right] \frac{e^{-m_\pi r}}{r} \tag{6.62}
\end{aligned}$$

The OPEP can give the radius of deuteron $r_D = 1.94$ fm, the quadrupole moment $Q = 0.284$ fm², which are in agreement with data. The OPEP can give the right description of the long range attractive part of the nuclear force, but not the short distance part, because of the small mass of pions.

6.6.2 One boson exchange potential

To describe the short and mediate distance of the nuclear force, one extends OPEP by including other bosons, i.e. one boson exchange potential (OBEP), see Table 6.4. The Lagrangian density for boson-nucleon couplings for various intermediate bosons are listed in Table 6.5.

In a similar way to one pion exchange, we can determine the potential from the σ exchange. As we know from Table 6.4 that σ is an isoscalar and scalar particle, the interaction term is $g_s \bar{\psi}\psi\phi_s$ with

vertex $i\Gamma = ig_s$. The T-matrix can be evaluated as

$$\begin{aligned}
i \langle p', h'_1, h'_2 | T | p, h_1, h_2 \rangle &= -\bar{u}_N(-p', h'_2) i\Gamma u_N(-p, h_2) \frac{i}{q^2 - m_\sigma^2} \bar{u}_N(p', h'_1) i\Gamma u_N(p, h_1) \\
&= i \frac{g_s^2}{q^2 - m_\sigma^2} \bar{u}_N(-p', h'_2) u_N(-p, h_2) \bar{u}_N(p', h'_1) u_N(p, h_1) \\
&\approx -i \frac{g_s^2}{\mathbf{q}^2 + m_\sigma^2} \langle \chi(2') | \left[1 - \frac{(\boldsymbol{\sigma} \cdot \mathbf{p}')(\boldsymbol{\sigma} \cdot \mathbf{p})}{4m_N^2} \right] | \chi(2) \rangle \\
&\quad \times \langle \chi(1') | \left[1 - \frac{(\boldsymbol{\sigma} \cdot \mathbf{p}')(\boldsymbol{\sigma} \cdot \mathbf{p})}{4m_N^2} \right] \tau_i | \chi(1) \rangle \\
&\approx -i \frac{g_s^2}{\mathbf{q}^2 + m_\sigma^2} \langle \chi(2') | \left[1 - \frac{\mathbf{p} \cdot \mathbf{p}'}{4m_N^2} - i \frac{\boldsymbol{\sigma} \cdot (\mathbf{p}' \times \mathbf{p})}{4m_N^2} \right] | \chi(2) \rangle \\
&\quad \times \langle \chi(1') | \left[1 - \frac{\mathbf{p} \cdot \mathbf{p}'}{4m_N^2} - i \frac{\boldsymbol{\sigma} \cdot (\mathbf{p}' \times \mathbf{p})}{4m_N^2} \right] | \chi(1) \rangle
\end{aligned} \tag{6.63}$$

We have used $\mathbf{q} = \mathbf{p} - \mathbf{p}'$ and we can also define $\mathbf{k} = (\mathbf{p} + \mathbf{p}')/2$. In terms of \mathbf{k} and \mathbf{q} , the potential in momentum space reads

$$\begin{aligned}
V_\sigma(\mathbf{q}) &= -\frac{g_s^2}{\mathbf{q}^2 + m_\sigma^2} \left[\left(1 - \frac{\mathbf{k}^2 - \mathbf{q}^2/4}{4m_N^2} \right)^2 + i \frac{\mathbf{S} \cdot (\mathbf{p}' \times \mathbf{p})}{2m_N^2} \left(1 - \frac{\mathbf{k}^2 - \mathbf{q}^2/4}{4m_N^2} \right) \right. \\
&\quad \left. - \frac{1}{16m_N^4} \boldsymbol{\sigma}_1 \cdot (\mathbf{p}' \times \mathbf{p}) \boldsymbol{\sigma}_2 \cdot (\mathbf{p}' \times \mathbf{p}) \right] \\
&\approx -\frac{g_s^2}{\mathbf{q}^2 + m_\sigma^2} \left[1 - \frac{\mathbf{k}^2 - \mathbf{q}^2/4}{2m_N^2} + \frac{i\mathbf{S} \cdot (\mathbf{k} \times \mathbf{q})}{2m_N^2} \right]
\end{aligned} \tag{6.64}$$

where we have kept the terms upto \mathbf{k}^2/m_N^2 or \mathbf{q}^2/m_N^2 . The term $i\mathbf{S} \cdot (\mathbf{k} \times \mathbf{q})$ gives the $\mathbf{L} \cdot \mathbf{S}$ coupling of the nuclear force. We only keep the leading order term we obtain

$$V_\sigma(\mathbf{q}) \approx -\frac{g_s^2}{\mathbf{q}^2 + m_\sigma^2} \rightarrow V_\sigma(r) \approx -\frac{g_s^2}{4\pi r} e^{-m_\sigma r} \tag{6.65}$$

which gives an attractive Yukawa potential.

Let us compute the potential from the exchange of the massive vector boson. The Lagrangian reads

$$L = -\frac{1}{4} F_{\mu\nu} F^{\mu\nu} + \frac{1}{2} m_v^2 V_\mu V^\mu \tag{6.66}$$

with $F^{\mu\nu} = \partial^\mu V^\nu - \partial^\nu V^\mu$ is the strength tensor for the vector field. We can write the vector field explicitly $V^\mu = (V^0, \mathbf{V})$ and $V_\mu = (V^0, -\mathbf{V})$. The equation of motion can be obtained from the Lagrangian equation,

$$\begin{aligned}
\partial_\lambda \frac{\partial L}{\partial(\partial_\lambda V_\sigma)} - \frac{\partial L}{\partial V_\sigma} &= 0 \\
-\frac{1}{2} \partial_\lambda F^{\mu\nu} (g_\mu^\lambda g_\nu^\sigma - g_\mu^\sigma g_\nu^\lambda) - m_v^2 V^\sigma &= 0 \\
\partial_\lambda F^{\lambda\sigma} + m_v^2 V^\sigma &= 0
\end{aligned} \tag{6.67}$$

The conjugate momenta are

$$\begin{aligned}
\Pi^\sigma &= \frac{\partial L}{\partial(\partial_0 V_\sigma)} = -\frac{1}{2} F^{\mu\nu} (g_\mu^0 g_\nu^\sigma - g_\mu^\sigma g_\nu^0) \\
&= (0, F^{i0}) = (0, \mathbf{E}) = (0, \boldsymbol{\Pi})
\end{aligned} \tag{6.68}$$

where

$$\mathbf{E} = \mathbf{\Pi} = -\nabla V_0 - \frac{\partial \mathbf{V}}{\partial t} \quad (6.69)$$

This indicates that there is no conjugate momentum of V_0 since the Lagrangian does not contain $\partial_0 V_0$. Actually V_0 is instantly obtained from Eq. (6.67),

$$V^0 = -\frac{1}{m_v^2} \partial_\lambda F^{\lambda 0} = -\frac{1}{m_v^2} \nabla \cdot \mathbf{\Pi} \quad (6.70)$$

So Eq. (6.69) becomes

$$\mathbf{E} = \mathbf{\Pi} = \frac{1}{m_v^2} \nabla (\nabla \cdot \mathbf{\Pi}) - \frac{\partial \mathbf{V}}{\partial t} \quad (6.71)$$

Taking the derivative of Eq. (6.67), we find

$$\partial_\sigma V^\sigma = 0 \quad (6.72)$$

The Hamiltonian can be found

$$\begin{aligned} H &= \Pi^\sigma \partial_0 V_\sigma - L = -\mathbf{\Pi} \cdot \dot{\mathbf{V}} - L \\ &= -\mathbf{\Pi} \cdot (-\mathbf{\Pi} - \nabla V^0) - \frac{1}{2} (\mathbf{E}^2 - \mathbf{B}^2) - \frac{1}{2m_v^2} (\nabla \cdot \mathbf{\Pi})^2 + \frac{1}{2} m_v^2 \mathbf{V}^2 \\ &= \frac{1}{2} (\mathbf{\Pi}^2 + \mathbf{B}^2) - \frac{1}{m_v^2} \mathbf{\Pi} \nabla \nabla \cdot \mathbf{\Pi} - \frac{1}{2m_v^2} (\nabla \cdot \mathbf{\Pi})^2 + \frac{1}{2} m_v^2 \mathbf{V}^2 \\ &= \frac{1}{2} \left[\mathbf{\Pi}^2 + \mathbf{B}^2 + \frac{1}{m_v^2} (\nabla \cdot \mathbf{\Pi})^2 + m_v^2 \mathbf{V}^2 \right] + \nabla \cdot (\mathbf{\Pi} V_0) \end{aligned} \quad (6.73)$$

which is definitely positive after dropping the last divergence term. Here we have used $\mathbf{B} = \nabla \times \mathbf{V}$. The quantization condition reads

$$[V^i(t, \mathbf{r}), \Pi^j(t, \mathbf{r}')] = -i \delta_{ij} \delta^{(3)}(\mathbf{r} - \mathbf{r}') \quad (6.74)$$

where the minus sign comes from the fact that $V_i = -V^i$ and Π^i are conjugate variables. Note that \mathbf{V} and $\mathbf{\Pi}$ satisfy the constraint (6.72),

$$\nabla \cdot \mathbf{V} - \frac{1}{m_v^2} \nabla \cdot \dot{\mathbf{\Pi}} = 0 \quad (6.75)$$

This is the binding condition for the longitudinal component of \mathbf{V} and $\mathbf{\Pi}$ along the direction of the wave vector.

Assume that \mathbf{V} expands as

$$\mathbf{V}(x) = \sum_{\mathbf{k}} \frac{1}{\sqrt{2E_k V}} \left(A_k^\lambda \boldsymbol{\varepsilon}_k^\lambda a_{k,\lambda} e^{-ik \cdot x} + A_k^{\lambda*} \boldsymbol{\varepsilon}_k^{\lambda*} a_{k,\lambda}^\dagger e^{ik \cdot x} \right) \quad (6.76)$$

where $k \cdot x = E_k t - \mathbf{k} \cdot \mathbf{x}$. We assume that $\boldsymbol{\varepsilon}_k^{1,2} \perp \mathbf{k}$ and $\boldsymbol{\varepsilon}_k^3 \parallel \mathbf{k}$. Similar to the expansion of \mathbf{V} , we can express $\mathbf{\Pi}$ in the following form,

$$\mathbf{\Pi}(x) = \sum_{\mathbf{k}} \frac{1}{\sqrt{2E_k V}} \left(C_k^\lambda \boldsymbol{\varepsilon}_k^\lambda a_{k,\lambda} e^{-ik \cdot x} + C_k^{\lambda*} \boldsymbol{\varepsilon}_k^{\lambda*} a_{k,\lambda}^\dagger e^{ik \cdot x} \right) \quad (6.77)$$

where the coefficients C_k^λ can be obtained by solving Eq. (6.71). Inserting the expansion of \mathbf{V} into Eq. (6.71), we obtain

$$\begin{aligned} -\frac{\partial \mathbf{V}(x)}{\partial t} &= i \sum_{\mathbf{k}} \frac{1}{\sqrt{2E_k V}} E_k \left(A_k^\lambda \boldsymbol{\varepsilon}_k^\lambda a_{k,\lambda} e^{-ik \cdot x} - A_k^{\lambda*} \boldsymbol{\varepsilon}_k^{\lambda*} a_{k,\lambda}^\dagger e^{ik \cdot x} \right) \\ &= \sum_{\mathbf{k}} \frac{1}{\sqrt{2E_k V}} \left[C_k^\lambda \left(1 + \frac{\mathbf{k}\mathbf{k}}{m_v^2} \right) \cdot \boldsymbol{\varepsilon}_k^\lambda a_{k,\lambda} e^{-ik \cdot x} + C_k^{\lambda*} \left(1 + \frac{\mathbf{k}\mathbf{k}}{m_v^2} \right) \cdot \boldsymbol{\varepsilon}_k^{\lambda*} a_{k,\lambda}^\dagger e^{ik \cdot x} \right] \end{aligned} \quad (6.78)$$

We can determine the coefficients,

$$C_k^{1,2} = iE_k A_k^{1,2}, \quad C_k^3 = i \frac{m_v^2}{E_k} A_k^3 \quad (6.79)$$

where we have used $\mathbf{k} \cdot \boldsymbol{\varepsilon}_k^{1,2} = 0$ and $\mathbf{k} \parallel \boldsymbol{\varepsilon}_k^3$. From the commutator (6.74), we obtain

$$\begin{aligned} [V^i(t, \mathbf{x}), \Pi^j(t, \mathbf{x}')] &= \sum_{\mathbf{k}, \mathbf{k}'} \frac{1}{\sqrt{2E_k V}} \frac{1}{\sqrt{2E_{k'} V}} \left[\left(A_k^\lambda \varepsilon_k^{i\lambda} a_{k, \lambda} e^{-ik \cdot x} + A_k^{\lambda*} \varepsilon_k^{i\lambda*} a_{k, \lambda}^\dagger e^{ik \cdot x} \right), \right. \\ &\quad \left. \left(C_{k'}^{\lambda'} \varepsilon_{k'}^{j\lambda'} a_{k', \lambda'} e^{-ik' \cdot x'} + C_{k'}^{\lambda'*} \varepsilon_{k'}^{j\lambda'*} a_{k', \lambda'}^\dagger e^{ik' \cdot x'} \right) \right] \\ &= \frac{1}{V} \sum_{\mathbf{k}, \mathbf{k}'} \frac{1}{\sqrt{2E_k}} \frac{1}{\sqrt{2E_{k'}}} \left\{ A_k^\lambda C_{k'}^{\lambda'*} \varepsilon_k^{i\lambda} \varepsilon_{k'}^{j\lambda'*} e^{-ik \cdot x + ik' \cdot x'} [a_{k, \lambda}, a_{k', \lambda'}^\dagger] \right. \\ &\quad \left. + A_k^{\lambda*} C_{k'}^{\lambda'} \varepsilon_k^{i\lambda*} \varepsilon_{k'}^{j\lambda'} e^{ik \cdot x - ik' \cdot x'} [a_{k, \lambda}^\dagger, a_{k', \lambda'}] \right\} \\ &= \frac{1}{V} \sum_{\mathbf{k}} \frac{1}{2E_k} \left\{ A_k^\lambda C_k^{\lambda*} \varepsilon_k^{i\lambda} \varepsilon_k^{j\lambda*} e^{i\mathbf{k} \cdot (\mathbf{x} - \mathbf{x}')} - A_k^{\lambda*} C_k^\lambda \varepsilon_k^{i\lambda*} \varepsilon_k^{j\lambda} e^{-i\mathbf{k} \cdot (\mathbf{x} - \mathbf{x}')} \right\} \\ &= -i \frac{1}{V} \sum_{\mathbf{k}, \lambda} \frac{1}{2} |A_k^\lambda|^2 \varepsilon_k^{i\lambda} \varepsilon_k^{j\lambda*} \left[e^{i\mathbf{k} \cdot (\mathbf{x} - \mathbf{x}')} + e^{-i\mathbf{k} \cdot (\mathbf{x} - \mathbf{x}')} \right] \\ &\quad - i \frac{1}{V} \sum_{\mathbf{k}} \frac{m_v^2}{2E_k^2} |A_k^3|^2 \varepsilon_k^{i3} \varepsilon_k^{j3*} \left[e^{i\mathbf{k} \cdot (\mathbf{x} - \mathbf{x}')} + e^{-i\mathbf{k} \cdot (\mathbf{x} - \mathbf{x}')} \right] \\ &= -i \delta_{ij} \delta^{(3)}(\mathbf{x} - \mathbf{x}') \end{aligned} \quad (6.80)$$

where $x = (t, \mathbf{x})$ and $x' = (t, \mathbf{x}')$. We have used $[a_{k, \lambda}, a_{k', \lambda'}^\dagger] = \delta_{\mathbf{k}, \mathbf{k}'} \delta_{\lambda, \lambda'}$ and assumed $\varepsilon_k^{i\lambda} \varepsilon_k^{j\lambda*}$ are real. The above requires

$$\sum_{\lambda=1,2} |A_k^\lambda|^2 \varepsilon_k^{i\lambda} \varepsilon_k^{j\lambda*} + \frac{m_v^2}{E_k^2} |A_k^3|^2 \varepsilon_k^{i3} \varepsilon_k^{j3*} = \delta_{ij} \quad (6.81)$$

If we assume $\boldsymbol{\varepsilon}_k^3 = (E_k/m_v) \hat{\mathbf{k}}$ and $A_k^1 = A_k^2 = A_k^3 = 1$, we get

$$\begin{aligned} \sum_{\lambda=1}^2 \varepsilon_k^{i\lambda} \varepsilon_k^{j\lambda*} &= \delta_{ij} - \frac{\mathbf{k}^i \mathbf{k}^j}{\mathbf{k}^2} \\ \sum_{\lambda=1}^3 \varepsilon_k^{i\lambda} \varepsilon_k^{j\lambda*} &= \delta_{ij} + \frac{\mathbf{k}^i \mathbf{k}^j}{m_v^2} \end{aligned} \quad (6.82)$$

The zero-component becomes

$$\begin{aligned} V^0 &= -\frac{1}{m_v^2} \nabla \cdot \boldsymbol{\Pi} \\ &= -\frac{i}{m_v^2} \sum_{\mathbf{k}} \frac{1}{\sqrt{2E_k V}} \left(C_k^\lambda \mathbf{k} \cdot \boldsymbol{\varepsilon}_k^\lambda a_{k, \lambda} e^{-ik \cdot x} - C_k^{\lambda*} \mathbf{k} \cdot \boldsymbol{\varepsilon}_k^{\lambda*} a_{k, \lambda}^\dagger e^{ik \cdot x} \right) \\ &= \sum_{\mathbf{k}} \frac{1}{\sqrt{2E_k V}} \frac{k}{m_v} \left(a_{k,3} e^{-ik \cdot x} + a_{k,3}^\dagger e^{ik \cdot x} \right) \end{aligned} \quad (6.83)$$

We can define the polarization tensor for V^0 ,

$$\varepsilon_k^{0,1} = \varepsilon_k^{0,2} = 0, \quad \varepsilon_k^{0,3} = \frac{k}{m_v} \quad (6.84)$$

Then the four-vector V^α reads

$$V^\alpha(x) = \sum_{\mathbf{k}} \frac{1}{\sqrt{2E_k V}} \left(\varepsilon_k^{\alpha,\lambda} a_{k,\lambda} e^{-ik \cdot x} + \varepsilon_k^{\alpha,\lambda} a_{k,\lambda}^\dagger e^{ik \cdot x} \right) \quad (6.85)$$

The orthogonal condition (6.82) can be written into a compact form,

$$\sum_{\lambda=1}^3 \varepsilon_k^{\alpha,\lambda} \varepsilon_k^{\beta,\lambda} = -g^{\alpha\beta} + \frac{k^\alpha k^\beta}{m_v^2} \quad (6.86)$$

The propagator can be obtained from Eq. (6.85),

$$\begin{aligned} iG &= \langle 0 | T [V^\alpha(x) V^\beta(x')] | 0 \rangle \\ &= \theta(t-t') \langle 0 | V^\alpha(x) V^\beta(x') | 0 \rangle + \theta(t'-t) \langle 0 | V^\beta(x') V^\alpha(x) | 0 \rangle \\ &= \theta(t-t') \sum_{\mathbf{k}, \mathbf{k}'} \frac{1}{V \sqrt{2E_k} \sqrt{2E_{k'}}} \varepsilon_k^{\alpha,\lambda} \varepsilon_{k'}^{\beta,\lambda'} e^{-ik \cdot x} e^{ik' \cdot x'} \langle 0 | a_{k,\lambda} a_{k',\lambda'}^\dagger | 0 \rangle \\ &\quad + \theta(t'-t) \sum_{\mathbf{k}, \mathbf{k}'} \frac{1}{V \sqrt{2E_k} \sqrt{2E_{k'}}} \varepsilon_k^{\alpha,\lambda} \varepsilon_{k'}^{\beta,\lambda'} e^{-ik' \cdot x'} e^{ik \cdot x} \langle 0 | a_{k',\lambda'} a_{k,\lambda}^\dagger | 0 \rangle \\ &= \theta(t-t') \sum_{\mathbf{k}} \frac{1}{2E_k V} \varepsilon_k^{\alpha,\lambda} \varepsilon_k^{\beta,\lambda} e^{-ik \cdot (x-x')} + \theta(t'-t) \sum_{\mathbf{k}} \frac{1}{2E_k V} \varepsilon_k^{\alpha,\lambda} \varepsilon_k^{\beta,\lambda} e^{ik \cdot (x-x')} \\ &\rightarrow \int \frac{d^4 k}{(2\pi)^4} \frac{i}{k^2 - m_v^2 + i\delta} \left(-g^{\alpha\beta} + \frac{k^\alpha k^\beta}{m_v^2} \right) \end{aligned} \quad (6.87)$$

So the propagator in momentum space is

$$iG = \frac{i}{k^2 - m_v^2 + i\delta} \left(-g^{\alpha\beta} + \frac{k^\alpha k^\beta}{m_v^2} \right) \quad (6.88)$$

Similarly we can compute the potential from the exchange of vector bosons. As we know from Table 6.4 that ρ and ω are vector mesons. We take the ω meson as an example, which is an isospin singlet. The interaction term is $g_v \bar{\psi} \gamma_\mu \psi \phi_\nu^\mu$ (vector coupling) with vertex $i\Gamma_\mu = ig_v \gamma_\mu$. The T-matrix is

$$\begin{aligned} i \langle p', h'_1, h'_2 | T | p, h_1, h_2 \rangle &= -\bar{u}_N(-p', h'_2) i\Gamma_\alpha u_N(-p, h_2) \\ &\quad \frac{i(-g^{\alpha\beta} + q^\alpha q^\beta / m_v^2)}{q^2 - m_v^2} \bar{u}_N(p', h'_1) i\Gamma_\beta u_N(p, h_1) \\ &= \frac{ig_v^2 (-g^{\alpha\beta} + q^\alpha q^\beta / m_v^2)}{q^2 - m_v^2} \\ &\quad \bar{u}_N(-p', h'_2) \gamma_\alpha u_N(-p, h_2) \bar{u}_N(p', h'_1) \gamma_\beta u_N(p, h_1) \end{aligned} \quad (6.89)$$

We can simplify

$$\begin{aligned} \bar{u}_N(p', h'_1) \gamma_0 u_N(p, h_1) &= \langle \chi(1') | \left(1 - \frac{\boldsymbol{\sigma} \cdot \mathbf{p}'}{2m_N} \right) \left(\frac{1}{2m_N} \right) | \chi(1) \rangle \\ &= \langle \chi(1') | \left[1 + \frac{(\boldsymbol{\sigma} \cdot \mathbf{p}')(\boldsymbol{\sigma} \cdot \mathbf{p})}{4m_N^2} \right] | \chi(1) \rangle, \\ \bar{u}_N(p', h'_1) \boldsymbol{\gamma} u_N(p, h_1) &= \langle \chi(1') | \frac{(\boldsymbol{\sigma} \cdot \mathbf{p}') \boldsymbol{\sigma}}{2m_N} + \frac{\boldsymbol{\sigma}(\boldsymbol{\sigma} \cdot \mathbf{p})}{2m_N} | \chi(1) \rangle \end{aligned} \quad (6.90)$$

The two terms are

$$\begin{aligned}
I_1 &= \bar{u}_N(-p', h'_2) \gamma_\alpha u_N(-p, h_2) \bar{u}_N(p', h'_1) \gamma^\alpha u_N(p, h_1) \\
&= \bar{u}_N(-p', h'_2) \gamma_0 u_N(-p, h_2) \bar{u}_N(p', h'_1) \gamma_0 u_N(p, h_1) \\
&\quad - \bar{u}_N(-p', h'_2) \gamma^i u_N(-p, h_2) \bar{u}_N(p', h'_1) \gamma^i u_N(p, h_1) \\
&= \langle \chi(2') | [1 + \frac{(\boldsymbol{\sigma} \cdot \mathbf{p}')(\boldsymbol{\sigma} \cdot \mathbf{p})}{4m_N^2}] | \chi(2) \rangle \langle \chi(1') | [1 + \frac{(\boldsymbol{\sigma} \cdot \mathbf{p}')(\boldsymbol{\sigma} \cdot \mathbf{p})}{4m_N^2}] | \chi(1) \rangle \\
&\quad + \frac{1}{4m_N^2} \langle \chi(2') | [(\boldsymbol{\sigma} \cdot \mathbf{p}')\sigma^i + \sigma^i(\boldsymbol{\sigma} \cdot \mathbf{p})] | \chi(2) \rangle \langle \chi(1') | [(\boldsymbol{\sigma} \cdot \mathbf{p}')\sigma^i + \sigma^i(\boldsymbol{\sigma} \cdot \mathbf{p})] | \chi(1) \rangle
\end{aligned}$$

and

$$\begin{aligned}
I_2 &= \bar{u}_N(-p', h'_2)(g_0\gamma_0 - \mathbf{q} \cdot \boldsymbol{\gamma})u_N(-p, h_2)\bar{u}_N(p', h'_1)(g_0\gamma_0 - \mathbf{q} \cdot \boldsymbol{\gamma})u_N(p, h_1) \\
&= \bar{u}_N(-p', h'_2)(\mathbf{q} \cdot \boldsymbol{\gamma})u_N(-p, h_2)\bar{u}_N(p', h'_1)(\mathbf{q} \cdot \boldsymbol{\gamma})u_N(p, h_1) \\
&= -\frac{1}{4m_N^2} \langle \chi(2') | [(\boldsymbol{\sigma} \cdot \mathbf{p}')(\boldsymbol{\sigma} \cdot \mathbf{q}) + (\boldsymbol{\sigma} \cdot \mathbf{q})(\boldsymbol{\sigma} \cdot \mathbf{p})] | \chi(2) \rangle \\
&\quad \times \langle \chi(1') | [(\boldsymbol{\sigma} \cdot \mathbf{p}')(\boldsymbol{\sigma} \cdot \mathbf{q}) + (\boldsymbol{\sigma} \cdot \mathbf{q})(\boldsymbol{\sigma} \cdot \mathbf{p})] | \chi(1) \rangle
\end{aligned} \tag{6.91}$$

where we have set $g_0 \approx 0$. The potential from vector meson exchange is

$$\begin{aligned}
V_\omega(\mathbf{q}) &= \frac{g_v^2}{\mathbf{q}^2 + m_v^2} \left\{ \left[1 + \frac{(\boldsymbol{\sigma}_1 \cdot \mathbf{p}')(\boldsymbol{\sigma}_1 \cdot \mathbf{p})}{4m_N^2} \right] \left[1 + \frac{(\boldsymbol{\sigma}_2 \cdot \mathbf{p}')(\boldsymbol{\sigma}_2 \cdot \mathbf{p})}{4m_N^2} \right] \right. \\
&\quad + \frac{1}{4m_N^2} [(\boldsymbol{\sigma}_1 \cdot \mathbf{p}')(\boldsymbol{\sigma}_2 \cdot \mathbf{p}')(\boldsymbol{\sigma}_1 \cdot \boldsymbol{\sigma}_2) + (\boldsymbol{\sigma}_1 \cdot \mathbf{p}')(\boldsymbol{\sigma}_1 \cdot \boldsymbol{\sigma}_2)(\boldsymbol{\sigma}_2 \cdot \mathbf{p}) \\
&\quad + (\boldsymbol{\sigma}_2 \cdot \mathbf{p}')(\boldsymbol{\sigma}_1 \cdot \boldsymbol{\sigma}_2)(\boldsymbol{\sigma}_1 \cdot \mathbf{p}) + (\boldsymbol{\sigma}_1 \cdot \boldsymbol{\sigma}_2)(\boldsymbol{\sigma}_1 \cdot \mathbf{p})(\boldsymbol{\sigma}_2 \cdot \mathbf{p})] \\
&\quad \left. - \frac{1}{4m_N^2} [(\boldsymbol{\sigma}_1 \cdot \mathbf{p}')(\boldsymbol{\sigma}_1 \cdot \mathbf{q})(\boldsymbol{\sigma}_2 \cdot \mathbf{p}')(\boldsymbol{\sigma}_2 \cdot \mathbf{q}) + (\boldsymbol{\sigma}_1 \cdot \mathbf{q})(\boldsymbol{\sigma}_1 \cdot \mathbf{p})(\boldsymbol{\sigma}_2 \cdot \mathbf{p}')(\boldsymbol{\sigma}_2 \cdot \mathbf{q}) \right. \\
&\quad \left. + (\boldsymbol{\sigma}_1 \cdot \mathbf{p}')(\boldsymbol{\sigma}_1 \cdot \mathbf{q})(\boldsymbol{\sigma}_2 \cdot \mathbf{q})(\boldsymbol{\sigma}_2 \cdot \mathbf{p}) + (\boldsymbol{\sigma}_1 \cdot \mathbf{q})(\boldsymbol{\sigma}_1 \cdot \mathbf{p})(\boldsymbol{\sigma}_2 \cdot \mathbf{q})(\boldsymbol{\sigma}_2 \cdot \mathbf{p}) \right] \}
\end{aligned} \tag{6.92}$$

If we make non-relativistic approximation, $|\mathbf{p}|, |\mathbf{p}'|, |\mathbf{q}| \ll m_N$, the potential becomes

$$V_\omega(\mathbf{q}) \approx \frac{g_v^2}{\mathbf{q}^2 + m_v^2} \rightarrow V_\omega(r) \approx \frac{g_v^2}{4\pi r} e^{-m_v r} \tag{6.93}$$

We can see that the potential resulting from vector boson exchange is repulsive.

Exercise 50. Try to derive Eq. (6.60) from Eq. (6.58). Try to extract the spin/isospin/space exchange potential in one pion exchange potential in Eq. (6.60).

Chapter 7

The structure of hadrons

7.1 Symmetries and Groups

Group theory is the branch of mathematics to deal with symmetry. We take the rotation group as an illustrative example. The set of rotations of a system form a group, each rotation being an element of the group. Let R_1 and R_2 be two successive rotations, then R_2R_1 are equivalent to a single rotation, another group element. The set of rotations is closed under multiplication. There is identity element corresponding to no rotation, and any rotation has an inverse, a back rotation. The product is not necessarily commutative, $R_2R_1 \neq R_1R_2$, but the associate law $R_3(R_2R_1) = (R_3R_2)R_1$ always holds. The rotation group is a Lie group, where every rotation can be expressed as the product of a succession of infinitesimal rotations. The group is then completely defined by the neighborhood of the identity.

The experimental results do not depend on the specific lab orientation of the system being measured. Rotation must form a symmetry group of a system. They are a subset of the Lorentz transformations. By definition, the physics is unchanged by a symmetry operation. In particular these operations leave the transition probabilities of the system invariant.

Suppose the states of a system under a rotation R transform as

$$|\psi'\rangle = U|\psi\rangle \quad (7.1)$$

The probability is unchanged

$$|\langle\phi|\psi\rangle|^2 = |\langle\phi'|\psi'\rangle|^2 = |\langle\phi|U^\dagger U|\psi\rangle|^2 \quad (7.2)$$

so U must be a unitary operator. The operators $U(R)$ form a group with the same structure as the original group R , they form a unitary representation of the rotation group.

Moreover the Hamiltonian is invariant under the rotation of the system, then we have

$$\langle\phi'|H|\psi'\rangle = \langle\phi|U^\dagger H U|\psi\rangle = \langle\phi|H|\psi\rangle \quad (7.3)$$

so we get $[H, U] = 0$, i.e. U is a constant of motion.

Now let us find the generators of U from infinitesimal rotations in the neighborhood of identity. Under the infinitesimal rotation R along the z-axis, the wave function transforms as

$$\begin{aligned} \psi'(\mathbf{r}) &= \psi(R^{-1}\mathbf{r}) = U\psi \\ &= \psi(x + \varepsilon y, y - \varepsilon x, z) \\ &= \psi(x, y, z) + \varepsilon\left(y\frac{\partial\psi}{\partial x} - x\frac{\partial\psi}{\partial y}\right) \\ &= [1 - i\varepsilon(xp_y - yp_x)]\psi \end{aligned} \quad (7.4)$$

where ε is a small rotational angle. Then the transformation matrix U becomes

$$U = 1 - i\varepsilon J_3 \quad (7.5)$$

with J_3 the angular momentum operator along the z-axis. A finite rotation can be built up from exponentiation,

$$U(\theta) = [U(\varepsilon)]^n = \left(1 - i\frac{\theta}{n}J_3\right)^n \rightarrow e^{-i\theta J_3} \quad (7.6)$$

The general form of the matrix along a rotational axis is

$$U(\boldsymbol{\theta}) = e^{-i\boldsymbol{\theta}\cdot\mathbf{J}} \quad (7.7)$$

The commutators of generators are

$$[J_i, J_j] = i\varepsilon_{ijk}J_k \quad (7.8)$$

A finite group is one which contains only a finite number of elements. Two examples are spatial reflection

$$P : \mathbf{r} \rightarrow -\mathbf{r}$$

and particle-antiparticle transformation or charge conjugation

$$C : A \rightarrow \bar{A}$$

where A denotes a particle and \bar{A} denotes its anti-particle. There are two elements in these groups: the identity e and an element g with $g^2 = e$, where g denotes the operation P or C . Invariance of the physics under g means that g is represented by a unitary (or anti-unitary) operator $U(g)$ satisfying

$$[U(g), H] = 0 \quad (7.9)$$

where $U(g)$ is a representation for the group. Time-reversal invariance is the only symmetry requiring an antiunitary operator. Here we take U to be unitary, i.e. $U^\dagger U = 1$, to represent spatial reflection or charge conjugation. For our two-element group, we have

$$U^2 = 1 \quad (7.10)$$

Since $U^{-1} = U^\dagger$, so $U = U^\dagger$, i.e. U is hermitian. Thus U itself is an observable conserved quantity, and its eigenvalues are conserved quantum number. If p is an eigenvalue of U corresponding to the eigenstate $|p\rangle$, i.e. $U|p\rangle = p|p\rangle$, then we have

$$U^2|p\rangle = p^2|p\rangle \quad (7.11)$$

leading to $p = \pm 1$. Invariance of the system under the symmetry operation g means that if the system is in eigenstate of U , the transition can only occur to eigenstates with the same eigenvalue. The eigenvalues of U are multiplicative quantum numbers. By contrast, the eigenvalues of the commuting generators of $SU(n)$ are additive quantum numbers.

The spatial reflection operation defines the parity property of a particle or a system, while the charge conjugation defines the C-parity.

Under the spatial reflection operation, the wave function changes as

$$\begin{aligned} P : \psi(t, \mathbf{r}) &\rightarrow \psi(t, -\mathbf{r}) \\ \psi(t, r, \theta, \phi) &\rightarrow \psi(t, r, \pi - \theta, \pi + \phi) \end{aligned} \quad (7.12)$$

The eigenvalues of the parity are ± 1 corresponding to the even/odd parity, i.e. $U(P)\psi(t, \mathbf{r}) = \pm\psi(t, -\mathbf{r})$. In central force potential the spatial wave-function can be written as

$$\psi(t, r, \theta, \phi) = R_n(r)P_l^m(\cos\theta)e^{im\phi} \quad (7.13)$$

Then under the transformation $\theta \rightarrow \pi - \theta$, $\phi \rightarrow \pi + \phi$, the wave function becomes

$$\begin{aligned}\psi(t, r, \pi - \theta, \pi + \phi) &= R_n(r) P_l^m(-\cos \theta) e^{im(\pi + \phi)} \\ &= R_n(r) (-1)^{l+m} P_l^m(\cos \theta) (-1)^m e^{im\phi} \\ &= (-1)^l \psi(t, r, \theta, \phi)\end{aligned}\quad (7.14)$$

So we see that the parity for a wave function in the central force potential is $(-1)^l$. We know that if the parity operator commutes with the Hamiltonian, the energy eigenstate has a specific parity. Then the parity of the state does not change with time. This is so-called the parity conservation. If the Hamiltonian is not invariant under the parity transformation, the parity conservation does not hold. For the strong and electromagnetic interaction, the parity is conserved, but it is violated in the weak interaction. Particles can also have intrinsic parity if their intrinsic wave functions have specific transformation property under the spatial reflection. It turns out that the intrinsic parity can only be defined for neutral particles, those with vanishing additive quantum numbers. The parities of non-neutral particles are not completely fixed. One can prove in field theory that the parity of a fermion is opposite in sign to its anti-fermion, and the parity of a boson is the same as that of its anti-boson. The parity of photons is negative because the vector potential \mathbf{A} for electromagnetic field is an axial vector, i.e. $P: \mathbf{A} \rightarrow -\mathbf{A}$.

The charge conjugation transforms a particle to its anti-particle. All additive quantum numbers, e.g. the charge, lepton number, baryon number, strange number etc., change their signs. The space-time, momentum and angular momentum do not change. Suppose a state $|A\rangle$ is transformed into its charge conjugate state $|\bar{A}\rangle$,

$$U(C) |A\rangle = \eta_A |\bar{A}\rangle \quad (7.15)$$

where η_A is a phase factor, $\eta_A \eta_A^* = 1$. We can transform the state twice,

$$U^2(C) |A\rangle = \eta_A \eta_{\bar{A}} |A\rangle = |A\rangle \quad (7.16)$$

which requires $\eta_A \eta_{\bar{A}} = 1$, then we get $\eta_{\bar{A}} = \eta_A^*$, i.e. the phase factor of a conjugate state is the complex conjugate of the factor of the state. According to the definition for the charge conjugation, Eq. (7.15), a charge neutral state is the eigenstate of $U(C)$. A neutral state is denoted by $|n\rangle$, then we have

$$U(C) |n\rangle = \eta_n |n\rangle \quad (7.17)$$

where $\eta_n = \pm 1$ is called the C-parity of the state. The C-parity is a multiplicative quantum number. Let us look at the C-parity of the photon. For photons, the charge conjugation changes the sign of the electric and magnetic fields. Thus the photon fields transform as

$$C: A_\mu = (\phi, \mathbf{A}) \rightarrow (-\phi, -\mathbf{A}) = -A_\mu \quad (7.18)$$

So the C-parity of photons is -1 .

For a neutral particle system composed of a particle and its anti-particle, the C-parity is given by $\eta_C = (-1)^{l+s}$. If we treat the system as consisting of identical particles by regarding the anti-particle as the particle with different additive quantum numbers, the general Pauli principle is applicable. Then interchanging particle labels $1 \leftrightarrow 2$ leads to the sign \pm for the bosonic and fermionic system respectively,

$$|1, 2\rangle = (-1)^l (-1)^{s-s_1-s_2} \eta_C |2, 1\rangle = \pm |2, 1\rangle \quad (7.19)$$

where $(-1)^l$ and $(-1)^{s-s_1-s_2}$ come from the angular momentum and spin sector respectively. η_C is the C-parity of the system. We get

$$\eta_C = (-1)^{l+s} \quad (7.20)$$

for both the bosonic and fermionic system.

The Strong and electromagnetic interactions are invariant under both the parity and charge conjugate transformation. The weak interactions do not respect these symmetries. However, to a good approximation, weak interactions are invariant under the product transformation CP .

7.1.1 The group SU(2)

We have discussed that the rotational symmetry is connected the angular momentum. In this subsection we will introduce the group related to the rotational symmetry.

The lowest-dimension nontrivial representation of the rotation group ($j = 1/2$) has generators,

$$J_i = \frac{1}{2}\sigma_i, \quad i = 1, 2, 3 \quad (7.21)$$

where the Pauli matrices are

$$\sigma_1 = \begin{pmatrix} 0 & 1 \\ 1 & 0 \end{pmatrix}, \sigma_2 = \begin{pmatrix} 0 & -i \\ i & 0 \end{pmatrix}, \sigma_3 = \begin{pmatrix} 1 & 0 \\ 0 & -1 \end{pmatrix}. \quad (7.22)$$

The basis for this representation is conventionally chosen to be the eigenvectors of σ_3 ,

$$\left| \frac{1}{2}, \frac{1}{2} \right\rangle = \begin{pmatrix} 1 \\ 0 \end{pmatrix} = \uparrow, \quad \left| \frac{1}{2}, -\frac{1}{2} \right\rangle = \begin{pmatrix} 0 \\ 1 \end{pmatrix} = \downarrow \quad (7.23)$$

The SU(2) transformation matrices are

$$U(\theta_i) = e^{-i\theta_i\sigma_i} \quad (7.24)$$

One can check,

$$U(\theta_i)U^\dagger(\theta_i) = 1, \quad \det(U(\theta_i)) = e^{-i\theta_i\text{Tr}(\sigma_i)} = 1 \quad (7.25)$$

There are $1, 2, 3, \dots$ dimensional representation of SU(2) corresponding to $j = 0, \frac{1}{2}, 1, \frac{3}{2}, \dots$, respectively. The two dimensional representation is called the fundamental representation of SU(2).

The combined angular momentum operators $\mathbf{J} = \mathbf{J}_A + \mathbf{J}_B$ also satisfy algebra (7.8). The Casimir operators J^2 , J_A^2 and J_B^2 have eigenvalues $J(J+1)$, $J_A(J_A+1)$ and $J_B(J_B+1)$. The product of the two irreducible representations of dimension $2J_A+1$ and $2J_B+1$ may be decomposed into the sum of irreducible representations of dimensions $2J+1$ with

$$J = |J_A - J_B|, |J_A - J_B| + 1, \dots, J_A + J_B \quad (7.26)$$

with basis $|JM\rangle$, where $M = m_A + m_B$. One basis can be expressed in terms of the other by,

$$|JM\rangle = \sum_{m_A, m_B} C(m_A m_B; JM) |J_A m_A, J_B m_B\rangle \quad (7.27)$$

where the coefficients C are called Clebsch-Gordan coefficients. These coefficients are readily calculated by repeatedly applying the step-down operator $J_- = J_{A-} + J_{B-}$ to the fully stretched state $|J, M = J\rangle = |J_A, M_A = J_A; J_B, M_B = J_B\rangle$ and using orthogonality.

We can denote the doublet [2] as

$$\left| \frac{1}{2}, \frac{1}{2} \right\rangle = \begin{pmatrix} 1 \\ 0 \end{pmatrix} = |\uparrow\rangle, \quad \left| \frac{1}{2}, -\frac{1}{2} \right\rangle = \begin{pmatrix} 0 \\ 1 \end{pmatrix} = |\downarrow\rangle \quad (7.28)$$

We may write the system with two spin-1/2 particles may have spin 1 and 0 as

$$[2] \otimes [2] = [3] \oplus [1] \quad (7.29)$$

Combining the third spin-1/2 particle, we have

$$([2] \otimes [2]) \otimes [2] = ([3] \otimes [2]) \oplus ([1] \otimes [2]) = [4] \oplus [2]_{MS} \oplus [2]_{MA} \quad (7.30)$$

where 'MS' and 'MA' mean mixed symmetric and mixed anti-symmetric. Normally the 4-plet completely symmetric and is expressed as

$$\frac{1}{\sqrt{3}}(\uparrow\uparrow\downarrow + \uparrow\downarrow\uparrow + \downarrow\uparrow\uparrow) \quad (7.31)$$

Figure 7.1: Clebsch-Gordan coefficients, from Particle Data Group, <http://pdg.lbl.gov>.

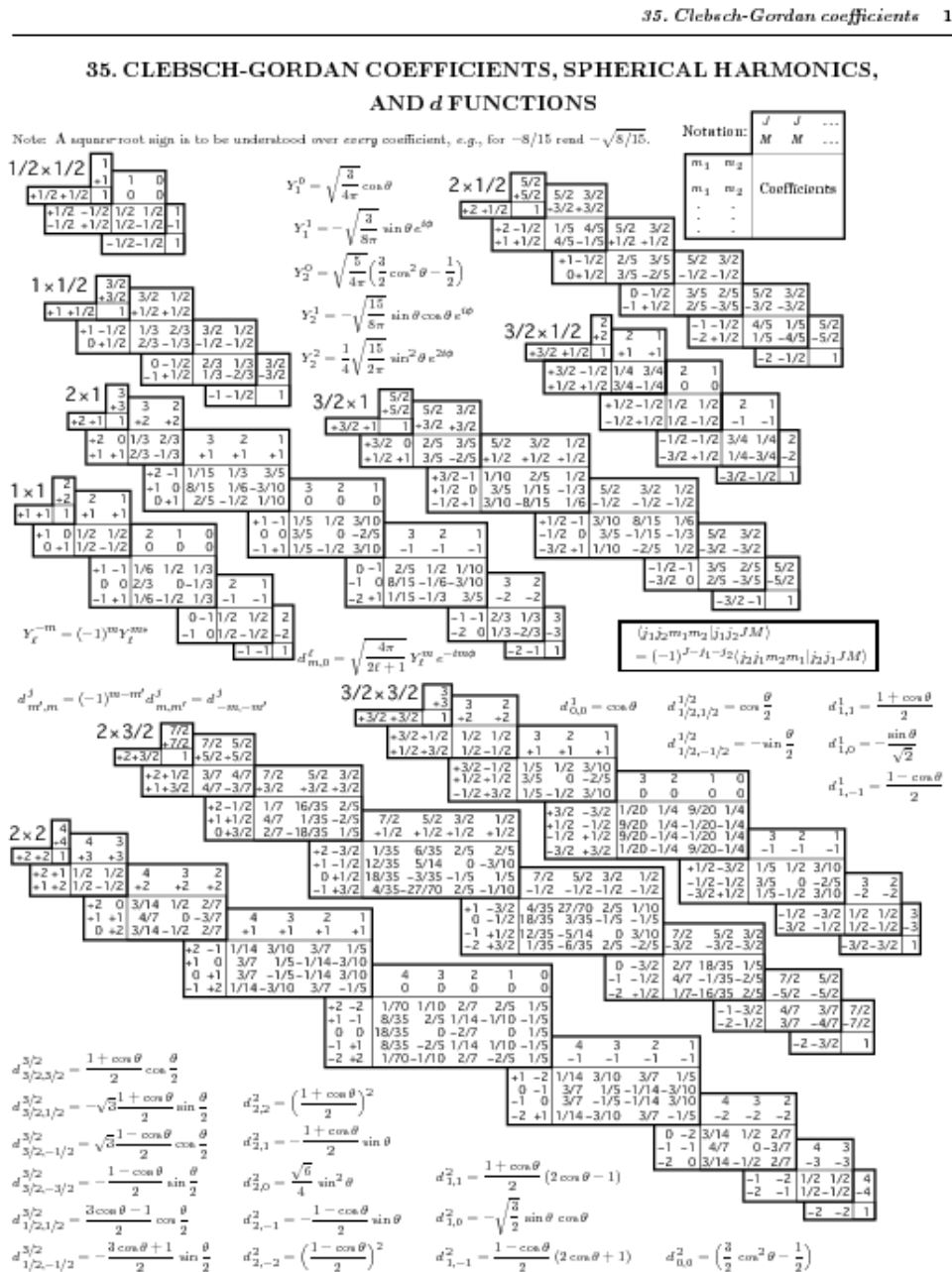


Figure 35.1: The sign convention is that of Wigner (*Group Theory*, Academic Press, New York, 1959), also used by Condon and Shortley (*The Theory of Atomic Spectra*, Cambridge Univ. Press, New York, 1953), Rose (*Elementary Theory of Angular Momentum*, Wiley, New York, 1957), and Cohen (*Tables of the Clebsch-Gordan Coefficients*, North American Rockwell Science Center, Thousand Oaks, Calif., 1974). The coefficients here have been calculated using computer programs written independently by Cohen and at LBNL.

$$\begin{aligned}
\left| \frac{3}{2}, \frac{3}{2} \right\rangle &= \uparrow\uparrow\uparrow \\
\left| \frac{3}{2}, \frac{1}{2} \right\rangle &= \sqrt{\frac{1}{3}} |1, 1\rangle \left| \frac{1}{2}, -\frac{1}{2} \right\rangle + \sqrt{\frac{2}{3}} |1, 0\rangle \left| \frac{1}{2}, \frac{1}{2} \right\rangle \\
&= \sqrt{\frac{1}{3}} \uparrow\uparrow\downarrow + \sqrt{\frac{2}{3}} \sqrt{\frac{1}{2}} (\uparrow\downarrow + \downarrow\uparrow) \uparrow \\
&= \sqrt{\frac{1}{3}} (\uparrow\uparrow\downarrow + \uparrow\downarrow\uparrow + \downarrow\uparrow\uparrow) \\
\left| \frac{3}{2}, -\frac{1}{2} \right\rangle &= \sqrt{\frac{2}{3}} |1, 0\rangle \left| \frac{1}{2}, -\frac{1}{2} \right\rangle + \sqrt{\frac{1}{3}} |1, -1\rangle \left| \frac{1}{2}, \frac{1}{2} \right\rangle \\
&= \sqrt{\frac{2}{3}} \sqrt{\frac{1}{2}} (\uparrow\downarrow + \downarrow\uparrow) \downarrow + \sqrt{\frac{1}{3}} \downarrow\downarrow\uparrow \\
&= \sqrt{\frac{1}{3}} (\uparrow\downarrow\downarrow + \downarrow\uparrow\downarrow + \downarrow\downarrow\uparrow) \\
\left| \frac{3}{2}, -\frac{3}{2} \right\rangle &= \downarrow\downarrow\downarrow
\end{aligned} \tag{7.32}$$

The 2-plet from $[1] \otimes [2]$ is expressed as

$$\begin{aligned}
\left| \frac{1}{2}, \frac{1}{2} \right\rangle_{MA} &= \sqrt{\frac{1}{2}} (\uparrow\downarrow - \downarrow\uparrow) \uparrow \\
\left| \frac{1}{2}, -\frac{1}{2} \right\rangle_{MA} &= \sqrt{\frac{1}{2}} (\uparrow\downarrow - \downarrow\uparrow) \downarrow
\end{aligned} \tag{7.33}$$

The 2-plet from $[3] \otimes [2] = [4] \oplus [2]$ is expressed as

$$\begin{aligned}
\left| \frac{1}{2}, \frac{1}{2} \right\rangle_{MS} &= -\sqrt{\frac{2}{3}} |1, 1\rangle \left| \frac{1}{2}, -\frac{1}{2} \right\rangle + \sqrt{\frac{1}{3}} |1, 0\rangle \left| \frac{1}{2}, \frac{1}{2} \right\rangle \\
&= -\sqrt{\frac{2}{3}} \uparrow\uparrow\downarrow + \sqrt{\frac{1}{3}} \sqrt{\frac{1}{2}} (\uparrow\downarrow + \downarrow\uparrow) \uparrow \\
&= \sqrt{\frac{1}{6}} [(\uparrow\downarrow\uparrow + \downarrow\uparrow\uparrow) - 2 \uparrow\uparrow\downarrow] \\
\left| \frac{1}{2}, -\frac{1}{2} \right\rangle_{MS} &= \sqrt{\frac{1}{3}} |1, 0\rangle \left| \frac{1}{2}, -\frac{1}{2} \right\rangle - \sqrt{\frac{2}{3}} |1, -1\rangle \left| \frac{1}{2}, \frac{1}{2} \right\rangle \\
&= \sqrt{\frac{1}{3}} \sqrt{\frac{1}{2}} (\uparrow\downarrow + \downarrow\uparrow) \downarrow - \sqrt{\frac{2}{3}} \downarrow\downarrow\uparrow \\
&= \sqrt{\frac{1}{6}} [(\uparrow\downarrow\downarrow + \downarrow\uparrow\downarrow) - 2 \downarrow\downarrow\uparrow]
\end{aligned} \tag{7.34}$$

7.1.2 $SU(2)$ isospin, fundamental representation

Isospin arises because the nucleon may be viewed as having an internal degree of freedom with two allowed states, the proton and neutron, which the nuclear interaction does not distinguish. We therefore have an $SU(2)$ symmetry in which the (p, n) form the fundamental representation.

$$p = \begin{pmatrix} 1 \\ 0 \end{pmatrix}, n = \begin{pmatrix} 0 \\ 1 \end{pmatrix} \tag{7.35}$$

Figure 7.2: Basic facts about proton and neutron. <http://pdg.lbl.gov>**P**

$$I(J^P) = \frac{1}{2}(\frac{1}{2}^+)$$

Mass $m = 1.00727646688 \pm 0.00000000013$ u
 Mass $m = 938.27203 \pm 0.00008$ MeV [a]
 $|m_p - m_{\bar{p}}|/m_p < 2 \times 10^{-9}$, CL = 90% [b]
 $|\frac{q_p}{m_p}|/(\frac{q_e}{m_e}) = 0.99999999991 \pm 0.00000000009$
 $|q_p + q_{\bar{p}}|/e < 2 \times 10^{-9}$, CL = 90% [b]
 $|q_p + q_e|/e < 1.0 \times 10^{-21}$ [c]
 Magnetic moment $\mu = 2.792847351 \pm 0.0000000028$ μ_N
 $(\mu_p + \mu_{\bar{p}})/\mu_p = (-2.6 \pm 2.9) \times 10^{-3}$
 Electric dipole moment $d < 0.54 \times 10^{-23}$ e cm
 Electric polarizability $\alpha = (12.0 \pm 0.6) \times 10^{-4}$ fm³
 Magnetic polarizability $\beta = (1.9 \pm 0.5) \times 10^{-4}$ fm³
 Charge radius = 0.875 ± 0.007 fm
 Mean life $\tau > 2.1 \times 10^{29}$ years, CL = 90% ($p \rightarrow$ invisible mode)
 Mean life $\tau > 10^{31}$ to 10^{33} years [d] (mode dependent)

N

$$I(J^P) = \frac{1}{2}(\frac{1}{2}^+)$$

Mass $m = 1.0086649156 \pm 0.0000000006$ u
 Mass $m = 939.56536 \pm 0.00008$ MeV [a]
 $m_n - m_p = 1.2933317 \pm 0.0000005$ MeV
 $= 0.0013884487 \pm 0.0000000006$ u
 Mean life $\tau = 885.7 \pm 0.8$ s
 $c\tau = 2.655 \times 10^8$ km
 Magnetic moment $\mu = -1.9130427 \pm 0.0000005$ μ_N
 Electric dipole moment $d < 0.29 \times 10^{-25}$ e cm, CL = 90%

7.1.3 Conjugate representation of $SU(2)$

Proton and neutron are up and down state in the fundamental representation of $SU(2)$. We can label antiparticle doublet (\bar{n}, \bar{p}) , which has $I_3 = (1/2, -1/2)$ just like (p, n) . This new representation is known as the conjugate representation. Use the following notation,

$$[2] = (p, n) \quad , \quad [2^*] = (\bar{n}, \bar{p}) \quad (7.36)$$

Here is the transformation for $\phi = \begin{pmatrix} p \\ n \end{pmatrix}$,

$$\phi' = \exp(i\theta \mathbf{n} \cdot \boldsymbol{\sigma})\phi = (\cos \theta + i \mathbf{n} \cdot \boldsymbol{\sigma} \sin \theta)\phi \quad (7.37)$$

Acting charge conjugation (complex conjugate) to the above equation, we have

$$\begin{aligned} \bar{\phi}' &= \exp(-i\theta \mathbf{n} \cdot \boldsymbol{\sigma}^*)\bar{\phi} = \exp(i\theta \sigma_2 \mathbf{n} \cdot \boldsymbol{\sigma} \sigma_2)\bar{\phi} \\ &= \sigma_2 \exp(i\theta \mathbf{n} \cdot \boldsymbol{\sigma})\sigma_2 \bar{\phi} \end{aligned} \quad (7.38)$$

where $\bar{\phi} = \begin{pmatrix} \bar{p} \\ \bar{n} \end{pmatrix}$ and we have used $\sigma_i^* = -\sigma_2 \sigma_i \sigma_2$. We can rewrite Eq. (7.38) as

$$\sigma_2 \bar{\phi}' = \exp(i\theta \mathbf{n} \cdot \boldsymbol{\sigma})\sigma_2 \bar{\phi}$$

Defining $\tilde{\phi} = \begin{pmatrix} -\bar{n} \\ \bar{p} \end{pmatrix} = -i\sigma_2 \bar{\phi}$, the above can be written as

$$\tilde{\phi}' = \exp(i\theta \mathbf{n} \cdot \boldsymbol{\sigma})\tilde{\phi} \quad (7.39)$$

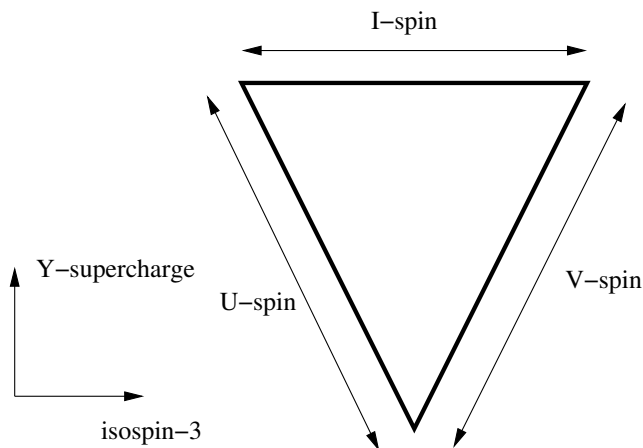
the same transformation form as ϕ .

For a rotation about the 2-axis, we have

$$\begin{pmatrix} p' \\ n' \end{pmatrix} = \begin{pmatrix} \cos \theta & \sin \theta \\ -\sin \theta & \cos \theta \end{pmatrix} \begin{pmatrix} p \\ n \end{pmatrix} \quad (7.40)$$

Now make charge conjugation on both side of the above equation, $p \rightarrow \bar{p}$ and $n \rightarrow \bar{n}$, we get

$$\begin{pmatrix} \bar{n}' \\ \bar{p}' \end{pmatrix} = \begin{pmatrix} \cos \theta & -\sin \theta \\ \sin \theta & \cos \theta \end{pmatrix} \begin{pmatrix} \bar{n} \\ \bar{p} \end{pmatrix} \quad (7.41)$$

Figure 7.3: $SU(3)$ triplet with I, U, V doublets.

Define the conjugate doublet as $\tilde{\phi} = \begin{pmatrix} -\bar{n} \\ \bar{p} \end{pmatrix}$, so that the transformation matrix is the same as that for ϕ ,

$$\tilde{\phi}' = \begin{pmatrix} \cos \theta & \sin \theta \\ -\sin \theta & \cos \theta \end{pmatrix} \tilde{\phi} \quad (7.42)$$

In general $SU(N)$ there are basic representation N and N^* . In $SU(2)$ we find $2 = 2^*$. For $N = 3, 4, \dots$, N and N^* are not equivalent.

Exercise 51. Pions $\pi^{\pm,0}$ are composed of (u, d) and (\bar{u}, \bar{d}) which obey $SU(2)$ fundamental representation. Pions are flavor triplet of $SU(2)$. Write down the flavor wave functions of pions.

7.1.4 $SU(3)$ symmetry

The extension from $SU(2)$ to $SU(3)$ is straightforward if we add a third component to a doublet to form a triplet in fundamental representation,

$$\phi = \begin{pmatrix} u \\ d \\ s \end{pmatrix} \quad (7.43)$$

The transformation is

$$\phi' = U\phi \quad (7.44)$$

where U is now a 3×3 unitary unimodular matrix,

$$U = \exp \left(\frac{1}{2} i \theta_i \lambda_i \right) \quad (7.45)$$

where λ_i are eight independent Hermitian traceless 3×3 matrices analogous to the σ_i of $SU(2)$. We can choose the form given by Gell-Mann,

$$\begin{aligned} \lambda_1 &= \begin{pmatrix} 0 & 1 & 0 \\ 1 & 0 & 0 \\ 0 & 0 & 0 \end{pmatrix}, & \lambda_2 &= \begin{pmatrix} 0 & -i & 0 \\ i & 0 & 0 \\ 0 & 0 & 0 \end{pmatrix}, & \lambda_3 &= \begin{pmatrix} 1 & 0 & 0 \\ 0 & -1 & 0 \\ 0 & 0 & 0 \end{pmatrix}, \\ \lambda_4 &= \begin{pmatrix} 0 & 0 & 1 \\ 0 & 0 & 0 \\ 1 & 0 & 0 \end{pmatrix}, & \lambda_5 &= \begin{pmatrix} 0 & 0 & -i \\ 0 & 0 & 0 \\ i & 0 & 0 \end{pmatrix}, \\ \lambda_6 &= \begin{pmatrix} 0 & 0 & 0 \\ 0 & 0 & 1 \\ 0 & 1 & 0 \end{pmatrix}, & \lambda_7 &= \begin{pmatrix} 0 & 0 & 0 \\ 0 & 0 & -i \\ 0 & i & 0 \end{pmatrix}, & \lambda_8 &= \frac{1}{\sqrt{3}} \begin{pmatrix} 1 & 0 & 0 \\ 0 & 1 & 0 \\ 0 & 0 & -2 \end{pmatrix} \end{aligned} \quad (7.46)$$

Normally we use $T_i = \frac{1}{2}\lambda_i$. The $SU(2)$ is subgroup of $SU(3)$. The $\lambda_{1,2}$ have the structure of $SU(2)$ in 12-block which is isospin subgroup. The $\lambda_{6,7}$ have the same structure in 23-block which is called U-spin. $\lambda_{4,5}$ is related to V-spin. See figures for their relation. The $SU(2)$ doublets are

$$u, d(I) \quad d, s(U) \quad u, s(V) \quad (7.47)$$

We can define ladder operators from T_i for isospin, U-spin and V-spin,

$$\begin{aligned} I_{\pm} &= T_1 \pm iT_2 = \begin{pmatrix} 0 & 1(0) & 0 \\ 0(1) & 0 & 0 \\ 0 & 0 & 0 \end{pmatrix} \\ U_{\pm} &= T_6 \pm iT_7 = \begin{pmatrix} 0 & 0 & 0 \\ 0 & 0 & 1(0) \\ 0 & 0(1) & 0 \end{pmatrix} \\ V_{\pm} &= T_4 \pm iT_5 = \begin{pmatrix} 0 & 0 & 1(0) \\ 0 & 0 & 0 \\ 0(1) & 0 & 0 \end{pmatrix} \end{aligned} \quad (7.48)$$

They satisfy

$$\begin{aligned} [I_+, I_-] &= 2I_3 = \text{diag}(1, -1, 0) \\ [U_+, U_-] &= \frac{3}{2}Y - I_3 = 2U_3 = \text{diag}(0, 1, -1) \\ [V_+, V_-] &= \frac{3}{2}Y + I_3 = 2V_3 = \text{diag}(1, 0, -1) \end{aligned} \quad (7.49)$$

where $I_3 = T_3 = \frac{1}{2}\lambda_3$ is the isospin operator since acting on u, d, s it has eigenvalues $\pm\frac{1}{2}, 0$ respectively. The hypercharge operator is

$$Y = \frac{2}{\sqrt{3}}T_8 = \frac{1}{\sqrt{3}}\lambda_8 \quad (7.50)$$

The Gell-Mann matrices satisfy the Lie algebra,

$$[T_i, T_j] = if_{ijk}T_k \quad (7.51)$$

with the anti-symmetric structure constants f_{ijk} given in Tab. 7.1. Also we have anti-commutator

$$\{T_i, T_j\} = \frac{1}{3}\delta_{ij} + d_{ijk}T_k \quad (7.52)$$

where symmetric structure constants d_{ijk} are given in Tab. 7.1.

Table 7.1: Structure constants of $SU(3)$.

$f_{123} = 1$
$f_{147} = f_{246} = f_{257} = f_{345} = f_{516} = f_{637} = 1/2$
$f_{458} = f_{678} = \sqrt{3}/2$
$d_{118} = d_{228} = d_{338} = -d_{888} = 1/\sqrt{3}$
$d_{146} = d_{157} = d_{256} = d_{344} = d_{355} = 1/2$
$d_{247} = d_{366} = d_{377} = -1/2$
$d_{448} = d_{558} = d_{668} = d_{778} = -1/(2\sqrt{3})$

We can generalise these results by defining $N \times N$ matrices T_i which satisfy Eq. (7.51) and transform N -dimensional states by

$$\phi \rightarrow \phi' = (1 + i\theta_i T_i)\phi \quad (7.53)$$

These states form N -dimensional multiplets of $SU(3)$.

A $SU(3)$ irreducible representation can be drawn in the $I_3 - Y$ diagram. We know that the eigenvalues of I_3 are $0, \pm\frac{1}{2}, \pm 1, \pm\frac{3}{2}, \dots$, so are U_3 and V_3 . From $Y = \frac{2}{3}(U_3 + V_3)$, the eigenvalues of hypercharge are $0, \pm\frac{1}{3}, \pm\frac{2}{3}, \pm 1, \pm\frac{4}{3}, \dots$. Then the basis vectors locate on the grid points with spacing $(\frac{1}{2}, \frac{1}{3})$ for I_3 and Y , see Fig. 7.4. The function of T_{\pm} is to change I_3 by ± 1 while keeping Y fixed. The operator U_{\pm} is to change (I_3, Y) by $(\mp\frac{1}{2}, \pm 1)$, while V_{\pm} is to change (I_3, Y) by $(\pm\frac{1}{2}, \pm 1)$. There are three kinds of irreducible representation: (1) There is one point on $(0, 0)$; (2) There is one point on $(0, \frac{2}{3})$; (3) There is one point on $(0, -\frac{2}{3})$. As an example, the weight diagram for the irreducible representation $(p, q) = (4, 1)$ is shown in Fig. 7.6 and 7.5. Any $SU(3)$ representation has a convex boundary in $I_3 - Y$ space. The maximum state ϕ_{max} can be defined by

$$I_+\phi_{max} = U_+\phi_{max} = V_+\phi_{max} = 0 \quad (7.54)$$

Let $I_3(\phi_{max}) = p/2$ and $U_3(\phi_{max}) = q/2$, we obtain for ϕ_{max}

$$(I_3, Y) = \left(\frac{p}{2}, \frac{p+2q}{3} \right) \quad (7.55)$$

The maximum state ϕ_{max} can also be defined in an alternative way,

$$I_+\phi_{max} = U_-\phi_{max} = V_+\phi_{max} = 0 \quad (7.56)$$

Then (I_{3z}, Y) for ϕ_{max} is obtained by acting $(U_-)^q$ on ϕ_{max} given in Eq. (7.55), changing (I_3, Y) by $(q/2, -q)$,

$$(I_3, Y) = \left(\frac{p+q}{2}, \frac{p-q}{3} \right) \quad (7.57)$$

Here we choose this ϕ_{max} , see Fig. 7.6. We see that the maximum state ϕ_{max} can be characterized by a pair of numbers (p, q) . The $SU(3)$ irreducible representation can be completely specified by a pair of number (p, q) , so we denote it as $D(p, q)$, see Tab. (7.2). The maximum state is composed of p -quarks and q -antiquarks. We will see in the next section that the irreducible representation notation $D(p, q)$ corresponds to a irreducible tensor representation $T_{a_1 \dots a_q}^{i_1 \dots i_p}$. The irreducible representation (p, q) can be classified into three categories by,

$$c(p, q) = p + 2q = (p - q) \pmod{3} \quad (7.58)$$

as: (1) $c(p, q) = 0$, C_2 and C_3 are integers, there is one point on $(0, 0)$ in (I_3, Y) plot; (2) $c(p, q) = \pm 1$, C_2 and C_3 are fractions, there is one point on $(0, -\frac{2}{3})$ and $(\frac{2}{3}, 0)$ respectively. If $c(p, q) = -c(q, p)$, where $c(q, p)$ is the c -number for its conjugate representation.

Figure 7.4: (I_3, Y) figure and U_{\pm}, V_{\pm} and I_{\pm} .

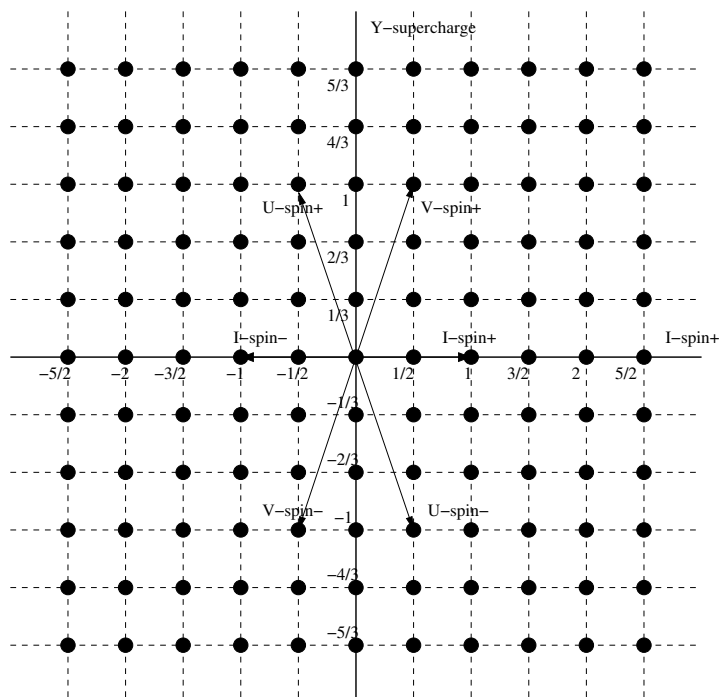


Figure 7.5: The irreducible representation $(p, q) = (4, 1)$. The weight of the states in the outer layer is 1, while that of the states surrounded by circles in the inner layers is 2.

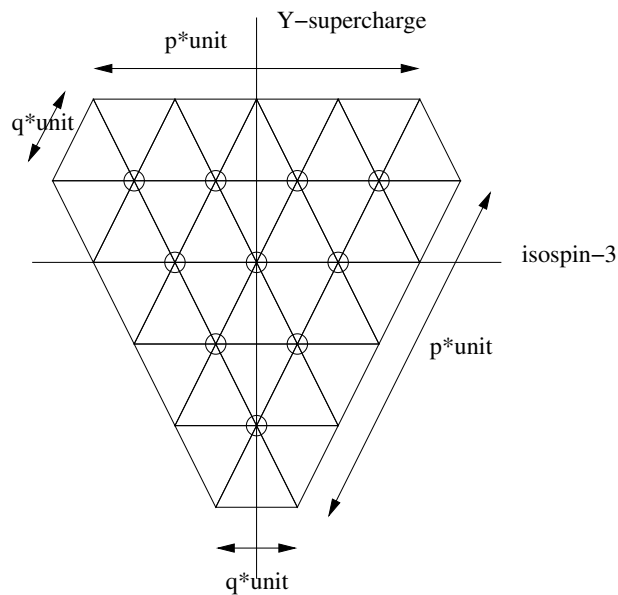
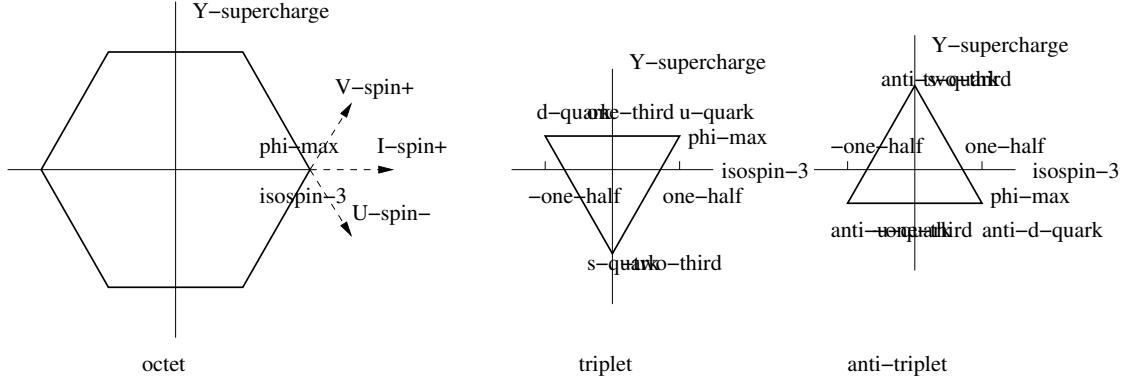


Figure 7.6: The maximum state ϕ_{max} given in Eq. (7.57) for the octet, triplet and anti-triplet.


The irreducible representation $D(p, q)$ can also be expressed by the Young tableaux as shown in Fig. 7.7.

There are two Casimir operators, C_2 and C_3 in $SU(3)$. The quadratic Casimir operator C_2 is defined by

$$C_2 = \sum_i T_i^2 = \frac{1}{2}\{I_+, I_-\} + I_3^2 + \frac{1}{2}\{U_+, U_-\} + \frac{1}{2}\{V_+, V_-\} + T_8^2 \quad (7.59)$$

We can compute the magnitude of the Casimir operator for any $SU(3)$ representation by acting with C_2 on the maximal state of that representation. We can rewrite C_2 by moving I_+ , V_+ and U_- are to the right side of any pair of operators

$$\begin{aligned} C_2 &= \frac{1}{2}\{I_+, I_-\} + I_3^2 + \frac{1}{2}\{U_+, U_-\} + \frac{1}{2}\{V_+, V_-\} + T_8^2 \\ &= I_- I_+ + I_3 + I_3^2 + U_+ U_- - U_3 + V_- V_+ + V_3 + T_8^2 \\ &= I_3^2 + 2I_3 + I_- I_+ + U_+ U_- + V_- V_+ + \frac{3}{4}Y^2 \end{aligned} \quad (7.60)$$

So we get

$$\langle \phi_{max} | C_2 | \phi_{max} \rangle = \langle I_3^2 \rangle + 2 \langle I_3 \rangle + \frac{3}{4}Y^2 \quad (7.61)$$

Then C_2 for $D(p, q)$ becomes

$$C_2 = \frac{1}{3}(p^2 + pq + q^2) + (p + q) \quad (7.62)$$

We see that C_2 is symmetric with respect to exchanging p and q . The values of C_2 for some representations are listed in Tab. (7.2).

The cubic Casimir operator C_3 is defined by

$$C_3 = -if_{i_1 j_1 j_2} if_{i_2 j_2 j_3} if_{i_3 j_3 j_1} T_{i_1} T_{i_2} T_{i_3} = -[T_{j_1}, T_{j_2}][T_{j_2}, T_{j_3}][T_{j_3}, T_{j_1}] \quad (7.63)$$

The eigenvalue of C_3 for the representation (p, q) is given by

$$C_3 = (p + 2q)(p + 2) - \frac{1}{9}(p - q)(2p^2 + 5pq + 2q^2) \quad (7.64)$$

Table 7.2: Irreducible representations for SU(3).

tensor	rank	dimension	C_2
T^i	(1,0)	3	4/3
T_a	(0,1)	$\bar{3}$	4/3
T_a^i	(1,1)	8	3
T^{ij}	(2,0)	6	10/3
T_{ab}	(0,2)	$\bar{6}$	10/3
T^{ijk}	(3,0)	10	6
T_{abc}	(0,3)	$\bar{10}$	6
T_{ab}^{ij}	(2,2)	27	8

We see that C_3 assumes different values for conjugate representation, i.e. it is not symmetric for p and q .

The commutation rule for SU(N) generators is given by,

$$[G_i, G_j] = if_{ijk}G_k, \quad (7.65)$$

where $i, j, k = 1, \dots, M$. The coefficients f_{ijk} are the structure constants of SU(N). There always exists a M-dimensional representation, the so-called *regular representation* or *adjoint representation* defined by the structure constants,

$$(G_i)_{jk} = -if_{ijk}. \quad (7.66)$$

One can prove that the above matrices in Eq. (7.66) satisfy the commutation rule (7.65) by using the Jacobi's identity,

$$[[G_i, G_j], G_k] + [[G_j, G_k], G_i] + [[G_k, G_i], G_j] = 0 \quad (7.67)$$

Exercise 52. Prove the Casimir operator C_2 is commutable with all Gell-Mann matrices T_i ($i = 1, \dots, 8$), $[C_2, T_i] = 0$.

7.1.5 Tensor representation of SU(3)

See Ref. [16]. Corresponding to the (n, m) irreducible representation, we have a (n, m) tensor $T_{a_1 \dots a_m}^{i_1 \dots i_n}$ transforming under SU(3),

$$T_{a_1 \dots a_m}^{i_1 \dots i_n} \rightarrow U_{j_1}^{i_1} \dots U_{j_n}^{i_n} U_{a_1}^{+b_1} \dots U_{a_m}^{+b_m} T_{b_1 \dots b_m}^{j_1 \dots j_n} \quad (7.68)$$

There are three special tensors.

(1) δ_j^i is a (1,1) tensor.

$$\delta_j^i \rightarrow U_{i_1}^i U_{j_1}^{+j_1} \delta_{j_1}^{i_1} = (UU^+)_{j_1}^i = \delta_j^i \quad (7.69)$$

(2) ϵ^{ijk} is a (3,0) tensor. ϵ_{ijk} is a (0,3) tensor.

$$\epsilon^{ijk} \rightarrow U_{i_1}^i U_{j_1}^j U_{k_1}^k \epsilon^{i_1 j_1 k_1} = \epsilon^{ijk} \det U = \epsilon^{ijk} \quad (7.70)$$

Using δ_j^i , ϵ^{ijk} and ϵ_{ijk} , we can form different tensors from $T_{a_1 \dots a_m}^{i_1 \dots i_n}$,

$$\begin{aligned} A_{a_2 \dots a_m}^{i_2 \dots i_n} &= \delta_{a_1}^{i_1} T_{a_1 \dots a_m}^{i_1 \dots i_n}, \\ B_{ba_1 \dots a_m}^{i_3 \dots i_n} &= \epsilon_{bi_1 i_2} T_{a_1 \dots a_m}^{i_1 i_2 i_3 \dots i_n}, \\ C_{a_3 \dots a_m}^{bi_1 \dots i_n} &= \epsilon^{ba_1 a_2} T_{a_1 a_2 a_3 \dots a_m}^{i_1 \dots i_n}, \end{aligned} \quad (7.71)$$

where A , B and C are $(n-1, m-1)$, $(n-2, m+1)$ and $(n+1, m-2)$ tensors respectively if they are not zero. We say that $T_{a_1 \dots a_m}^{i_1 \dots i_n}$ is reducible.

A irreducible (n, m) tensor $T_{a_1 \dots a_m}^{i_1 \dots i_n}$ has following properties: (1) Symmetric under interchange of any two subscript and superscript indices; (2) Contraction of any one superscript and one subscript indices gives zero.

An irreducible (n, m) tensor $T_{a_1 \dots a_m}^{i_1 \dots i_n}$ form a basis for the irreducible representation of $SU(3)$. The dimension of the representation is given by

$$d = (1+n)(1+m)[1+(n+m)/2]. \quad (7.72)$$

Now we give a proof. We first focus on the upper indices. Due to the symmetry, the order of the indices is irrelevant. Suppose we put the indices in such an order: ones, twos and threes. If there are j ones, and then $(n-j)$ twos and threes. There are $(n-j+1)$ combinations in this case. In total the number of different components is then

$$\sum_{j=0}^n (n-j+1) = \frac{1}{2}(n+1)(n+2) \quad (7.73)$$

Similarly for lower indices there are $\frac{1}{2}(m+1)(m+2)$ linearly independent components. So a (n, m) tensor has $\frac{1}{4}(m+1)(m+2)(n+1)(n+2)$ independent components. The trace of the tensor is a $(n-1, m-1)$. The traceless requirement leads to $\frac{1}{4}m(m+1)n(n+1)$ conditions. The dimension of the irreducible representation is then

$$\begin{aligned} d &= \frac{1}{4}(m+1)(m+2)(n+1)(n+2) - \frac{1}{4}m(m+1)n(n+1) \\ &= \frac{1}{2}(m+1)(n+1)(m+n+2) \end{aligned} \quad (7.74)$$

Suppose A_j^i and B_j^i are two irreducible $(1,1)$ tensors (octet), so they are traceless. We can construct a $(2,2)$ tensor $T_{ab}^{ij} = A_a^i B_b^j$ which can be reduced to tensors in Tab. (7.3). For example the 27-plet is

$$\begin{aligned} T_{ab}^{ij} &= A_a^i B_b^j + A_b^i B_a^j + A_a^j B_b^i + A_b^j B_a^i - \delta_a^i (A_b^c B_c^j + A_c^j B_b^c) - \delta_a^j (A_c^i B_b^c + A_b^c B_c^i) \\ &\quad - \delta_b^i (A_a^c B_c^j + A_c^j B_a^c) - \delta_b^j (A_c^i B_a^c + A_a^c B_c^i) \end{aligned} \quad (7.75)$$

Exercise 53. Consider the tensor decomposition of $D(2,0) \otimes D(0,2)$.

7.1.6 Reduction of direct product of irreducible representations in $SU(3)$

There are many ways to reduce the direct product of two irreducible representations. Here we take Young tableaux method as an example. As we have learned that an IR representation $D(p, q)$ can be represented by a Young table with the first and second rows to have $p+q$ and q boxes, as shown in Fig. 7.7. The dimension of the representation is given in Eq. (7.72). Consider the following reduction $D(3,1) \otimes D(1,1)$. The procedure is (1) Fix the first one $D(3,1)$, label each box of $D(1,1)$ by its row number; (2) Move each box from $D(1,1)$ to $D(3,1)$ one by one; (3) For the labelled boxes which are in

Table 7.3: Irreducible tensor from $T_{ab}^{ij} = A_a^i B_b^j$.

tensor	rank	dim
$S = A_a^i B_i^a$	(0,0)	1
$F_a^i = A_j^i B_a^j - B_j^i A_a^j$	(1,1)	8
$D_a^i = A_j^i B_a^j + B_j^i A_a^j - \frac{2}{3} \delta_j^i S$	(1,1)	8
$A_a^i B_b^j \epsilon^{abk} + \text{all permutations of (i,j,k)}$	(3,0)	10
$A_a^i B_b^j \epsilon_{ijc} + \text{all permutations of (a,b,c)}$	(0,3)	$\overline{10}$
$A_a^i B_b^j + \text{symmetric term-(trace)}$	(2,2)	27

the same row, the order of numbers from the left to the right should not decrease (equal or increase); (4) For the labelled boxes which are in the same column, the numbers should be all different, and should increase from up to down; (5) Counting labelled boxes from up-right to down-left, the number of boxes labelled by 1 should be no less than that labelled by 2 in each step of the counting. (6) Delete any column with 3 or more boxes.

The result of the reduction is then,

$$D(3, 1) \otimes D(1, 1) = D(4, 2) \oplus D(5, 0) \oplus D(2, 3) \oplus D(3, 1) \oplus D(3, 1) \oplus D(2, 0) \quad (7.76)$$

The dimension of an IR representation $D(p, q)$ can also be computed by using the Young tableaux. The dimension is given by d_1/d_2 where d_1 and d_2 are products of two series of numbers filled in each box of the Young tableaux. The rule of the filling for d_1 is: (1) fill one number in each box; (2) fill 3 [for SU(3)] in the upper-left box; (3) the number increases by 1 when moving to the right and decreases by 1 when moving to down. The rule for d_2 is: fill one number in each box, which is the number of boxes counting from this box to its right end plus that to its lower end and minus 1. For example, we can compute the dimension of $D(1, 1) = 8$ according to this rule, see Fig. 7.8.

Exercise 54. Consider the decomposition of $D(3, 2) \otimes D(2, 1)$ in Young tableaux.

7.1.7 Quarks as building blocks for hadrons

According to the quark model, all hadrons are made up of a small variety of more basic entities, called quarks, bound together in different ways. The fundamental representation of SU(3), the multiplet from which all other multiplets can be built, is a triplet. There are also anti-quark multiplets in which the signs of additive quantum numbers are reversed. Each quark is assigned spin 1/2 and baryon number $B = 1/3$. See Fig. (7.6). Baryons are made of three quarks (qqq) and mesons of quark-anti-quark ($q\bar{q}$). A new additive quantum number is called the hypercharge, i.e. the sum of the baryon number and the strangeness number,

$$Y = B + S \quad (7.77)$$

The charge, Qe , is given by the Gell-mann-Nishijima relation,

$$Q = I_3 + \frac{Y}{2} \quad (7.78)$$

The quantum number of the quarks are listed in Tab. (7.4).

Figure 7.7: Young tableaux and reduction of the direct product.

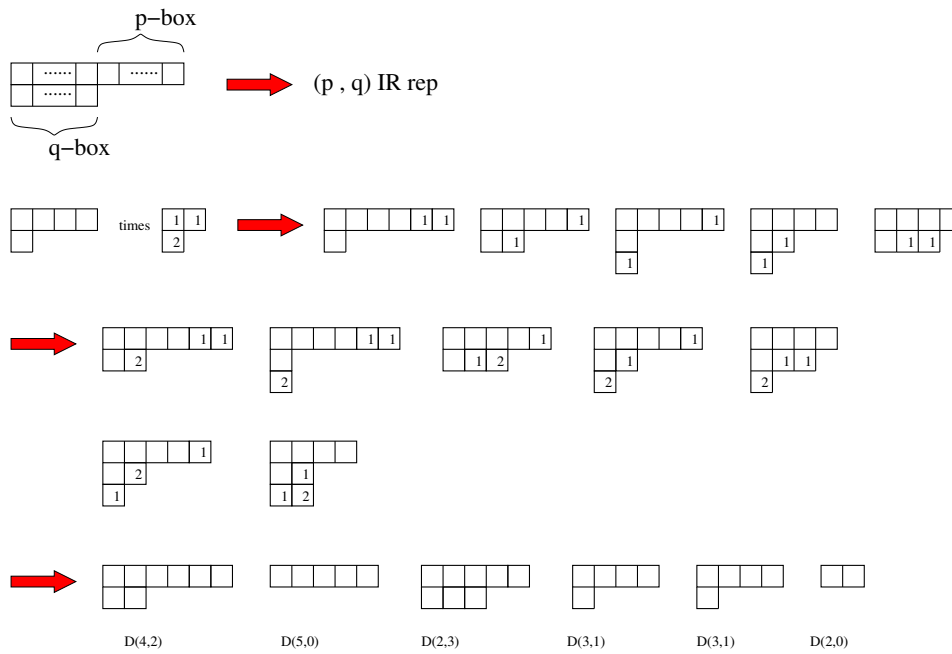


Figure 7.8: The dimension of $D(3,1)$.

$$\begin{array}{|c|c|c|c|} \hline 3 & 4 & 5 & 6 \\ \hline 2 & & & \\ \hline \end{array}
 \quad \underline{\hspace{10em}} \quad = \quad 24$$

$$\begin{array}{|c|c|c|c|} \hline 5 & 3 & 2 & 1 \\ \hline 1 & & & \\ \hline \end{array}$$

Table 7.4: Quantum numbers of the quarks.

quark	spin	B	Q	I_3	S	Y
u	1/2	1/3	2/3	1/2	0	1/3
d	1/2	1/3	-1/3	-1/2	0	1/3
s	1/2	1/3	-1/3	0	-1	-2/3

7.1.8 Mesons as quark-anti-quark states

In the quark model, mesons are bound states made of a quark and an anti-quark. Consider two flavor case, $q = (u, d)$, $\bar{q} = (-\bar{d}, \bar{u})$, the mesons are in isotriplet and isosinglet, i.e. $[2] \otimes [2] = [3] \oplus 1$ in $SU(2)$,

$$\begin{aligned}
 |I = 1, I_3 = 1\rangle &= -u\bar{d} \\
 |I = 1, I_3 = 0\rangle &= \frac{1}{\sqrt{2}}(u\bar{u} - d\bar{d}) \\
 |I = 1, I_3 = -1\rangle &= d\bar{u} \\
 |I = 0, I_3 = 0\rangle &= \frac{1}{\sqrt{2}}(u\bar{u} + d\bar{d})
 \end{aligned} \tag{7.79}$$

They are pions: $\pi^+ = u\bar{d}$ (we neglect the minus sign), $\pi^- = d\bar{u}$ and $\pi^0 = \frac{1}{\sqrt{2}}(u\bar{u} - d\bar{d})$. The masses of pion are about: 140 MeV (π^\pm) and 135 MeV (π^0). The spin, parity and C-parity of pions are $J^{PC} = 0^{-+}$. The isospin scalar $\frac{1}{\sqrt{2}}(u\bar{u} + d\bar{d})$ will be mixed with other $I_3 = Y = 0$ states.

For three flavor case, $q = (u, d, s)$, $\bar{q} = (\bar{u}, \bar{d}, \bar{s})$, there are nine possible combinations. See Fig. (7.9) for resulting meson nonet. The nine states divide into an $SU(3)$ octet and an $SU(3)$ singlet. The decomposition can be written as

$$\begin{aligned}
 [3] \otimes [3^*] &= [8] \oplus [1] \\
 D(1, 0) \otimes D(0, 1) &= D(1, 1) \oplus D(0, 0)
 \end{aligned} \tag{7.80}$$

Three states, A, B and C, have $I_3 = Y = 0$. These are linear combinations of $u\bar{u}$, $d\bar{d}$, and $s\bar{s}$ states. The singlet combination, C, must contain each quark flavor on an equal footing, so we have

$$C = \frac{1}{\sqrt{3}}(u\bar{u} + d\bar{d} + s\bar{s}) \tag{7.81}$$

State A is taken to be a member of the isospin triplet ($d\bar{u}$, A, $-u\bar{d}$) and so we have

$$A = \frac{1}{\sqrt{2}}(u\bar{u} - d\bar{d}) \tag{7.82}$$

By orthogonality to A and C, we can find B,

$$B = \frac{1}{\sqrt{6}}(u\bar{u} + d\bar{d} - 2s\bar{s}) \tag{7.83}$$

We often use the notation ($SU(3), SU(2)$),

$$\begin{aligned}
 A &= \pi^0, \rho^0([8], [3]) \\
 B &= \eta_8, \omega_8([8], [1]) \\
 C &= \eta_1, \omega_1([1], [1])
 \end{aligned} \tag{7.84}$$

The physical η and η' or ω and ϕ are mixtures of $\eta_{1,8}$ and $\omega_{1,8}$ respectively. The η and η' are almost octet and singlet respectively,

$$\begin{aligned}
 \eta &\approx \eta_8 = \frac{1}{\sqrt{6}}(u\bar{u} + d\bar{d} - 2s\bar{s}), \\
 \eta' &\approx \eta_1 = \frac{1}{\sqrt{3}}(u\bar{u} + d\bar{d} + s\bar{s}).
 \end{aligned}$$

Here are their masses and spin-parities: $\eta(548)$ and $\eta'(958)$, $J^{PC} = 0^{-+}$. The physical ω and ϕ appear to be ideal mixture:

$$\begin{aligned}\phi &= \frac{1}{\sqrt{3}}\omega_1 - \sqrt{\frac{2}{3}}\omega_8 = s\bar{s} \\ \omega &= \sqrt{\frac{2}{3}}\omega_1 + \frac{1}{\sqrt{3}}\omega_8 = \frac{1}{\sqrt{2}}(u\bar{u} + d\bar{d})\end{aligned}\quad (7.85)$$

Their masses and spin-parities are $\phi(1020)$, $\omega(1420)$, $J^{PC} = 1^{-}$.

Octet mesons can be expressed by

$$[8] \rightarrow M = q^a q_b - \frac{1}{3}\delta_b^a q^c q_c \quad (7.86)$$

where q^i is the quark field and q_i is its Hermite conjugation (antiquark). Under the SU(3) transformation $q \rightarrow Uq$, the meson tensor transforms as

$$M \rightarrow U M U^+ \quad (7.87)$$

Matrix form

$$M = \begin{pmatrix} \frac{\pi^0}{\sqrt{2}} + \frac{\eta_8}{\sqrt{6}} & \pi^+ & K^+ \\ \pi^- & -\frac{\pi^0}{\sqrt{2}} + \frac{\eta_8}{\sqrt{6}} & K^0 \\ K^- & \bar{K}^0 & -\frac{2}{\sqrt{6}}\eta_8 \end{pmatrix} = \frac{1}{\sqrt{2}}\xi_a \lambda_a \quad (7.88)$$

where

$$\begin{aligned}\pi^\pm &= \frac{1}{\sqrt{2}}(\xi_1 \mp i\xi_2), \quad \pi^0 = \xi_3 \\ K^\pm &= \frac{1}{\sqrt{2}}(\xi_4 \mp i\xi_5), \quad K^0/\bar{K}^0 = \frac{1}{\sqrt{2}}(\xi_6 \mp i\xi_7) \\ \eta_8 &= \xi_8\end{aligned}\quad (7.89)$$

The singlet can be written as

$$[1] \rightarrow S = \frac{1}{3}\delta_b^a q^c q_c = \frac{\eta_1}{\sqrt{3}} \begin{pmatrix} 1 & 0 & 0 \\ 0 & 1 & 0 \\ 0 & 0 & 1 \end{pmatrix} \quad (7.90)$$

One can verify

$$\begin{aligned}M + S &= \begin{pmatrix} \frac{\pi^0}{\sqrt{2}} + \frac{\eta_8}{\sqrt{6}} + \frac{\eta_1}{\sqrt{3}} & \pi^+ & K^+ \\ \pi^- & -\frac{\pi^0}{\sqrt{2}} + \frac{\eta_8}{\sqrt{6}} + \frac{\eta_1}{\sqrt{3}} & K^0 \\ K^- & \bar{K}^0 & -\frac{2}{\sqrt{6}}\eta_8 + \frac{\eta_1}{\sqrt{3}} \end{pmatrix} \\ &= \begin{pmatrix} u \\ d \\ s \end{pmatrix} (\bar{u}, \bar{d}, \bar{s}) = \begin{pmatrix} u\bar{u} & u\bar{d} & u\bar{s} \\ d\bar{u} & d\bar{d} & d\bar{s} \\ s\bar{u} & s\bar{d} & s\bar{s} \end{pmatrix}\end{aligned}\quad (7.91)$$

Here are masses and spin-parity for kaons: $K^\pm(494)$, $K^0(498)$ and $\bar{K}^0(498)$, $J^P = 0^-$.

Like any quantum-mechanical bound system, the $q\bar{q}$ pair will have a discrete energy level spectrum corresponding to the different modes of $q\bar{q}$ excitations. The intrinsic spin of $q\bar{q}$ is $S = 0, 1$. The spin

Figure 7.9: Meson nonet as $q\bar{q}$ bound states. A, B, C are states with $Y = I_3 = 0$ composed of $u\bar{u}, d\bar{d}, s\bar{s}$.

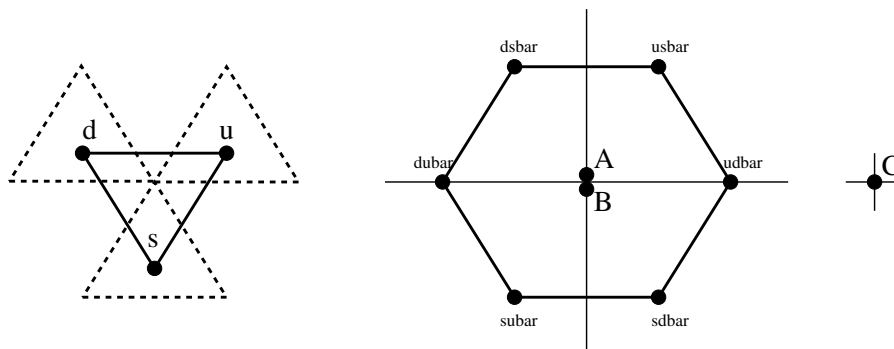


Table 7.5: Some examples of J^P (spin-parity) about meson multiplets (nonets). We have used abbreviation “S”=scalar, “PS”=pseudoscalar, “V”=vector, “AV”=axial vector, “T”=tensor, “AT”=axial tensor.

multiplets	S	PS	V	AV	T	AT
J^P	0^+	0^-	1^-	1^+	2^+	2^-

J of the composite meson is the vector sum of this spin and the relative orbital angular momentum L of the q and \bar{q} . The parity of the meson is,

$$P = (-1)^{L+1} \quad (7.92)$$

where the minus sign arises because the q and \bar{q} have opposite intrinsic parity, and $(-1)^L$ arises from the space inversion replacements $\theta \rightarrow \pi - \theta$, $\phi \rightarrow \pi + \phi$ in the angular part of the $q\bar{q}$ wavefunction $Y_{LM}(\theta, \phi)$. A neutral $q\bar{q}$ system is an eigenstate of the particle-anti-particle conjugation operator C . The value of C can be deduced by $q \leftrightarrow \bar{q}$ and then interchanging their positions and spins. The combined operation gives

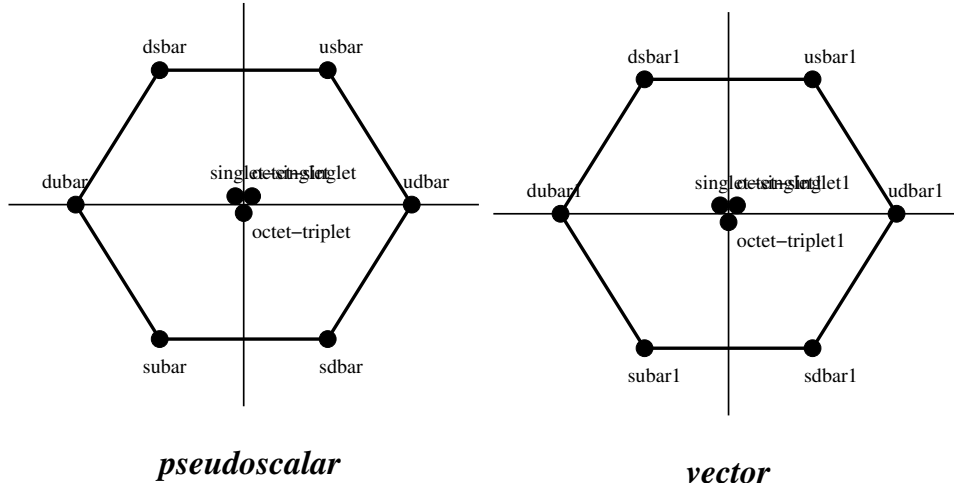
$$C = -(-1)^{S+1}(-1)^L = (-1)^{L+S} \quad (7.93)$$

where the minus sign arises from interchanging fermions, the $(-1)^{S+1}$ from the symmetry of the $q\bar{q}$ spin states, and the $(-1)^L$ from the angular momentum. Here S is the total intrinsic spin of the $q\bar{q}$ pair. The total meson spin J is given by $|L - S| < J < |L + S|$.

The C-parity is only defined for neutral particles or systems. Now we extend the C-parity by introducing the G-parity which is not limited to neutral systems or particles. The $u\bar{d}$ state can be

Table 7.6: Some examples of J^{PC} (spin-parity-C-parity) about ground state ($L = 0$) and first excited ($L = 1$) mesons. We have used abbreviation “PS”=pseudoscalar, “V”=vector, “S”=scalar, “AV”=axial vector, “T”=tensor.

multiplets	PS ($L = 0$)	V ($L = 0$)	S ($L = 1$)	AV ($L = 1$)	T ($L = 1$)
J^{PC}	0^{-+}	1^{--}	0^{++}	$1^{++}, 1^{+-}$	2^{++}

Figure 7.10: Pseudoscalar ($J^P = 0^-$) and vector mesons ($J^P = 1^-$).


either symmetric or anti-symmetric

$$\begin{aligned}\phi_S &= \frac{1}{\sqrt{2}}(u\bar{d} + \bar{d}u) \\ \phi_A &= \frac{1}{\sqrt{2}}(u\bar{d} - \bar{d}u)\end{aligned}$$

These states are distinguished by G -parity defined by

$$G = Ci\tau_2 = C \begin{pmatrix} 0 & 1 \\ -1 & 0 \end{pmatrix}$$

where C is the charge conjugation operator. Let's see

$$\begin{aligned}G \begin{pmatrix} u \\ d \end{pmatrix} &= C \begin{pmatrix} 0 & 1 \\ -1 & 0 \end{pmatrix} \begin{pmatrix} u \\ d \end{pmatrix} = C \begin{pmatrix} d \\ -u \end{pmatrix} = \begin{pmatrix} \bar{d} \\ -\bar{u} \end{pmatrix} \\ G \begin{pmatrix} \bar{d} \\ -\bar{u} \end{pmatrix} &= G^2 \begin{pmatrix} u \\ d \end{pmatrix} = - \begin{pmatrix} u \\ d \end{pmatrix}\end{aligned}$$

so we have

$$\begin{aligned}G\phi_S &= \frac{1}{\sqrt{2}}G(u\bar{d} + \bar{d}u) = -\frac{1}{\sqrt{2}}(\bar{d}u + u\bar{d}) = -\phi_S \\ G\phi_A &= \frac{1}{\sqrt{2}}G(u\bar{d} - \bar{d}u) = \frac{1}{\sqrt{2}}(-\bar{d}u + u\bar{d}) = \phi_A\end{aligned}$$

We can see

$$\begin{aligned}\pi^0 &\sim \frac{1}{2}[(u\bar{u} - d\bar{d}) + (\bar{u}u - \bar{d}d)] = \phi_S^0 \\ \rho^0 &\sim \frac{1}{2}[(u\bar{u} - d\bar{d}) - (\bar{u}u - \bar{d}d)] = \phi_A^0\end{aligned}$$

This definition is consistent to the fact about the C -parity,

$$C\phi_S^0 = \phi_S^0, C\phi_A^0 = -\phi_A^0$$

Table 7.7: $q\bar{q}$ representations with explicit G-parity

$K^+(K^{+*})$	$\frac{1}{\sqrt{2}}(u\bar{s} \pm \bar{s}u)$
$K^0(K^{0*})$	$\frac{1}{\sqrt{2}}(d\bar{s} \pm \bar{s}d)$
$K^-(K^{-*})$	$\frac{1}{\sqrt{2}}(s\bar{u} \pm \bar{u}s)$
$\bar{K}^0(\bar{K}^{0*})$	$-\frac{1}{\sqrt{2}}(s\bar{d} \pm \bar{d}s)$
$\pi^+(\rho^+)$	$-\frac{1}{\sqrt{2}}(u\bar{d} \pm \bar{d}u)$
$\pi^-(\rho^-)$	$\frac{1}{\sqrt{2}}(d\bar{u} \pm \bar{u}d)$
$\pi^0(\rho^0)$	$\frac{1}{2}[(u\bar{u} - d\bar{d}) \pm (\bar{u}u - \bar{d}d)]$
$\eta_8^0(\omega_8^0)$	$\frac{1}{2\sqrt{3}}[(u\bar{u} + d\bar{d} - 2s\bar{s}) \pm (\bar{u}u + \bar{d}d - 2\bar{s}s)]$
$\eta_1^0(\omega_1^0)$	$\frac{1}{\sqrt{6}}[(u\bar{u} + d\bar{d} + s\bar{s}) \pm (\bar{u}u + \bar{d}d + \bar{s}s)]$

Therefore 0^- mesons (pseudoscalar) are the symmetric states with negative G-parity, while 1^- mesons (vector) are anti-symmetric states with positive G-parity.

Combining with spins, we have following possibilities for the symmetry property of SU(3)-SU(2) wave function ϕ_χ under the interchange of 1 and 2,

$$\begin{aligned} \text{symmetric} & : \phi_S\chi_S, \phi_A\chi_A \\ \text{anti-symmetric} & : \phi_S\chi_A, \phi_A\chi_S \end{aligned}$$

where χ_A denotes the spin single wave function and χ_S the triplet wave function. The 0^- and 1^- mesons are totally anti-symmetric because the wave functions for neutral particles are

$$\begin{aligned} \pi^0 & \sim \phi_S^0\chi_A \\ \rho^0 & \sim \phi_A^0\chi_S \end{aligned}$$

Hence the wave functions for the 0^- mesons are $\phi_S\chi_A$ while that for the 1^- mesons are $\phi_A\chi_S$.

7.1.9 Baryons as three-quark states

A baryon is a bound state of three quarks. First we combine two quarks,

$$[3] \otimes [3] = [6] \oplus [\bar{3}] \quad (7.94)$$

Then the third one,

$$\begin{aligned} ([3] \otimes [3]) \otimes [3] &= ([6] \oplus [\bar{3}]) \otimes [3] = [6] \otimes [3] + [\bar{3}] \otimes [3] \\ &= [10] \oplus [8]_{MS} \oplus [8]_{MA} \oplus [1] \end{aligned} \quad (7.95)$$

where 'MS' and 'MA' mean mixed symmetric and mixed anti-symmetric SU(3) multiplets. As an example, we construct 'uud' whose combinations are denoted as Δ , p_{MS} , and p_{MA} . Combining the non-strange member of the $[\bar{3}]$ with the u quark of the $[3]$, we have

$$p_{MA} = \frac{1}{\sqrt{2}}(ud - du)u \quad (7.96)$$

Note that $(ud - du)$ behaves like a \bar{s} in $SU(3)_f$. The decuplet states are totally symmetric under interchange of quarks, as evidenced by the uuu, ddd, and sss members. The symmetric combination of 'uud' is

$$\Delta = \frac{1}{\sqrt{3}}[udu + duu + uud] \quad (7.97)$$

Requiring orthogonality of the remaining 'uud' state to both p_{MA} and Δ gives

$$p_{MS} = \frac{1}{\sqrt{6}}[(ud + du)u - 2uud] \quad (7.98)$$

The states p_{MS} and p_{MA} have mixed symmetry, they are analogous to $|\frac{1}{2}, \pm\frac{1}{2}\rangle_{MA}$ in Eq. (7.33) and $|\frac{1}{2}, \pm\frac{1}{2}\rangle_{MS}$ Eq. (7.34). The quark structure of other states can be readily obtained in a similar way by using U or V spin. The singlet is (Problem: prove this)

$$\begin{aligned} (qqq)_{[1]} &= \frac{1}{\sqrt{6}}[u(ds - sd) + s(ud - du) + d(su - us)] \\ &\sim \frac{1}{\sqrt{6}}[u\bar{u} + s\bar{s} + d\bar{d}] \end{aligned} \quad (7.99)$$

The reduction of direct product of three spin-1/2 states is given in Eq. (7.30). The spin states are displayed in Eq. (7.32)-(7.34). The two doublets have mixed symmetry that the spin states are symmetric or anti-symmetric with interchange of two quarks. We can label states by (SU(3),SU(2)),

$$\begin{aligned} S &: ([10], [4]) + ([8], [2]) \\ MS &: ([10], [2]) + ([8], [4]) + ([8], [2]) + ([1], [2]) \\ MA &: ([10], [2]) + ([8], [4]) + ([8], [2]) + ([1], [2]) \\ A &: ([1], [4]) + ([8], [2]) \end{aligned} \quad (7.100)$$

The ground state baryons fit into the $J^P = (3/2)^+$ decuplet and the $J^P = (1/2)^+$ octet. See Fig. 7.13. Their spatial wave functions are symmetric, belonging to the S wave ($L = 0$) in orbital angular momentum. Their spin and flavor or SU(6) wavefunctions are totally symmetric. The total wave functions for ground state baryons must be anti-symmetric. Then a new degree of freedom for quarks, whose wave function is anti-symmetric, is needed for ground state baryons (and for all baryons). This new degree of freedom is called the color. We will discuss it in Section 7.2. The decuplet and octet ground state baryons belong to $([10], [4])$ and $([8], [2])$ respectively. For example, the wave function of spin-up proton is

$$\begin{aligned} \left| p, J_z = \frac{1}{2} \right\rangle &= \frac{1}{\sqrt{2}} \left[p_{MS} \left| \frac{1}{2}, \frac{1}{2} \right\rangle_{MS} + p_{MA} \left| \frac{1}{2}, \frac{1}{2} \right\rangle_{MA} \right] \\ &= \frac{1}{\sqrt{18}} \left\{ \frac{1}{2}(udu + duu - 2uud)(\uparrow\downarrow\uparrow + \downarrow\uparrow\uparrow - 2\uparrow\uparrow\downarrow) \right. \\ &\quad \left. + \frac{3}{2}(udu - duu)(\uparrow\downarrow\uparrow - \downarrow\uparrow\uparrow) \right\} \\ &= \frac{1}{\sqrt{18}} \{ udu(2\uparrow\downarrow\uparrow - \uparrow\uparrow\downarrow - \downarrow\uparrow\uparrow) + duu(2\downarrow\uparrow\uparrow - \uparrow\uparrow\downarrow - \uparrow\downarrow\uparrow) \\ &\quad + uud(2\uparrow\uparrow\downarrow - \uparrow\downarrow\uparrow - \downarrow\uparrow\uparrow) \} \end{aligned} \quad (7.101)$$

where spin wave functions $|\frac{1}{2}, \frac{1}{2}\rangle_{MA,MS}$ are given by Eq.(7.33,7.34).

A simple way to get the spin-flavor wave functions is to start from the simplest known wave functions of certain baryons and to use the spin ladder operators. For example, starting from

$$\begin{aligned} \left| \Delta^+, J_z = \frac{3}{2} \right\rangle &= \frac{1}{\sqrt{3}} \mathcal{P}(|u\uparrow, u\uparrow, d\uparrow\rangle) \\ &= \frac{1}{\sqrt{3}} (|u\uparrow, u\uparrow, d\uparrow\rangle + |u\uparrow, d\uparrow, u\uparrow\rangle + |d\uparrow, u\uparrow, u\uparrow\rangle) \end{aligned} \quad (7.102)$$

where $\mathcal{P}(|u \uparrow, u \uparrow, d \uparrow\rangle)$ is to sum over all different permutations, we can derive $|\Delta^+, J_z = \frac{1}{2}\rangle$ by using the spin ladder operator $S_- = s_{1-} + s_{2-} + s_{3-}$,

$$\begin{aligned}
|\Delta^+, J_z = \frac{1}{2}\rangle &= S_- \left| \Delta^+, J_z = \frac{3}{2}\right\rangle \\
&= \frac{1}{\sqrt{3}}(s_{1-} + s_{2-} + s_{3-})(|u \uparrow, u \uparrow, d \uparrow\rangle + |u \uparrow, d \uparrow, u \uparrow\rangle + |d \uparrow, u \uparrow, u \uparrow\rangle) \\
&= \frac{1}{2\sqrt{3}} \{ |u \downarrow, u \uparrow, d \uparrow\rangle + |u \downarrow, d \uparrow, u \uparrow\rangle + |d \downarrow, u \uparrow, u \uparrow\rangle \\
&\quad + |u \uparrow, u \downarrow, d \uparrow\rangle + |u \uparrow, d \downarrow, u \uparrow\rangle + |d \uparrow, u \downarrow, u \uparrow\rangle \\
&\quad + |u \uparrow, u \uparrow, d \downarrow\rangle + |u \uparrow, d \uparrow, u \downarrow\rangle + |d \uparrow, u \uparrow, u \downarrow\rangle \} \\
&\rightarrow \frac{1}{3} [\mathcal{P}(|u \downarrow, u \uparrow, d \uparrow\rangle) + \mathcal{P}(|u \uparrow, u \downarrow, d \uparrow\rangle) + \mathcal{P}(|u \uparrow, u \uparrow, d \downarrow\rangle)] \quad (7.103)
\end{aligned}$$

One can verify that the spin-up proton is the orthogonal state to $|\Delta^+, J_z = \frac{1}{2}\rangle$ with the same values of I_3 and S_z .

Exercise 55. Write down the spin-flavor wave functions for the ground state decuplet $(3/2)^+$ and octet $(1/2)^+$ baryons, and show that they are totally symmetric under the interchange of two quark labels. The decuplet $(3/2)^+$ and octet $(1/2)^+$ baryons are shown in the left and right panel of Fig. 7.13 respectively.

Exercise 56. Starting from $|\Sigma^{*+}, J_z = \frac{3}{2}\rangle = |u \uparrow, u \uparrow, s \uparrow\rangle$, find the spin-isospin function of $|\Sigma^0, J_z = \frac{1}{2}\rangle$ and $|\Lambda, J = \frac{1}{2}\rangle$.

Exercise 57. For a non-relativistic particle with the charge Q and the mass m , its magnetic moment is given by,

$$\boldsymbol{\mu} = \frac{Q}{2m} g \mathbf{s} \quad (7.104)$$

where $g = 2$ is the g -factor for elementary particles. We know that the magnetic moment of a proton (neutron) is $\mu_p = 2.79\mu_N$ ($\mu_n = -1.91\mu_N$) with $\mu_N = \frac{e}{2m_p}$ the nuclear magneton, which corresponds to $g_p = 5.6$ ($g_n = -3.82$). Since the neutron is a neutral particle, its magnetic moment indicates that it is made of electrically charged particles: quarks. Show the following relation with the wave functions of proton and neutron,

$$\frac{\langle p, \frac{1}{2} | \mu_p^z | p, \frac{1}{2} \rangle}{\langle n, \frac{1}{2} | \mu_n^z | n, \frac{1}{2} \rangle} = -\frac{3}{2} \quad (7.105)$$

where

$$\mu_{p,n}^z = \frac{g_q}{2m_q} \sum_{i=1}^3 Q_i s_{iz}$$

where $g_q = 2$, m_q and Q_i are the g -factor, mass and charges for quarks.

Figure 7.11: The qq multiplet of $SU(3)$. $3 \otimes 3 = 6 \oplus \bar{3}$.

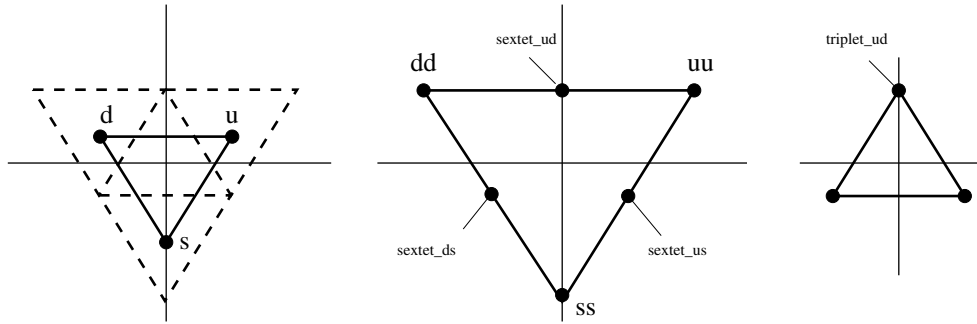


Figure 7.12: The qqq multiplet of $SU(3)$. $3 \otimes 3 \otimes 3 = 10 \oplus 8 \oplus 8 \oplus 1$.

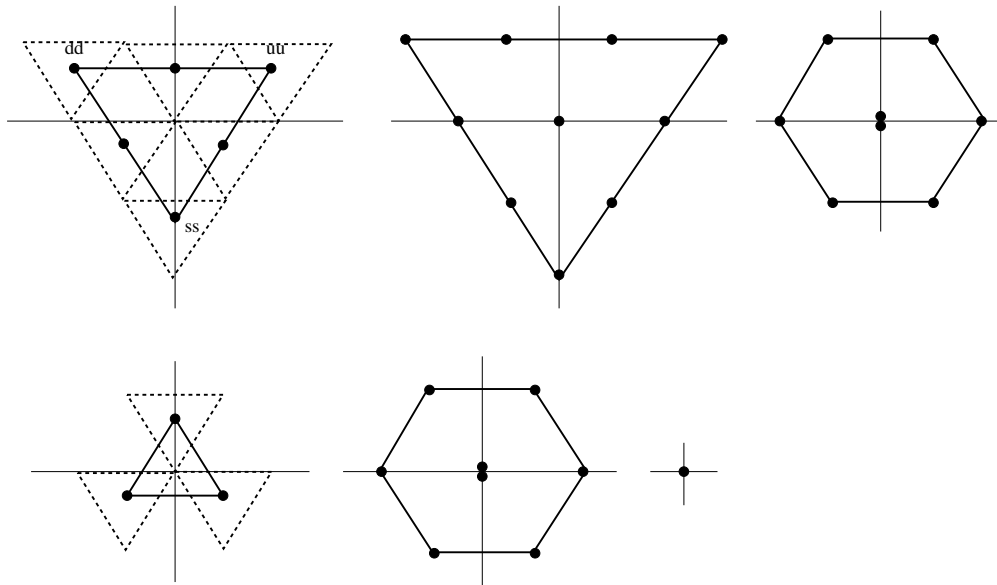
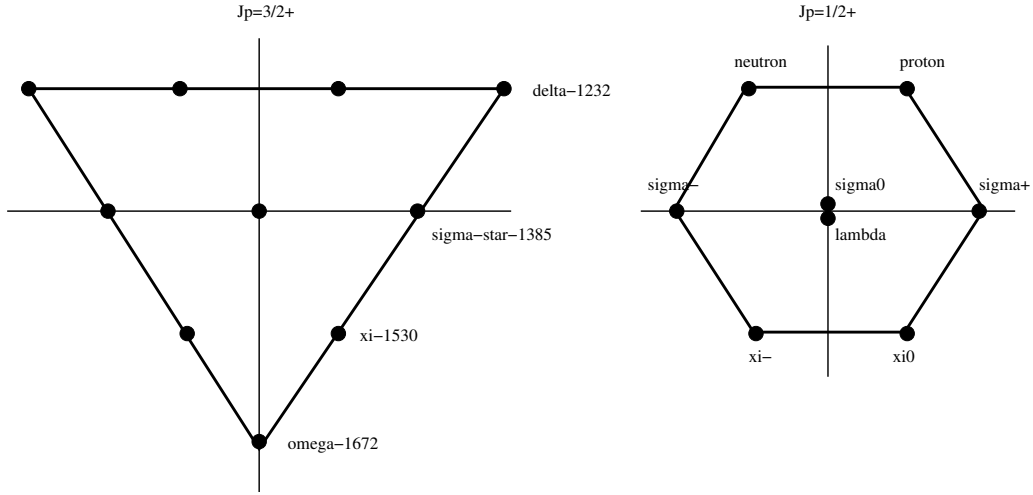


Figure 7.13: Ground state baryons, the decuplet [$J^P = (3/2)^+$] and octet [$J^P = (1/2)^+$].

7.1.10 Gell-Mann-Okubo relations

Similarly as in Eq. (7.88), the flavor contents of the baryon and anti-baryon octets can also be written as

$$\begin{aligned}
 B &= \begin{pmatrix} \frac{\Sigma^0}{\sqrt{2}} + \frac{\Lambda}{\sqrt{6}} & \Sigma^+ & p \\ \Sigma^- & -\frac{\Sigma^0}{\sqrt{2}} + \frac{\Lambda}{\sqrt{6}} & n \\ \Xi^- & \Xi^0 & -\frac{2}{\sqrt{6}}\Lambda \end{pmatrix} \\
 \bar{B} &= \begin{pmatrix} \frac{\bar{\Sigma}^0}{\sqrt{2}} + \frac{\bar{\Lambda}}{\sqrt{6}} & \bar{\Sigma}^- & \bar{\Xi}^- \\ \bar{\Sigma}^+ & -\frac{\bar{\Sigma}^0}{\sqrt{2}} + \frac{\bar{\Lambda}}{\sqrt{6}} & \bar{\Xi}^0 \\ \bar{p} & \bar{n} & -\frac{2}{\sqrt{6}}\bar{\Lambda} \end{pmatrix}
 \end{aligned} \tag{7.106}$$

It can be proved that B_j^i can also be written in the form,

$$B_j^i \sim q^i q^a q^b \epsilon_{abj} - \frac{1}{3} \delta_j^i q^k q^a q^b \epsilon_{abk}$$

The baryons and anti-baryons transform in $SU(3)$ as

$$\begin{aligned}
 B &\rightarrow UBU^+ \\
 \bar{B} &\rightarrow U\bar{B}U^+
 \end{aligned} \tag{7.107}$$

We can write the strong Hamiltonian as

$$H = H_{sys} + H_{asym} \tag{7.108}$$

where H_{sys} is invariant under $SU(3)$ transformation. The $SU(3)$ violated term is denoted by H_{asym} . To make the baryon number conserve in H_{asym} , H_{asym} has to be in the bilinear form (as it gives the masses of baryons) and traceless in flavor indices,

$$S_i^j \sim q_i \gamma_0 q^j - \frac{1}{3} \delta_i^j q_i \gamma_0 q^j \sim \psi_i^\dagger \gamma_0 \psi_j - \frac{1}{3} \delta_i^j \psi_k^\dagger \gamma_0 \psi_k \tag{7.109}$$

where $q^i \sim \psi_i$ and $q_i \sim \psi_i^\dagger$ with ψ_i and ψ_i^\dagger spinors and i the flavor index. Assume that $H_{asym} \ll H_{sys}$, so H_{asym} can be regarded as perturbation. Suppose $|h\rangle$ is the eigenstate of H_{sys} ,

$$H_{sys} |h\rangle = \gamma |h\rangle \quad (7.110)$$

So the energy expectation value becomes

$$E_h \approx \gamma + \langle h | H_{asym} | h \rangle \quad (7.111)$$

Let's determine the form of $\langle h | H_{asym} | h \rangle$. Note that $|h\rangle$ are eigenstates of H_{sys} and belong to the representation of SU(3). The matrix $\langle h | H_{asym} | h \rangle$ can be regarded as the transition amplitude of the process

$$h \rightarrow h + S_j^i \quad (7.112)$$

where S_j^i is the pseudoparticle which belongs to SU(3) octet. Let's discuss a special case $S_j^i = S_3^3 \delta_{i3} \delta_{j3}$. Denote $|h\rangle = B_j^i$, the gedanken process is

$$B_j^i \rightarrow B_b^a + S_3^3 \quad (7.113)$$

The perturbation H_{asym} can be regarded as formed by three octets, B_j^i , \bar{B}_b^a and S_j^i ,

$$\begin{aligned} H_{asym} &\sim (\alpha \bar{B}_a^i B_j^a + \beta \bar{B}_j^a B_a^i) S_i^j \sim \alpha \bar{B}_a^3 B_3^a + \beta \bar{B}_3^a B_a^3 \\ &= \alpha(\bar{p}p + \bar{n}n + \frac{2}{3}\bar{\Lambda}\Lambda) + \beta(\bar{\Xi}^- \Xi^- + \bar{\Xi}^0 \Xi^0 + \frac{2}{3}\bar{\Lambda}\Lambda) \\ &= \alpha(\bar{p}p + \bar{n}n) + \beta(\bar{\Xi}^- \Xi^- + \bar{\Xi}^0 \Xi^0) + \frac{2}{3}(\alpha + \beta)\bar{\Lambda}\Lambda \end{aligned} \quad (7.114)$$

The total energy is then

$$E_h \approx \gamma + \alpha(\bar{p}p + \bar{n}n) + \beta(\bar{\Xi}^- \Xi^- + \bar{\Xi}^0 \Xi^0) + \frac{2}{3}(\alpha + \beta)\bar{\Lambda}\Lambda \quad (7.115)$$

We can derive

$$\begin{aligned} E_\Sigma &= \gamma \\ E_\Lambda - E_\Sigma &= \frac{2}{3}(\alpha + \beta) \\ E_N - E_\Sigma &= \alpha \\ E_\Xi - E_\Sigma &= \beta \end{aligned} \quad (7.116)$$

So we derive

$$3(E_\Lambda - E_\Sigma) = 2(E_N - E_\Sigma) + 2(E_\Xi - E_\Sigma) \quad (7.117)$$

which becomes

$$3E_\Lambda + E_\Sigma - 2E_N - 2E_\Xi = 0 \quad (7.118)$$

The above relation can be transformed into that of mesons by replacing $\Lambda \rightarrow \eta$, $N \rightarrow K$, $\Xi \rightarrow K$,

$$3E_\eta + E_\pi - 4E_K = 0 \quad (7.119)$$

The above relations can be casted into ultra-relativistic case, where

$$E_i = \sqrt{p^2 + m_i^2} \sim p + \frac{m_i^2}{2p} \quad (7.120)$$

Table 7.8: Masses of octet baryons and mesons. Unit=MeV.

N	939	π	140
Λ	1116	K, \bar{K}	495
Σ	1192	η	549
Ξ	1315		

The above equations become

$$\begin{aligned} 3m_\Lambda^2 + m_\Sigma^2 - 2m_N^2 - 2m_\Xi^2 &= 0 \\ 3m_\eta^2 + m_\pi^2 - 4m_K^2 &= 0 \end{aligned} \quad (7.121)$$

Here we have assumed that $|h\rangle$ is a state with momentum $p \gg m_i$. For non-relativistic case we have

$$\begin{aligned} 3m_\Lambda + m_\Sigma - 2m_N - 2m_\Xi &= 0 \\ 3m_\eta + m_\pi - 4m_K &= 0 \end{aligned} \quad (7.122)$$

We can check the above relations (7.121) and (7.122) by inserting baryon and meson masses given in Table (7.8).

The baryon decuplet can be expressed by,

$$B^{ijk} = \frac{1}{n} \sum_P q^{P(i)} q^{P(j)} q^{P(k)} \quad (7.123)$$

where the sum is over all different permutations and n is its number. The normalized state is given by

$$\frac{1}{\sqrt{n}} \sum_P q^{P(i)} q^{P(j)} q^{P(k)} \quad (7.124)$$

Then we have, e.g.

$$\begin{aligned} B^{333} &= \Omega \\ B^{133} &= \frac{1}{\sqrt{3}} \Xi^{*0} \\ B^{113} &= \frac{1}{\sqrt{3}} \Sigma^{*+} \\ B^{123} &= \frac{1}{\sqrt{6}} \Sigma^{*0} \end{aligned} \quad (7.125)$$

For the baryon decuplet, the mass formula can be derived in a similar way. The virtual process can be written by

$$B^{lmn} \rightarrow B^{abc} + S_j^i \quad (7.126)$$

where we also take $S_j^i = S_3^3 \delta_{i3} \delta_{j3}$. The SU(3) violated Hamiltonian is then in the form,

$$H_{asym} \sim \left(\bar{B}_{iab} B^{jab} - \frac{1}{3} \delta_i^j \bar{B}_{dab} B^{dab} \right) S_j^i \sim \beta \left(\bar{B}_{3ab} B^{3ab} - \frac{1}{3} \bar{B}_{dab} B^{dab} \right) \quad (7.127)$$

The total energy is

$$\begin{aligned}
E_h &\sim \alpha + \beta \left(\bar{B}_{3ab} B^{3ab} - \frac{1}{3} \bar{B}_{dab} B^{dab} \right) \\
&= \alpha + \beta \left[\frac{2}{3} \bar{\Omega} \Omega + \frac{1}{3} (\bar{\Xi}^{*0} \Xi^{*0} + \bar{\Xi}^{*-} \Xi^{*-}) \right. \\
&\quad \left. - \frac{1}{3} (\bar{\Delta}^{++} \Delta^{++} + \bar{\Delta}^+ \Delta^+ + \bar{\Delta}^0 \Delta^0 + \bar{\Delta}^- \Delta^-) \right]
\end{aligned} \tag{7.128}$$

This gives the result that the masses of isospin multiplets Δ , Σ^* , Ξ^* and Ω are equal-distant,

$$m_{\Sigma^*} - m_{\Delta} = m_{\Xi^*} - m_{\Sigma^*} = m_{\Omega} - m_{\Xi^*} = \frac{\beta}{3} \tag{7.129}$$

One can check the above formula by inserting the mass values of the decuplet baryons. Eq. (7.121), (7.122) and (7.129) can be summarized into the so-called Gell-Mann-Okubo relations [17, 18],

$$m = a + bY + c \left[I(I+1) - \frac{1}{4}Y^2 \right] \tag{7.130}$$

Exercise 58. Use the Gell-Mann-Okubo mass formula to obtain the masses of ground state baryons, $(1/2)^+$ and $(3/2)^+$.

Exercise 59. We can define a matrix in terms of meson octet in Eq. (7.88) $U = e^{i\xi_a \lambda_a / f}$, where λ_a are Gell-Mann matrices in Eq. (7.46), ξ_a are meson fields given in Eq. (7.89), and f is a constant. Then the Lagrangian due to the quark masses is given by

$$L_m \sim \frac{f^2}{4} \{ \text{Tr}[M(U + U^\dagger)] \} \tag{7.131}$$

where $M = \text{diag}(m_u, m_d, m_s)$ is the quark mass matrix. Derive the masses for the mesons by extracting the coefficients of quadratic terms of mesonic fields.

7.2 Quarks and gluons

7.2.1 Color degrees of freedom

There are many evidences for the existence of color degree of freedom. We only take some of them as examples.

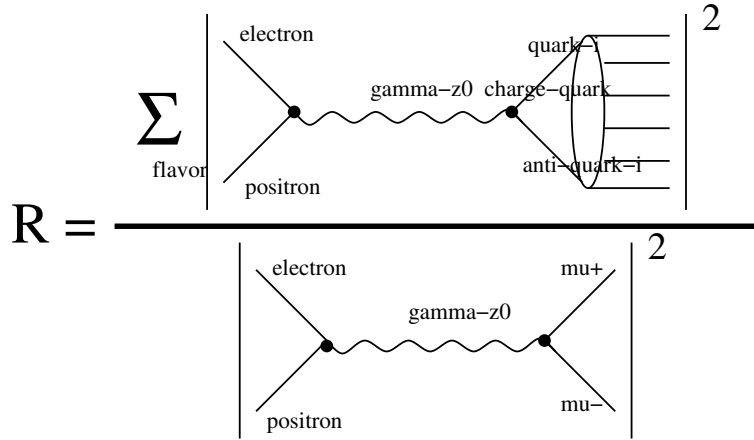
The first one is from the baryons $\Omega(sss)$, $\Delta^{++}(uuu)$ and $\Delta^-(ddd)$ with the same flavor content. We know that they belong to the ground state with orbital angular momentum $L = 0$, whose wave function is symmetric. The flavor wave function is also symmetric. This seems to violate the Pauling principle for a fermionic system. So quarks must carry another degree of freedom - color. There are three colors, R , G and B which makes a color triplet. The color wave function for three quarks should be a color singlet which is anti-symmetric,

$$(qqq)_{[1]} = [(RB - BR)G + (BG - GB)R + (GR - RG)B]/\sqrt{6} \tag{7.132}$$

By the way, the color wave function for mesons is

$$(q\bar{q})_{[1]} = (R\bar{R} + G\bar{G} + B\bar{B})/\sqrt{3} \tag{7.133}$$

Figure 7.14: The definition of the R factor.



The second evidence is the R factor defined by

$$R = \frac{\sigma(e^+e^- \rightarrow q\bar{q} \rightarrow \text{hadrons})}{\sigma(e^+e^- \rightarrow \mu^+\mu^-)} \quad (7.134)$$

Both reactions are electromagnetic interactions. Both quarks and electrons are pointlike particles. The only differences are that muons carry unit charges, while quarks carry fractional charges, flavors and colors. The number of colors can be determined by measuring R . The factor can be written as

$$R = N_c \sum_f Q_f^2 \quad (7.135)$$

where Q_f is the quark electric charge for flavor f and N_c the number of colors. In the energy range where only light quarks (u, d, s) are produced, $R = \frac{2}{3}N_c$. When the charm quark threshold is reached, the factor becomes $R = \frac{10}{9}N_c$. When the bottom quark is produced, we have $R = \frac{11}{9}N_c$. All these values can be compared to data which show a clear evidence for $N_c = 3$.

The third evidence is the decay rate of $\pi^0 \rightarrow \gamma + \gamma$, see Fig. 7.16. for illustration. The rate is given by

$$\Gamma(\pi^0 \rightarrow 2\gamma) = N_c^2 (Q_u^2 - Q_d^2)^2 \frac{\alpha^2 m_\pi^2}{64\pi^3 f_\pi^2} \quad (7.136)$$

where $\alpha = e^2/4\pi = 1/137$, N_c is the number of colors, m_π is the mass of neutral pion, $Q_{u,d}$ are charges of u and d quarks, f_π is the pion decay constant for $\pi \rightarrow \mu\nu$. We can estimate the rate by substituting $N_c = 3$, $Q_u = 2/3$, $Q_d = 1/3$, $m_\pi = 140$ MeV and $f_\pi = 91$ MeV,

$$\Gamma(\pi^0 \rightarrow 2\gamma) \approx 9 \times \frac{1}{9} \frac{1}{137^2} \frac{1}{64\pi^3} \left(\frac{140}{91}\right)^2 \text{ MeV} \approx 7.6 \text{ eV} \quad (7.137)$$

which agree with the data very well,

$$\Gamma^{\text{exp}}(\pi^0 \rightarrow 2\gamma) = 7.48 \pm 0.33 \text{ eV} \quad (7.138)$$

If quarks carry no color, the measured decay rate in experiments is about 9 times larger than the theoretical prediction.

Color degrees of freedom respect $SU(3)_c$ symmetry. Unlike flavor $SU(3)_f$ which is an approximated symmetry, this is an exact symmetry and has dynamic effects.

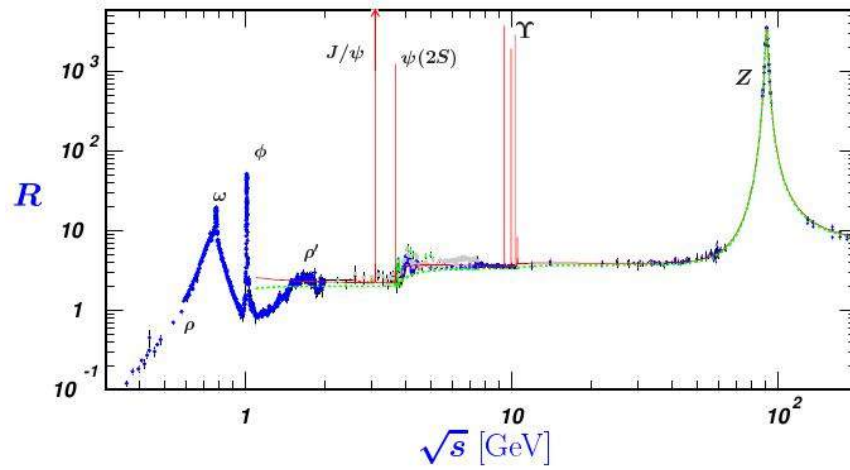
Figure 7.15: The data for R [19].

Figure 7.16: Pions decay to two photons via axial vector current.

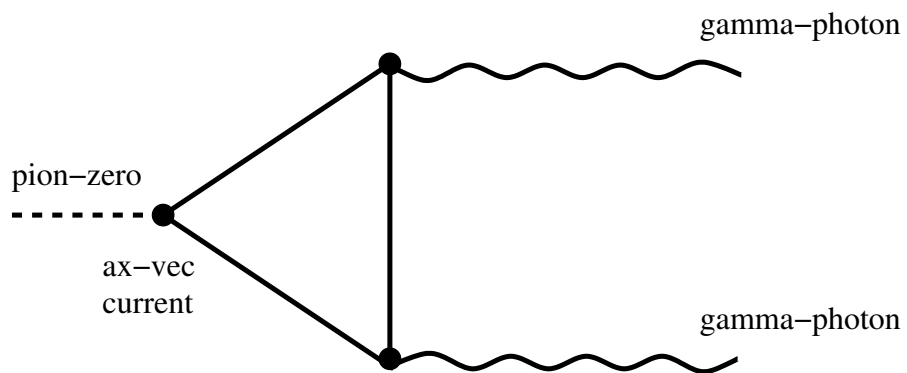


Table 7.9: Part of color factors c for one gluon exchange. $T_i = \lambda_i/2$ with λ_i the Gell-Mann matrices in Eq. (7.46).

initial	final	gluon	color factor c
BB	BB	A_8	$(T_8)_{33}(T_8)_{33} = \frac{1}{3}$
RR	RR	A_3, A_8	$(T_3)_{11}(T_3)_{11} + (T_8)_{11}(T_8)_{11} = \frac{1}{3}$
RB	RB	A_8	$(T_8)_{11}(T_8)_{33} = -\frac{1}{6}$
RB	BR	A_4, A_5	$(T_4)_{31}(T_4)_{13} + (T_5)_{31}(T_5)_{13} = \frac{1}{2}$
$B\bar{B}$	$B\bar{B}$	A_8	$-(T_8)_{33}(T_8)_{33} = -\frac{1}{3}$
$B\bar{B}$	$R\bar{R}$	A_4, A_5	$-(T_4)_{31}(T_4)_{13} - (T_5)_{31}(T_5)_{13} = -\frac{1}{2}$
BB	$G\bar{G}$	A_6, A_7	$-(T_6)_{23}(T_6)_{32} - (T_7)_{23}(T_7)_{32} = -\frac{1}{2}$

7.2.2 Gluons as color carriers

The color interaction between quarks are carried by gluons. Gluons carry colors and anti-colors and belong to a color octet. According to group theory, $[3] \otimes [3] = [1] \oplus [8]$, the direct product of two triplets can be reduced to a singlet and a octet. The gluon octet can be represented by g_i ($i = 1, \dots, 8$),

$$\begin{aligned}
\begin{pmatrix} R \\ G \\ B \end{pmatrix} (\bar{R}, \bar{G}, \bar{B}) &= \begin{pmatrix} \frac{1}{3}(2R\bar{R} - G\bar{G} - B\bar{B}) & R\bar{G} & R\bar{B} \\ GR & \frac{1}{3}(2G\bar{G} - R\bar{R} - B\bar{B}) & G\bar{B} \\ B\bar{R} & B\bar{G} & \frac{1}{3}(2B\bar{B} - R\bar{R} - G\bar{G}) \end{pmatrix} \\
&+ \frac{1}{3}(R\bar{R} + G\bar{G} + B\bar{B}) \begin{pmatrix} 1 & 0 & 0 \\ 0 & 1 & 0 \\ 0 & 0 & 1 \end{pmatrix} \\
&= \begin{pmatrix} \frac{A_3 + A_8}{\sqrt{2}} & \frac{A_1 - iA_2}{\sqrt{2}} & \frac{A_4 - iA_5}{\sqrt{2}} \\ \frac{A_1 + iA_2}{\sqrt{2}} & -\frac{A_3 + A_8}{\sqrt{2}} & \frac{A_6 - iA_7}{\sqrt{2}} \\ \frac{A_4 + iA_5}{\sqrt{2}} & \frac{A_6 + iA_7}{\sqrt{2}} & -\frac{2A_8}{\sqrt{6}} \end{pmatrix} + \frac{1}{\sqrt{3}}A_0 \begin{pmatrix} 1 & 0 & 0 \\ 0 & 1 & 0 \\ 0 & 0 & 1 \end{pmatrix} \\
&= \frac{1}{\sqrt{2}}T^a A^a + \frac{1}{\sqrt{3}}A_0 \mathbf{1} \tag{7.139}
\end{aligned}$$

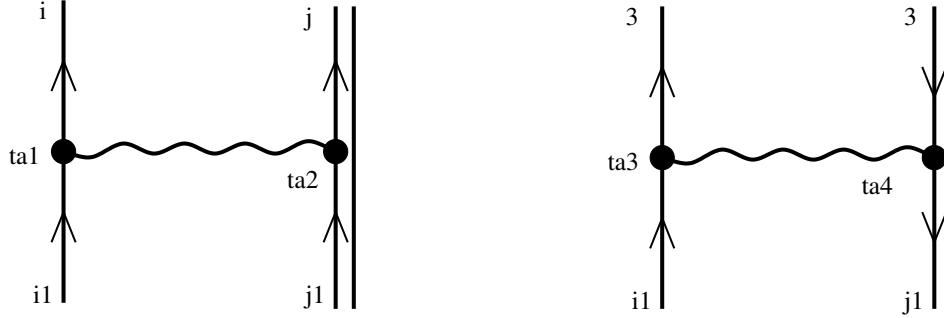
where A_0 is the color singlet and A_1, \dots, A_8 are color singlet and defined by,

$$\begin{aligned}
A_0 &= (R\bar{R} + G\bar{G} + B\bar{B})/\sqrt{3}, \\
A_1 &= (R\bar{G} + G\bar{R})/\sqrt{2}, \\
A_2 &= i(R\bar{G} - G\bar{R})/\sqrt{2}, \\
A_3 &= (R\bar{R} - G\bar{G})/\sqrt{2}, \\
A_4 &= (R\bar{B} + B\bar{R})/\sqrt{2}, \\
A_5 &= i(R\bar{B} - B\bar{R})/\sqrt{2}, \\
A_6 &= (G\bar{B} + B\bar{G})/\sqrt{2}, \\
A_7 &= i(G\bar{B} - B\bar{G})/\sqrt{2}, \\
A_8 &= (R\bar{R} + G\bar{G} - 2B\bar{B})/\sqrt{6} \tag{7.140}
\end{aligned}$$

The singlet gluon couples equally to all quarks, and is independent of the octet.

The strength of the interaction coupling for the exchange of a single gluon between two colored quarks is $c\alpha_s$, where c is the color factor that can be deduced from Eq. (7.139). Part of color factors for one gluon exchange are listed in Tab. 7.9.

Figure 7.17: One gluon exchange in baryons and mesons. The wavy lines denote gluons. Solid lines are quarks.



The color factor for two quarks inside a baryon can be determined as follows. The color wave function for a baryon is

$$(qqq)_{[1]} = \frac{1}{\sqrt{6}}[R(GB - BG) + B(RG - GR) + G(BR - RB)] \quad (7.141)$$

For the RG term, i.e. the second term in the color wave function (7.141), the color amplitude is

$$\begin{aligned} & \frac{1}{\sqrt{6}}(\delta_{i1}\delta_{j2} - \delta_{i2}\delta_{j1})(T_a)_{i'i}(T_a)_{j'j} \frac{1}{\sqrt{6}}(\delta_{i'1}\delta_{j'2} - \delta_{i'2}\delta_{j'1}) \\ &= \frac{1}{\sqrt{6}}(\delta_{i1}\delta_{j2} - \delta_{i2}\delta_{j1}) \left[\frac{1}{6}(\delta_{ii'}\delta_{jj'} + \delta_{ij'}\delta_{ji'}) - \frac{1}{3}(\delta_{ii'}\delta_{jj'} - \delta_{ij'}\delta_{ji'}) \right] \frac{1}{\sqrt{6}}(\delta_{i'1}\delta_{j'2} - \delta_{i'2}\delta_{j'1}) \\ &= -\frac{1}{18}(\delta_{i1}\delta_{j2} - \delta_{i2}\delta_{j1})(\delta_{ii'}\delta_{jj'} - \delta_{ij'}\delta_{ji'}) (\delta_{i'1}\delta_{j'2} - \delta_{i'2}\delta_{j'1}) \\ &= -\frac{2}{9} \end{aligned} \quad (7.142)$$

where i, j denote the initial state color indices and i', j' denote the final state color indices. We have used the formula,

$$\begin{aligned} (T_a)_{i'i}(T_a)_{j'j} &= \frac{1}{2}\delta_{ij'}\delta_{ji'} - \frac{1}{6}\delta_{ii'}\delta_{jj'} \\ &= \frac{1}{6}(\delta_{ii'}\delta_{jj'} + \delta_{ij'}\delta_{ji'}) - \frac{1}{3}(\delta_{ii'}\delta_{jj'} - \delta_{ij'}\delta_{ji'}) \end{aligned} \quad (7.143)$$

or

$$T_a(1)T_a(2) = \frac{1}{2} \left(P_{12} - \frac{1}{N} \right) \quad (7.144)$$

for $SU(N)$ group, where P_{12} is the permutation operator for indices 1 and 2. For other terms in (7.141), the result is the same. So the color factor for any two quarks inside a baryon is $c_{baryon} = 3 \times (-2/9) = -2/3$.

The color singlet wave function for a meson is,

$$(q\bar{q})_{[1]} = \frac{1}{\sqrt{3}}(R\bar{R} + G\bar{G} + B\bar{B}) \quad (7.145)$$

In the same way, we can determine the color factor for quark and anti-quark inside a meson $c = -4/3$,

Figure 7.18: The first evidence for three-jet events in e^+e^- collisions at Petra [20, 21]. European Physical Society high energy and particle physics prize (1995) by P. Söding, B. Wiik, G. Wolf, S.L. Wu.

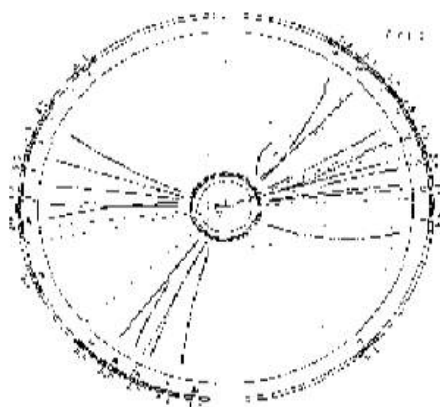


FIG. 18. A flat hadronic event in the JADE detector. The solid lines indicate the trajectories of the charged tracks. The dotted lines from the intersection point are the detected neutral particle directions.

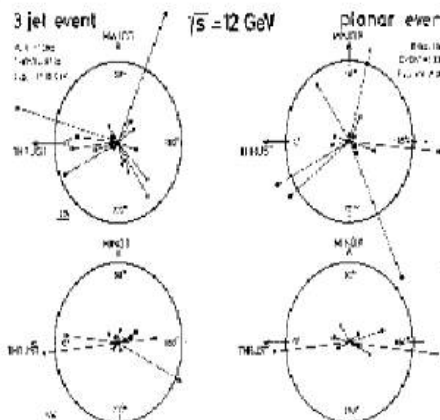


FIG. 19. Energy flow diagrams. Two events measured at $\sqrt{s} = 12 \text{ GeV}$ with the lines showing the directions and magnitudes of energy deposited in the calorimeters divided in two pseudorapidity regions. The events appear to have a similar structure to the three-jet event. The jets within the pseudorapidity bands show the same structure.

For the initial state $B\bar{B}$, the color amplitude is

$$\begin{aligned} & \frac{1}{\sqrt{3}}(T_a)_{i'3}(-T_a)_{3j'}\frac{1}{\sqrt{3}}\delta_{j'i'} \\ &= -\frac{1}{3}(T_a)_{3i'}(T_a)_{i'3} = -\frac{4}{9} \end{aligned} \quad (7.146)$$

where the minus sign in $(-T_a)_{3j'}$ comes from the anti-quark. For other terms in 7.145 the result is the same, so we have the factor 3 for the total result $c_{meson} = 3 \times (-4/9) = -4/3$.

Thus the Coulomb potentials between two quarks inside a baryon and a meson are

$$\begin{aligned} V_C(r) &= -\frac{2}{3}\frac{\alpha_S}{r}, \text{ inside baryon} \\ &= -\frac{4}{3}\frac{\alpha_S}{r}, \text{ inside meson} \end{aligned} \quad (7.147)$$

Note that the negative sign indicates that the force is attractive. In order to take into account the confinement, one should include the confinement potential which prevent two quarks from separating to large distance,

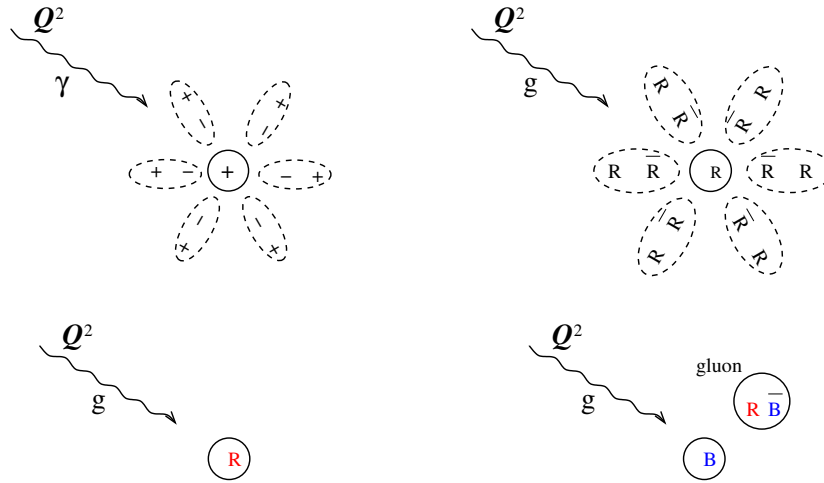
$$V(r) = C\frac{\alpha_S}{r} + Ar \quad (7.148)$$

where $A \approx 0.18 \text{ GeV}^2 \approx 0.9 \text{ GeV/fm}$ is the string tension.

Exercise 60. There are three constituent quarks inside a baryon. There are one quark and one anti-quark in a meson. Each quark carries a color R , G or B . Each anti-quark carries an anti-color \bar{R} , \bar{G} or \bar{B} . Write down the color wave functions for a baryon and a meson. What is the connection between baryon and meson color wave functions? Why?

Exercise 61. Describe why the color degrees of freedom is necessary for the baryon Ω^- .

Figure 7.19: Illustration of how vacuum polarization in QED and QCD shield a test charge. In QCD there is another process which is absent in QED, i.e. a red charge can turn to be B or G by radiating a gluon with $R\bar{B}$ or $R\bar{G}$.



7.2.3 Asymptotic Freedom

The electric charge can be probed by photons. The higher the energy of the photon, the smaller size it can probe. The wave length of the photon can be defined by the inverse of an energy scale $\lambda \sim 1/\sqrt{Q^2}$. It can be proved that as the energy of the photon increases, the effective coupling in quantum electrodynamics changes as

$$\alpha_{QED}(Q^2) \equiv \alpha_{eff}(Q^2) = \frac{\alpha}{1 - \frac{\alpha}{3\pi} \ln \frac{Q^2}{m_e^2}} \quad (7.149)$$

We see that $\alpha_{eff}(Q^2)$ increases as Q^2 increases. The physical reason for the rising effective charge with the increased Q^2 of the probing photon is illustrated in Fig. 7.19. If Q^2 is small then the photon cannot resolve small distances and sees a point charge shielded by the vacuum polarization of the infinite sea of electron-positron pairs. As Q^2 increases, the photon sees a smaller and smaller spatial area and the shielding effect of the pair fluctuation becomes less and less.

In quantum chromodynamics (QCD), things get complicated. We know that photons as a carrier of electromagnetic force are charge neutral. But this is not the case in QCD. The strong coupling constant is defined by $\alpha_s = g_s^2/(4\pi)$ with g_s the coupling of quark-gluon and gluon-gluon vertices, whose running behavior is governed by

$$\mu \frac{\partial \alpha_s}{\partial \mu} = 2\beta(\alpha_s) \quad (7.150)$$

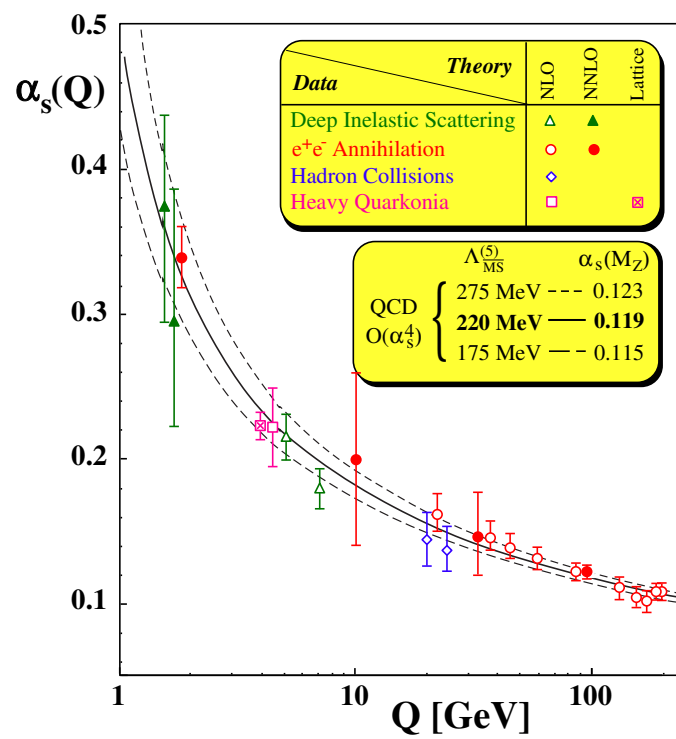
where the beta-function is given by

$$\beta(\alpha_s) = - \left(11 - \frac{2}{3}n_f \right) \frac{\alpha_s^2}{4\pi} \quad (7.151)$$

with n_f the number of flavors. We obtain

$$\begin{aligned} \ln \frac{\mu^2}{\mu_0^2} &= \int_{\alpha_s(\mu_0)}^{\alpha_s(\mu)} \frac{d\alpha_s}{\beta(\alpha_s)} \\ \alpha_s(\mu) &= \frac{1}{\frac{1}{\alpha_s(\mu_0)} + \frac{1}{4\pi} (11 - \frac{2}{3}n_f) \ln \frac{\mu^2}{\mu_0^2}} = \frac{\alpha_s(\mu_0)}{1 + \alpha_s(\mu_0) \frac{1}{4\pi} (11 - \frac{2}{3}n_f) \ln \frac{\mu^2}{\mu_0^2}} \end{aligned} \quad (7.152)$$

Figure 7.20: Running coupling constant [22].



We see that when $11 - \frac{2}{3}n_f > 0$, $\alpha_s(\mu) < \alpha_s(\mu_0)$ for $\mu > \mu_0$. We can make expansion of the inverse of $\ln \frac{\mu^2}{\mu_0^2}$, we get the leading term,

$$\alpha_s(Q^2) = \frac{4\pi}{(11 - 2n_f/3) \ln(Q^2/\Lambda^2)} \quad (7.153)$$

where Λ is an arbitrary energy scale. One observes that the essential difference of $\alpha_S(Q^2)$ from $\alpha_{QED}(Q^2)$ is that $\alpha_S(Q^2)$ decreases as Q^2 increases, just opposite to $\alpha_{QED}(Q^2)$. This is called the asymptotic freedom. The physics is shown in Fig. 7.19. The quark-antiquark vacuum polarization screen the color charge in a similar way as in QED. But there is another process which cannot be found in QED: a color charge can turn into another color charge by radiating a gluon carrying away the original charge. The contribution of this process dominate over the QED-like one provided $11 > 2n_f/3$ which is true for $n_f = 6$ in the real world. The data and theoretical predictions for $\alpha_s(Q^2)$ are shown in Fig. 7.20.

The running coupling constant can be very large at the infrared end which means strong couplings. This indicates a very important effect, color confinement, where quarks and gluons can not be seen freely at low energies. We will explain the color confinement in the next section.

7.2.4 Phenomenological illustration of the confinement [7]

Consider a system of quarks and gluons in a volume of L^3 , the coupling constant at length scale l is given by g_l , one can prove $g_L > g_l$ for $L > l$. Let's introduce a color dielectric constant in vacuum κ_L and a renormalized coupling constant $g \equiv g_l$ where l is the length in the order of proton radius. Then κ_L is defined by

$$g_L^2 = \frac{g^2}{\kappa_L} \quad (7.154)$$

So when $L = l$, we have $\kappa_l = 1$ and

$$\kappa_L < \kappa_l, \text{ for } L > l \quad (7.155)$$

The perturbation theory gives to the leading order,

$$\frac{\kappa_L}{\kappa_l} = \frac{1}{1 + \frac{\alpha_s}{2\pi} (11 - \frac{2}{3}n_f) \ln \frac{L}{l}} \quad (7.156)$$

When $L \rightarrow \infty$, we have $\kappa_\infty = 0$ and $g_\infty^2 \rightarrow \infty$. So the vacuum is a medium with extremely strong couplings.

In electromagnetism, the dielectric constant is $\kappa_{\text{vacuum}} = 1$. One can prove that $\kappa \geq 1$ for all physical dielectric media. This can be seen by the electric displacement vector,

$$\mathbf{D} = \mathbf{E} + 4\pi\mathbf{P} = \kappa\mathbf{E} \quad (7.157)$$

where the polarization vector \mathbf{P} is parallel to \mathbf{E} , so one has $\kappa \geq 1$.

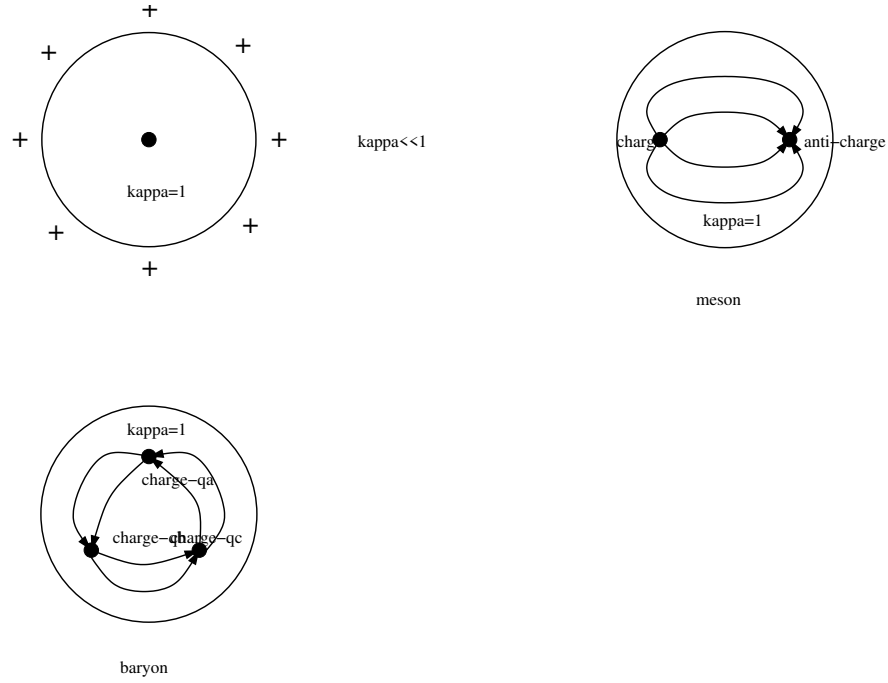
There is an electromagnetism analogy to the color confinement. We consider a hypothetical medium with a small dielectric constant,

$$\kappa \equiv \kappa_m \ll 1 \text{ or } = 0 \quad (7.158)$$

i.e. the medium is anti-screening because the polarization vector is anti-parallel to the electric field. If we put a test charge into the medium, a hole must be formed as shown in Fig. 7.21. Inside the hole is the perturbative vacuum with $\kappa = 1$. We can estimate the radius of this hole. Assume E_{out} , D_{out} , E_{in} and D_{in} are normal components of the fields outside and inside the sphere. We have

$$\begin{aligned} D_{\text{in}} &= E_{\text{in}} = D_{\text{out}} = \frac{e}{R^2} \\ E_{\text{out}} &= \frac{e}{\kappa_m R^2} \end{aligned} \quad (7.159)$$

Figure 7.21: The effect of a test charge in an anti-screening medium.



where e is the total electric charge of a charge distribution and R is the radius of the hole. The electric energies in the medium and vacuum are given by

$$\begin{aligned}
 U_{out}^m &= \frac{1}{8\pi} \int_R^\infty d\Omega dr r^2 \mathbf{D} \cdot \mathbf{E} = \frac{1}{2} \frac{e^2}{\kappa_m R} \\
 U_{out}^{vac} &= \frac{1}{2} \frac{e^2}{R}
 \end{aligned} \tag{7.160}$$

where U_{out}^{vac} So the energy difference is

$$\Delta U_e = \frac{1}{2} \frac{e^2}{R} \left(\frac{1}{\kappa_m} - 1 \right) \tag{7.161}$$

One needs an energy U_{hole} to create a hole. It has two parts: the volume energy and the surface one,

$$U_{hole} \sim C_1 \frac{4\pi}{3} R^3 + C_2 4\pi R^2 \tag{7.162}$$

where C_1 and C_2 are two constants. The total energy is then

$$U = U_{out}^m + U_{hole} \tag{7.163}$$

When $\kappa_m \rightarrow 0$ and $U_{hole} \sim C_1 \frac{4\pi}{3} R^3$, i.e. dominated by the volume energy, we can find the minimum of U as,

$$\begin{aligned}
 \frac{dU}{dR} &= \frac{d}{dR} \left(\frac{1}{2} \frac{e^2}{\kappa_m R} + C_1 \frac{4\pi}{3} R^3 \right) \\
 &= -\frac{1}{2} \frac{e^2}{\kappa_m R^2} + C_1 4\pi R^2 = 0
 \end{aligned} \tag{7.164}$$

Figure 7.22: The splitting of a bag.

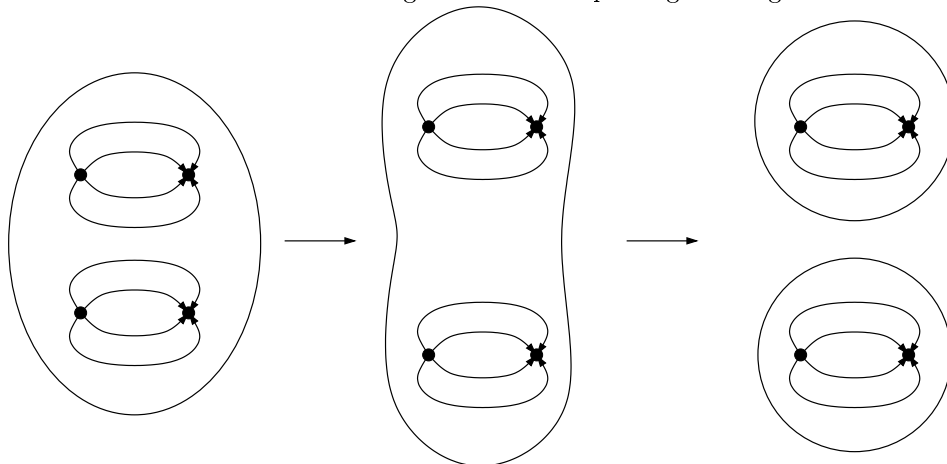


Table 7.10: Comparison with superconductivity.

superconductivity (QED)	hadron (QCD)
H	E^a
$\mu_{in} = 0$	$\kappa_{vac} = 0$
$\mu_{vac} = 1$	$\kappa_{in} = 1$
internal	external
external	internal

which gives

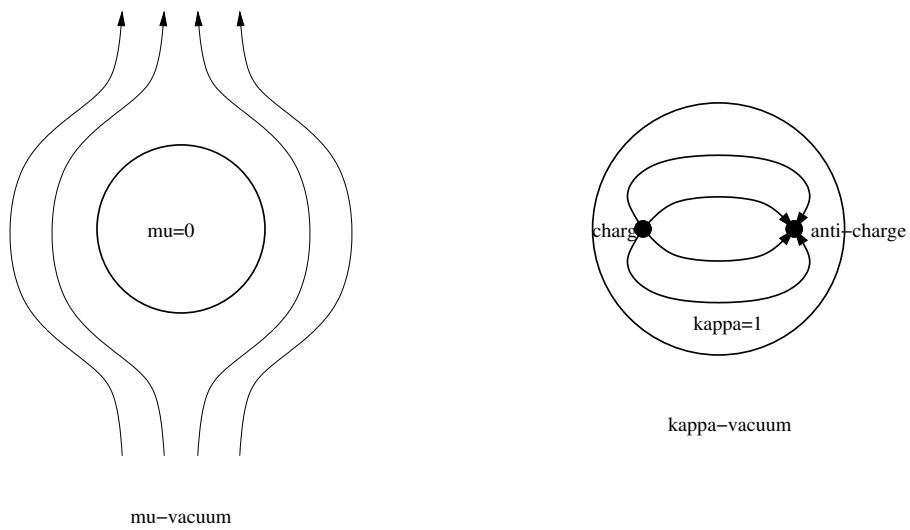
$$\begin{aligned}
 R_{\min} &= \left(\frac{e^2}{8\pi\kappa_m C_1} \right)^{1/4} \\
 U_{\min} &= \frac{1}{2} \frac{e^2}{\kappa_m R_{\min}} + C_1 \frac{4\pi}{3} R_{\min}^3 \\
 &\sim \frac{4}{3} \left(\frac{e^2}{2\kappa_m} \right)^{3/4} (4\pi C_1)^{1/4}
 \end{aligned} \tag{7.165}$$

One can extend this example by introducing two test particles in opposite charges into the vacuum. Similar to the case of one test charge, a hole containing the two charges will form. This is the picture for mesons with two opposite color charges. See Fig. 7.21.

When the couplings are extremely strong, there exists a strong repulsive force exerting on the color charges. This is analogous to Van der Waals force between two helium atoms. There is also an analogy between the Meissner effect in a superconductor and the color confinement. See Table 7.10 and Fig. 7.23.

Exercise 62. Determine R_{\min} and U_{\min} when $U_{\text{hole}} \sim C_2 4\pi R^2$, i.e. the hole energy is only from the surface.

Figure 7.23: Comparison of superconductivity and hadron.



Chapter 8

Acknowledgement

The author thanks following students who took this course and pointed out several errors in this lecture note: Dai Lei (2008-09 fall semester), Wu Ying-hai (2008-09 fall semester), Chen Peng-fei (2009-10 fall semester), Liu Pei-fan (2014 spring semester).

Appendix A

Nucleon-nucleon scattering theory

A.1 Nucleon-nucleon scatterings

The nucleon-nucleon interaction is a basic for understanding the nuclear force, for a review of this topic, see, e.g., Ref. [29]. The scattering experiments is one of the most efficient tools to detect the properties of particles. They are widely used in nuclear and particle physics. One of the earliest attempt was made in the Rutherford's experiment where the alpha-particles were used to bombard the atoms. It shows that there is a nucleus inside the atom. In 1960s, in order to find the structure of nucleons Hofstadter used high energy electron-nucleon scatterings, which uncovers that the nucleon is not a point-like particle but has a finite size.

A.2 The stationary scattering wave function

Let us consider the non-relativistic scattering of a spinless particle of mass m by a central potential $V(r)$. The time-dependent Schroedinger equation is

$$\left[-\frac{1}{2m}\nabla^2 + V(r) \right] \psi(t, \mathbf{r}) = i \frac{\partial \psi(t, \mathbf{r})}{\partial t} \quad (\text{A.1})$$

For stationary solution,

$$\psi(t, \mathbf{r}) = e^{-iEt} \psi(\mathbf{r}) \quad (\text{A.2})$$

where $E = k^2/2m$. So the time-independent Schroedinger equation becomes

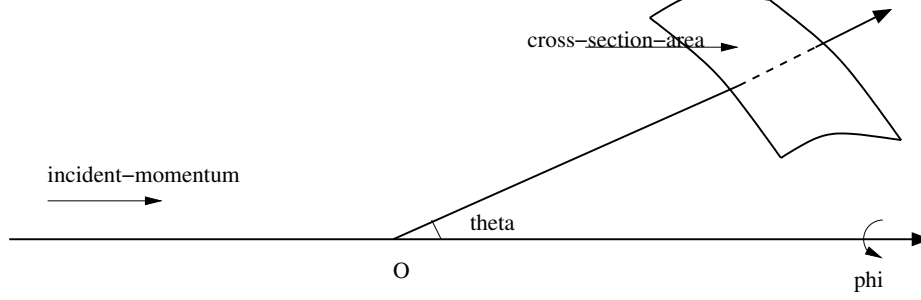
$$[\nabla^2 + k^2 - 2mV(r)] \psi(\mathbf{r}) = 0 \quad (\text{A.3})$$

We assume that the potential $V(r)$ tends to zero faster than $1/r$ as r goes to infinity. The asymptotic form of the wave function at $r \rightarrow \infty$ is denoted by $\psi_{\mathbf{k}}^{(+)}(\mathbf{r})$,

$$\psi_{\mathbf{k}}^{(+)}(\mathbf{r}) \rightarrow A \left[e^{i\mathbf{k}\cdot\mathbf{r}} + f(\theta, \phi) \frac{e^{ikr}}{r} \right] \quad (\text{A.4})$$

where the first term of Eq. (A.4) is the incident wave along \mathbf{k} , while the second term is the scattering wave. We can choose the incident momentum $\mathbf{k} = k\hat{\mathbf{z}}$ along the z -axis, so $f(\theta, \phi) = f(\theta)$ depending only on the polar angle. This is because the incident wave has rotational symmetry which is conserved during the scattering by a central potential.

Figure A.1: Scattering of a plane wave.



A.3 Cross section

The cross section $\sigma(\Omega)d\Omega = \frac{d\sigma}{d\Omega}d\Omega$ is the number of particles emitted per unit time and unit incident flux within the solid angle $d\Omega$ about the direction $\Omega(\theta, \phi)$. One can obtain it by computing the outgoing flux of particles scattered through the spherical surface $r^2d\Omega$ divided by the incident flux.

The probability current density is

$$\mathbf{j}(\mathbf{r}) = -i\frac{1}{2m}[\psi^*\nabla\psi - (\nabla\psi^*)\psi] = \frac{1}{m}\text{Im}(\psi^*\nabla\psi) \quad (\text{A.5})$$

It satisfies the continuity equation,

$$\nabla \cdot \mathbf{j} + \frac{\partial \rho}{\partial t} = 0 \quad (\text{A.6})$$

where $\rho = |\psi|^2$ is the probability density. Since $\frac{\partial \rho}{\partial t} = 0$ in the stationary case, one has

$$\nabla \cdot \mathbf{j} = 0 \quad (\text{A.7})$$

Now we try to calculate the current density. In spherical coordinates, we have

$$\nabla = \hat{\mathbf{r}}\frac{\partial}{\partial r} + \hat{\theta}\frac{1}{r}\frac{\partial}{\partial \theta} + \hat{\phi}\frac{1}{r\sin\theta}\frac{\partial}{\partial \phi} \quad (\text{A.8})$$

The radial outgoing flux is

$$\begin{aligned} \mathbf{j} \cdot \hat{\mathbf{r}} &= \frac{1}{m}\text{Im} \left\{ AA^* \left[e^{-ikz} + f^*(\theta)\frac{e^{-ikr}}{r} \right] \frac{\partial}{\partial r} \left[e^{ikz} + f(\theta)\frac{e^{ikr}}{r} \right] \right\} \\ &= \frac{1}{m}|A|^2\text{Im} \left[e^{-ikz} \frac{\partial}{\partial r} e^{ikz} \right] + \frac{1}{m}|A|^2|f(\theta)|^2\text{Im} \left[\frac{e^{-ikr}}{r} \frac{\partial}{\partial r} \frac{e^{ikr}}{r} \right] \\ &\quad + \frac{1}{m}|A|^2\text{Im} \left[f(\theta)e^{-ikz} \frac{\partial}{\partial r} \frac{e^{ikr}}{r} + f^*(\theta)\frac{e^{-ikr}}{r} \frac{\partial}{\partial r} e^{ikz} \right] \\ &= (\mathbf{j}_{\text{inc}} + \mathbf{j}_{\text{out}} + \mathbf{j}_{\text{int}}) \cdot \hat{\mathbf{r}} \end{aligned} \quad (\text{A.9})$$

Here the flux corresponding to the incident wave

$$\psi_{k\hat{\mathbf{z}}}(\mathbf{r}) = Ae^{ikz} \quad (\text{A.10})$$

is given by

$$\mathbf{j}_{\text{inc}} = \frac{1}{m}\hat{\mathbf{z}}|A|^2\text{Im} \left[e^{-ikz} \frac{\partial}{\partial z} e^{ikz} \right] = \hat{\mathbf{z}}|A|^2\frac{k}{m} = \hat{\mathbf{z}}|A|^2v \quad (\text{A.11})$$

One can verify

$$\mathbf{j}_{\text{inc}} \cdot \hat{\mathbf{r}} = \frac{1}{m} |A|^2 \text{Im} \left[e^{-ikz} \frac{\partial}{\partial r} e^{ikz} \right] = |A|^2 \frac{1}{m} k \cos \theta \quad (\text{A.12})$$

The outgoing flux is

$$\begin{aligned} \mathbf{j}_{\text{out}} \cdot \hat{\mathbf{r}} &= \frac{1}{m} |A|^2 |f(\theta)|^2 \text{Im} \left[\frac{e^{-ikr}}{r} \frac{\partial}{\partial r} \frac{e^{ikr}}{r} \right] \\ &\approx |A|^2 \frac{|f(\theta)|^2}{r^2} \frac{k}{m} + O(1/r^3) \end{aligned} \quad (\text{A.13})$$

The interference term is given by

$$\begin{aligned} \mathbf{j}_{\text{int}} \cdot \hat{\mathbf{r}} &= \frac{1}{m} |A|^2 \text{Im} \left[f(\theta) e^{-ikz} \frac{\partial}{\partial r} \frac{e^{ikr}}{r} + f^*(\theta) \frac{e^{-ikr}}{r} \frac{\partial}{\partial r} e^{ikz} \right] \\ &= |A|^2 \frac{k}{m} \frac{1}{r} \text{Re} \left[f(\theta) e^{ik(r-z)} + f^*(\theta) \cos \theta e^{-ik(r-z)} \right] + O(1/r^2) \end{aligned} \quad (\text{A.14})$$

We see that as $r \rightarrow \infty$, the exponential factor $e^{\pm ik(r-z)}$ oscillates drastically except at the forward direction at $\theta = 0$. The interference term can be neglected except at forward direction.

The particle outgoing flux through the spherical area $r^2 d\Omega$ is

$$|A|^2 \frac{|f(\theta)|^2}{r^2} \frac{k}{m} r^2 d\Omega = |A|^2 \frac{k}{m} |f(\theta)|^2 d\Omega \quad (\text{A.15})$$

Dividing by the incident flux $|A|^2 v$, one gets the differential cross section,

$$\frac{d\sigma}{d\Omega} = |f(\theta, \phi)|^2 \quad (\text{A.16})$$

The total cross section is then

$$\sigma = \int d\Omega \frac{d\sigma}{d\Omega} = \int d\Omega |f(\theta, \phi)|^2 \quad (\text{A.17})$$

A.4 The optical theorem

Now consider the forward scattering at $\theta = 0$. Let us compute the flux at forward direction from Eq. (A.14),

$$\begin{aligned} \int_{\theta=0} d\Omega r^2 \mathbf{j}_{\text{int}} \cdot \hat{\mathbf{r}} &\approx \int_{\theta=0} d\Omega r^2 |A|^2 \frac{k}{m} \frac{1}{r} \text{Re} \left[f(\theta=0) e^{ikr(1-\cos\theta)} + f^*(\theta=0) e^{-ikr(1-\cos\theta)} \right] \\ &= r |A|^2 \frac{k}{m} 4\pi \int_{\cos\delta\theta}^1 d\cos\theta \text{Re} \left[f(\theta=0) e^{ikr(1-\cos\theta)} \right] \\ &\approx r |A|^2 \frac{k}{m} 4\pi \text{Re} \left[\frac{i}{kr} f(\theta=0) (1 - e^{ikr(1-\cos\delta\theta)}) \right] \\ &\approx r |A|^2 \frac{k}{m} 4\pi \text{Re} \left[\frac{i}{kr} f(\theta=0) (1 - e^{ikr\delta\theta^2/2}) \right] \\ &\approx -|A|^2 \frac{1}{m} 4\pi \text{Im} f(\theta=0) \end{aligned} \quad (\text{A.18})$$

We have used the fact that $kr\delta\theta^2/2 \rightarrow \infty$ when $r \rightarrow \infty$, so the phase factor $e^{ikr\delta\theta^2/2}$ drastically fluctuates and is negligible. We see in Eq. (A.18) that the total flux from $\mathbf{j}_{\text{int}} \cdot \hat{\mathbf{r}}$ is negative which means it goes inside the sphere. In contrast the total flux from incident wave is zero,

$$\int d\Omega \mathbf{j}_{\text{inc}} \cdot \hat{\mathbf{r}} = 0 \quad (\text{A.19})$$

which is easy to understand: the incident wave goes inside the region at $\theta = \pi$ and leaves the region at $\theta = 0$.

From the continuity equation $\nabla \cdot \mathbf{j} = 0$, we have

$$r^2 \int d\Omega \mathbf{j} \cdot \hat{\mathbf{r}} = 0 \quad (\text{A.20})$$

which reads

$$r^2 \int d\Omega (\mathbf{j}_{\text{out}} + \mathbf{j}_{\text{int}}) \cdot \hat{\mathbf{r}} = 0 \quad (\text{A.21})$$

and can be written as

$$|A|^2 \frac{1}{m} \left[k \int d\Omega |f(\Omega)|^2 - 4\pi \text{Im}f(\theta = 0) \right] = 0 \quad (\text{A.22})$$

So the total cross section is related to the imaginary part of the scattering amplitude in the forward direction,

$$\sigma_{\text{tot}} = \frac{4\pi}{k} \text{Im}f(\theta = 0) \quad (\text{A.23})$$

This is called the optical theorem, a result of probability conservation, which states that the total cross section is given by the imaginary part of the forward scattering amplitude. This proof is based on the elastic scattering.

A.5 Partial wave method

We consider a central potential $V(r)$. In spherical coordinates, the Hamiltonian $H = -(1/2m)\nabla^2 + V$ reads,

$$\begin{aligned} H &= -\frac{1}{2m} \left[\frac{1}{r^2} \frac{\partial}{\partial r} \left(r^2 \frac{\partial}{\partial r} \right) + \frac{1}{r^2 \sin \theta} \frac{\partial}{\partial \theta} \left(\sin \theta \frac{\partial}{\partial \theta} \right) + \frac{1}{r^2 \sin^2 \theta} \frac{\partial^2}{\partial \phi^2} \right] + V(r) \\ &= -\frac{1}{2m} \left[\frac{1}{r^2} \frac{\partial}{\partial r} \left(r^2 \frac{\partial}{\partial r} \right) - \frac{L^2}{r^2} \right] + V(r) \end{aligned} \quad (\text{A.24})$$

with L^2 given by

$$L^2 = - \left[\frac{1}{\sin \theta} \frac{\partial}{\partial \theta} \left(\sin \theta \frac{\partial}{\partial \theta} \right) + \frac{1}{\sin^2 \theta} \frac{\partial^2}{\partial \phi^2} \right] \quad (\text{A.25})$$

One can verify

$$[H, L^2] = [H, L_z] = 0 \quad (\text{A.26})$$

Because the operators $\{H, L^2, L_z\}$ all commute to each other, the state can be labeled by quantum numbers $\{n, l, m\}$, where n labels the energy level, l the angular momentum, m the projection to the third axis. The scattering wave function $\psi_{\mathbf{k}}^{(+)}$ can be expanded in partial waves as

$$\psi_{\mathbf{k}}^{(+)}(k, \mathbf{r}) = \sum_{l=0}^{\infty} \sum_{m=-l}^{+l} c_{lm}(k) R_{lm}(k, r) Y_{lm}(\theta, \phi) \quad (\text{A.27})$$

If there is no dependence on the magnetic quantum number m , so $R_{lm}(k, r)$ is written as $R_l(k, r)$. We obtain

$$\left[\frac{d^2}{dr^2} + \frac{2}{r} \frac{d}{dr} + k^2 - \frac{l(l+1)}{r^2} - U(r) \right] R_l(k, r) = 0 \quad (\text{A.28})$$

It is convenient to use

$$R_l(k, r) = \frac{u_l(k, r)}{r} \quad (\text{A.29})$$

to rewrite Eq. (A.28) as

$$\left[\frac{d^2}{dr^2} + k^2 - \frac{l(l+1)}{r^2} - U(r) \right] u_l(k, r) = 0 \quad (\text{A.30})$$

For $V(r) = 0$, we can also use variable $\rho = kr$ to rewrite Eq. (A.28) as

$$\left[\frac{d^2}{d\rho^2} + \frac{2}{\rho} \frac{d}{d\rho} + 1 - \frac{l(l+1)}{\rho^2} \right] R_l(\rho) = 0 \quad (\text{A.31})$$

whose solution is the spherical Bessel function.

For free particles with $V(r) = 0$, the solutions to Eq. (A.31) are spherical Bessel functions

$$R_l(kr) = C_l^{(1)}(k) j_l(kr) + C_l^{(2)}(k) n_l(kr) \quad (\text{A.32})$$

or

$$R_l(kr) = D_l^{(1)}(k) h_l^{(1)}(kr) + D_l^{(2)}(k) h_l^{(2)}(kr) \quad (\text{A.33})$$

At $r \rightarrow 0$ only $j_l(kr)$ is finite and all others diverge. At $r \rightarrow \infty$, we have

$$\begin{aligned} R_l(k, r) &\rightarrow C_l^{(1)}(k) \frac{1}{kr} \sin\left(kr - \frac{l}{2}\pi\right) - C_l^{(2)}(k) \frac{1}{kr} \cos\left(kr - \frac{l}{2}\pi\right) \\ &\sim \frac{1}{kr} \sqrt{[C_l^{(1)}(k)]^2 + [C_l^{(2)}(k)]^2} \\ &\quad \times \left[\frac{C_l^{(1)}(k) \sin\left(kr - \frac{l}{2}\pi\right)}{\sqrt{[C_l^{(1)}(k)]^2 + [C_l^{(2)}(k)]^2}} - \frac{C_l^{(2)}(k) \cos\left(kr - \frac{l}{2}\pi\right)}{\sqrt{[C_l^{(1)}(k)]^2 + [C_l^{(2)}(k)]^2}} \right] \\ &\sim \frac{1}{kr} A_l(k) \sin\left[kr - \frac{l}{2}\pi + \delta_l(k)\right] \end{aligned} \quad (\text{A.34})$$

where we have used

$$\begin{aligned} A_l(k) &= \sqrt{[C_l^{(1)}(k)]^2 + [C_l^{(2)}(k)]^2} \\ \tan \delta_l(k) &= -\frac{C_l^{(2)}(k)}{C_l^{(1)}(k)} \end{aligned} \quad (\text{A.35})$$

and $\delta_l(k)$ is called the phase shift. The usual normalizations of scattering wave functions at $r \rightarrow \infty$ are $A_l(k) = 1$ or $A_l(k) = 1/\cos \delta_l$.

A.5.1 Scattering amplitude and cross section

The scattering wave function at $r \rightarrow \infty$ is

$$\psi_{\mathbf{k}}^{(+)}(\mathbf{r}) \rightarrow A \left[e^{ikz} + f(\theta) \frac{e^{ikr}}{r} \right] \quad (\text{A.36})$$

where the first term is the incident wave and the second term is the scattering wave. It is easy to verify that both terms are eigen wave function of the Schroedinger equation at $r \rightarrow \infty$ where $l(l+1)/r^2 \rightarrow 0$ and $V(r) \rightarrow 0$. We can expand the plane wave e^{ikz} as

$$e^{ikz} = \sum_{l=0}^{\infty} (2l+1) i^l j_l(kr) P_l(\cos \theta) \quad (\text{A.37})$$

The proof can be found in the Appendix. Then the scattering wave function can be written as

$$\begin{aligned}
\psi_{\mathbf{k}}^{(+)}(\mathbf{r}) &\sim \sum_{l=0}^{\infty} (2l+1) i^l j_l(kr) P_l(\cos \theta) + f(\theta) \frac{e^{ikr}}{r} \\
&\sim \sum_{l=0}^{\infty} (2l+1) i^l \frac{1}{kr} \sin\left(kr - \frac{l}{2}\pi\right) P_l(\cos \theta) + f(\theta) \frac{e^{ikr}}{r} \\
&\sim \sum_{l=0}^{\infty} (2l+1) i^l \frac{1}{2ikr} \left\{ \exp\left[i\left(kr - \frac{l}{2}\pi\right)\right] - \exp\left[-i\left(kr - \frac{l}{2}\pi\right)\right] \right\} P_l(\cos \theta) \\
&\quad + f(\theta) \frac{e^{ikr}}{r}
\end{aligned} \tag{A.38}$$

If we assume for real $\delta_l(k)$,

$$\begin{aligned}
f(\theta) &= \sum_{l=0}^{\infty} (2l+1) f_l P_l(\cos \theta) \\
&= \frac{1}{2ik} \sum_{l=0}^{\infty} (2l+1) \{ \exp[2i\delta_l(k)] - 1 \} P_l(\cos \theta) \\
&= \frac{1}{2ik} \sum_{l=0}^{\infty} (2l+1) \{ \exp[2i\delta_l(k)] - 1 \} P_l(\cos \theta) \\
&= \frac{1}{k} \sum_{l=0}^{\infty} (2l+1) \exp[i\delta_l(k)] \sin \delta_l(k) P_l(\cos \theta)
\end{aligned} \tag{A.39}$$

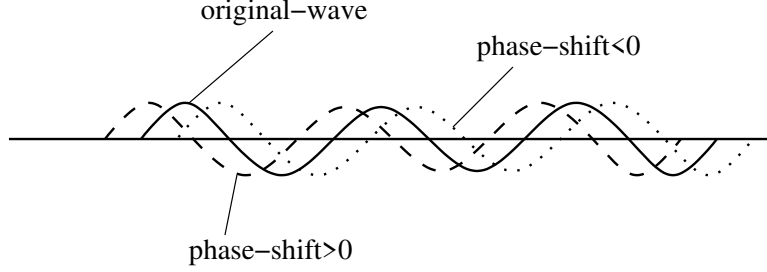
where the partial wave scattering amplitude is written as $f_l = (S_l - 1)/(2ik)$ where $S_l = e^{2i\delta_l(k)}$. We then obtain

$$\begin{aligned}
\psi_{\mathbf{k}}^{(+)}(\mathbf{r}) &\sim \sum_{l=0}^{\infty} (2l+1) i^l \frac{1}{2ikr} P_l(\cos \theta) \\
&\quad \times \left\{ \exp\left[i\left(kr - \frac{l}{2}\pi + 2\delta_l(k)\right)\right] - \exp\left[-i\left(kr - \frac{l}{2}\pi\right)\right] \right\} \\
&\sim \sum_{l=0}^{\infty} (2l+1) i^l \frac{1}{2ikr} \exp[i\delta_l(k)] P_l(\cos \theta) \\
&\quad \times \left\{ \exp\left[i\left(kr - \frac{l}{2}\pi + \delta_l(k)\right)\right] - \exp\left[-i\left(kr - \frac{l}{2}\pi + \delta_l(k)\right)\right] \right\} \\
&\sim \sum_{l=0}^{\infty} (2l+1) i^l \frac{1}{kr} \exp[i\delta_l(k)] P_l(\cos \theta) \sin\left(kr - \frac{l}{2}\pi + \delta_l\right)
\end{aligned} \tag{A.40}$$

The differential cross section is given by

$$\begin{aligned}
\frac{d\sigma}{d\Omega} &= |f(\theta)|^2 = \frac{1}{k^2} \sum_{l,l'=0}^{\infty} (2l+1)(2l'+1) \exp[i\delta_l(k)] \exp[-i\delta_{l'}(k)] \\
&\quad \times \sin \delta_l(k) \sin \delta_{l'}(k) P_l(\cos \theta) P_{l'}(\cos \theta)
\end{aligned} \tag{A.41}$$

Figure A.2: The positivity of the phase shift.



The total cross section is then

$$\begin{aligned}
 \sigma_{tot} &= \int d\Omega |f(\theta, \phi)|^2 \\
 &= 2\pi \frac{1}{k^2} \int_{-1}^1 d(\cos \theta) \sum_{l, l'=0}^{\infty} (2l+1)(2l'+1) \exp[i\delta_l(k)] \exp[-i\delta_{l'}(k)] \\
 &\quad \times \sin \delta_l(k) \sin \delta_{l'}(k) P_l(\cos \theta) P_{l'}(\cos \theta) \\
 &= 4\pi \frac{1}{k^2} \sum_{l, l'=0}^{\infty} \delta_{ll'} (2l+1) \exp[i\delta_l(k)] \exp[-i\delta_{l'}(k)] \sin \delta_l(k) \sin \delta_{l'}(k) \\
 &= \frac{4\pi}{k^2} \sum_{l=0}^{\infty} (2l+1) \sin^2 \delta_l(k)
 \end{aligned} \tag{A.42}$$

where we have used

$$\int_{-1}^1 dx P_l(x) P_{l'}(x) = \frac{2}{2l+1} \delta_{ll'} \tag{A.43}$$

The phase shift reflect if the force is attractive or repulsive, one can see from $\psi_{\mathbf{k}}^{(+)}$ in Eq. (A.40)

$$\delta_l = \begin{cases} > 0, & \text{attractive force} \\ < 0, & \text{repulsive force} \end{cases} \tag{A.44}$$

See Fig. A.2 for illustration.

We can estimate the maximum value of l_{max} as follows

$$l_{max} \sim ka \tag{A.45}$$

where a is the interaction range. For example, the range of nuclear force is about a few fm, for a particle with the incident energy $k \sim 20$ MeV/c,

$$ka \sim 20 \times \frac{1}{197} \sim 0.1 \tag{A.46}$$

So the partial wave one has to take into account is s and p wave.

A.5.2 Inelastic scattering and total cross section

The wave function at $r \rightarrow \infty$ is given in Eq. (A.40), we rewrite it here,

$$\begin{aligned}
\psi(\mathbf{r}) &\sim \sum_{l=0}^{\infty} (2l+1) \frac{1}{2ikr} i^l \{S_l \exp[i(kr - l\pi/2)] - \exp[-i(kr - l\pi/2)]\} P_l(\cos\theta) \\
&= \sum_{l=0}^{\infty} \frac{2l+1}{2ikr} [S_l \exp(ikr) + (-1)^{l+1} \exp(-ikr)] P_l(\cos\theta)
\end{aligned} \tag{A.47}$$

For elastic scatterings, δ_l is real and S_l is a purely phase factor, $|S_l| = 1$. For inelastic scatterings, δ_l is complex and $|S_l| \neq 1$. The probability current density is given in Eq. (A.5), its radial part is given by

$$\begin{aligned}
j_r(r) &= \frac{1}{m} \text{Im}(\psi^* \partial_r \psi) = \frac{1}{m} \text{Im} \sum_{l=0}^{\infty} i \frac{2l+1}{2kr} [S_l^* \exp(-ikr) + (-1)^{l+1} \exp(ikr)] P_l(\cos\theta) \\
&\times \sum_{l'=0}^{\infty} \frac{2l'+1}{2ikr} ik [S_{l'} \exp(ikr) - (-1)^{l'+1} \exp(-ikr)] P_{l'}(\cos\theta) \\
&= \frac{1}{m} \frac{1}{4kr^2} \text{Im} \sum_{l,l'=0}^{\infty} i(2l+1)(2l'+1) P_l(\cos\theta) P_{l'}(\cos\theta) \\
&\times [S_l^* S_{l'} - (-1)^{l+l'} - (-1)^{l'+1} S_l^* \exp(-2ikr) + (-1)^{l+1} S_{l'} \exp(2ikr)]
\end{aligned} \tag{A.48}$$

We can compute the outgoing flow,

$$\begin{aligned}
\int d\Omega j_r(r) r^2 &= \frac{\pi}{2mk} \text{Im} \sum_{l,l'=0}^{\infty} i(2l+1)(2l'+1) \frac{2}{2l+1} \delta_{ll'} \\
&\times [S_l^* S_l - 1 + 2i(-1)^{l+1} \text{Im}[S_l \exp(2ikr)]] \\
&= \frac{\pi}{mk} \sum_{l=0}^{\infty} (2l+1) (|S_l|^2 - 1)
\end{aligned} \tag{A.49}$$

When $|S_l|^2 = 1$, no outgoing flow occurs, this corresponds to elastic scatterings. When $|S_l|^2 < 1$, there is negative flow, this corresponds to an absorption. The differential and total cross sections for inelastic scattering can be obtained by dividing the above by the incident flow k/m ,

$$\begin{aligned}
\frac{d\sigma_{in}}{d\Omega} &= \frac{r^2 j_r(r)}{k/m} \\
\sigma_{in} &= \frac{\int d\Omega j_r(r) r^2}{k/m} = \frac{\pi}{k^2} \sum_{l=0}^{\infty} (2l+1) (1 - |S_l|^2)
\end{aligned} \tag{A.50}$$

The total elastic cross section is

$$\begin{aligned}
\sigma_{el} &= \int d\Omega |f|^2 = \frac{1}{4k^2} \sum_{l,l'=0}^{\infty} (2l+1)(2l'+1) (S_l - 1)(S_l^* - 1) P_l(\cos\theta) P_{l'}(\cos\theta) \\
&= \frac{\pi}{k^2} \sum_{l=0}^{\infty} (2l+1) |1 - S_l|^2 = 4\pi \sum_{l=0}^{\infty} (2l+1) |f_l|^2
\end{aligned} \tag{A.51}$$

where the scattering amplitude f is given in by Eq. (A.39). The total cross section is then

$$\sigma_{tot} = \sigma_{el} + \sigma_{in} = \frac{2\pi}{k^2} \sum_{l=0}^{\infty} (2l+1) (1 - \text{Re}S_l) \tag{A.52}$$

The scattering amplitude in general case is similar to Eq. (A.39)

$$f(\theta) = \frac{1}{2ik} \sum_{l=0}^{\infty} (2l+1)(S_l - 1) P_l(\cos \theta)$$

so we have

$$\text{Im}f(0) = \frac{1}{2k} \sum_{l=0}^{\infty} (2l+1)(1 - \text{Re}S_l) \quad (\text{A.53})$$

Comparing Eq. (A.52) and (A.53) we obtain the optical theorem (A.23) in general case with elastic and in-elastic scatterings.

A.5.3 Phase shifts in square well scattering

Let us consider the scattering of a particle in a square well potential in a sphere,

$$V(r) = \begin{cases} -V_0, & r < a \\ 0, & r > a \end{cases} \quad (\text{A.54})$$

where $V_0 > 0$. We consider only the s-wave scattering. In the range $r < a$,

$$\begin{aligned} \frac{d^2u}{dr^2} + (k^2 + k_0^2)u &= 0 \\ k &= \sqrt{2mE}, \quad k_0 = \sqrt{2mV_0} \end{aligned} \quad (\text{A.55})$$

The boundary condition is $u(0) = 0$. The solution is

$$\begin{aligned} u(r) &= \sin k_1 r \\ k_1 &= \sqrt{k^2 + k_0^2} = \sqrt{2m(E + V_0)} \end{aligned} \quad (\text{A.56})$$

In the range $r > a$, the Schroedinger equation becomes

$$\frac{d^2u}{dr^2} + k^2u = 0 \quad (\text{A.57})$$

with the solution

$$u(r) = A \sin(kr + \delta_0) \quad (\text{A.58})$$

The boundary condition at $r = a$ should be that the wave function and its derivative must be continuous, then we have

$$\frac{1}{k} \tan(ka + \delta_0) = \frac{1}{k_1} \tan(k_1 a) \quad (\text{A.59})$$

or

$$\frac{1}{k} \frac{\tan(ka) + \tan \delta_0}{1 - \tan(ka) \tan \delta_0} = \frac{1}{k_1} \tan(k_1 a) \quad (\text{A.60})$$

Then we get $\tan \delta_0$,

$$\begin{aligned} \tan \delta_0 &= \frac{k \tan(k_1 a) - k_1 \tan(ka)}{k_1 + k \tan(ka) \tan(k_1 a)} \\ \delta_0 &= -ka + \tan^{-1} \left[\frac{k}{k_1} \tan(k_1 a) \right] \end{aligned} \quad (\text{A.61})$$

At $ka \ll 1$, we can Taylor expand the above with respect to k , and obtain

$$k \cot \delta_0 = \frac{1}{a} \frac{k_1 a + ka \tan(ka) \tan(k_1 a)}{\tan(k_1 a) - (k_1 a/ka) \tan(ka)} \approx -\frac{1}{a_s} + \frac{1}{2} r_{eff} k^2 \quad (\text{A.62})$$

We see that δ_0 must be of the order k at the limit $k \rightarrow 0$. Here the scattering length is

$$a_s = -\lim_{k \rightarrow 0} \frac{\tan \delta_0(k)}{k} = a \left[1 - \frac{\tan(k_0 a)}{k_0 a} \right] \quad (\text{A.63})$$

Note that $a_s < 0$ and $\delta_0(k) > 0$ for attractive interaction. For $a_s < 0$, $k_0 a$ must be in $[0, \pi/2]$. We have used

$$\frac{1}{a} \frac{k_1 a + ka \tan(ka) \tan(k_1 a)}{\tan(k_1 a) - (k_1 a/ka) \tan(ka)} \approx -\frac{1}{a_s} + \frac{1}{2} r_{eff} k^2 \quad (\text{A.64})$$

where

$$r_{eff} = a - \frac{a^3}{3a_s^2} - \frac{1}{k_0^2 a_s} \quad (\text{A.65})$$

Because for s-wave and low energy, then the total cross section is

$$\sigma_{tot} = 4\pi \frac{\sin^2 \delta_0}{k^2} = \frac{4\pi}{k^2 + k^2 \cot^2 \delta_0} = \frac{4\pi}{k^2 + (-1/a_s + \rho k^2/2)^2} \approx 4\pi a^2 \left[1 - \frac{\tan(k_0 a)}{k_0 a} \right]^2 + O(k^2) \quad (\text{A.66})$$

When $k_0 a = \pi/2$,

$$\delta_0 = \pi/2 \quad (\text{A.67})$$

In this case the scattering length and cross section turn to negative infinity. This corresponds to zero energy resonance. Note that $k_0 a = \pi/2$ is also the threshold for the appearance of one s-wave bound state. When $\pi/2 < k_0 a < \pi$, there is one bound state, so the scattering length is positive. When $k_0 a < \pi/2$, there is no bound state, the scattering amplitude is negative.

A.5.4 Breit-Wigner formula

We consider the elastic scattering for simplicity. The total cross section is

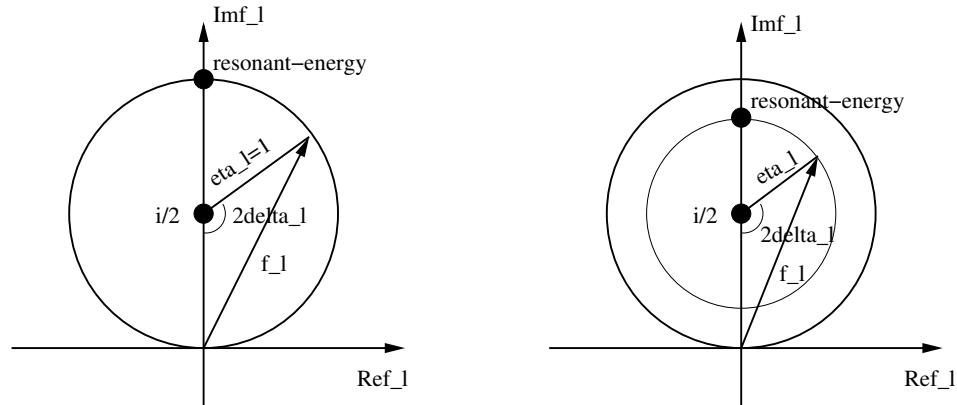
$$\sigma_{tot} = \frac{4\pi}{k^2} \sum_{l=0}^{\infty} (2l+1) \sin^2 \delta_l(E) \quad (\text{A.68})$$

When $\delta_l(E)$ satisfy

$$\delta_l(E) \sim (n+1/2)\pi, \text{ or } \sin^2 \delta_l(E) \sim 1 \quad (\text{A.69})$$

the partial wave cross section reaches maximum and the resonant states occur. We can expand near the resonant energy $E = E_0$ as

$$\begin{aligned} \sin \delta_l(E) &\approx \sin \delta_l(E_0) + \left[\cos \delta_l(E) \frac{d\delta_l}{dE} \right]_{E_0} (E - E_0) \approx 1 \\ \cos \delta_l(E) &\approx \cos \delta_l(E_0) - \left[\sin \delta_l(E) \frac{d\delta_l}{dE} \right]_{E_0} (E - E_0) \\ &= - \left. \frac{d\delta_l}{dE} \right|_{E_0} (E - E_0) = -\frac{2}{\Gamma} (E - E_0) \end{aligned} \quad (\text{A.70})$$

Figure A.3: Argand plot for the partial wave amplitude. (a) $\eta_l = 1$; (b) $\eta_l < 1$.

where we have defined

$$\Gamma = 2 \left/ \frac{d\delta_l}{dE} \right|_{E_0} \quad (\text{A.71})$$

So the partial wave amplitude is

$$\begin{aligned} f_l &= \exp[i\delta_l(k)] \sin \delta_l(k) \\ &= \frac{\sin \delta_l(k)}{\cos \delta_l(k) - i \sin \delta_l(k)} \\ &\approx \frac{1}{-\frac{2}{\Gamma}(E - E_0) - i} = \frac{-\Gamma/2}{(E - E_0) + i\Gamma/2} \\ |f_l|^2 &= \frac{\Gamma^2/4}{(E - E_0)^2 + \Gamma^2/4} \end{aligned} \quad (\text{A.72})$$

If at $E \sim E_0$, the partial wave l is dominant, the cross section so we have

$$\sigma_l^{tot} = \frac{4\pi}{k^2} (2l+1) \frac{\Gamma^2/4}{(E - E_0)^2 + \Gamma^2/4} \quad (\text{A.73})$$

Generally the partial wave amplitude can be written as

$$f_l = \frac{1}{2i} (\eta_l e^{2i\delta_l} - 1) = \frac{i}{2} - \frac{i}{2} \eta_l e^{2i\delta_l} \quad (\text{A.74})$$

The amplitude f_l can be plotted on the Argand plot of $\text{Im}f_l$ versus $\text{Re}f_l$. The center of the circle is at $(0, i/2)$. The resonant energy is located at $(0, i(1 + \eta_l)/2)$ which corresponds to $\delta_l = \pi/2$.

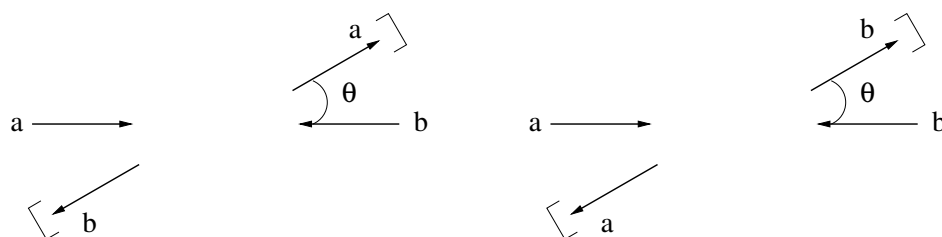
A.6 Scatterings of identical particles

There are two cases for scatterings of identical particles.

(1) Two incident particles with spin-0. One cannot distinguish which particle is captured by the detector. The differential cross section is then

$$\frac{d\sigma}{d\Omega} = |f(\theta) + f(\pi - \theta)|^2 \quad (\text{A.75})$$

Figure A.4: Identicle scatterings.



In the c.m.s frame, the differential cross section is symmetric with respect to $\theta = \pi/2$. In terms of the partial wave decomposition, the differential cross section can be written

$$\begin{aligned} \frac{d\sigma}{d\Omega} &= \frac{1}{4k^2} \left| \sum_{l=0}^{\infty} (2l+1) \{ \exp[2i\delta_l(k)] - 1 \} [P_l(\cos\theta) + P_l(-\cos\theta)] \right|^2 \\ &= \frac{1}{4k^2} \left| \sum_{l=\text{even}}^{\infty} (2l+1) \{ \exp[2i\delta_l(k)] - 1 \} P_l(\cos\theta) \right|^2 \end{aligned} \quad (\text{A.76})$$

where we have used Eq. (A.39) and $P_l(-\cos\theta) = (-1)^l P_l(\cos\theta)$.

(2) Scatterings of two identical spin-1/2 particles. The wave function of two fermions are anti-symmetric. The spin states are $S = 0$ and 1. For $S = 0$, the spatial wave function must be symmetric. For $S = 1$, the spatial wave function must be anti-symmetric. So we have

$$\begin{aligned} \frac{d\sigma}{d\Omega} &= |f(\theta) + f(\pi - \theta)|^2, \quad S = 0 \\ \frac{d\sigma}{d\Omega} &= |f(\theta) - f(\pi - \theta)|^2, \quad S = 1 \end{aligned} \quad (\text{A.77})$$

For the second line, the partial wave decomposition reads

$$\frac{d\sigma}{d\Omega} = \frac{1}{4k^2} \left| \sum_{l=\text{odd}}^{\infty} (2l+1) \{ \exp[2i\delta_l(k)] - 1 \} P_l(\cos\theta) \right|^2 \quad (\text{A.78})$$

If the incident particles are not polarized, the probability in spin-0 state is 1/4, while that in spin-1 state is 3/4. So the total differential cross section is

$$\left(\frac{d\sigma}{d\Omega} \right)_{\text{tot}} = \frac{1}{4} \left(\frac{d\sigma}{d\Omega} \right)_{S=0} + \frac{3}{4} \left(\frac{d\sigma}{d\Omega} \right)_{S=1} \quad (\text{A.79})$$

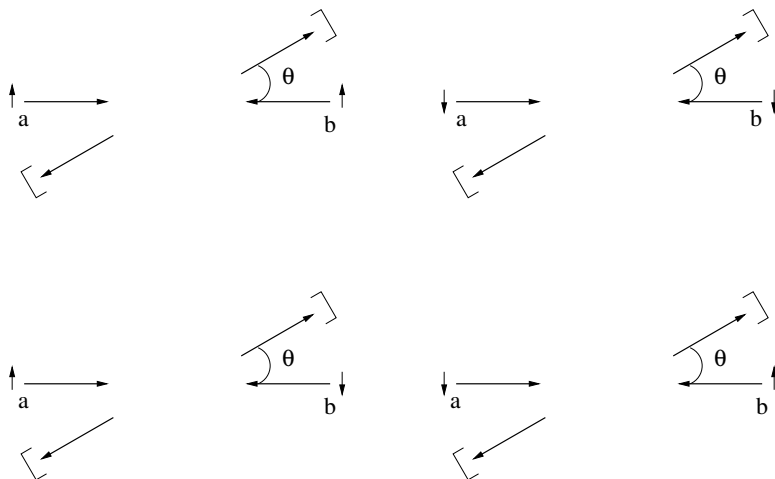
A.7 Lippman-Schwinger equation and Green function method

We now introduce another method for scattering problems: Lippman-Schwinger or Green function method. This method is suitable for high energy particle scatterings. The time-independent Schrödinger equation reads

$$(\nabla^2 + k^2)\psi(\mathbf{r}) = U(\mathbf{r})\psi(\mathbf{r}) \quad (\text{A.80})$$

where $k^2 = 2mE$ and $U(\mathbf{r}) = 2mV(\mathbf{r})$. The wave function satisfies the boundary condition at $r \rightarrow \infty$, Eq. (A.4). The solution $\psi(\mathbf{r})$ is composed of a general solution of the homogeneous equation and a

Figure A.5: Scatterings of identical spin-1/2 particles.



special solution of the full equation,

$$\psi(\mathbf{r}) = \phi_{\mathbf{k}}(\mathbf{r}) + \int d^3\mathbf{r}_1 G_0(\mathbf{r} - \mathbf{r}_1) U(\mathbf{r}_1) \psi(\mathbf{r}_1) \quad (\text{A.81})$$

where $\phi_{\mathbf{k}}(\mathbf{r})$ is a general solution of

$$(\nabla^2 + k^2)\phi_{\mathbf{k}}(\mathbf{r}) = 0$$

The Green function $G_0(\mathbf{r} - \mathbf{r}')$ satisfies

$$(\nabla^2 + k^2)G_0(\mathbf{r} - \mathbf{r}_1) = \delta^3(\mathbf{r} - \mathbf{r}_1) \quad (\text{A.82})$$

Obviously one can verify that $\psi(\mathbf{r})$ of the form in Eq. (A.81) obey the Schrödinger equation. Eqs. (A.81) can be written in a symbolic form

$$|\psi\rangle = |\phi\rangle + G_0 U |\psi\rangle$$

where $|\psi\rangle$ can be solved by

$$|\psi\rangle = (1 - G_0 U)^{-1} |\phi\rangle = (1 + G U) |\phi\rangle \quad (\text{A.83})$$

Note that G_0 and U can thought of matrices in symbolic space. Here we have defined the full Green function G ,

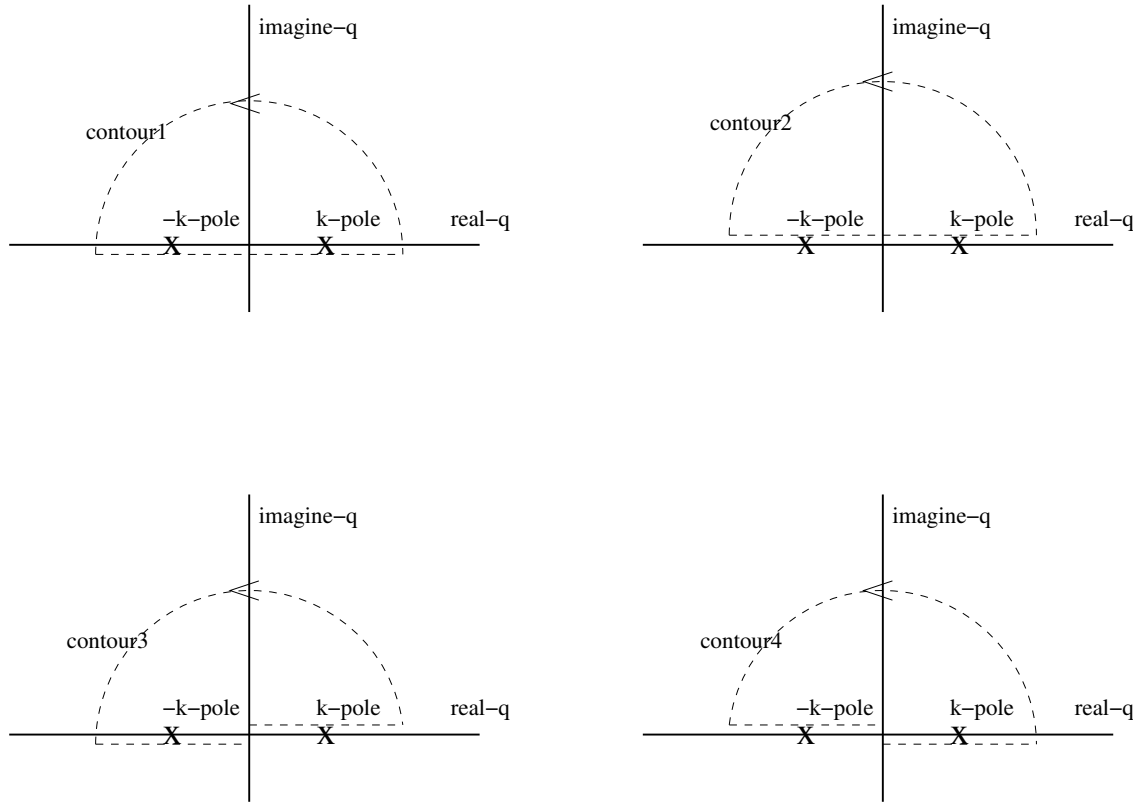
$$G = (1 - G_0 U)^{-1} G_0$$

The Green function G satisfies

$$[\nabla^2 + k^2 - U(\mathbf{r})]G(\mathbf{r} - \mathbf{r}_1) = \delta^3(\mathbf{r} - \mathbf{r}_1) \quad (\text{A.84})$$

So we can verify that $|\psi\rangle$ satisfies Eq. (A.80).

Figure A.6: The possible contours for the integral in Eq. (A.85).



We can solve $G_0(\mathbf{r} - \mathbf{r}_1)$ as

$$\begin{aligned}
 G_0(\mathbf{r}) &= - \int \frac{d^3 \mathbf{q}}{(2\pi)^3} e^{i\mathbf{q}\cdot\mathbf{r}} \frac{1}{q^2 - k^2} = - \frac{1}{(2\pi)^2} \int dq d\theta \sin \theta e^{iqr \cos \theta} \frac{q^2}{q^2 - k^2} \\
 &= \frac{i}{(2\pi)^2} \frac{1}{r} \int_0^\infty dq \frac{q}{q^2 - k^2} \int_{-1}^1 d(iqr \cos \theta) e^{iqr \cos \theta} \\
 &= \frac{i}{(2\pi)^2} \frac{1}{r} \int_0^\infty dq \frac{q}{q^2 - k^2} (e^{iqr} - e^{-iqr}) = \frac{i}{(2\pi)^2} \frac{1}{r} \int_{-\infty}^\infty dq \frac{qe^{iqr}}{q^2 - k^2} \\
 &= \frac{i}{2(2\pi)^2} \frac{1}{r} \int_{-\infty}^\infty dq e^{iqr} \left(\frac{1}{q - k} + \frac{1}{q + k} \right) \tag{A.85}
 \end{aligned}$$

We can extend q to complex plane and make it to the contour integral along C . To make the integral converge, we assume $\text{Im}q > 0$ close the contour in the upper plane because $e^{iqr} \rightarrow 0$ in the upper half circle at $r \rightarrow \infty$. There are four contours $C_{1,2,3,4}$. The integrals of contour $C_{1,2,3}$ give contributions proportional to $e^{ikr} + e^{-ikr}$, 0, and e^{-ikr} respectively. For the outgoing wave we need the contribution proportional to e^{ikr} which comes only from C_4 . The choice of C_4 can be implemented by making the replacement $\frac{1}{q^2 - k^2} \rightarrow \frac{1}{q^2 - k^2 - i\epsilon}$. Eq. (A.85) can be carried out

$$G_0(\mathbf{r}) = -\frac{1}{4\pi} \frac{1}{r} e^{ikr} \tag{A.86}$$

If we treat the potential as perturbation, i.e. we take Born approximation, in the leading order

Eq. (A.81) or (A.83) becomes

$$\begin{aligned}
\psi(\mathbf{r}) &\approx \phi_{\mathbf{k}}(\mathbf{r}) - \frac{1}{4\pi} \int d^3\mathbf{r}_1 \frac{1}{|\mathbf{r} - \mathbf{r}_1|} e^{ik|\mathbf{r} - \mathbf{r}_1|} U(\mathbf{r}_1) \phi_{\mathbf{k}}(\mathbf{r}_1) \\
&\approx \phi_{\mathbf{k}}(\mathbf{r}) - \frac{1}{4\pi} \int d^3\mathbf{r}_1 \frac{1}{r - r_1 \cos\theta} e^{ik(r - r_1 \cos\theta)} U(\mathbf{r}_1) \phi_{\mathbf{k}}(\mathbf{r}_1) \\
&\approx e^{i\mathbf{k}\cdot\mathbf{r}} - \frac{1}{4\pi r} e^{ikr} \int d^3\mathbf{r}_1 e^{-i(\mathbf{k}_f - \mathbf{k})\cdot\mathbf{r}_1} U(\mathbf{r}_1)
\end{aligned} \tag{A.87}$$

where $\mathbf{k}_f = k\mathbf{r}/r$. The scattering amplitude is then

$$f(\mathbf{k}_f, \mathbf{k}) = -\frac{1}{4\pi} \int d^3\mathbf{r}_1 e^{-i(\mathbf{k}_f - \mathbf{k})\cdot\mathbf{r}_1} U(\mathbf{r}_1) = -\frac{1}{4\pi} \tilde{U}(\mathbf{k}_f - \mathbf{k}) \tag{A.88}$$

Appendix B

A: Bessel functions

The Bessel equation reads

$$\frac{d^2 y}{dx^2} + \frac{1}{x} \frac{dy}{dx} + \left(1 - \frac{\nu^2}{x^2}\right) y = 0 \quad (\text{B.1})$$

where ν and x are any complex number. The solutions are the Bessel functions $J_\nu(x)$ of the first kind,

$$J_\nu(x) = \sum_{k=0}^{\infty} (-1)^k \frac{1}{k!} \frac{1}{\Gamma(\nu + k + 1)} \left(\frac{x}{2}\right)^{2k+\nu} \quad (\text{B.2})$$

If ν is not an integer, then $J_{-\nu}(x)$ is another independent solution. If $J_\nu(x) = n$ an integer, then we have

$$\begin{aligned} J_{-n}(x) &= \sum_{k=0}^{\infty} (-1)^k \frac{1}{k!} \frac{1}{\Gamma(-n + k + 1)} \left(\frac{x}{2}\right)^{2k-n} \\ &= \sum_{l=0}^{\infty} (-1)^{l+n} \frac{1}{(l+n)!} \frac{1}{l!} \left(\frac{x}{2}\right)^{2l+n} \\ &= (-1)^n J_n(x) = J_n(-x) \end{aligned} \quad (\text{B.3})$$

where we have used the fact that $1/(-l)! = 0$ with $l > 0$. This means $J_n(x)$ and $J_{-n}(x)$ are basically the same solution of the Bessel equation. Another independent solution is the Bessel function of second kind. When x is real, $J_n(x)$ is an oscillating function with a damping amplitude.

The generating function of Bessel functions is

$$e^{x(t-t^{-1})/2} = \sum_{n=-\infty}^{\infty} J_n(x) t^n, \quad (0 < |t| < \infty) \quad (\text{B.4})$$

One can write it in a different way by using $t = ie^\varphi$, $x = kr$,

$$\begin{aligned} e^{ikr \cos \theta} &= \sum_{n=-\infty}^{\infty} J_n(kr) i^n e^{in\theta} \\ &= J_0(kr) + \sum_{n=1}^{\infty} [J_n(kr) i^n e^{in\theta} + J_{-n}(kr) i^{-n} e^{-in\theta}] \\ &= J_0(kr) + 2 \sum_{n=1}^{\infty} i^n J_n(kr) \cos n\theta \end{aligned} \quad (\text{B.5})$$

where we have used $J_{-n}(x) = (-1)^n J_n(x)$.

The Bessel function of the second kind is defined by

$$Y_\nu(x) = \frac{J_\nu(x) \cos \nu\pi - J_{-\nu}(x)}{\sin \nu\pi} \quad (\text{B.6})$$

If ν is not an integer, obviously $Y_\nu(x)$ is independent of $J_\nu(x)$. One can prove that if $\nu = n$, $Y_n(x)$ is also an independent solution of $J_n(x)$. Note that $Y_n(x)$ diverges at $x = 0$. For example, at $x \rightarrow 0$,

$$\begin{aligned} Y_0(x) &= \frac{2}{\pi} \ln \frac{x}{2} \\ Y_n(x) &= -\frac{(n-1)!}{\pi} \left(\frac{x}{2}\right)^{-n} \end{aligned} \quad (\text{B.7})$$

Bessel functions of third kind $H_\nu^{(1)}(x)$ and $H_\nu^{(2)}(x)$ are defined by

$$\begin{aligned} H_\nu^{(1)}(x) &= J_\nu(x) + iY_\nu(x) \\ H_\nu^{(2)}(x) &= J_\nu(x) - iY_\nu(x) \end{aligned} \quad (\text{B.8})$$

The asymptotic forms of Bessel functions at $|\arg(x)| < \pi$, $|x| \rightarrow \infty$ are

$$\begin{aligned} J_\nu(x) &= \sqrt{\frac{2}{\pi x}} \cos\left(x - \frac{\nu\pi}{2} - \frac{\pi}{4}\right) + O(x^{-3/2}), \\ Y_\nu(x) &= \sqrt{\frac{2}{\pi x}} \sin\left(x - \frac{\nu\pi}{2} - \frac{\pi}{4}\right) + O(x^{-3/2}), \\ H_\nu^{(1)}(x) &= \sqrt{\frac{2}{\pi x}} \exp\left[i\left(x - \frac{\nu\pi}{2} - \frac{\pi}{4}\right)\right] + O(x^{-3/2}), \\ H_\nu^{(2)}(x) &= \sqrt{\frac{2}{\pi x}} \exp\left[-i\left(x - \frac{\nu\pi}{2} - \frac{\pi}{4}\right)\right] + O(x^{-3/2}), \end{aligned} \quad (\text{B.9})$$

The spherical Bessel functions are solutions of

$$\frac{d^2 y}{dx^2} + \frac{2}{x} \frac{dy}{dx} + \left[1 - \frac{l(l+1)}{x^2}\right] y = 0 \quad (\text{B.10})$$

Using $y(x) = x^{-1/2}\eta(x)$ and

$$\begin{aligned} \frac{dy}{dx} &= -\frac{1}{2} \frac{1}{x\sqrt{x}} \eta(x) + \frac{1}{\sqrt{x}} \frac{d\eta(x)}{dx} \\ \frac{d^2 y}{dx^2} &= \frac{3}{4} x^{-5/2} \eta(x) - x^{-3/2} \eta'(x) + x^{-1/2} \eta''(x) \\ \frac{d^2 y}{dx^2} + \frac{2}{x} \frac{dy}{dx} &= \frac{3}{4} x^{-5/2} \eta(x) - x^{-3/2} \eta'(x) + x^{-1/2} \eta''(x) \\ &\quad + \frac{2}{x} \left[-\frac{1}{2} \frac{1}{x\sqrt{x}} \eta(x) + \frac{1}{\sqrt{x}} \frac{d\eta(x)}{dx} \right] \\ &= -\frac{1}{4} x^{-5/2} \eta(x) + x^{-3/2} \eta'(x) + x^{-1/2} \eta''(x) \end{aligned} \quad (\text{B.11})$$

Then the spherical Bessel equation becomes the Bessel one

$$\begin{aligned} &\frac{d^2 y}{dx^2} + \frac{2}{x} \frac{dy}{dx} + \left[1 - \frac{l(l+1)}{x^2}\right] y \\ &= x^{-1/2} \left[\frac{d^2 \eta}{dx^2} + \frac{1}{x} \frac{d\eta}{dx} + \left(1 - \frac{(l+1/2)^2}{x^2}\right) \eta \right] = 0 \end{aligned} \quad (\text{B.12})$$

whose solution is the Bessel function $\eta \sim J_{l+1/2}, Y_{l+1/2}$. The solutions $y = x^{-1/2}\eta(x)$ to the spherical Bessel equation are spherical Bessel functions

$$\begin{aligned} j_l(x) &= \sqrt{\frac{\pi}{2x}} J_{l+1/2}(x) \\ n_l(x) &= \sqrt{\frac{\pi}{2x}} Y_{l+1/2}(x) \\ h_l^{(1)} &= \sqrt{\frac{\pi}{2x}} H_{l+1/2}^{(1)}(x) = j_l(x) + in_l(x) \\ h_l^{(2)} &= \sqrt{\frac{\pi}{2x}} H_{l+1/2}^{(2)}(x) = j_l(x) - in_l(x) \end{aligned} \quad (\text{B.13})$$

They satisfy

$$\begin{aligned} \psi_{l-1} + \psi_{l+1} &= \frac{2l+1}{x} \psi_l \\ l\psi_{l-1} - (l+1)\psi_{l+1} &= (2l+1)\psi_l' \end{aligned} \quad (\text{B.14})$$

where ψ_l stands for $j_l(x), n_l(x), h_l^{(1)}$ or $h_l^{(2)}$.

We can expand the plane wave e^{ikz} in terms of Legendre polynomials

$$e^{ikr \cos \theta} = \sum_{l=0}^{\infty} c_l(kr) P_l(\cos \theta)$$

where

$$\begin{aligned} c_l(kr) &= \frac{2l+1}{2} \int_{-1}^1 dx e^{ikrx} P_l(x) \\ &= \frac{2l+1}{2^{l+1}} \frac{1}{l!} \int_{-1}^1 dx e^{ikrx} \frac{d^l}{dx^l} (x^2-1)^l \\ &= \frac{2l+1}{2^{l+1}} \frac{1}{l!} (-ikr) \int_{-1}^1 dx e^{ikrx} \frac{d^{l-1}}{dx^{l-1}} (x^2-1)^l \\ &= \frac{2l+1}{2^{l+1}} \frac{1}{l!} (-ikr)^l \int_{-1}^1 dx e^{ikrx} (x^2-1)^l \\ &= \frac{2l+1}{2^{l+1}} \frac{1}{l!} (-ikr)^l \sum_{m=0}^{\infty} \frac{(ikr)^m}{m!} \int_{-1}^1 dx x^m (x^2-1)^l \\ &= \frac{2l+1}{2^{l+1}} \frac{1}{l!} (-ikr)^{l,2} \sum_{s=0}^{\infty} \frac{(ikr)^{2s}}{(2s)!} \int_0^1 dx x^{2s} (x^2-1)^l \end{aligned} \quad (\text{B.15})$$

where we have used

$$\left. \frac{d^{l-n}}{dx^{l-n}} (x^2-1)^l \right|_{-1}^1 = 0 \quad (\text{B.16})$$

where $n = 1, 2, \dots, l-1$. The integral is evaluated as

$$\begin{aligned} \int_{-1}^1 dx x^{2s} (x^2-1)^l &= (-1)^l \frac{1}{2} \int_0^1 du u^{s-1/2} (1-u)^l \\ &= (-1)^l \frac{1}{2} \frac{\Gamma(s+1/2) \Gamma(l+1)}{\Gamma(l+s+3/2)} \\ &= \frac{(-1)^l l! (2s)! \sqrt{\pi}}{2^{2s+1} s! \Gamma(l+s+3/2)} \end{aligned} \quad (\text{B.17})$$

where we have used

$$\Gamma(s + 1/2) = \Gamma(2s + 1)2^{-2s}\sqrt{\pi}/\Gamma(s + 1) = \frac{(2s)! \sqrt{\pi}}{2^{2s} s!} \quad (\text{B.18})$$

Eq. (B.15) becomes

$$\begin{aligned} c_l(kr) &= \frac{2l+1}{2} i^l (kr/2)^l \sum_{s=0}^{\infty} (-1)^s (kr/2)^{2s} \frac{\sqrt{\pi}}{s! \Gamma(l+s+3/2)} \\ &= (2l+1) i^l \sqrt{\frac{\pi}{2kr}} \sum_{s=0}^{\infty} (-1)^s (kr/2)^{2s+l+1/2} \frac{1}{s! \Gamma(l+s+3/2)} \\ &= (2l+1) i^l \sqrt{\frac{\pi}{2kr}} J_{l+1/2}(kr) = (2l+1) i^l j_l(kr) \end{aligned} \quad (\text{B.19})$$

Appendix C

B: Spherical harmonic functions

A few lowest order harmonic functions. The Legendre and associated Legendre polynomials are given by

$$\begin{aligned} P_l(x) &= \frac{1}{2^l l!} \frac{d^l}{dx^l} (x^2 - 1)^l \\ P_l^m(x) &= (1 - x^2)^{m/2} \frac{d^m}{dx^m} P_l(x) \\ &= \frac{(1 - x^2)^{m/2}}{2^l l!} \frac{d^{l+m}}{dx^{l+m}} (x^2 - 1)^l \end{aligned}$$

Note that for the associated Legendre functions, the first equality holds for $l \geq m \geq 0$, but the second one holds for all $|m| \leq l$. They satisfy

$$\begin{aligned} P_l(-x) &= (-1)^l P_l(x) \\ \int_{-1}^1 dx P_l(x) P_k(x) &= \frac{2}{2l+1} \delta_{lk} \\ \int_{-1}^1 dx P_l^m(x) P_k^m(x) &= \frac{(l+m)!}{(l-m)!} \frac{2}{2l+1} \delta_{lk} \end{aligned}$$

A few lowest order terms are

$$\begin{aligned} P_0(x) &= 1, \quad P_1(x) = x, \quad P_2(x) = \frac{1}{2}(3x^2 - 1), \\ P_3(x) &= \frac{1}{2}(5x^3 - 3x), \quad P_4(x) = \frac{1}{8}(35x^4 - 30x^2 + 3) \\ P_5(x) &= \frac{1}{8}(63x^5 - 70x^3 + 15x), \\ P_6(x) &= \frac{1}{16}(231x^6 - 315x^4 + 105x^2 - 5) \end{aligned}$$

The spherical harmonic functions are defined

$$\begin{aligned} Y_{lm} &= (-1)^m \sqrt{\frac{2l+1}{4\pi}} \sqrt{\frac{(l-m)!}{(l+m)!}} P_l^m(\cos\theta) e^{im\varphi}, \quad |m| \leq l \\ Y_{lm}^* &= (-1)^m Y_{l,-m} \end{aligned}$$

For $m \neq 0$, we have

$$Y_{l,0} = \sqrt{\frac{2l+1}{4\pi}} P_l(\cos\theta)$$

The orthogonal and complete property,

$$\int d\Omega Y_{lm}^* Y_{l'm'} = \delta_{ll'} \delta_{mm'}$$

A few lowest order functions

$$\begin{aligned} Y_{00} &= \sqrt{\frac{1}{4\pi}} \\ Y_{10} &= \sqrt{\frac{3}{4\pi}} \cos \theta, \quad Y_{1,\pm 1} = \mp \sqrt{\frac{3}{8\pi}} \sin \theta e^{\pm i\varphi} \\ Y_{20} &= \frac{1}{2} \sqrt{\frac{5}{4\pi}} (3 \cos^2 \theta - 1), \quad Y_{2,\pm 1} = \mp \sqrt{\frac{15}{8\pi}} \sin \theta \cos \theta e^{\pm i\varphi}, \\ Y_{2,\pm 2} &= \frac{1}{2} \sqrt{\frac{15}{8\pi}} \sin^2 \theta e^{\pm 2i\varphi} \end{aligned}$$

Vector spherical harmonic functions are

$$\mathbf{Y}_{LM}(\theta, \phi) = \sum_{m,n} C_{lm,1n}^{LM} Y_{lm}(\theta, \phi) \mathbf{e}_n \quad (\text{C.1})$$

The gradient formula

$$\begin{aligned} \nabla[f(r)Y_{lm}(\theta, \phi)] &= Y_{lm} \nabla f(r) + f(r) \nabla Y_{lm} \\ &= f'(r) \mathbf{r} Y_{lm} + \mathbf{e}_\theta f(r) \frac{1}{r} \frac{\partial Y_{lm}}{\partial \theta} + \mathbf{e}_\phi f(r) \frac{1}{r \sin \theta} \frac{\partial Y_{lm}}{\partial \phi} \end{aligned}$$

where we have used

$$\begin{aligned} \nabla &= \mathbf{e}_r \frac{\partial}{\partial r} + \mathbf{e}_\theta \frac{\partial}{r \partial \theta} + \mathbf{e}_\phi \frac{\partial}{r \sin \theta \partial \phi} \\ \frac{\partial Y_{lm}}{\partial \theta} &= (-1)^{m+1} \frac{1}{\sin \theta} \sqrt{\frac{2l+1}{4\pi}} \sqrt{\frac{(l-m)!}{(l+m)!}} \sin^2 \theta \frac{d}{d \cos \theta} P_l^m(\cos \theta) e^{im\phi} \\ &= (-1)^{m+1} \frac{1}{\sin \theta} \sqrt{\frac{2l+1}{4\pi}} \sqrt{\frac{(l-m)!}{(l+m)!}} \\ &\quad \times \left[\frac{(l+1)(l+m)}{2l+1} P_{l-1}^m(\cos \theta) - \frac{l(l-m+1)}{2l+1} P_{l+1}^m(\cos \theta) \right] e^{im\phi} \\ &= -\frac{1}{\sin \theta} (l+1) \sqrt{\frac{(l-m)(l+m)}{(2l-1)(2l+1)}} Y_{l-1,m} + \frac{1}{\sin \theta} l \sqrt{\frac{(l-m+1)(l+m+1)}{(2l+1)(2l+3)}} Y_{l+1,m} \\ &= \frac{1}{\sin \theta} (-c_1 Y_{l-1,m} + c_2 Y_{l+1,m}) \\ \frac{\partial Y_{lm}}{\partial \phi} &= im Y_{lm} \\ \mathbf{e}_\theta &= \mathbf{e}_x \cos \theta \cos \phi + \mathbf{e}_y \cos \theta \sin \phi - \mathbf{e}_z \sin \theta \\ &= -\mathbf{e}_1 \frac{1}{\sqrt{2}} \cos \theta e^{-i\phi} + \mathbf{e}_{-1} \frac{1}{\sqrt{2}} \cos \theta e^{i\phi} - \mathbf{e}_z \sin \theta \\ \mathbf{e}_\phi &= -\mathbf{e}_x \sin \theta + \mathbf{e}_y \cos \theta \\ &= \frac{1}{\sqrt{2}} (\sin \theta + i \cos \theta) \mathbf{e}_1 + \frac{1}{\sqrt{2}} (-\sin \theta + i \cos \theta) \mathbf{e}_{-1} \\ \mathbf{e}_x &= \frac{1}{\sqrt{2}} (-\mathbf{e}_1 + \mathbf{e}_{-1}) \\ \mathbf{e}_y &= \frac{i}{\sqrt{2}} (\mathbf{e}_1 + \mathbf{e}_{-1}) \end{aligned}$$

We obtain

$$\begin{aligned}
& \mathbf{e}_\theta f(r) \frac{1}{r} \frac{\partial Y_{lm}}{\partial \theta} + \mathbf{e}_\phi f(r) \frac{1}{r \sin \theta} \frac{\partial Y_{lm}}{\partial \phi} \\
= & \frac{f(r)}{r \sin \theta} (-c_1 Y_{l-1,m} + c_2 Y_{l+1,m}) \\
& \left(-\mathbf{e}_1 \frac{1}{\sqrt{2}} \cos \theta e^{-i\phi} + \mathbf{e}_{-1} \frac{1}{\sqrt{2}} \cos \theta e^{i\phi} - \mathbf{e}_z \sin \theta \right) \\
& + \frac{f(r)}{r \sin \theta} i m Y_{lm} \left[\frac{1}{\sqrt{2}} (\sin \theta + i \cos \theta) \mathbf{e}_1 + \frac{1}{\sqrt{2}} (-\sin \theta + i \cos \theta) \mathbf{e}_{-1} \right]
\end{aligned}$$

Appendix D

Solutions to problems

Exercises in (6.3.2). We use $S_{12} = T^{ij} \sigma_{1i} \sigma_{2j} = 2T^{ij} S_i S_j$ where $T^{ij} = 3\hat{r}_i \hat{r}_j - \delta_{ij}$ and $S_i = \frac{1}{2}(\sigma_{1i} + \sigma_{2i})$. We can express the total spin operators in terms of ladder operators $S_{\pm} = S_1 \pm iS_2$ with

$$\begin{aligned} S_{\pm} \chi_{1,m} &= \sqrt{(1 \mp m)(1 \pm m + 1)} \chi_{1,m \pm 1} \\ S_{\pm} \chi_{1,1} &= 0, \sqrt{2} \chi_{1,0} \\ S_{\pm} \chi_{1,0} &= \sqrt{2} \chi_{1,\pm 1} \\ S_{\pm} \chi_{1,-1} &= \sqrt{2} \chi_{1,0}, 0 \end{aligned}$$

with

$$\begin{aligned} S_1 &= \frac{1}{2}(S_+ + S_-) \\ S_2 &= \frac{1}{2i}(S_+ - S_-) \\ S_1^2 &= \frac{1}{4}(S_+^2 + S_-^2 + S_+ S_- + S_- S_+) \\ S_1 S_2 &= -\frac{i}{4}(S_+^2 - S_-^2 - S_+ S_- + S_- S_+) \\ S_2^2 &= -\frac{1}{4}(S_+^2 + S_-^2 - S_+ S_- - S_- S_+) \\ S_2 S_1 &= -\frac{i}{4}(S_+^2 - S_-^2 + S_+ S_- - S_- S_+) \end{aligned}$$

We get

$$\begin{aligned} S_i S_j \chi_{1,1} &= \begin{pmatrix} \frac{1}{2}(\chi_{1,-1} + \chi_{1,1}) & \frac{i}{2}(\chi_{1,-1} + \chi_{1,1}) & \frac{\sqrt{2}}{2} \chi_{1,0} \\ \frac{i}{2}(\chi_{1,-1} - \chi_{1,1}) & \frac{1}{2}(-\chi_{1,-1} + \chi_{1,1}) & \frac{\sqrt{2}}{2} i \chi_{1,0} \\ 0 & 0 & \chi_{1,1} \end{pmatrix} \\ S_i S_j \chi_{1,0} &= \begin{pmatrix} \chi_{1,0} & 0 & 0 \\ 0 & \chi_{1,0} & 0 \\ \frac{\sqrt{2}}{2}(\chi_{1,1} - \chi_{1,-1}) & -\frac{\sqrt{2}}{2} i(\chi_{1,1} + \chi_{1,-1}) & 0 \end{pmatrix} \\ S_i S_j \chi_{1,-1} &= \begin{pmatrix} \frac{1}{2}(\chi_{1,1} + \chi_{1,-1}) & -\frac{i}{2}(\chi_{1,1} + \chi_{1,-1}) & -\frac{\sqrt{2}}{2} \chi_{1,0} \\ -\frac{i}{2}(\chi_{1,1} - \chi_{1,-1}) & -\frac{1}{2}(\chi_{1,1} - \chi_{1,-1}) & i \frac{\sqrt{2}}{2} \chi_{1,0} \\ 0 & 0 & \chi_{1,-1} \end{pmatrix} \end{aligned}$$

where we have used for $\chi_{1,1}$,

$$\begin{aligned}
S_1 S_1 \chi_{1,1} &= \frac{1}{4}(S_-^2 + S_+ S_-) \chi_{1,1} = \frac{1}{2}(\chi_{1,-1} + \chi_{1,1}) \\
S_1 S_2 \chi_{1,1} &= \frac{i}{4}(S_-^2 + S_+ S_-) \chi_{1,1} = \frac{i}{2}(\chi_{1,-1} + \chi_{1,1}) \\
S_1 S_3 \chi_{1,1} &= S_1 \chi_{1,1} = \frac{1}{2}(S_+ + S_-) \chi_{1,1} = \frac{\sqrt{2}}{2} \chi_{1,0} \\
S_2 S_1 \chi_{1,1} &= \frac{i}{4}(S_-^2 - S_+ S_-) \chi_{1,1} = \frac{i}{2}(\chi_{1,-1} - \chi_{1,1}) \\
S_2 S_2 \chi_{1,1} &= -\frac{1}{4}(S_-^2 - S_+ S_-) \chi_{1,1} = \frac{1}{2}(-\chi_{1,-1} + \chi_{1,1}) \\
S_2 S_3 \chi_{1,1} &= -\frac{1}{2i} S_- \chi_{1,1} = \frac{\sqrt{2}}{2} i \chi_{1,0} \\
S_3 S_1 \chi_{1,1} &= \frac{1}{2} S_3 (S_+ + S_-) \chi_{1,1} = \frac{1}{2} S_3 (S_+ + S_-) \chi_{1,1} = 0 \\
S_3 S_2 \chi_{1,1} &= \frac{1}{2i} S_3 (S_+ - S_-) \chi_{1,1} = 0 \\
S_3 S_3 \chi_{1,1} &= \chi_{1,1}
\end{aligned}$$

and for $\chi_{1,0}$,

$$\begin{aligned}
S_1 S_1 \chi_{1,0} &= \frac{1}{4}(S_+ S_- + S_- S_+) \chi_{1,0} = \chi_{1,0} \\
S_1 S_2 \chi_{1,0} &= -\frac{i}{4}(-S_+ S_- + S_- S_+) \chi_{1,0} = 0 \\
S_1 S_3 \chi_{1,0} &= 0 \\
S_2 S_1 \chi_{1,0} &= -\frac{i}{4}(S_+ S_- - S_- S_+) \chi_{1,0} = 0 \\
S_2 S_2 \chi_{1,0} &= -\frac{1}{4}(-S_+ S_- - S_- S_+) \chi_{1,0} = \chi_{1,0} \\
S_2 S_3 \chi_{1,0} &= 0 \\
S_3 S_1 \chi_{1,0} &= \frac{1}{2} S_3 (S_+ + S_-) \chi_{1,0} = \frac{\sqrt{2}}{2} (\chi_{1,1} - \chi_{1,-1}) \\
S_3 S_2 \chi_{1,0} &= \frac{1}{2i} S_3 (S_+ - S_-) \chi_{1,0} = -\frac{\sqrt{2}}{2} i (\chi_{1,1} + \chi_{1,-1}) \\
S_3 S_3 \chi_{1,0} &= 0
\end{aligned}$$

and for $\chi_{1,-1}$,

$$\begin{aligned}
S_1 S_1 \chi_{1,-1} &= \frac{1}{4}(S_+^2 + S_- S_+) \chi_{1,-1} = \frac{1}{2}(\chi_{1,1} + \chi_{1,-1}) \\
S_1 S_2 \chi_{1,-1} &= -\frac{i}{4}(S_+^2 + S_- S_+) \chi_{1,-1} = -\frac{i}{2}(\chi_{1,1} + \chi_{1,-1}) \\
S_1 S_3 \chi_{1,-1} &= -\frac{1}{2}(S_+ + S_-) \chi_{1,-1} = -\frac{\sqrt{2}}{2} \chi_{1,0} \\
S_2 S_1 \chi_{1,-1} &= -\frac{i}{4}(S_+^2 - S_- S_+) \chi_{1,-1} = -\frac{i}{2}(\chi_{1,1} - \chi_{1,-1}) \\
S_2 S_2 \chi_{1,-1} &= -\frac{1}{4}(S_+^2 - S_- S_+) \chi_{1,-1} = -\frac{1}{2}(\chi_{1,1} - \chi_{1,-1}) \\
S_2 S_3 \chi_{1,-1} &= i\frac{1}{2}(S_+ - S_-) \chi_{1,-1} = i\frac{\sqrt{2}}{2} \chi_{1,0} \\
S_3 S_1 \chi_{1,-1} &= \frac{1}{2} S_3 (S_+ + S_-) \chi_{1,-1} = 0 \\
S_3 S_2 \chi_{1,-1} &= \frac{1}{2i} S_3 (S_+ - S_-) \chi_{1,-1} = 0 \\
S_3 S_3 \chi_{1,-1} &= \chi_{1,-1}
\end{aligned}$$

Then we obtain

$$\begin{aligned}
S_{12} \phi_S^{11} &= 2 \frac{1}{\sqrt{4\pi}} T^{ij} S_i S_j \chi_{1,1} \\
&= 2 \frac{1}{\sqrt{4\pi}} \left[T^{11} \frac{1}{2} (\chi_{1,-1} + \chi_{1,1}) + T^{12} \frac{i}{2} (\chi_{1,-1} + \chi_{1,1}) + T^{13} \frac{\sqrt{2}}{2} \chi_{1,0} \right. \\
&\quad \left. + T^{21} \frac{i}{2} (\chi_{1,-1} - \chi_{1,1}) + T^{22} \frac{1}{2} (-\chi_{1,-1} + \chi_{1,1}) + T^{23} \frac{\sqrt{2}}{2} i \chi_{1,0} + T^{33} \chi_{1,1} \right] \\
&= \frac{1}{\sqrt{4\pi}} \left[(T^{11} - T^{22} + iT^{12}) \chi_{1,-1} + \sqrt{2}(T^{13} + iT^{23}) \chi_{1,0} + T^{33} \chi_{1,1} \right] \\
&= \sqrt{8} \phi_D^{11} \\
\\
S_{12} \phi_S^{10} &= 2 \frac{1}{\sqrt{4\pi}} T^{ij} S_i S_j \chi_{1,0} \\
&= 2 \frac{1}{\sqrt{4\pi}} \left[T^{11} \chi_{1,0} + T^{22} \chi_{1,0} + T^{31} \frac{\sqrt{2}}{2} (\chi_{1,1} - \chi_{1,-1}) - T^{32} \frac{\sqrt{2}}{2} i (\chi_{1,1} + \chi_{1,-1}) \right] \\
&= \frac{1}{\sqrt{4\pi}} \left[2(T^{11} + T^{22}) \chi_{1,0} + \sqrt{2}(T^{13} - iT^{23}) \chi_{1,1} - \sqrt{2}(T^{13} + iT^{23}) \chi_{1,-1} \right] \\
&= \sqrt{8} \phi_D^{10}
\end{aligned}$$

$$\begin{aligned}
S_{12}\phi_S^{1,-1} &= 2\frac{1}{\sqrt{4\pi}}T^{ij}S_iS_j\chi_{1,-1} \\
&= 2\frac{1}{\sqrt{4\pi}}\left[T^{11}\frac{1}{2}(\chi_{1,1} + \chi_{1,-1}) - iT^{12}\chi_{1,1} - T^{13}\frac{\sqrt{2}}{2}\chi_{1,0}\right. \\
&\quad \left.- T^{22}\frac{1}{2}(\chi_{1,1} - \chi_{1,-1}) + iT^{23}\frac{\sqrt{2}}{2}\chi_{1,0} + T^{33}\chi_{1,-1}\right] \\
&= \frac{1}{\sqrt{4\pi}}\left[(T^{11} - T^{22} - i2T^{12})\chi_{1,1} + \sqrt{2}(-T^{13} + iT^{23})\chi_{1,0} + T^{33}\chi_{1,-1}\right] \\
&= \sqrt{8}\phi_D^{1,-1}
\end{aligned}$$

where ϕ_D^{1m} are given by

$$\begin{aligned}
\phi_D^{11} &= \sum_{m_1, m_2} c(1; m_1, m_2)Y_{2m_1}(\theta, \varphi)\chi_{1m_2} \\
&= \sqrt{\frac{3}{5}}Y_{2,2}(\theta, \varphi)\chi_{1,-1} - \sqrt{\frac{3}{10}}Y_{2,1}(\theta, \varphi)\chi_{1,0} + \sqrt{\frac{1}{10}}Y_{2,0}(\theta, \varphi)\chi_{1,1} \\
&= \sqrt{\frac{3}{5}}\frac{1}{4}\sqrt{\frac{15}{2\pi}}\frac{1}{3}(T^{11} - T^{22} + i2T^{12})\chi_{1,-1} + \sqrt{\frac{3}{10}}\sqrt{\frac{15}{8\pi}}\frac{1}{3}(T^{13} + iT^{23})\chi_{1,0} + \sqrt{\frac{1}{10}}\frac{1}{2}\sqrt{\frac{5}{4\pi}}T^{33}\chi_{1,1} \\
&= \frac{1}{4}\frac{1}{\sqrt{2\pi}}(T^{11} - T^{22} + i2T^{12})\chi_{1,-1} + \frac{1}{4}\frac{1}{\sqrt{\pi}}(T^{13} + iT^{23})\chi_{1,0} + \frac{1}{4}\frac{1}{\sqrt{2\pi}}T^{33}\chi_{1,1} \\
&= \frac{1}{\sqrt{4\pi}}\frac{1}{\sqrt{8}}\left[(T^{11} - T^{22} + i2T^{12})\chi_{1,-1} + \sqrt{2}(T^{13} + iT^{23})\chi_{1,0} + T^{33}\chi_{1,1}\right]
\end{aligned}$$

$$\begin{aligned}
\phi_D^{10} &= \sum_{m_1, m_2} c(0; m_1, m_2)Y_{2m_1}(\theta, \varphi)\chi_{1m_2} \\
&= \sqrt{\frac{3}{10}}Y_{2,1}(\theta, \varphi)\chi_{1,-1} - \sqrt{\frac{2}{5}}Y_{2,0}(\theta, \varphi)\chi_{1,0} + \sqrt{\frac{3}{10}}Y_{2,-1}(\theta, \varphi)\chi_{1,1} \\
&= -\sqrt{\frac{3}{10}}\sqrt{\frac{15}{8\pi}}\frac{1}{3}(T^{13} + iT^{23})\chi_{1,-1} - \sqrt{\frac{2}{5}}\frac{1}{2}\sqrt{\frac{5}{4\pi}}T^{33}\chi_{1,0} + \sqrt{\frac{3}{10}}\sqrt{\frac{15}{8\pi}}\frac{1}{3}(T^{13} - iT^{23})\chi_{1,1} \\
&= -\frac{1}{4\sqrt{\pi}}(T^{13} + iT^{23})\chi_{1,-1} - \frac{\sqrt{2}}{2\sqrt{\pi}}T^{33}\chi_{1,0} + \frac{1}{4\sqrt{\pi}}(T^{13} - iT^{23})\chi_{1,1} \\
&= \frac{1}{\sqrt{4\pi}}\frac{1}{\sqrt{8}}\left[-\sqrt{2}(T^{13} + iT^{23})\chi_{1,-1} - 4T^{33}\chi_{1,0} + \sqrt{2}(T^{13} - iT^{23})\chi_{1,1}\right]
\end{aligned}$$

$$\begin{aligned}
\phi_D^{1,-1} &= \sum_{m_1, m_2} c(-1; m_1, m_2)Y_{2m_1}(\theta, \varphi)\chi_{1m_2} \\
&= \sqrt{\frac{3}{5}}Y_{2,-2}(\theta, \varphi)\chi_{1,1} - \sqrt{\frac{3}{10}}Y_{2,-1}(\theta, \varphi)\chi_{1,0} + \sqrt{\frac{1}{10}}Y_{2,0}(\theta, \varphi)\chi_{1,-1} \\
&= \sqrt{\frac{3}{5}}\frac{1}{4}\sqrt{\frac{15}{2\pi}}\frac{1}{3}(T^{11} - T^{22} - i2T^{12})\chi_{1,-1} - \sqrt{\frac{3}{10}}\sqrt{\frac{15}{8\pi}}\frac{1}{3}(T^{13} - iT^{23})\chi_{1,0} + \sqrt{\frac{1}{10}}\frac{1}{2}\sqrt{\frac{5}{4\pi}}T^{33}\chi_{1,-1} \\
&= \frac{1}{4}\frac{1}{\sqrt{2\pi}}(T^{11} - T^{22} - i2T^{12})\chi_{1,-1} - \frac{1}{4}\frac{1}{\sqrt{\pi}}(T^{13} - iT^{23})\chi_{1,0} + \frac{1}{4}\frac{1}{\sqrt{2\pi}}T^{33}\chi_{1,-1} \\
&= \frac{1}{\sqrt{4\pi}}\frac{1}{\sqrt{8}}\left[(T^{11} - T^{22} - i2T^{12})\chi_{1,-1} - \sqrt{2}(T^{13} - iT^{23})\chi_{1,0} + T^{33}\chi_{1,-1}\right]
\end{aligned}$$

Now we have proved $S_{12}\phi_S^{1m} = \sqrt{8}\phi_D^{1m}$. By acting S_{12} on it again and use

$$\begin{aligned}
S_{12}^2 &= [3(\hat{\mathbf{r}} \cdot \boldsymbol{\sigma}_1)(\hat{\mathbf{r}} \cdot \boldsymbol{\sigma}_2) - (\boldsymbol{\sigma}_1 \cdot \boldsymbol{\sigma}_2)][3(\hat{\mathbf{r}} \cdot \boldsymbol{\sigma}_1)(\hat{\mathbf{r}} \cdot \boldsymbol{\sigma}_2) - (\boldsymbol{\sigma}_1 \cdot \boldsymbol{\sigma}_2)] \\
&= 9 + (\boldsymbol{\sigma}_1 \cdot \boldsymbol{\sigma}_2)^2 - 3(\hat{\mathbf{r}} \cdot \boldsymbol{\sigma}_1)\sigma_{1i}(\hat{\mathbf{r}} \cdot \boldsymbol{\sigma}_2)\sigma_{2i} - 3\sigma_{1i}(\hat{\mathbf{r}} \cdot \boldsymbol{\sigma}_1)\sigma_{2i}(\hat{\mathbf{r}} \cdot \boldsymbol{\sigma}_2) \\
&= 9 + (\boldsymbol{\sigma}_1 \cdot \boldsymbol{\sigma}_2)^2 - 3\hat{r}_a\hat{r}_c(\delta_{ia} - i\epsilon_{iab}\sigma_{1b})(\delta_{ic} - i\epsilon_{icd}\sigma_{2d}) - 3\hat{r}_a\hat{r}_c(\delta_{ia} + i\epsilon_{iab}\sigma_{1b})(\delta_{ic} + i\epsilon_{icd}\sigma_{2d}) \\
&= 3 + (\boldsymbol{\sigma}_1 \cdot \boldsymbol{\sigma}_2)^2 + 3\hat{r}_a\hat{r}_c\epsilon_{iab}\epsilon_{icd}\sigma_{1b}\sigma_{2d} + 3\hat{r}_a\hat{r}_c\epsilon_{iab}\epsilon_{icd}\sigma_{1b}\sigma_{2d} \\
&= 3 + (\boldsymbol{\sigma}_1 \cdot \boldsymbol{\sigma}_2)^2 + 6\hat{r}_a\hat{r}_c(\delta_{ac}\delta_{bd} - \delta_{ad}\delta_{bc})\sigma_{1b}\sigma_{2d} \\
&= 3 + (\boldsymbol{\sigma}_1 \cdot \boldsymbol{\sigma}_2)^2 + 6(\delta_{bd} - \hat{r}_b\hat{r}_d)\sigma_{1b}\sigma_{2d} \\
&= 3 + (\boldsymbol{\sigma}_1 \cdot \boldsymbol{\sigma}_2)^2 - 4(\boldsymbol{\sigma}_1 \cdot \boldsymbol{\sigma}_2) - 2S_{12} \\
&= (\boldsymbol{\sigma}_1 \cdot \boldsymbol{\sigma}_2 + 2)^2 - 1 - 2S_{12}
\end{aligned}$$

we get

$$\begin{aligned}
S_{12}^2\phi_S^{1m} &= \sqrt{8}S_{12}\phi_D^{1m} = 8\phi_S^{1m} - 2S_{12}\phi_S^{1m} \\
S_{12}\phi_D^{1m} &= \sqrt{8}\phi_S^{1m} - 2\phi_D^{1m}
\end{aligned}$$

Exercises in (3.6).

In order to change the life of the energy level in second into the energy width in eV, we use the relation in the natural unit, $c = 3 \times 10^{23}$ fm/s = 1, which gives 1 s = 3×10^{23} fm. So the width is

$$\Gamma \sim \frac{1}{\tau} \approx \frac{1}{1.4 \times 3 \times 10^{13}} \text{ fm}^{-1} \approx \frac{197}{1.4 \times 3 \times 10^{13}} \text{ MeV} \approx 4.7 \times 10^{-12} \text{ MeV}$$

The recoil energy is about

$$E_R = \frac{p^2}{2m} \approx \frac{(0.12)^2}{2 \times 191 \times 940} \text{ MeV} \approx \frac{(0.12)^2}{2 \times 191 \times 940} \text{ MeV} \approx 4 \times 10^{-8} \text{ MeV}$$

For the resonant absorption to take place, one need at least

$$N \sim \frac{4 \times 10^{-8}}{4.7 \times 10^{-12}} \approx 8.5 \times 10^3$$

atoms to reduce the recoil energy.

Exercises in (3.5). For the γ -decay $2^+ \rightarrow 1^-$, according to the parity selection rule, $P_i P_f = (-1)^L$, $(-1)^{L+1}$ for EL and ML radiation which requires L be odd and even for EL and ML radiation respectively. E1 and M2 are the lowest possible radiation. But the strength of M2 is much less than E1. So the answer is E1 radiation.

Bibliography

- [1] Natural Units and the Scales of Fundamental Physics in MIT Quantum Theory Notes, R. L. Jaffe, 2007.
- [2] Fundamental nuclear physics: particles and nuclei, Ping-zhi Ning, Lei Li and De-fen Min, High Education Press 2003. (in Chinese)
- [3] Nuclear Physics, Xi-ting Lu, Atomic Energy Press 2000 (in Chinese).
- [4] Introductory Nuclear Physics, Kenneth S. Krane, John-Wiley and Sons, 1988.
- [5] Nuclear Physics in a Nutshell, Carlos A. Bertulani, Princeton University Press, 2007.
- [6] M.G. Bowler, Nuclear Physics, Pergamon Press, 1973.
- [7] Field theory and particle physics, T. D. Lee, Scientific Press 1981. (in Chinese)
- [8] Quantum mechanics, Jin-yan Zeng, Scientific Press 1981. (in Chinese)
- [9] Advanced Quantum Mechanics, Guang-jiong Ni and Su-Qing Chen, Fudan University Press 2004. (in Chinese)
- [10] Lectures in particle and nuclear physics, Chong-shou Gao and Jin-yan Zeng, High Education Press 1990. (in Chinese)
- [11] Group theory and its application in particle physics, Chong-shou Gao, High Education Press 1992. (in Chinese)
- [12] An introduction to quarks and partons, F. E. Close, Academic Press 1979.
- [13] Quarks & Leptons: An Introduction Course in Modern Particle Physics, F. Halzen and A.D. Martin, John Wiley & Sons 1984.
- [14] Quantum Collision Theory, Charles J. Joachain, North-Holland Publishing Company 1975.
- [15] Classical quark models: an introduction, A. W. Thomas and S. V. Wright, nucl-th/9808008.
- [16] J. J. De Swart, Rev. Mod. Phys. **35**, 916(1963).
- [17] S. Okubo, Prog. Theor. Phys. **27**, 949 (1962).
- [18] M. Gell-Mann and Y. Neeman, The eightfold way: a review with a collection of reprints, W. A. Benjamin, Publisher, 1964.
- [19] W. M. Yao *et al.* [Particle Data Group], J. Phys. G **33**, 1 (2006).
- [20] D. P. Barber *et al.*, Phys. Rev. Lett. **43**, 830 (1979).
- [21] W. Bartel *et al.* [JADE Collaboration], Phys. Lett. B **91**, 142 (1980).

- [22] S. Bethke, arXiv:hep-ex/9812026.
- [23] H. F. Ehrenberg, et al, Phys. Rev. **113**, 666(1959).
- [24] R. Davis, Jr., Phys. Rev. **86**, 976 (1952).
- [25] F. Reines and C. L. Cowan, Phys. Rev. **113**, 273 (1959); F. Reines, C. L. Cowan, F. B. Harrison, A. D. McGuire and H. W. Kruse, Phys. Rev. **117**, 159 (1960).
- [26] C. S. Wu, E. Ambler, R. W. Hayward, D. D. Hoppes and R. P. Hudson, Phys. Rev. **105**, 1413 (1957).
- [27] Nuclear Data Online Services at Peking University (NDOS), <http://ndos.nst.pku.edu.cn/>.
- [28] IAEA nuclear data services, <http://www-nds.iaea.org/>
- [29] R. Machleidt and I. Slaus, J. Phys. G **27**, R69 (2001) [arXiv:nucl-th/0101056].
- [30] J. Maruhn and W. Greiner, Phys. Rev. Lett. **32**, 548 (1974).
- [31] G.S. Boykov, V.D. Dmitriev, G.A. Kudyaev, Yu.B. Ostapenko, M.I. Svirin, G.N. Smirenkin, Yad. Fiz. 53 (1993) 628.
- [32] T. Ethvignot et al., Physics Letters **B575**, 221(2003).
- [33] G.S. Boykov, V.D. Dmitriev, G.A. Kudyaev, Yu.B. Ostapenko, M.I. Svirin, G.N. Smirenkin, Yad. Fiz. 53 (1993) 628.
- [34] M. G. Fuda, Am. J. Phys. 52, 838(1984).
- [35] A. Bohm, M. Gadella, G. Bruce Mainland, Am. J. Phys. 57, 1103(1989).
- [36] J. N. Bahcall, *Solving the Mystery of the Missing Neutrinos*, "http://www.nobelprize.org/nobel_prizes/physics/articles/bahcall/".
- [37] K. Heyde, *Basic ideas and concepts in nuclear physics*, second edition, IOP Publishing Ltd 1994, 1999.